**UNIVERSITY OF ARCHITECTURE,
CIVIL ENGINEERING AND GEODESY**

Eng. Tzvetan Stefanov Georgiev

STUDY ON SEISMIC BEHAVIOR OF "X" CBFs WITH REDUCED DIAGONAL SECTIONS

AUTHOR'S SUMMARY of PhD THESIS

Extended English version

**For the award of educational
and scientific degree "doctor"**

SOFIA, January 2013

The thesis contains 462 pages, including 404 figures or photos and 78 tables. It is structured in 5 chapters. The exposition of the thesis is presented in Chapters 1, 2, 3 and 4. Chapter 1 provides an introduction to the subject, literary review of the problem, formulation of a proposal for CBFs having "X"-shaped configuration of diagonals and Reduced Cross Sections (RCS). The chapter summarizes also the purpose of the thesis. Chapter 2 presents analytical studies of the geometry and kinematics of the proposed type of structures and represents a series of numerical studies of the effects of the use of RCS (structural fuses) in diagonals of proposed CBFs. Chapter 3 presents the experimental program and depicts the planned experimental set-up, experimental models and equipment and provides a detailed picture of the ongoing experiments. Chapter 4 contains an analysis of the experimental results and the conclusions and findings arising thereof. Chapter 5 summarizes and structures main findings of the study. The exposition is followed by formulating of the pretensions on scientific and applied-science contributions of the author, guidelines for future studies, literature used and acknowledgments. The bibliography includes 103 titles out of which 29 in Cyrillic and 74 in Latin. The dissertation ends with a description of publications related to the topic of this development and statement of privacy. Part of the thesis where have been published mainly results of conducted analytical studies is presented in 3 Appendices of 32 pages in total. Appendices include 21 figures and 3 tables.

The thesis is discussed at scientific seminar in Department "Steel, Timber and Plastic Structures" at the UACEG in November 14, 2012 and is targeted for defense.

The doctoral student is enrolled for free doctorate at Department "Steel, Timber and Plastic Structures" of UACEG in 25.01.2012 with Protocol ¯ 196 / 01.25.2012 and a deadline for completion of the doctoral studies: 12 months after the date of enrollment or not later than the end of January 2013.

The public presentation of the thesis will take place on March 20, 2013 in Hall 226 of UACEG 1 Hristo Smirnenski Blvd., 1046 Sofia, Bulgaria from 17.00 hours.

Materials for defense will be available to those interested in the study in office room ı 737 UACEG, 1 Hristo Smirnenski Blvd., 1046 Sofia, Bulgaria and are uploaded to the website of the university www.uacg.bg.

Author: Eng. Tzvetan Stefanov Georgiev
Title: Study on seismic behavior of ñXòCBFs with reduced diagonal sections

CONTENTS

Chapter 1. Formulation of study and a literary review on the subject

1.1. Introduction

Bracing systems are well represented in the overall evolution of the steel structures. Bracing systems are an ensemble of structural elements where to the traditional rectangular frame are added diagonals (braces). The diagonals intersect axially with the elements of the frame thus forming a structure that bears horizontal loads by the operation of its members mainly being subjected to axial forces.

Seismic Engineering in the field of steel structures began its differentiation in the first decades of the 20th century. Historically it relies on the accumulated knowledge of the theory and practice of structures but extends the theory and practice viewed in the light of specific seismic actions. Earthquakes might cause very significant damages on structures but the probability of their occurrence during the lifetime of the building or facility is very small. This led to the development of engineering concept for the design of energy dissipating structures that may successfully absorb seismic energy and to preserve their bearing capacity during and after the seismic impact. The most common class of energy dissipating structures are those that rely on the ductile characteristics of material and of the ductile response of the elements and structural subsystems by which they are composed of. In this sense bracing systems being systems that can effectively operate in presence of horizontal forces and loads are widely used in seismic engineering and especially in seismic engineering of steel structures.

Bracing systems used to sustain the effects of seismic actions operate in elasto-plastic phase and are subjected to large displacements and produced by them significant deformations. Since the response of such bracing system differs significantly from the operation of a bracing system in elastic phase in global technical and normative literature has become popular the term *Concentrically Braced Frames (CBFs)*. Under CBFs we shall understand bracing systems designed for reversal inelastic response ensuring sustainable hysteretic behavior and leading to absorption of seismic energy without a significant decline in bearing capacity (ductile behavior). CBFs consist of two main components (members) ï a frame and diagonals (bracings). Diagonals are the hallmark of the bracing system. They define its significant stiffness and stressed state in the elements of which they are composed. The frame consists of vertical elements mostly columns and horizontal members mostly beams or struts. Horizontal and vertical members form the frame. Diagonals can be called also bracings. The connection between the frame and diagonals is performed in joints. The main geometrical parameters characterizing CBFs are the distance between columns *b* (span) the distance between the beams *h* (inter storey height). The area enclosed by the span *b* and inter storey height *h* we shall call *sub-assembly*.

1.2 Short classification

Because of its advantages bracing systems are traditionally used in steel structure of buildings. This has led to a serious variety of configurations that can be classified under different features of theirs as functionality, mode of diagonals, number of floors, number of spans, according to the geometry of the diagonals in respect to the frame and etc. Given the focus of this study in here we shall point out just some features that are directly related to the seismic behavior of bracing structures.

According to the alignment of the axes of the diagonals *- bracing systems are subclassed into concentrically braced frames (CBFs), Figure 1-8 a and b and eccentrically braced frames (EBFs), Figure 1-8 c and d).*

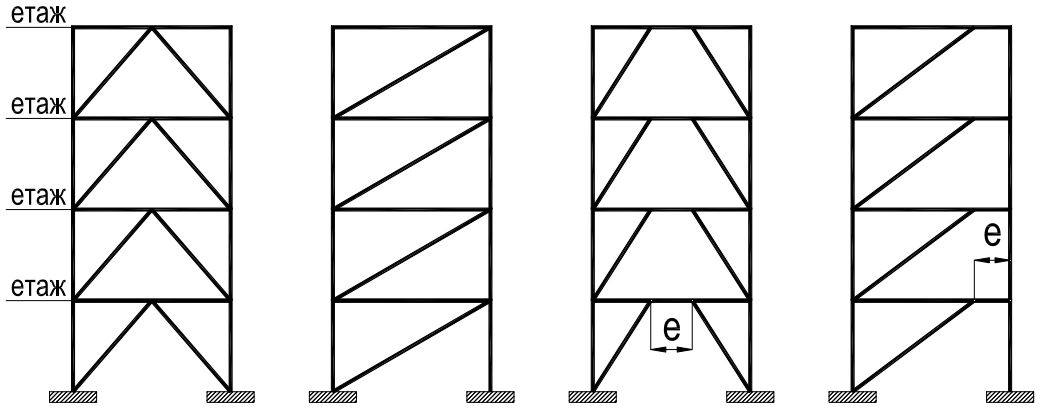

a) b) c) d)

Fig. 1-8 *– Concentrically braced frames a), b) and eccentrically braced frames c), d)*

According to the behavior of the diagonals – there are three types of braces.

- **"Tension diagonal only"" –** bracing systems where in practice operates only the diagonal subjected to tension. Pressed diagonal is of such slenderness that it buckles to the emergence of even the lowest compression in it. These were the prevailing number of bracings in the very beginning of steel construction.
- **Ductile Vertical Braces** in which the diagonals obtain limit slenderness within certain range so that pressed diagonal operates until a certain frame drift and then buckles and continues to work effectively only the tensioned diagonal.
- **BRB (**buckling restrained bracings) **bracing systems** where the diagonals are designed so that they do not lose stability. This can be achieved by filling diagonals having box-shaped cross sections with incompressible mortar or by placing the diagonal in steel jacket.

According to the choice of energy dissipation zones

- The first type CBFs are systems in which the energy dissipation is forwarded to the diagonals and the diagonals themselves are bare members without any specifics details. Arguably the most widely encountered are braced frames with energy dissipating zones in diagonals for the simple reason that this is the guiding recommendation as per seismic codes (such as EN 1998-1 [2], AISC 341-10 [31] and etc.).
- The second type CBFs are systems where energy dissipation is directed into connections. In recent years research interest in developing different kinds of joints and connections in the presence of guaranteed ductile behavior is enhanced. As a consequence thereof were performed various studies and patented developments in which energy dissipation element appears to be the connection.
- To the third type of bracing systems belongs a very important aspect which is the focus of this PhD thesis subject. These are braced frames in which energy dissipating elements are the diagonals but within the length of the diagonals are formed the so called reduced cross sections or structural fuses (SFs) - Figure 1-12. SFs are places where by design improvements is intended to be directed the development of inelastic deformations and to be achieved improvement of overall ductile behavior of the CBF. To this type of bracing systems is dedicated the present study.
-

Fig. 1-12 *– An example of a diagonal in CBF with modification of the original cross section (structural fuses) for directing the dissipation of seismic energy, literary source [95]*

1.3. Reference on current understanding of the factors that influence energy dissipation by structures under seismic action

The modern approach laid down in the codes for earthquake resistant design of structures is based on the response spectrum method and elastic analysis with reduced seismic forces. It is due to the presumption that structural systems are energy dissipating, based on ductile behavior. Despite the many criticisms on this approach solid research data base, accumulated worldwide design code experience and the ability to use computer aided analysis are its main advantages making it still the most widely used method in practice. For this reason the philosophy set out in the behavior factor (*the integral parameter that reflects the complex ability of given structure to bear the effects of strong seismic impacts*) will be briefly interpreted in this item. A similar interpretation could be found in literary sources [38], [42], [54], [77] and others. In summary of the worldwide experience can be used the equation $q = q_{\mu}.q_{\Omega}$ where q is a factor under Eurocode 8, q_{μ} reflects the contribution of partial ductility and q_{Ω} reflects the contribution of the overstrength. ***It is evident that the ability of structures to withstand destructive earthquakes depends on two main parameters –ductility and overstrength.*** Both factors could be improved or make worse through the structural design. Therefore an obvious is the conclusion that they must be studied in details for each class of structures. This conclusion directly reflects on the subject of this PhD thesis. The proposed study of CBFs using diagonals with implementation of reduced cross sections could be a key to improve the structural ductility and hence the coefficient q_{μ}. The proposed details in diagonals are active tool in the hands of the designer for proper reduction of the cross section. Thus could be achieved redistribution of plasticization of the diagonals along the height of the building and obtaining the desired yielding mechanism. The latter in turn affects the coefficient q_{Ω}.

1.4. Formulating the idea and philosophy of the proposed CBFs

Based on the conclusions set out in item 1.3 and considering the personal experience of the author in designing bracing systems has been reached the conclusion of proposing two types of structural improvements in CBFs and "X"-shaped configuration of the bracings. The idea is based on the implementation of the strategy for reducing the cross section (weakening) of the diagonal and the strategy of joint strengthening in order to be achieved predictable and stable hysteretic behavior. The proposed feasible solution is illustrated in Figures 1-14. It can be best represented by a brief description of its main constituent components.

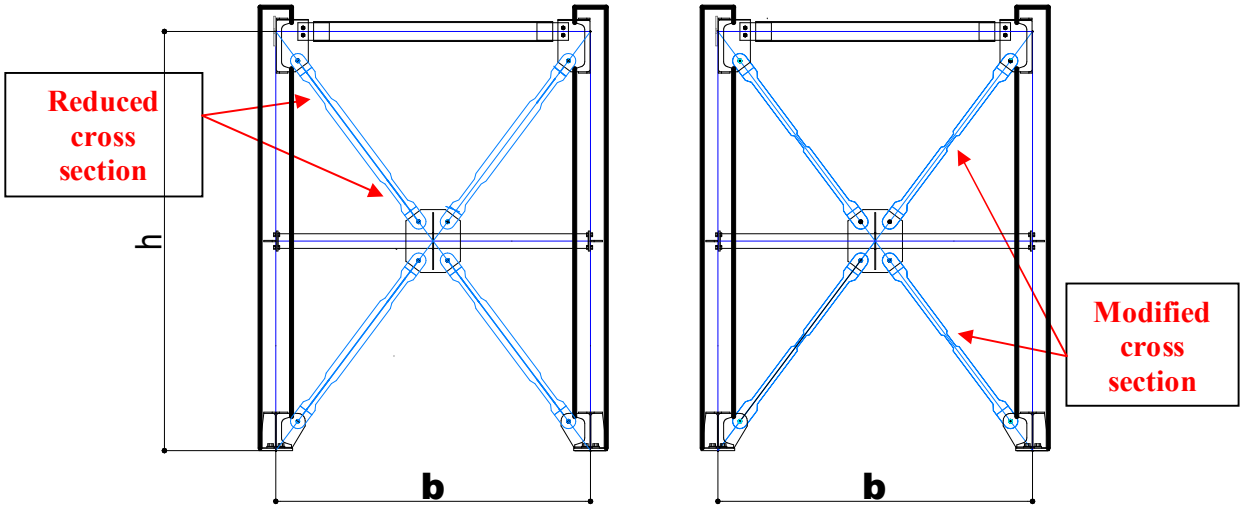

Fig. 1-14 *- geometry and composition of the solutions offered for CBFs and SFs. Proposal with SFs – at left; Proposal with modified middle section – at right;*

The geometry of a subassembly of the proposed bracing system is characterized by concentrically alignment of the diagonals at the corners of the frame. In the composition of the subassembly when compared to the known designs for "X" configuration of the diagonals is made an innovation. Diagonals are interrupted by a horizontal intermediate member whose role is to split them in half so they should not have physical contact with each other. The second role of the introduced horizontal intermediate member is to provide out-of-plane support of the intersection joint. Third possible positive effect of the presence of the horizontal intermediate member is halving the height of the column and reducing its buckling length beyond the plane of the frame.

Cross sections are "H" type for the diagonals and sections "H" type for the horizontal intermediate member. In this study was suggested the diagonals to be made of welded built-up cross sections. An advantage of this choice has been found in the ability to easily compile cross sections with the needed geometric and inertia characteristics at very affordable technological price. Columns and the beam are made of traditional profiles, HEB for the columns and HEA for the beam.

The joints are designed as simple pin joint - Figure 1-16. It is proposed the use of single bolt connections. The purpose is to be provided free rotation of the diagonal in the end cross section and the prediction of the mode of the diagonal buckling.

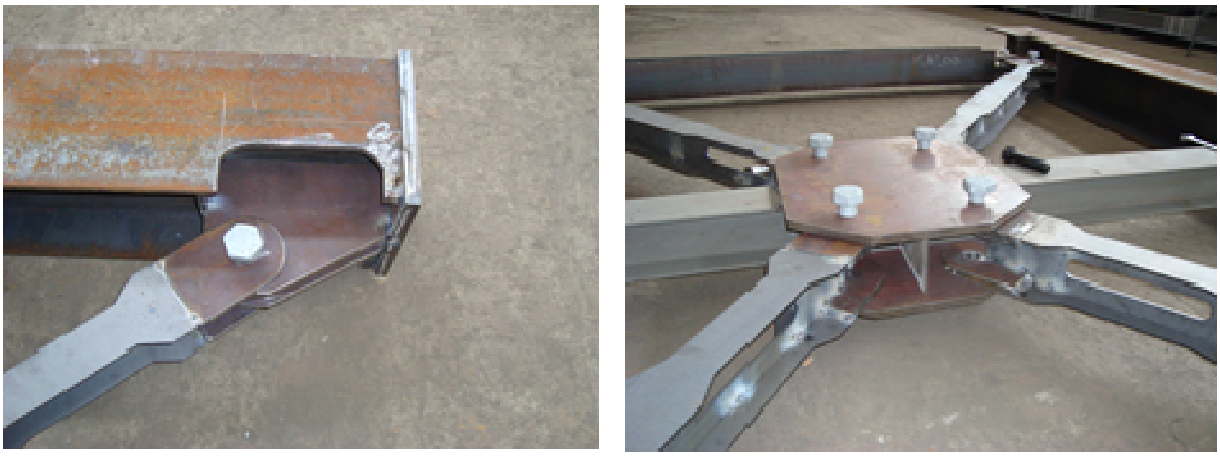

Fig. 1-16 *– general view of the joints in the proposed type of CBFs with SFs*

Energy dissipation members are the diagonals***.*** They are proposed in two variants. Variant with reduced cross section - Figure 1-17, implemented in models H1 and H2. Variant obtaining a modified cross section in the middle - Figure 1-19, implemented in model H3. Within the length of the diagonal are defined the following cross sections. ***Strengthened cross section,*** it is in the area of the joint. Through the use of strengthened cross section in the area of the joint is guaranteed the elastic operation of this connection and the avoidance of potential forms of brittle failure.

Reduced section, it is in areas close to the joint and at a distance not less than the height of the cross section. Through the use of reduced cross sections is aimed to control the location of inelastic deformations within the SF and predictability of the behavior of the diagonal in plastic phase.

Basic cross section, it represents the rest of the diagonal unaffected by the application of the two strategies of strengthening and of weakening of the cross section.

Modified cross section – this is a cross section which bending stiffness is reduced and the area of the cross section is increased - Figure 1-19 below.

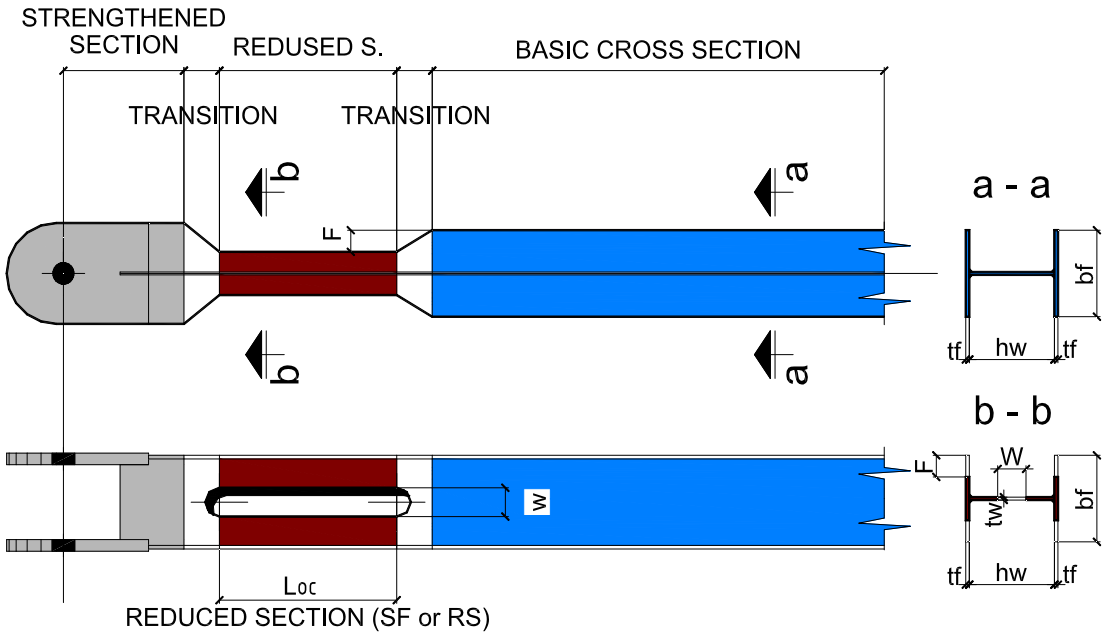

***Fig. 1-17** - diagonal, definition of strengthened, reduced and basic cross section*

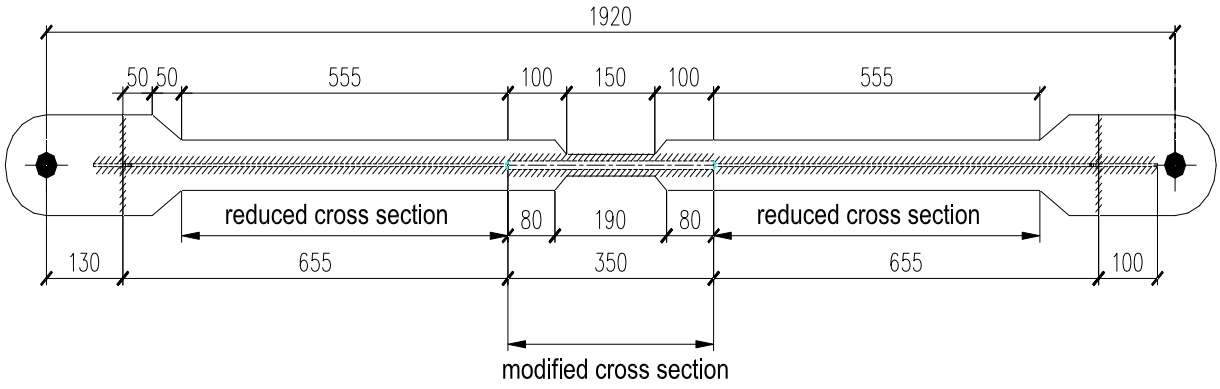

***Fig. 1-19** - fragment of diagonal in model H3 with modified cross section in the middle of the diagonal, drawing of the diagonal;*

1.5. Literary overview

CBFs viewed in the light of the needs of seismic engineering are subject to researchers' studies by the end of the 70s of the last century.

The efforts of researchers and scholars are concentrated on experimental studies, theoretical research and analysis of behavior of structures having CBFs in past earthquakes. In pursuit of these three aspects is structured a part of the literary overview on the subject of this PhD thesis.

After about 30 years of worldwide research interest are clearly outlined the pros and cons in the elasto-plastic behavior of bracing structures. This naturally raises the interest of scientists of how to achieve improvements in this behavior without losing its strengths. Thus was born the trend of seeking of improved behavior through different design methods. Studies and publications on the subject of improved behavior of CBFs or similar are also included in this overview.

1.5.1. Experimental studies

In the literary overview of the PhD thesis has been covered a number of experimental studies related to CBFs. Due to the limited size of the author's summary here they will only be generalized. The overview of experimental studies covers 23 studies conducted in the period as of 1976 until 2012 in North America, Europe, Japan and New Zealand [69], [67.68], [39], [34, 35 and 36], [51] [75] [33] [101] [100] [38.98] [40] [49] [50] [58] [74, 37], [41], [56] and [65].

1.5.2. Theoretical models used in the study of hysteretic behavior of CBFs

In the thesis there is a brief overview of the types of theoretical models as they are divided into phenomenological models [63, 73], physical models [64] and models based on finite elements [62].

1.5.3. Behavior of CBFs in past earthquakes

Certainly the analysis of the performed behavior of steel structures designed to withstand strong earthquakes through CBFs is the source from which engineers and researchers can draw information and to make conclusions about the appropriateness of the applied design techniques and methods of analysis. In the thesis are dealt the experience gained from three previous earthquakes. It have been reviewed in details publications of ***Trembly, Timler, Bruneau and Filiatrault*** (1995) about the earthquake in Northridge [96], publication of ***Trembly, Bruneau, Nakashina, Prion, Filiatrault and DeVal*** (1996) [97] of the Kobe earthquake. It has been included the extensive comparative analysis concerning on the one hand Japanese practice for design and construction in seismic areas and on the other hand Canadian practice. In the thesis is examined also the earthquake in **the region of Kocaeli**, Turkey. It is of interest in view of the fact that Turkey is our neighboring country with similar construction practices. Kocaeli earthquake happened on 17 August 1999 and had a magnitude of 7.6 on the Richter scale. The author has personal experience of this earthquake as in the period 19^{th} to 21^{st} of August, together with Dr. eng. Jordan Milev has visited the epicentrum area. Part of the personal experience of the author is given in the overview of the thesis. Furthermore has been prepared an extensive report on this earthquake and the consequences thereof presented by ***Scawthorn et al (2000)*** [89].

1.5.4. Summary of the performed behavior of CBFs in past earthquakes

Behavior of CBFs in past earthquakes can be summarized as follows:

- CBFs show low cycle fatigue failure especially in cases of diagonals having box cross sections and of low slenderness;
- A common mode of failure of box diagonals is the fracture of the reduced cross section in the connection between the box and the gusset plate or block shear in connections;
- CBFs with slender diagonals when being framed by a continuous members and having capacity designed gusset plate welds, demonstrated surprisingly good behavior in the Kobe earthquake.
- The loss of stability of a pressed diagonal out of the plane of the frame results in the destruction of the cladding. The destruction of cladding and falling of debris from it is a potential danger to human life;

1.5.5. Improved behavior of CBFs

Improvement of the behavior of concentrically braced frames is the subject that matches the concept of this thesis. Therefore we shall make more diverse literary review of publications that extend beyond the studied type of structures but show the demand for various methods for improvement of the hysteretic behavior. In 1990 at an IABSE Symposium in Brussels ***Andre Plumier*** (1990) [85] reported the idea of reducing a part of the cross section of a frame beam and directing plastic deformations in the reduced cross section. This idea has been patented by ARBED. Another article by *Andre Plumier* [86] comes 7 years after the first publication [85]. This is the time in which happened Nortridge earthquake in 1994 and the time in which ARBED released the patent for RBS (*reduced beam section*). The period 1994-1997 was one of the most dynamic periods in the history of seismic engineering therefore the series of questions and comments about the "pros and cons" RBS is quite natural. Article [86] is a kind of response to the requisite questions, doubts and criticisms and provides detailed information about test results that proved the improved hysteretic frame behavior by using RBS.

In the period 1999-2001 has been held the European International Research Projects ***Inco Copernicus – RECOS***. Within this project the Bulgarian research team consisting of *Peter Sotirov, Nicholai Rangelov, Jordan Milev, Tzvetan Georgiev, Ognyan Ganchev and Zdravko Bonev* [90.92] developed a frame joint by combined application of the strategy of the weakening and the strategy of strengthening by haunching. Within the project has been tested 6 experimental models made in full-size scale. Models were frame sub-assembly, composed of column, frame beam and frame joint. The studies made reveal improved hysteretic behavior of models. In none of the performed tests were registered modes of brittle failure neither in joints nor in welded connections. The results of

the study are reported in details in [90] and the entire project is summarized and published in [92]. ***Piluso, Montuori and Longo*** (2005) [84] during EURO Steel 2005 reported on innovative design of diagonals for CBFs in which is used *reduced section solution* (RSS). In this article the authors give rise of an idea which according to them represents a solution to the conflicting requirements set out in Eurocode 8. They address the requirements of [2] for reduction of the slenderness of the diagonals and at the same time the fulfillment of the obligation of making the frame of greater bearing capacity then the diagonals themselves. The authors offer through the use of reduced cross section to be lightened the contour columns and beams without reducing slenderness and respectively the energy dissipation abilities of the CBF.

The overview of recent studies in one way or another presents examples of research works that rely on the concept of structural fuses. An interesting fact is that after the entry into force of the new regulations in the U.S. and Canada respectively [31, 82], has been emerged an interest and arose an objective need to seek constructive methods to implement this concept in CBFs designed for low-rise buildings. Such an important example is the ongoing research project between *CISC - Ecole Polytechnique* and *the University of Berkeley in California UBC*. According to the researchers being key participants in the project ***Timler, Prion, Tremblay, Bouatay*** (2011) [95] the reasons for this choice of the two leading universities are rooted in the traditions of research in the fields of CBFs and seismic behavior of structures. Project [95] is under development and its final results are not published yet. The subject of the research is CBFs in which use box-shaped cross sections (so popular in North America) and in which are applied various structural elements aiming reduction or modification - Figure 1-12. Within the ***European ECSC research project (2004)*** are combined the efforts of four European universities[1] and an industrial partner as is *Archelor/ARBED* aiming the development of a new type of energy dissipation connections INERD (Figure 1-55) for use in CBFs. The aim of this research project is to improve the behavior of systems providing absorption of seismic forces by introducing energy dissipation elements in the connections of the diagonals. Leaders of research teams ***Vayas, Castiglioni, Plumier and Calado*** (2004) see serious advantage in the concept INERD elements to be part of the connections. According to them after a strong earthquake these elements could be easily replaced without affecting the system of bearing of vertical loads. Research work is a series of experimental tests of single sub-assembly of CBF in full-size [99, 88] and a series of analytical studies aimed at obtaining an affordable way of designing of INERD and the simulation of the behavior of multi-storey frames with implemented INERD connections [99].

[1] ATU ï technical university of Athens, Polytechnic Institute of Milan, University of Liège and IST Lisbon

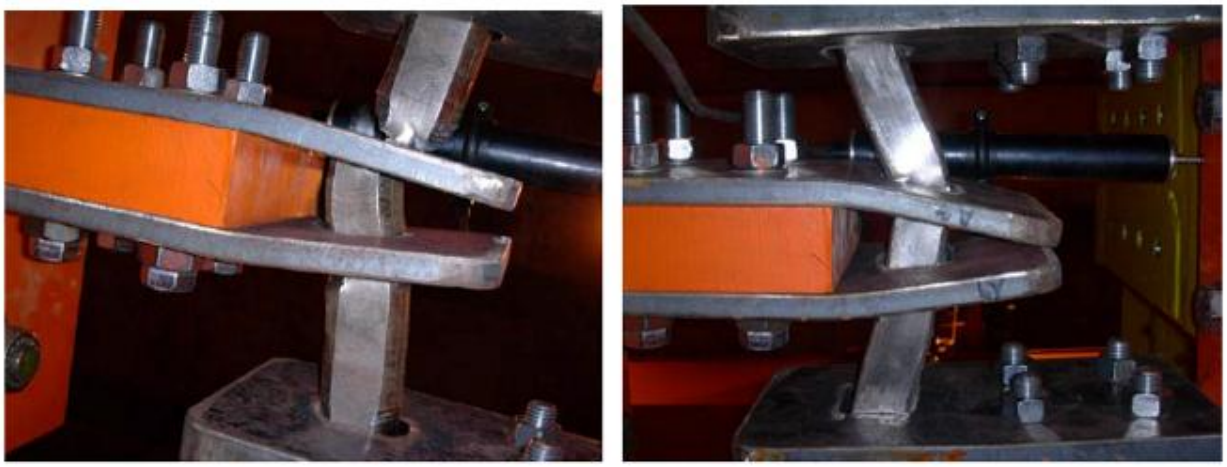

Fig. 1-55 *- experimental set-up for the study of "U"-shaped INERD connection (right), forms of destruction of rectangular pin INERD connections (left) – literary source [48].*

1.5.6. Studies and publications of Bulgarian scientists

In the thesis are examined also a number of publications of Bulgarian scientists which are related to the subject of study. This includes 17 publications from the period as of 1990 until 2012 concerning the problems of seismic behavior of steel structures or seismic design of building structures according to Eurocode 8 [28], [23], [7], [27], [80, 81, 91, 93], [22], [21], [12], [9], [16], [24, 25], [19] and [3]. By the performed review of studies of Bulgarian scientists could be drawn the following conclusions:

- In our country and in particular within the premises of UACEG has been conducted a sufficient number of experimental studies in the application of static cyclic loading (pseudo dynamic test)*;*
- The field of seismic engineering is of interest to many researchers but the subject of examining Concentrically Braced Frames has not been concerned in depth;
- It would be of interest to our scientific and professional community the experimental study of the behavior of ñXöCBFs in conditions of hysteretic behavior. Of interest is the better understanding of the behavior, evaluation of the impact of local factors (market available steels, production technology) and the establishment of Bulgarian research experience.

1.6. Analysis of code requirements for designing of CBFs

In order to be acquainted with the current state of the problem in some leading codes in the thesis are discussed recent editions of the codes in the United States of America, published by the American Institute of Steel Construction (AISC 341-05 [30] and 341-10 [31]) and the General European Standard Eurocode 8 (EN 1998-1 [2]). Attention is paid to the Bulgarian State Standards NPSSZR 1987. A comparison of these three

normative documents is made. Purpose of this comparison is to be demonstrated how two of the world's leading standards address designing of CBFs with an "X"-shaped diagonals and where is the place of Bulgarian standards [17].

1.7. Defining the objectives of the PhD thesis

After performing an analysis of the problem we formulate the following objectives of the thesis:

- To be developed CBFs applicable in Bulgarian construction realities by which to be made easy designing of the non-dissipative frame (counter columns and beams) and joints*;*
- To be studied the hysteretic behavior of the proposed frames and to be derived parameters that characterize it. Obtained and analyzed information to serve as basis for future analytical models;
- To be studied the influence of the reduced cross section on the stressed state and on the stability of the diagonal.

Chapter 2. Kinematics of CBFs and analysis of the effects of the proposed Reduced Cross Sections

2.1. Kinematics of "X"-shaped Concentrically Braced Frames

The geometry of "X"-shaped CBFs is considered in accordance with the accepted in Figure 2-1 basic parameters. As a result of an analysis have been derived the following key relationships that will characterize the kinematics of the system.

The relationship between inter-storey displacement Δ and lengthening of the diagonal δ are derived in assumptions of axially non deformed columns, truss model and small structural displacements. Then

$$\delta = \sqrt{(b+\Delta)^2 + h^2} - \sqrt{b^2 + h^2} \qquad (2.1\text{-}1)$$

by making some simplifications is reached the equation:

$$\delta = \Delta.\cos\alpha_1 \qquad (2.1\text{-}2)$$

In the course of these considerations and on the condition that the displacements are small of certain accuracy could be assumed that $\cos\alpha_1 \approx \cos\alpha$ and hence the equation (2.1-2) will be transformed into $\delta = \Delta.\cos\alpha$ (2.1-3)

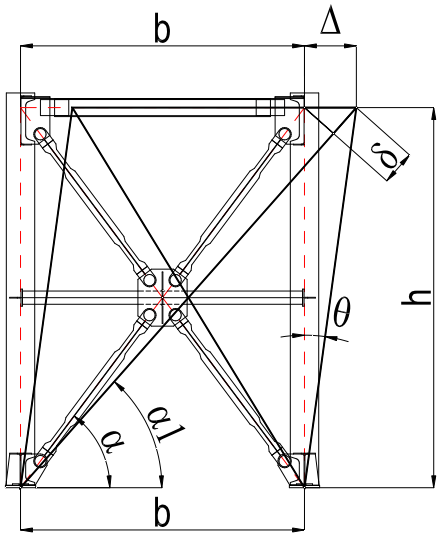

- span b;
- inter-storey height h;
- drift (inter-storey) displacement q;
- angle of inclination of the diagonal U;
- U1 angle of inclination of the diagonal after occurrence of drift q;
- relative inter-storey displacement d,

$$\vartheta = \frac{\Delta}{h};$$

- elongation of the tensioned diagonal u.

***Fig. 2-1** - main geometric parameters that characterize the kinematics of the truss model system for "X"-shaped CBF sub-assembly*

Another important parameter that is derived as a function of inter-storey displacement Δ is the size of the Maximum Transverse Displacement (MTD) named *f* of the buckled compressed diagonal. Consideration is made on the assumption for polygonal deformed line as per Figure 2-2.

Then $f = \frac{\sqrt{\Delta.b}}{2}$. After considering that $\Delta = \theta.h$, the equation can be written as $f = \frac{\sqrt{\theta.h.b}}{2}$. If we introduce the "normalized *f*" with the equation $\bar{f} = \frac{f}{L}$

After short trigonometric transformations has been derived the equation $\bar{f} = \frac{\sqrt{\sin\alpha.\cos\alpha}}{2}.\sqrt{\theta}$. It has been taken in mind that the angle of inclination of the diagonal in practice varies from 30 to 60 degrees and is derived an approximately simple and universal equation $\bar{f} = 0.353.\sqrt{\theta}$.

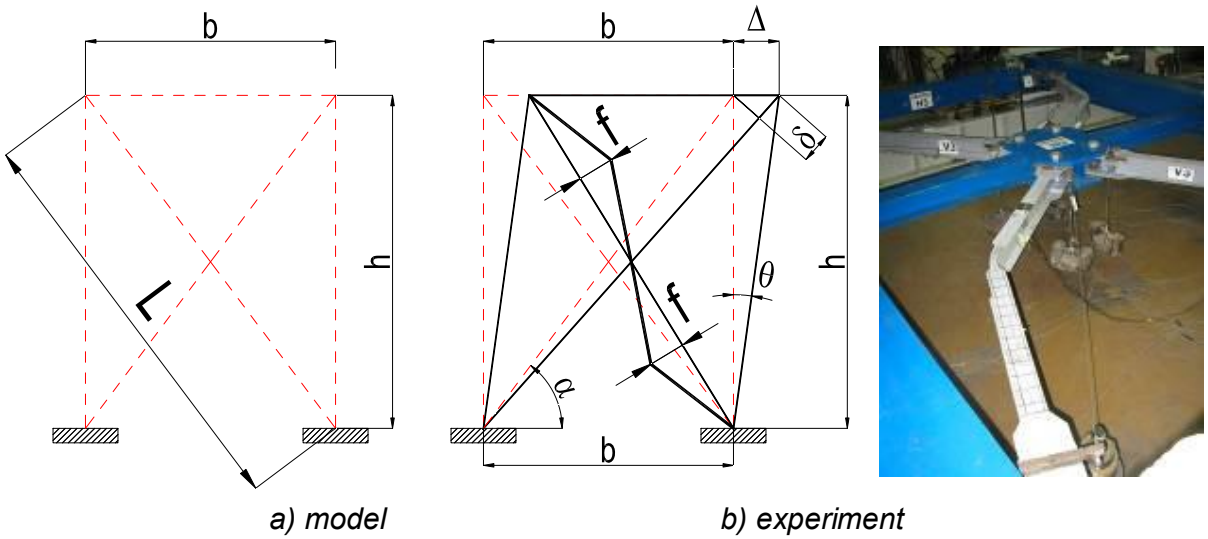

a) model *b) experiment*

***Fig. 2-2** - a theoretical model for determining the parameter f in buckling*

2.2. Analysis of the effects of applying Reduced Cross Sections in the diagonal

2.2.1. Parametric study and computational model

The reduction of the cross section in the diagonal is achieved by cutting Θpart of the flange of the free side and by making a slot through the cross section of the web. The transition between the Reduced Cross Section (RCS) and the non-reduced is smooth. To be studied whether the RCS does not affect negatively the ability for development of inelastic deformations in it have been made a series of numerical models of various cases of reduction ratio. The main design parameters are trimming of the flange ***F*** and the width of the slot in the web ***W*** - Figure 2-6. These parameters are varied and has been studied whether through increasing them (i.e. reducing the cross section) could be influenced the development of plastic deformations in the diagonal.

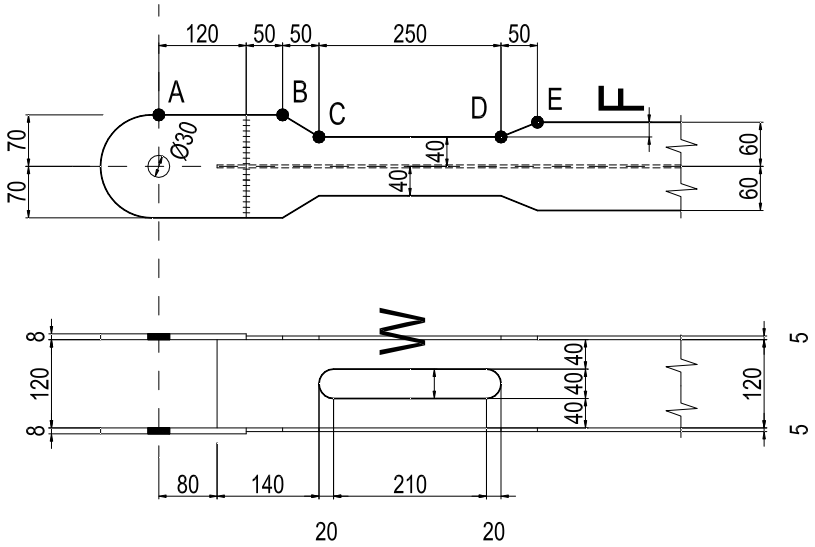

***Fig. 2-6** - defining parameter **F** for trimming the flange and parameter **W** for reducing the cross section of the web*

Calculation model was used with solid finite elements which accurately reproduces the geometry of the reduced cross section and the design of the part through which is performed connection to the column - Figure 2-9. The study was conducted by the use of ANSYS V12.

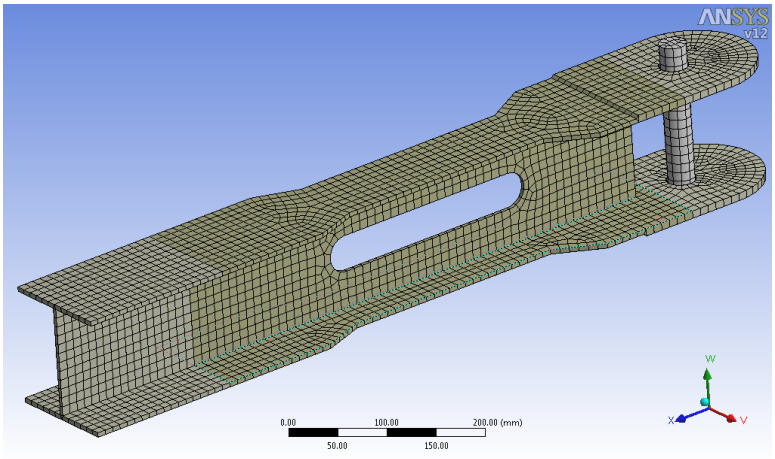

***Fig. 2-9** - Mesh of FE used in the calculation model. Areas in pale grey obtain fully elastic behavior of the material*

Stress-strain diagram of the material is synthesized based on literary data. Have been used elastic branch, yielding plateau and a branch of strain hardening of material.

2.2.2. Parametric study on the assessment of the influence of reduction ratio (degree of reduction in cross section)

Have been made a series of numerical simulations of different models with altered degree of reduction of the cross section. For this purpose parameters ***F*** and ***W*** were varied as defined in item 2.2.1. Have been formed three series for testing in which were varied respectively flange trimming (parameter F), reduction of the cross section of the web

(parameter W) and combinations thereof. The as created plan for the numerical experiment targets to establish on how the parameters ***F*** and ***W*** influence separately and in interaction the elastic-plastic behavior of the member in the area of reduced cross section. Methodology of study involves the derivation of graphs representing force against displacement for each model and the search of relationships between the main parameters characterizing the behavior of the member and the degree of reduction of the cross section $\frac{A_{OC}}{A}$ (reduction ratio).

In the course of the study arose also the need of defining the following parameters: γ_{SH} - Strain-hardening coefficient. It is a coefficient that reflects the increase in force Fy (the force causing yielding) due to the material strain-hardening or other factors contributing to this.

Here is the place to make a detour concerning the strain-hardening coefficient. According to the author it is influenced by the following factors: hardening caused by the shape of the cross section, material strain-hardening, strain rate and the influence of the joint ribs and connections. On the basis of the study in this thesis and in conjunction with [11] and [58] the author considers that this coefficient (γ_{SH}) should attain its differentiated value and the end result to be a number significantly higher than the presently stated in [2] value of 1,1.

The results obtained in format "force-displacement" are summarized in the relevant Figures and only Figures 2-15 and 2-17 are published also in this summary.

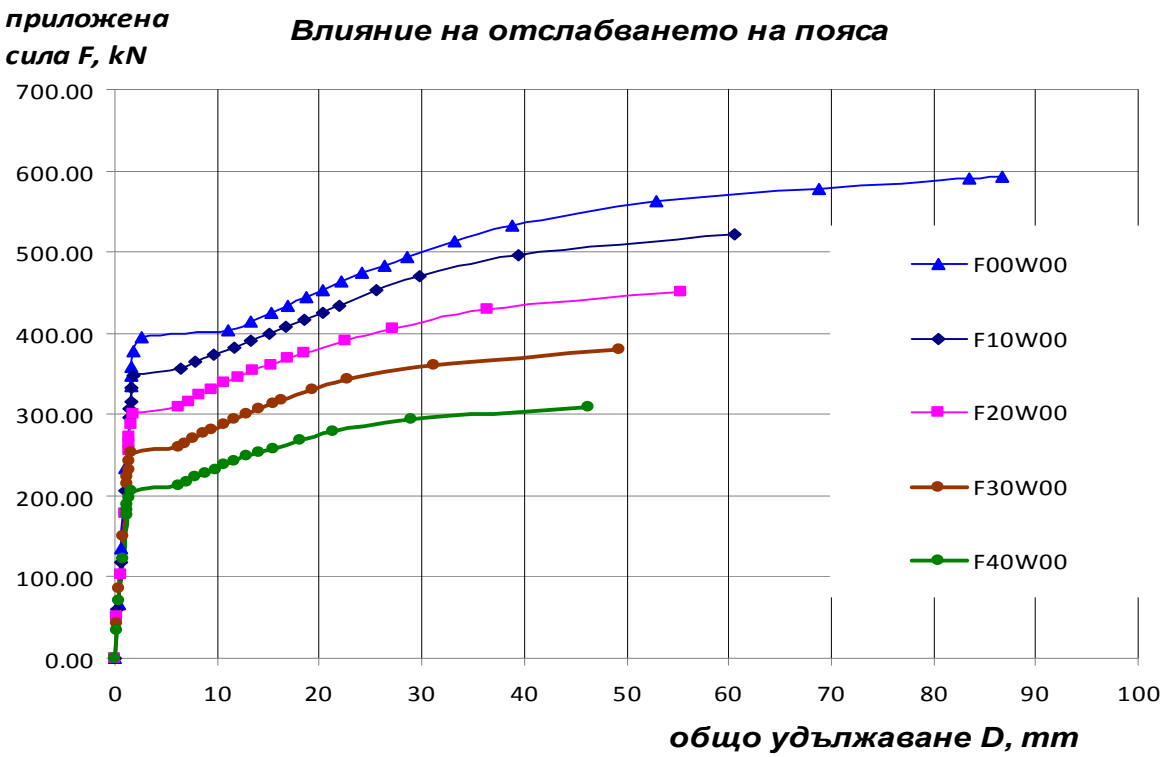

Fig. 2-15 *– relationship "force - displacement" for models of series 1.*

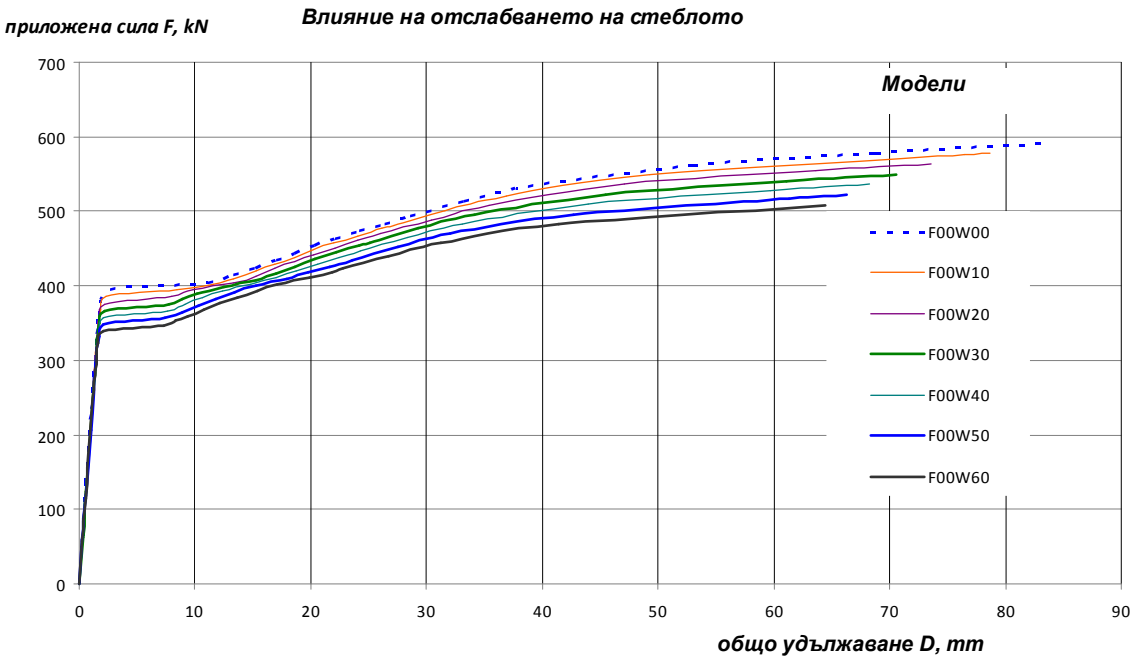

Fig. 2-17 *– relationship "force - displacement" for models of series 2.*

By the above analysis we may conclude that the reduction of the cross section does not lead to occurrence of brittle mode of behavior. Instead there is presence of plastic work. It is also clear that RCS leads to some reduction of the plastic elongation and this reduction increases with increasing the reduction ratio. Assessment of the effect of hardening could be made as follows. If we take into consideration the assumption of small displacements then by the geometry of the braced frame we may express the necessary lengthening of the tensioned diagonal as a function of the storey drift - Figure 2-25.

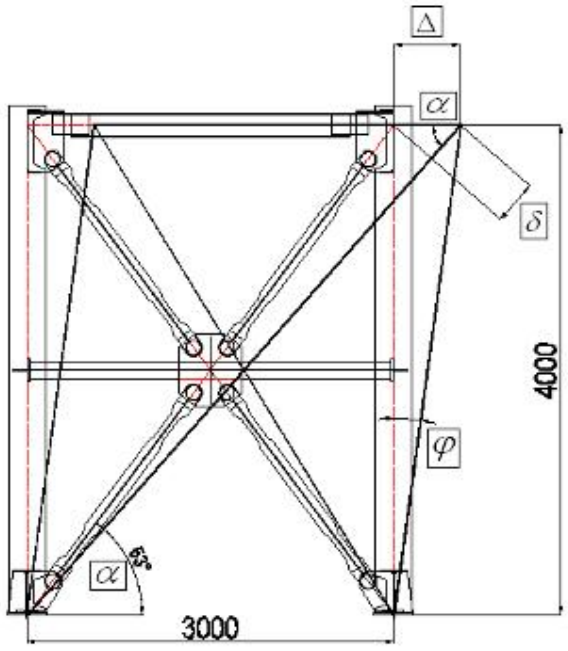

$\delta = \Delta.\cos(\alpha)$ (2.1-3), If we use the criteria, that for CBFs of ductility class "mediumò (DCM), the drift Δ should correspond to a rotation of the column $\varphi = 0.025rad$ and in ductility class "high" (DCH), the drift Δ should correspond to a rotation of the column $\varphi = 0.035rad$, then we may easily calculate, that for this example in height 4000 mm and a span between the columns of 3000 mm shall be obtained:

For DCM - $\Delta = 100mm \Rightarrow \delta = 60mm;$ and for DCH - $\Delta = 140mm \Rightarrow \delta = 84mm;$

Fig. 2-25 *- geometric relationships "drift - lengthening of the diagonal"*

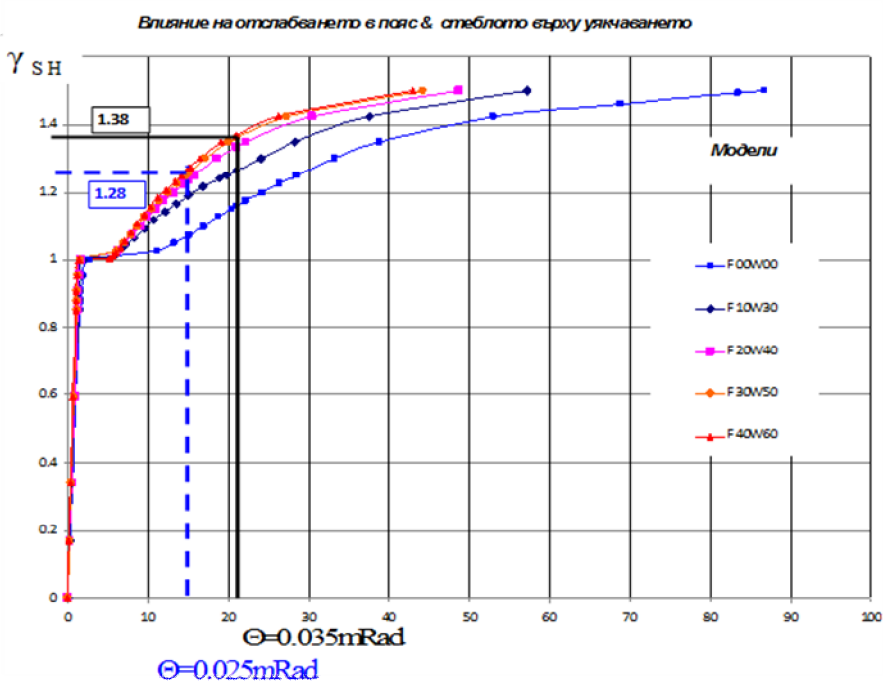

***Fig. 2-27** - of strain-hardening coefficient γ_{SH} in ductility classes DCM & DCH – models of series 3*

Within one diagonal there has 4 pieces of reduced cross section. Therefore any reduction in cross section must ensure elastic-plastic lengthening of 15 mm for ductility class "medium" and 21 mm for ductility class "high". In the occurrence of as designated elongations could be monitored also the corresponding work of the material in strain hardening phase. Figure 2-27 shows the relationships between obtained elastic-plastic elongations in the diagonal and the corresponding hardening. Figures 2-28 and 2-29 show the relationships between the degree of reduction in cross section and the coefficient of normal stress increase in the diagonal due to hardening γ_{SH}.

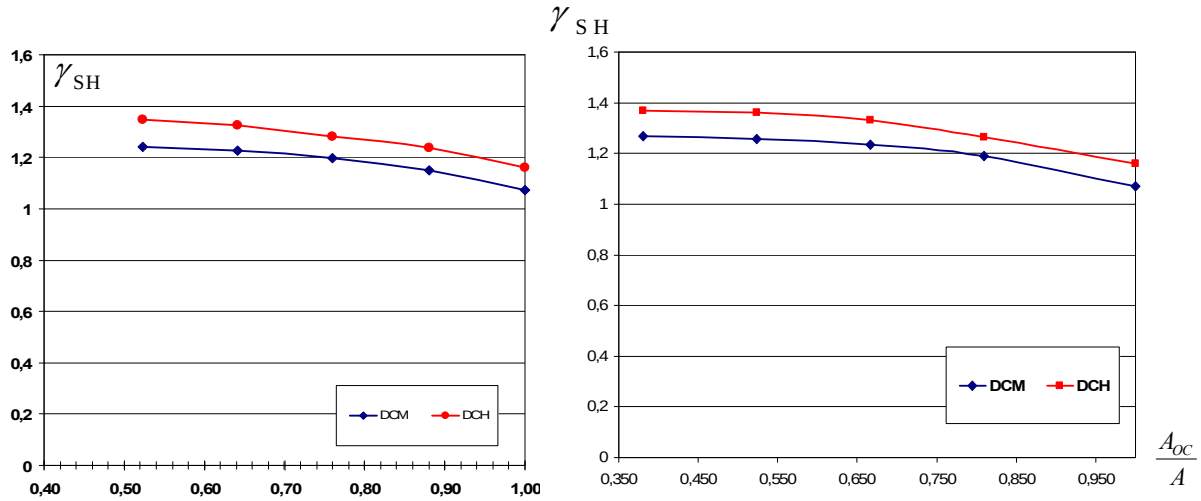

***Fig. 2-28 and Fig. 2-29** - variation in the coefficient of strain-hardening γ_{SH} depending on the reduction ratio – models of series 1 (at left), models of series 3 (at right)*

According to Eurocode 8 [2] there has not been shown differentiated value of coefficient γ_{SH} and the same was assumed to be of value equal to 1,1, irrespective of the type of cross section or class of ductility. This study shows that there is a need of differentiated selection of the coefficient by taking into account hardening whether it's hardening arising from the work of the material or it is hardening resultant from the type of the cross section. In the cases reviewed γ_{SH} ranged from 1,07 to 1,28 for DCM and from 1,16 to 1,38 for DCH. We note that even in case of non-reduced cross section (model F00W00) in the assumed criteria for ductility of class "high" (DCH) was obtained value $\gamma_{SH} = 1{,}16$, which exceeds the estimated value in Eurocode 8 equal to 1,1. The explanation of the author is that always in the joint area there is a reason to expect 2D stressed state that leads to a hardening effect. We believe that the value of 1,1 set out in this European code is undervalued and should have more differentiated form.

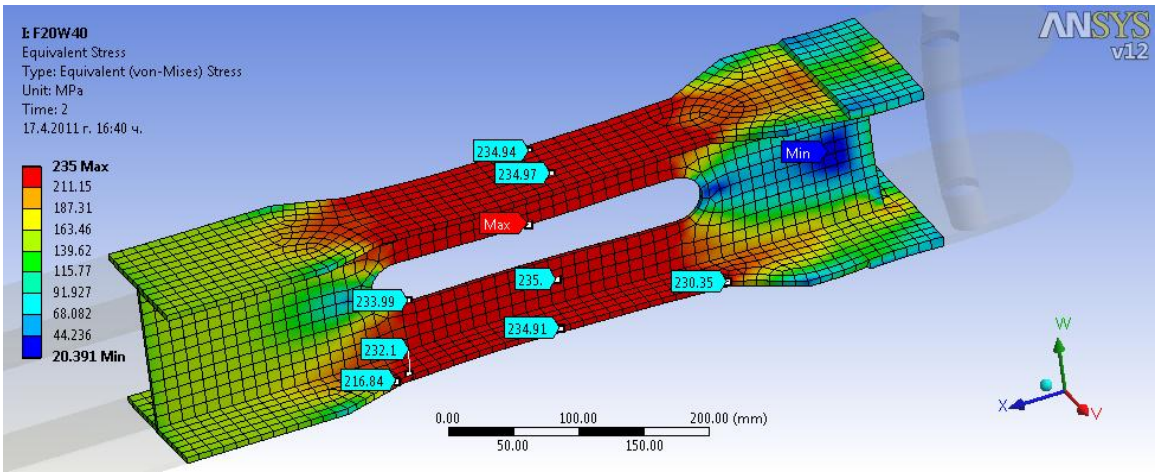

***Fig. 2-32** - picture of stressed state under von-Mises for model F20W40 in application of force F=1.0Fy*

Picture of development of normal strains for model F20W40 at different levels of applied tensile force is shown in Figure 2-32. Given the large number of models and the shortened volume of the author's summary here is only information for model F20W40. For all other models the information is shown in Appendix 2.2 to the thesis.

2.2.3. Influence of the length of the reduced cross section

All models described in item 2.2.2 are of length of reduced cross section equal to 250 mm. The logical question is how by changing the length of the reduced cross section will be affected the elastic-plastic behavior of the studied part of the member. To perform such an analysis has been selected model F20W40 by varying the length of the reduced cross section from 100 to 350 mm. Thus were achieved derivatives of models being of varying length of the RCS. For all models was applied static non-linear analysis using ANSYS V12. Principles and approaches adopted in the numerical model described in item 2.2.1 are also applied here. By the analysis of results could be drawn the following conclusions:

- there is a match between the theoretical force that produces yielding and the same force obtained by FEM analysis;
- the displacements in member D_y corresponding to force F_y increase with the growth of length of the reduced cross section;
- plastic deformations develop mainly in the area of reduced cross section;
- with increasing the length of reduced cross section increases also the ductility of the element. Put another way if we need to increase the inter-storey displacement and recall the relationships in equation (2.1-3) then the way we can do that is by increasing the length of the RCS zone.

Of particular interest is the determination of the minimum length of the area of reduced cross section. Such a study would allow us to determine when the reduced area begins to act as a concentrator of plastic deformations. Figure 2-36 shows a graphical relationship between the coefficient of strain-hardening $\gamma_{SH} = \frac{F}{F_y}$, the length of reduced cross section area and the resultant elongation of the investigated member. Figure 2-36 shows how by shortening the reduced cross section area is observed decrease in plastic plateau and increase of hardening.

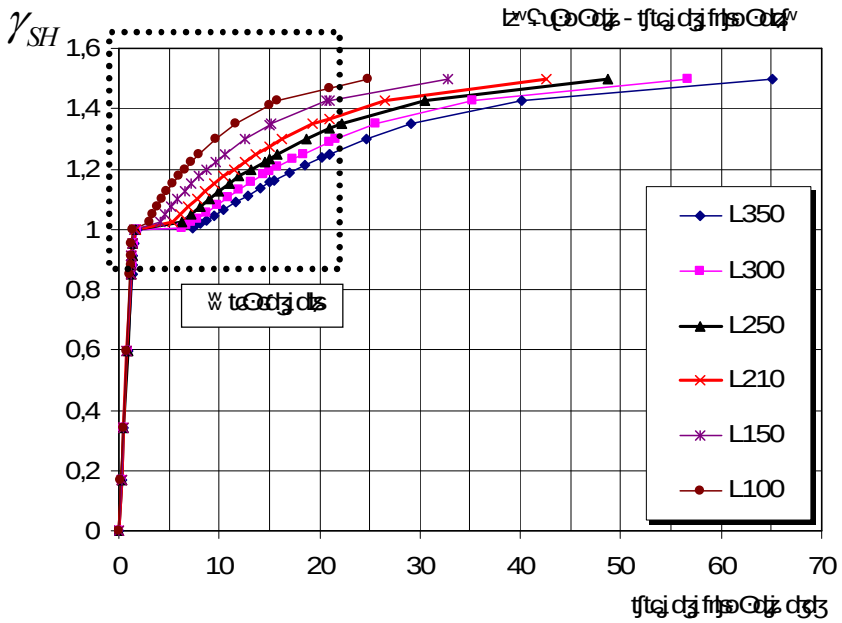

Fig. 2-36 *- relationships "hardening – displacement" in changing the length of the reduced cross section.*

It is noteworthy that when the length of the area of reduced cross section becomes smaller than approximately 1.5H (height of member) there is a visible reduction of plastic plateau and increase in hardening. If we take into consideration standard ISO 6892-1 which regulates the standard tensile test then there is a requirement according to which the minimum length of the narrowed part of the specimen to be greater than $5.65\sqrt{\grave{A}}$. It is

considered that this criterion provides a smooth transition between the reduced cross section and non-reduced cross section and that length is sufficient to minimize the effects of stress concentration due to structural reduction of cross sections. Such assumption is made also by *Vincenzo Piluso* et al in [84]. We apply the same approach and summarize it in Figure 2-38. Once we have defined criteria for the minimum length of the reduced cross section we may derive maximum value of coefficients γ_{SH} for ductility class "medium" DCM (obtained elongation of 15 mm) and ductility class "high" DCH (obtained elongation 21 mm). This is done in Figure 2-38. The conclusion is that the minimum acceptable length of the area of reduced cross section shall be formulated by the equation $L_{OC,\min} = 5.65\sqrt{A_{OC}} = 189mm$. As a practical alternative criterion can be formulated that the minimum length of the reduced cross section area should not be shorter than 1.5H (height of the member). When the reduced cross section area is of less length it acts as a concentrator which causes a reduction of the plastic work of the material and rapid increase of the force in the member.

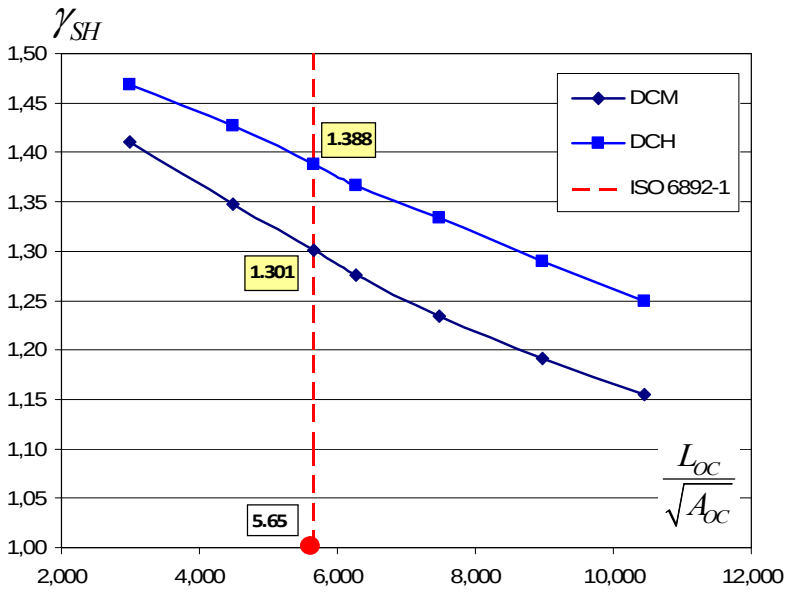

***Fig. 2-38** - relationship of the coefficient of strain-hardening as a function of the normalized length against net cross section*

2.2.4. Influence of the shape of the reduced cross section

Have been designed five different models in which the reduction ration of the cross section $k = \frac{A_{OC}}{A}$ is one and the same, the length of the area of reduced cross section is one and the same and the only changed parameter is the shape by which the reduced cross section is achieved. Have been used model F2f20W40 (reducing of the flange by making two openings of Ø 20), model F4f20W40 (reducing of the flange by making 4 openings of Ø 20), F20Wf40 (reducing of the flange by making 2 openings of Ø 20) and model F20DBW40 - Figure 2-47, the dog bone shape. Model F20W40, shown in Figure 2-32 is well known and studied in previous items. At this stage it will be used as a base

(referential) model whose behavior shall be compared to the behavior of other new models. Models in question were tested using the same experimental set-up and the same way of applying axial force F through computer finite elements model explained in item 2.2.1. To make conclusion from the obtained results has been prepared Figure 2-48. It appears that when reduction in cross-section is achieved by local opening (such as round holes in flanges or the web) then such a structural arrangement acts as an abrupt concentrator of strain. There are both hardening effects and also reduction of plastic work in reduced cross section. Only the shape of the flange trimming of type "dog bone" in fig. 2-47 does not lead to a difference between the theoretical force $F_{y,theory}$ causing yielding and force F_y obtained by non-linear static analysis.

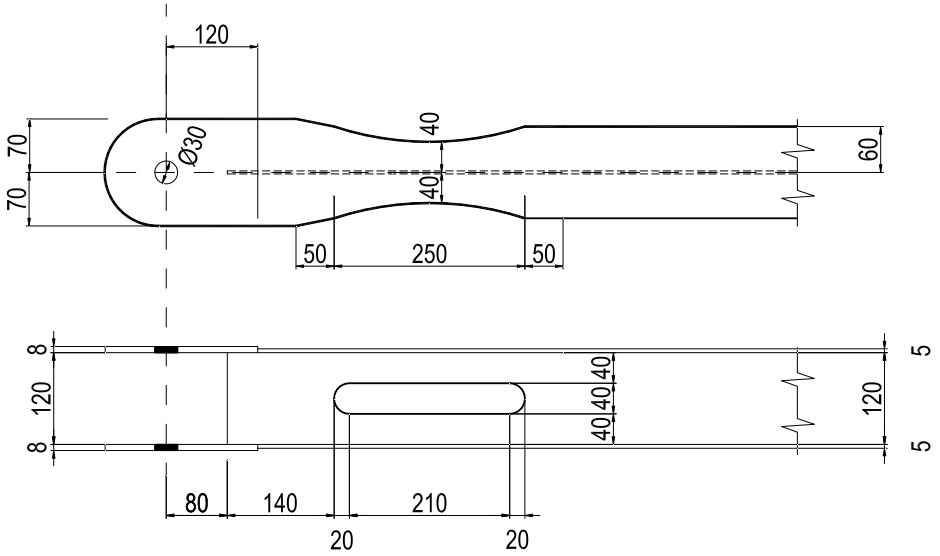

***Fig. 2-47** - model F20DBW40, trimming of the flange is obtained by type Dog Bone*

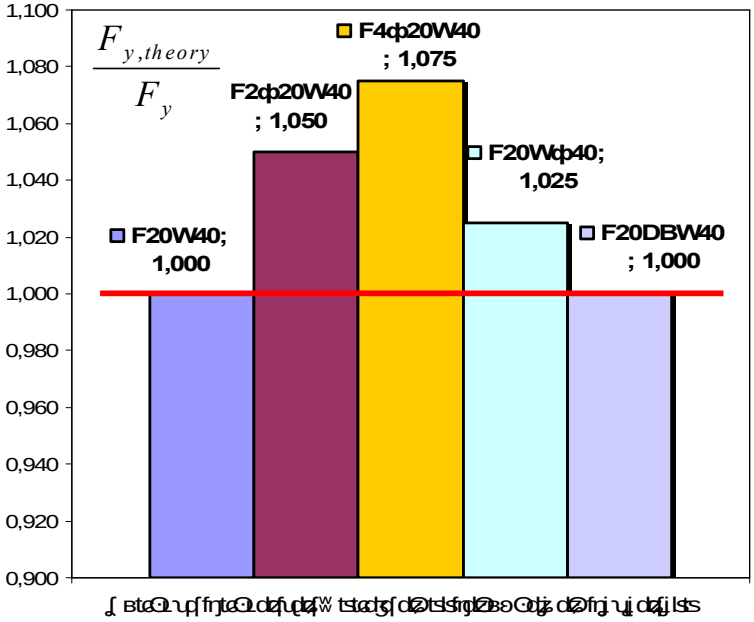

***Fig. 2-48** - assessment of the hardening depending on the shape of the RCS*

Structural design of type "dog bone" gradually reduces the cross section and it does not create hardening effects - Figure 2-48. Summary of the influence of the shape of the structural trimming (reduction of cross section) on the development of plastic deformations is shown in Figure 2-49. As shown in Figure 2-49 there are two significant effects on the behavior of the members generated by the shape of the reduced cross section. The first effect can be defined as an increase of the elastic branch of the work of the member (hardening). The increase is from 2.5% to 7.5% depending on the type of trimming. Using a small number of round openings as in model F2F20W40 is the most inappropriate from this point of view. The second very important effect is the strong reduction of plastic deformations.

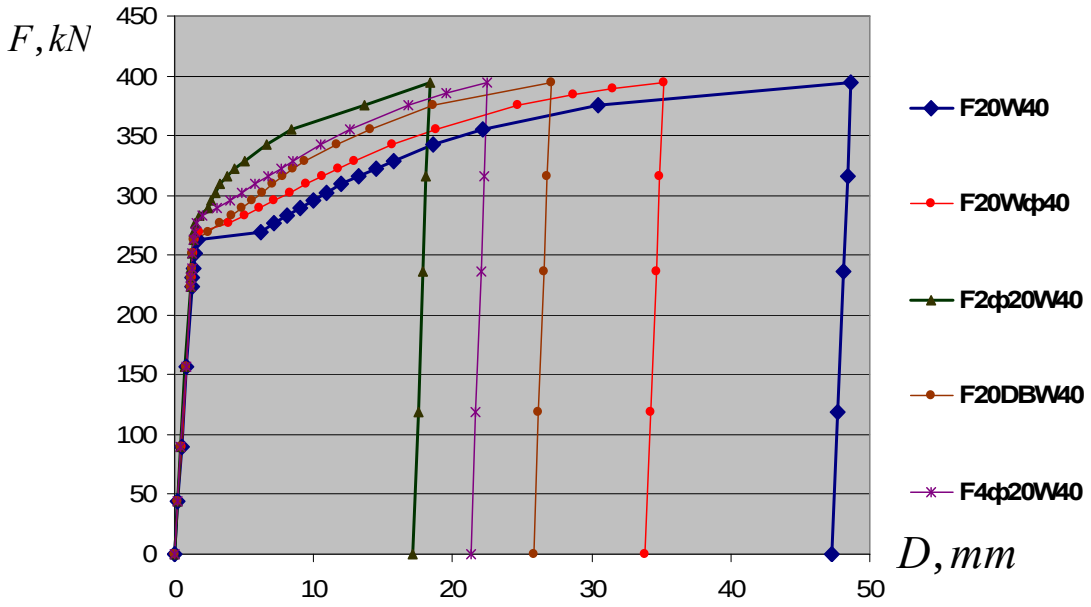

***Fig. 2-49** – relationship force - displacement in changing the shape of the RCS*

In conclusion it can be said that all proposed alternative ways of shaping the reduced cross section gives a worse result compared to the basic way of trimming of the cross section. The worst behavior is that of model F4Ø20W40 and the weakest negative effect is by using the form of model F20WØ40. The use of trimming of type "dog bone" is also not recommended, although this form is used widely in frame beams having moment resisting joints.

2.2.5. Influence of RCS on the slenderness of the diagonal

Structural fuses in the diagonal (RCS) influence the slenderness. To a similar conclusion has reached *Vicenco Piluso* et al in its article [84]. Has been conducted parametric study for determining on how the length of the proposed reduced cross section and the reduction ratio affect the slenderness of the diagonal. Have been used series of diagonal models of varying degrees of reduction of cross section and different length of reduced cross section. For each model has been solved the stability equation in order to

be determined the critical buckling force in given diagonal and coefficient ε. Has been used software SAP2000 V14. The influence of the length of the trimmed cross section on coefficient μ depending on the varying degree of reduction in cross section is examined and summarized in Figure 2-61. In this study has been artificially varied the length L_{OC} while the two trimmings join together. Through an analysis and summarization of the obtained results was derived equation (2.2-1) by which could be determined coefficient μ.

$$\mu = \frac{\lambda_{eq}}{\lambda} = \left(0.42\frac{L_{OC}}{L} + 0.89\right)\left(\frac{I_{Z,OC}}{I_Z}\right)^{-(\frac{L_{OC}}{L}+0.14)} \geq 1.0 \qquad (2.2\text{-}1),$$

The equation has a range of validity $0.95 \geq k = \frac{A_{OC}}{A} \geq 0.50$ and $0.25 \geq \frac{L_{OC}}{L} \geq 0.10$.

Has been performed comparison of results obtained by equation (2.2-1) and those obtained by the solution based on the finite elements method. Has been discusses various models that fall within the range of validity of the equation. Comparison shows that the equation gives results that are always on the safe side and differences vary but do not exceed 9%.

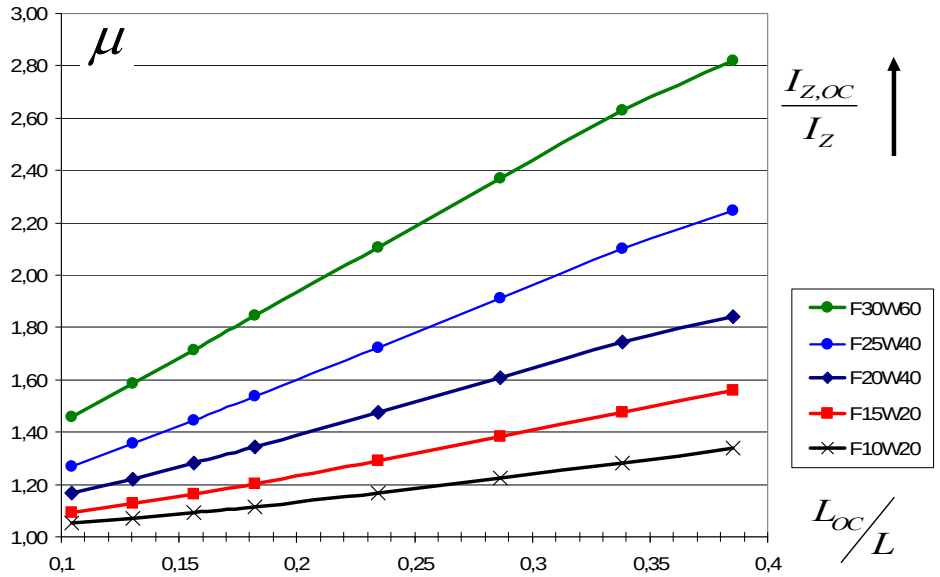

Fig. 2-61 *- influence of the length of the reduced cross section* L_{OC} *in series having a different ratio* $\frac{I_{Z,OC}}{I_Z}$ *on coefficient* μ *expressed by* $\frac{L_{OC}}{L}$

2.3. Conclusions and generalizations made from the analytical studies

➢ The proposed equation (2.1-3) is the most convenient expression for calculating the relationship between inter-floor displacement and the lengthening of the diagonal. In the general practical case the equation leads to an error of up to 3% compared to other

equations (2.1-1) and (2.1-2). The equation has been checked also experimentally (see results described in Chapter 4);

- The proposed equation (2.1-6) shows the relationship between the occurring inter-floor displacement and the MTD of the diagonal in buckling. The equation has been checked also experimentally (see results described in Chapter 4);
- The proposed numerical model gives reliable results for the assessment of the effects of stress concentration. As a conclusion from the performed numerical parametric study can be formulated the assertions that the reduction of the cross section in the proposed way does not act as a concentrator. Plastic deformations develop within the area of the reduced cross section. The presence of reduced cross section reduces plastic elongations between 25 and 45% depending on the degree of trimming. However this plastic phase is absolutely sufficient for obtaining of dissipative behavior relying on ductile work. Trimming of the web makes the characteristic diagram of the member almost unchanged.
- The length of the area of reduced cross section directly affects the ductility of the member. Short lengths of area of RCS may act as a stress concentrator leading to the reduction of plastic work of the member. The study confirms that the minimum length of the area of reduced cross section could be determined by the equation $L_{OC,\min} = 5.65\sqrt{A_{OC}}$. A similar recommendation was given by Professor Vincenzo Piluso et al in [84]. The author offers also a second criterion $L_{OC,\min} = 1.5H$.
- The degree of trimming of the cross section, the degree of development of plastic deformations, the length of the area of implemented RCS and the hardening caused by the presence of the Structural Fuses are in interaction. In significant reduction of the cross section, hardening may ignore the effect of trimming. Proper setting of the behavior could be obtained by increasing the length of the area of reduced cross section.
- Connecting the dissipative member and the non-dissipative frame is realized in joints. To ensure elastic behavior of the frame should be kept in mind the occurrence of potential hardening in the dissipative member. This should become with the use of coefficient γ_{SH} called a coefficient of strain-hardening. On the value of the coefficient of strain-hardening according to the author influence the following factors:
  - Hardening caused by the operation of material within the reduced cross section zone, after reaching the end of plastic plateau;
  - Hardening caused by the shape of the cross section and of the layout of the joint ribs and connections;
  - Hardening due to the strain rate in seismic situation;
  - Hardening dependent on the class of ductility of the designed structure (DCH or DCM);

The author proposes for structures or members sensitive to overloading the value of the coefficient in question to be $\gamma_{SH} = 1,3$. The author believes that value 1,1 set out in the European code is undervalued and should have more differentiated form in accordance with the factors described above. Such a conclusion is also well supported in study [58],

where Goggins, Broderick and Elghazouli report about forces of 20% higher than the expected one and explain the difference with the dynamic nature of the study.

- Of the studied 5 different designs of the area reduced in cross section the proposed version has the best impact on the elastic-plastic behavior of the member. The variants related to reduction of the cross section through drilling of openings act as stress concentrators. The variant related to reduction of the cross section by the implementation of trimming of type "dog bone" is not acting as a stress concentrator but reduces the plastic work of the member.
- By introducing reduced cross sections along the diagonal is affected the slenderness of the member. The length of the trimmed cross section is a geometrical parameter that significantly affects the equivalent slenderness of the diagonal λ_{eq}. In order to take into account the effect of the reduced cross section has been derived an analytical equation (2.2-1) which covers cases of practical interest of such type of diagonals that obtain structural fuses. The accuracy of the equation is compared with the results obtained by solution of FEM and has been proven for cross section of height of 130 mm, width of 120 mm, flange thickness of 5 mm and web thickness of 4 mm. The equation always gives values on the safe side. The average deviation of the values obtained by equation (2.2-1) is 4.46% and the maximum deviation is 8.65%. The proposed equation is compared with the equation proposed by Vincenzo Piluso et al in [84]. The results of comparison are published in Appendix 2.3 of the thesis.

Chapter 3. Experimental program

3.1. Experimental program, aims and objectives of the experiments

A key stage in this study is the realization of an experimental program aiming to prove or disprove the applicability of the concept of implementation of Reduced Cross Sections (structural fuses) in the diagonals of the proposed type of CBFs. The program includes three types of experiments with a total of six tests and is illustrated on the block diagram shown below.

№	Description of the experiment	Abbreviation	Model
1	Study on a fragment of a diagonal having SF - alternating static loading	Experiment 1-1	D1
2		Experiment 1-2	D2
3	Study on a fragment of concentrically braced frame - static, cyclic, alternating loading	Experiment 2-1	H1
4		Experiment 2-2	H2
5		Experiment 2-3	H3
6		Experiment 3	Bare Frame

3.2. Experiment 1 – separate study on a fragment of a diagonal with reduced cross section

There were conducted two experiments (experiments 1-1 and 1-2) in which models represent an "abstract" of the area of the diagonal in CBF. They are designed with the same size and thickness as well as models prepared for Experiment 2. The structural joint for junction with the column is detailed in the same way as in the CBF sub-assembly prototype shown in Figure 1-16 of item 1.4. The type of experimental models designed for Experiment 1 and the experimental set-up are shown in Figure 3-2. Experimental models for experiments 1-1 and 1-2 are called respectively models D1 and D2 and with the use of this designation will be referred to in point 4.

Fig. 3-2 *–Experiments 1 – experimental set-up and models*

3.3. Experiment 2 – study on single storey, single span CBF

Experimental models represent a model in geometric scale of 1:2 of single storey, single span CBF. The models are designed by using a scale for the geometry. The cross

sections of the bracings of the frame are designed so they should have stressed state like their prototypes of an actual structure. The frame (columns and beams) is designed to retain its elastic behavior during the experiment. Thus in various tests have been replaced the diagonals and the frame was used repeatedly. During an experiment 2 were used 3 experimental models called H1, H2 & H3. For clarity and easy orientation in the attached further on in the exposition photographs we need to define that the frame is painted in blue, the diagonals of H1 in red, diagonals of H2 in yellow and diagonals of H3 in grey. The following Figures 3-9, 3-11 and 3-13 show photographs of the experimental models.

Fig. 3-9 *- experimental model H1;*

Fig. 3-11 *- experimental model H2;*

Fig. 3-13 *– experimental model H3 – general view*

The experimental set-up is shown in Figure 3-15. It is achieved by a supporting stand (position 1), loading system ï a hydraulic actuator (position 2), an experimental model (position 4) and stability bracing system (position 3). Experiment 2 was implemented in a planar set-up and horizontal position of the model and the loading system. Given the available equipment in the laboratory and the capabilities of the universal laboratory stand this was the optimal set-up for conducting experiment 2.

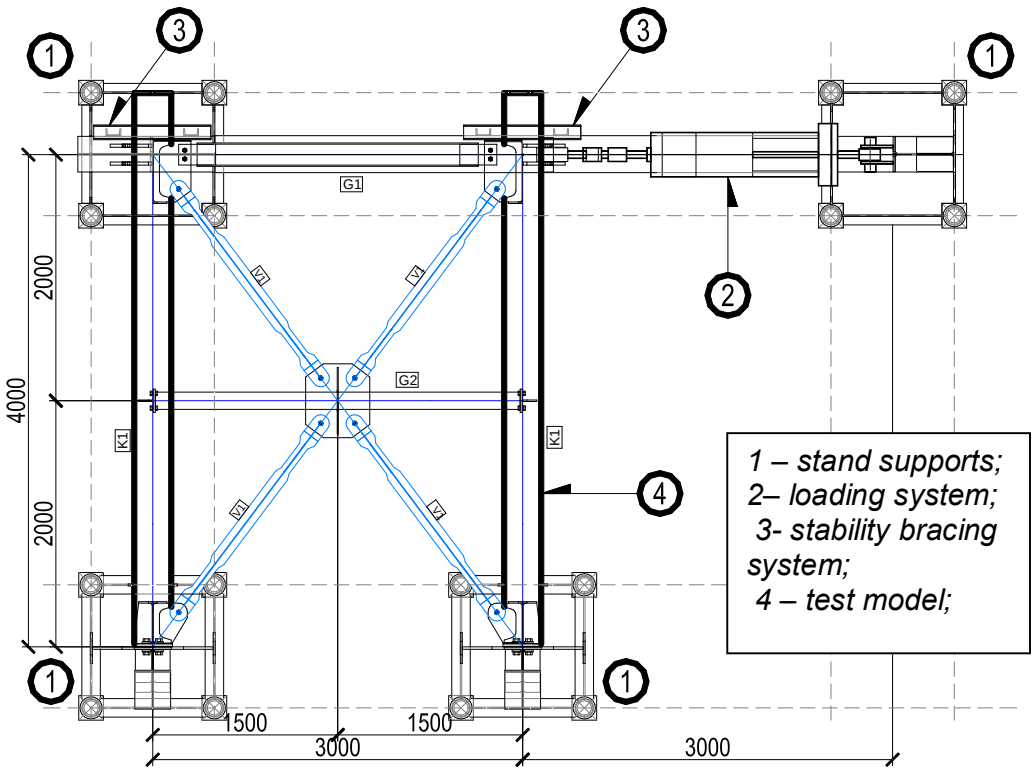

***Fig. 3-15** - Experiment 2 - experimental set-up, basic dimensions;*

3.4. Experiment 3 – study on a separate frame of single storey, single span CBF

Experiment 3 did not need a separate model. For such was used the frame which consisted of two pieces of columns K1, one horizontal intermediate member (a strut) G1 and a beam G2. The experimental set-up is similar to the set-up of Experiment 2 but with diagonals removed from the models.

3.5. Loading procedure

Loading is realized by controlled displacement at the top of the frame. Displacement is applied statically and the loading cycle is reversal and symmetrical. Cycles in which has been registered growth of plastic deformations were repeated up to 3 times and was checked whether there is a degradation of the bearing capacity (resistance) in applying of one and the same displacement. Cycling loading continues in as described rhythm until the occurrence of fracture in the diagonal due to a low cycle fatigue or to an exhaustion of the tensile strength. The as described protocol of loading is consistent with the recommendations of the ECCS [48] and meets the test for cyclic loading with increasing of the applied displacement.

3.6. Instrumentation and sensors

All experiments were conducted in the Teaching and Research Laboratory of the Department of Steel, Timber and Plastic Structures of UACEG Sofia during 15.10.2011 to 20.11.2011. The experiment was conducted according to the adopted experimental set-up (Figure 3-15) by performing a displacement control and measurement of the applied force.

Loading system (servo-actuator Caproni) had been receiving signals for the applied displacements through the software system for management and control. Data on the level of applied force were received from sensor 0 (force sensor) - Figure 3-51. All the data in the experiments were recorded digitally. During the experiments were located 13 pcs of inductive sensors. Layout of inductive sensors used for experiments 2-1 is shown in Figure 3-51.

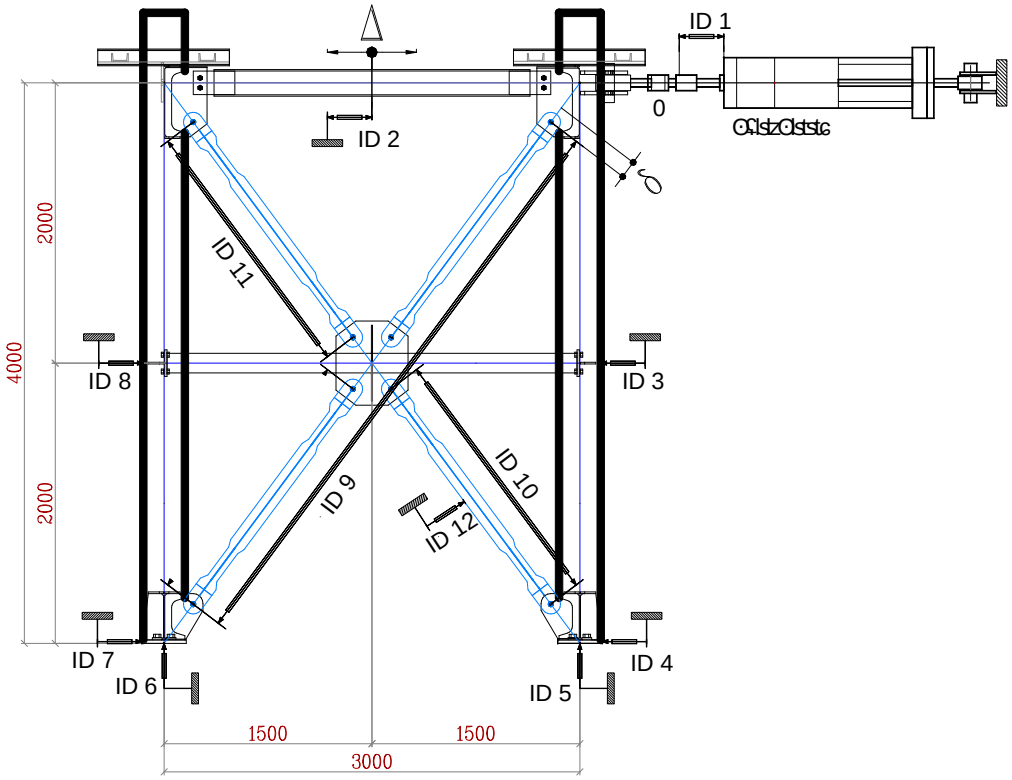

***Fig. 3-51** - layout of inductive sensors on model H1*

For obtaining information about the stressed state in the pressed and tensioned diagonal strain gauges (SG) were located. In various experiments was agreed to be operated from 16 to 20 pcs of SG Hotinger. The location of SG was defined so that they could provide data as long as possible i.e. until the occurrence of plastic deformations in the place of their installation. Layout scheme of SG for experiment 2-1 and their numbers are shown in Figure 3-52.

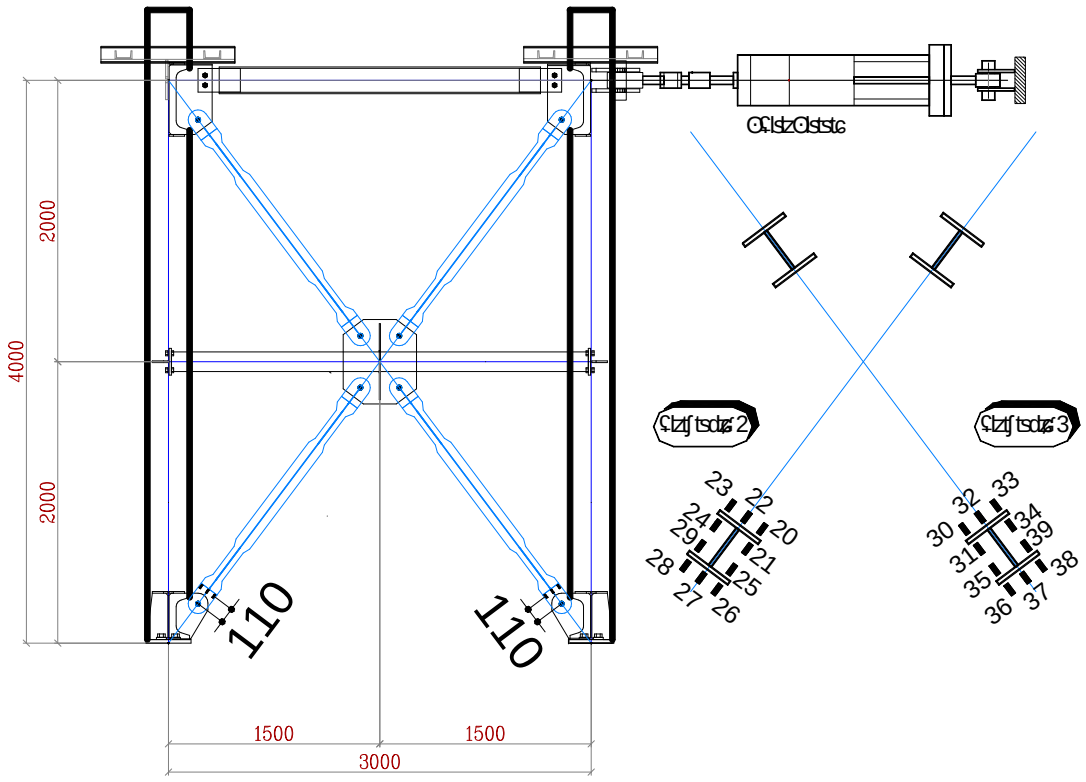

***Fig. 3-52** - layout scheme of ERS on model H1;*

All experiments were conducted in keeping of detailed diary and photo reports. The data for the experiments performed are described in details in Chapter 3 of the PhD thesis and could be successfully used also by other interested researchers.

Chapter 4. Analysis of experimental results

4.1. Experimental series 1

The main objective of the experiments in series 1 was to determine whether the area of reduced cross section (structural fuse) is able to develop inelastic deformations along the entire trimmed area under reversal cyclic loading. The focus of the experiments was to establish whether it is reached the stress concentration and impractical reduction of the plastic phase of behavior of the material due to the change in the shape of the cross section of the member. Due to the limited size of the author's summary and given the similar results between the two experiments here will be given only a brief analysis of experiment 1-2 (Model D2). The reader is kindly invited to get acquainted with the extensive analysis in Chapter 4 of the PhD Thesis.

4.2. Analysis of the results of experiment 1-2

Further on in the analysis of Figure 4-3 are shown the locations and numbers of used inductive sensors and similar characteristic relationships between the force measured and the displacement measured are presented on the following figures. During the installation of inductive sensors 3 and 4 had been used such an approach so that ID3 was aimed to cover the Reduced Cross Section as well as the transitional area (zone) while sensor ID4 covered only the RCS. Thus by the difference in readings between the two sensors can be judged the impact of the transitional zone to the development of inelastic deformations.

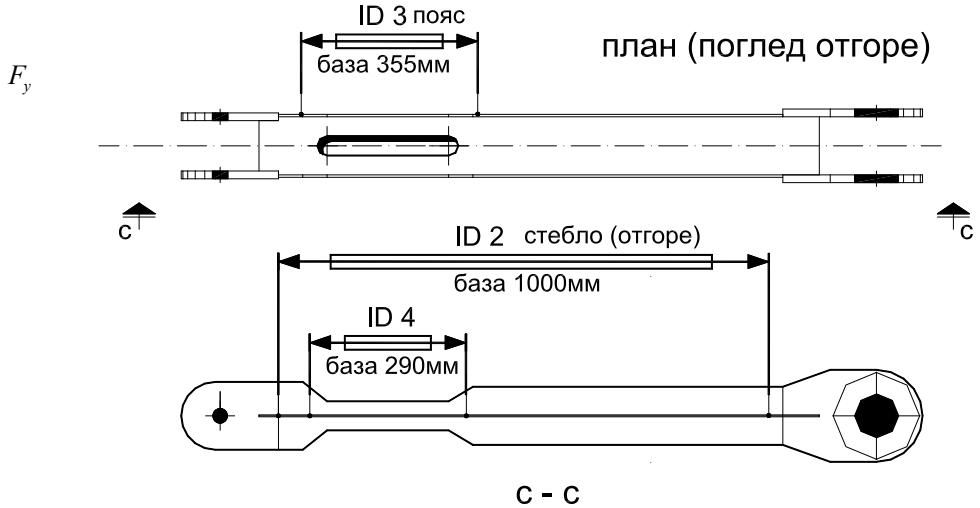

***Fig. 4-3** – location of the inductive sensors (ID2, ID3 & ID4) in experiment 1-2, model D2;*

Through the data obtained from ID2 again will be monitored the overall elongation of model D2 within the working length and ID3 and ID4 will monitor what part of the axial displacements occur in the RCS and the transitional zone and what part occur only in the structural fuse. Figures 4-4 show graphs of the measured force in the force sensor as a function of the maximum measured displacement in the corresponding sensor in each cycle of loading. By the analysis of Figure 4-4 could be drawn the following conclusions: In the elastic phase deformations develop both in the RCS and in the non-trimmed cross section. Transitional zone also contributes to final elongations. After the occurrence of

plasticization of material inelastic deformations focus only on the RCS but we have reasons to believe that partial plasticization covers also the transitional zone. The contribution of elastic deformations to the overall elongation of the member is about 8,1%. It could be said that inelastic deformations in the flange and the web of the RCS are identical. The contribution of the transitional zone to the plastic strains is estimated within 7.5% to 8.0%.

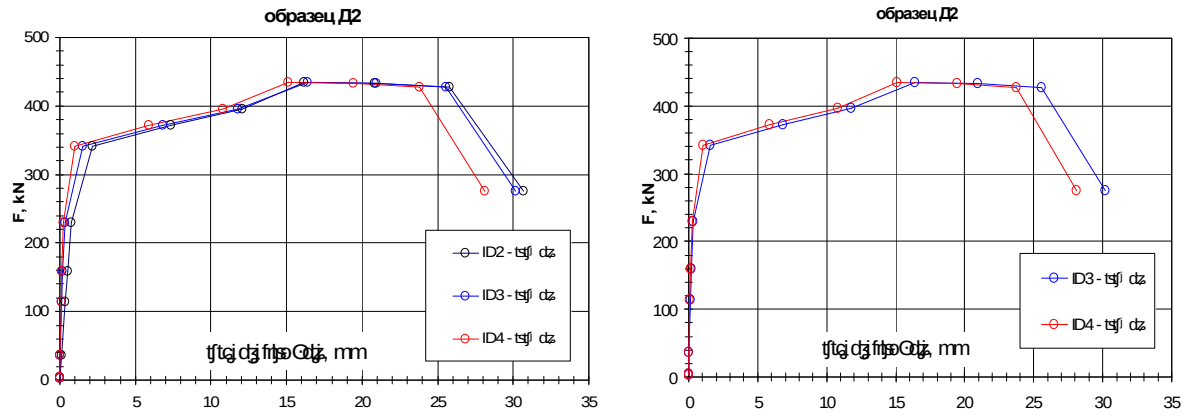

Fig. 4-4 *- graphs of measured force F as a function of the measured maximal axial displacements in sensors (ID2, ID3 & ID4 – at left and ID3 & ID4 at right) in experiment 1-2, model D2;*

This conclusion has been reached by comparing the reports of reading of ID3 & ID4 shown in Figure 4-4. The maximal relative deformations that occurred within the structural fuse are $\varepsilon_{pl,OC} = 0,087 - 0,096$.

For the study of the stressed state in the RCS of model D2 were installed 12 pcs of SG and whose numerical designation and location is shown in Figure 4-9. The next figures reveal the stresses in 3 typical sections (beginning, mid-part and end of the RCS and in 4 typical profiles (flange in respect to section c-c by the use of sensors 10, 11 and 12, flange in respect to section d-d by the use of sensors 13, 14 and 15, web 1 by the use of sensors 16, 17 and 18 and web 2 by the use of sensors 20, 21 and 22). Model D2 was retrofitted by placing additional SG 23 which will help us to trace the picture of normal stresses in the web. Figure 4-11 shows a change in the normal stresses in points of cross sections 1, 2 and 3 in flanges and in the web. It is worth noting the greater difference in data from sensor readings in comparison of the data from the readings for model D1. A similar pattern was observed also in cycles 3, 4, 5, 6, 7 and 8. After cycle 8 some of the sensors stop functioning properly due to the occurred inelastic deformations. The difference thus registered in reports the author explains with the reported in item 3.7.2. of Chapter 3 (of the PhD Thesis) phenomena of lack of centricity in the assembly of the model and the generated from this lack of eccentricity bending of the member. This argument can be confirmed if Figure 4-11 is considered. There could be clearly noted the report's reversibility of cross sections 1 and 3 for the sensors in the web. Since model D2 was retrofitted with an additional sensor ¯ 23 (just below sensor 21) that allow to be a made an excerpt of the development of normal stresses in the middle of the web for cycles 3, 4,

5 and 8 - Figure 4-12. The results' analysis in Figure 4-12 shows that the maximal normal stress in cycles 3, 4, 5 and 8 in the middle of the web are virtually identical. Again we may clarify that registered misalignment causes bend

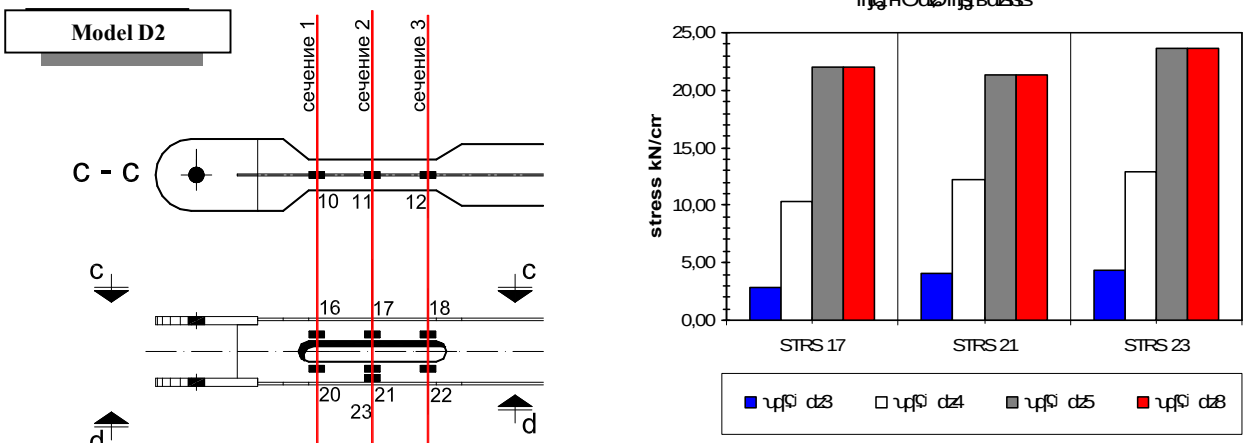

Fig. 4-12 *- graphs of normal stresses in the middle part of the web in cycles of loading 3, 4, 5 and 8, model D2;*

Fig. 4-9 *– experiment 1-2, model D2; location and numerical designation of SG*

mostly at the beginning and at the end of the RCS i.e. in sections 1 and 3. That is where could be observed larger differences in readings of the inductive sensors.

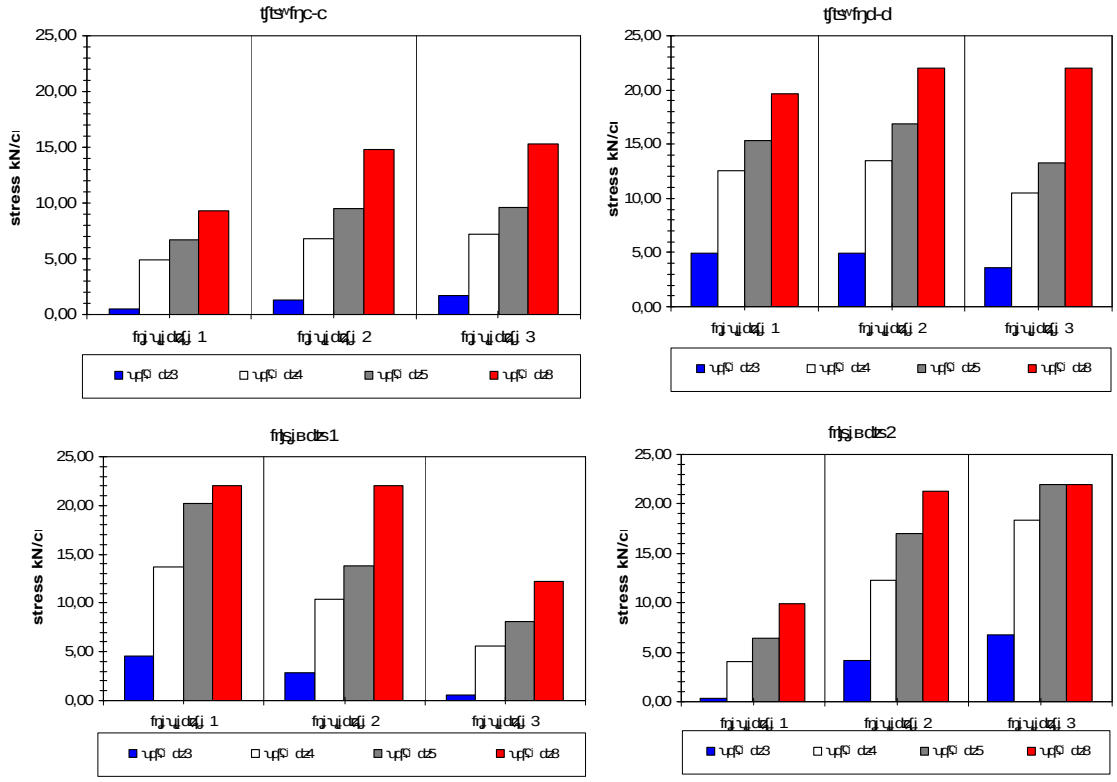

Fig. 4-12 *- graphs of normal stresses by profiles in cycles of loading 3, 4, 5 and 8, model D2;*

Despite the occurrence of atypical bending in the diagonal of CBF the author believes that it has an effect on the stressed state of the RCS only in the elastic phase of deformation of the member. In actual inelastic phase the accompanying bending virtually plays no effect.

Final stage of the comprehensive analysis of the results of experimental series 1 was to be compared the theoretical tearing force and the experimental maximal force registered during the corresponding experiment. Subject of analysis is also the type of the form of fracture of the experimental model. The theoretical maximal force that can be borne by the member is defined under the equation: $F_u = A_{w,OC}.f_{u,w} + A_{f,OC}.f_{u,f}$

For model D1 it is respectively $F_u^{D1} = (320.451,5 + 600.570,5).\frac{1}{1000} = 486,78kN$, and for model D2 the force is $F_u^{D2} = (320.324 + 800.351,7).\frac{1}{1000} = 385,04kN$. Recorded maximal values of axial forces in models D1 and D2 and comparison between theoretical and experimental value are given in Table 4-3.

Table 4-3

Experimental model	Theoretical value kN	Experimental value kN	Difference %
D1	486,78	461,86	5,4%
D2	385,04	434,5	12,8%

Figure 4-14 shows a typical instant of the inelastic behavior of model D2. Upon occurrence of longitudinal elongation corresponding to strains $\varepsilon_{pl,OC} \approx 0,05$ visually could be observed transverse shrinkage of the RCS due to the effect of Poisson.

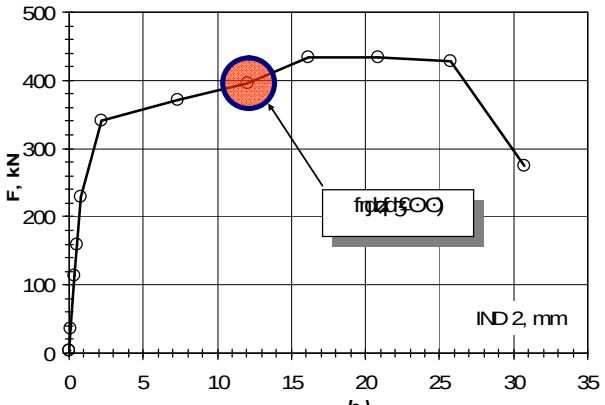

a) b)

Fig. 4-14 *- visible traces of the effect of Poisson. Shrinkage of the RCS – photo a) on the left and graph "F-δ" – the Figure to the right b); This condition is registered in loading cycle number 18;*

4.2.1. Particular conclusions derived by the analysis of experiments 1-1 and 1-2

By the analysis made of performed experiments 1-1 and 1-2 could be drawn the following particular conclusions and generalizations:

- Combining two classes of steel for RCS is a mistake and leads to a reduction of the plastic elongation of the member. Main characterizing parameter for the ductile behavior of the steel is the residual elongation.
- It is advisable to manufacture RCS from steel of the same cast. This can be done by working with only one thickness for all steel plates (flange and web) or by producing a casting patch of the RCS (Structural Fuse).
- Inelastic deformations in a member subjected to tension under conditions of cyclic reversals of increasing tension and compression develop mainly in the RCS. Part of inelastic strains could occur in the transitional zone between the RCS and the normal cross section. This part of additional inelastic deformations the author estimated to 8% of the plastic strains in the RCS.
- Plastic strains along the area of Reduced Cross Section which occur in the flanges and the web are practically identical.
- Elastic deformations develop along the entire effective length of the member as their overall contribution to the final displacement in respect to the specific geometry is 10%.
- The stressed state in the RCS is close to the state of uniform distribution of stresses. Notable differences are observed at the beginning and at the end of web slot.
- There have not been observed any significant forms of stress concentrations in the RCS.
- Factors such as non-centrically transmission of forces or initial geometric imperfections or a combination thereof lead to a change in the uniformity of the stresses in the RCS but are of significance only in the elastic phase of the response of the member.
- The observed modes of failure are due to dominant exhaustion of limit deformations of the material in case of tension. A dominant form of low cycle fatigue was not observed although it is present as an accompanying effect in fracture.

4.2.2. Analytical bi-linear model of a diagonal having RCS

The performed experimental series 1 allows by an analysis of the obtained results and findings from 4.2.1 to be compiled an analytical model for the inelastic behavior. The model covers a diagonal with designed RCS subjected to tension and considering the presumption of an alternating cyclic loading. Such a model can serve as a basis for modeling the inelastic behavior of the diagonal when designing a sophisticated FE non-linear model of CBF by using plastic hinges. For that purpose in handling of the proposed by the author model is necessary to be determined the following basic parameters. They are defined in Figure 4-16.

δ_y *- maximal elastic elongation of the diagonal*

This is the elongation of the diagonal beyond which begins the occurrence of yielding. It can be defined by the expression

$$\delta_y = L.\varepsilon_y = L.0,002 \qquad (4.1\text{-}1)$$

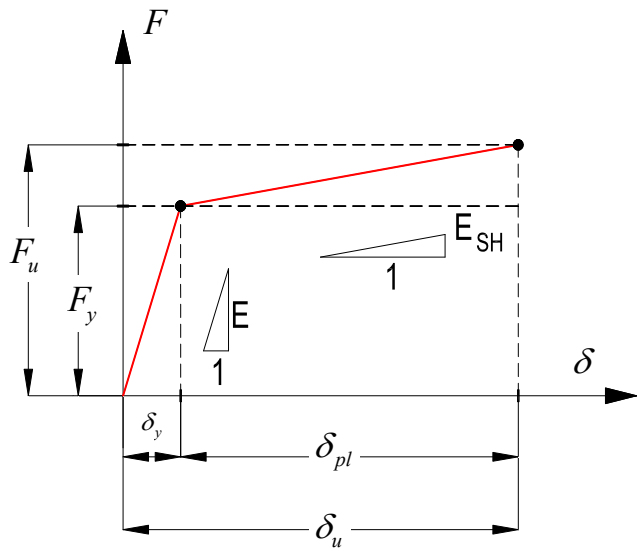

We make the assumption that the maximum elastic deformations are 0.2% and multiply them by the working length of the diagonal L. Working length of the diagonal is the axial length of the member excluding the length of the joints. For these experimental models working length coincides with the base of inductive sensor ID2 and is about 1000 mm. The author

***Fig. 4-16** - basic parameters characterizing the non-linear behavior of tensioned diagonal having RCS (structural fuses);*

believes that in defining of δ_y, the suggested equation includes also the deformations within the joint because value $\varepsilon_y = 0,002$ is above the average one but the length L is less than the axial length. So at the end the result is realistic. Below we'll define also the remaining basic concepts underlying in the theoretical model.

F_y *- yielding force in bi-linear pattern of behavior*

This is the axial force in the member which when being reached the behavior of the member ceases to be elastic and enters into the phase of inelastic behavior. Plastic strains concentrate in the RCS and the rest of the member has an elastic behavior. The author suggests the force F_y to be determined by the following formula:

$F_y = A_{w,OC}.f_{y,w} + A_{f,OC}.f_{y,f}$ (4.1-2) where:

$f_{y,w}$ - yield strength of the material used for the web of the RCS;

$f_{y,f}$ - yield strength of the material used for the flanges of the RCS;

$A_{w,OC}$ - cross sectional area of the web at the place of the structural fuse; $A_{f,OC}$ - cross sectional area of the flanges at the place of the structural fuse;

Logically the area of the SF (Reduced Cross Section) is $A_{OC} = A_{w,OC} + A_{f,OC}$.

Thus the coordinates of the transitional point are uniquely identified. Under a transitional point we will understand the point of intersection of the two lines defining the bilinear inelastic model of behavior. The elastic stiffness E of the member is defined by the expression: $E = \frac{F_y}{\delta_y}$ (4.1-3), and the stiffness in strain hardening range is defined as part of the elastic stiffness. The author proposes the equation:

$$E_{SH} = \frac{E}{30} \qquad (4.1\text{-}4),$$

In order to be determined distinctly the bilinear pattern of behavior should be calculated parameter δ_{pl} .

δ_{pl} - this is the elongation of the member which occurs in the inelastic phase of behavior. This elongation is formed by the plastic strains of the structural fuse within its length L_{OC} and to it should be added the elastic elongations of that part of the diagonal which is outside the structural fuse. The author suggests the following equation for the definition of δ_{pl} .

$$\delta_{pl} = k_1.(L_{OC}.\varepsilon_{pl,OC}) + (L - L_{OC})\frac{\gamma_{SH}.F_y}{A.E} \qquad (4.1\text{-}5) \text{ where:}$$

The first part of the equation (4.1-5) is the inelastic elongation of the RCS and the second part of the equation is the addition of the elastic elongations of the non-plasticized parts of the member. Newly introduced parameters are:

k_1 - coefficient which takes into account that in the transitional zones of the RCS there is a presence of partial plasticization of the section. By analyzing the results of the located inductive sensors has been reached the following proposal $k_1 = 1.08$. L_{OC} - Length of the structural fuse (this is the part of the member that is designed as RCS). In this case for models D1 and D2 L_{OC}=250dd3 γ_{SH} - coefficient of strain-hardening. This coefficient takes into account the phenomenon that in the inelastic phase the force in the member increases in respect to the initial value of Fy. The author offers a summarized and averaged value $\gamma_{SH} = 1.3$. A - an area of the cross section of the diagonal outside the structural fuse. E - Modulus of elastic deformations. In the present case has been assumed $E = 210000\frac{N}{mm^2}$. $\varepsilon_{pl,OC}$ - maximal possible plastic deformations in the structural fuse. This parameter is the most important for credible and reliable determination of the inelastic behavior of the member. On the other hand it should be able to be determined by the initial outputs of the physical and mechanical properties of the material from which has been produced the structural fuse. The author proposes to start from the minimal standard elongation of the steels used in the RCS by offering the equation:

$$\varepsilon_{pl,OC} = 0,25.\bar{A}_{[\%]} \qquad (4.1\text{-}6) \text{ where:}$$

$\bar{A}_{[\%]}$ - final elongation of a standard specimen subjected to uniaxial tension. This value is taken from the certificate of the steel or by a laboratory test protocol. Here is the place where we should give some clarifications on the origin of equation (4.1-6). According to the standard tensile tests performed the author observed a relationship that the maximal tensile stress f_u (tensile strength) occurs in deformations equal to $\varepsilon_u \approx (0,5-0,6).\bar{A}_{[\%]}$. On the other hand within the RCS there is a bi-axial stress state due to the implemented trimming (narrowing) of the flanges and the slot opening in the web and the member is not

able to realize strains reaching ε_u (see also Chapter 2). From the effected measurements of deformations and by introducing a certain computational reserve the author has come to the conclusion that $\varepsilon_{pl,OC} \approx 0,5.\varepsilon_u$. Thus has been reached the conservative but simple enough equation (4.1-6).

To compare the results of the proposed theoretical model with experimentally obtained characteristic relationships "applied force - axial displacement" in respect to experimental models D1 and D2 were made the necessary calculations according to equation (4.1-5). For working length of the member L we shall accept the location base of inductive sensor ID2. In this way we will be able to make accurate comparison between theoretical results and the experimental result. Graphical interpretation of that comparison is shown in Figures 4-18 and 4-19.

Gained theoretical and experimental results for model D2 are compared in Table 4-8.

Table 4-8

Model D2	$F_y\ [kN]$	$F_u\ [kN]$	$\delta_u\ [мм]$	$\frac{F_u}{F_y}$	$\mu_0 = \frac{\delta_u}{\delta_y}$
Theoretical model	302,7	397,8	20,86	1,314	10,43
Experiment 1-2	341,3	433,6	20,845	1,27	9,56
Difference %	12,8%	8,99%	0,07%	3,4%	9,1%

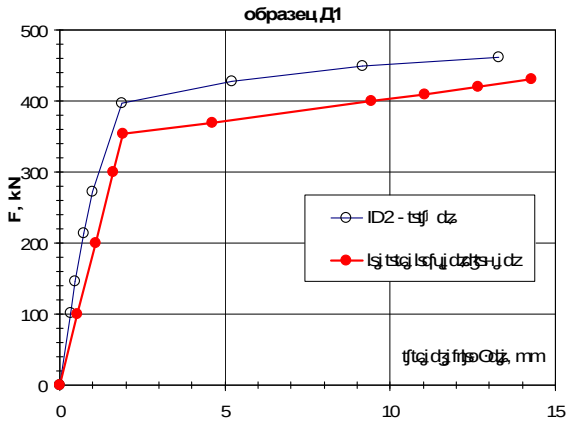

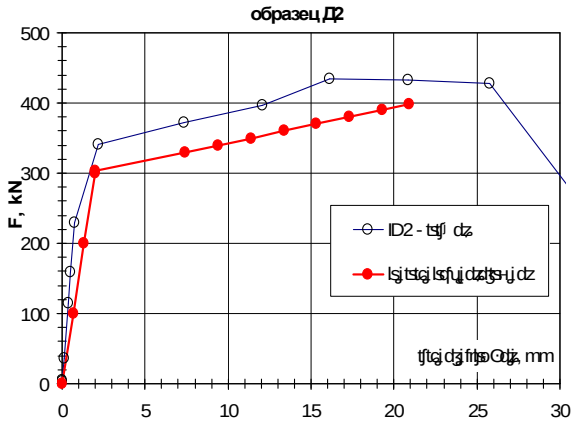

***Fig. 4-18 (at left)** - model D1, comparison of the characteristic curve "F-δ" of the analytical model and experiment 1-1;* ***Fig. 4-19 (at right)** - model D2, comparison of the characteristic curve "F-δ" of the analytical model and experiment 1-2;*

By the as derived analytical bi-linear model and comparisons made with experimental results we make the following conclusions and generalizations.

- The analytical model gives good results as registered differences are up to 13%.
- The main difference is the determination of the theoretical force F_y. The author believes that the reason for the difference as registered is the fact that the structural fuse is composed of steel plates of different thicknesses and different physical and mechanical properties. In the use of steel plates with different thicknesses there is always a chance the steel from the one type of steel plate to be of higher strength or

the yield of the material to occur at different strains. Therefore emerge effects of hardening of one of the materials and finally real force F_y is greater than the theoretically determined. One possibility of solving this problem is to introduce a correction factor for the theoretically obtained force F_y . According to the author other much realistic opportunity for matching the analytical and experimental result is the use of only one type of steel in the process of preparing of the RCS (structural fuse). This can be done by using steel plates of the same thickness for the flanges and for the web as these steel plates must be a part of one production casting batch. An important addition to the correct prediction of the actual behavior is the implementation of procedure of testing of the material used for preparing the structural fuse after its delivery in the production premises of the factory. As an alternative idea of solving the problem related to the different characteristics of the steels used for the flanges and the web of the structural fuse, the author sees in the possibility of implementing pre manufactured steel castings. This idea could be further improved if the steel used for making these castings is of guaranteed yield strength and improved plastic properties.

- The analytical model could be used in the evaluation of the inelastic behavior of the diagonals of models H1, H2 and H3. Through the analytical bi-linear model can be determined the extent of development of plastic strains in the diagonals of the CBF and to be determined whether deformations develop in all RCS.

4.3. Methods for the analysis of experimental results of experimental series 2

4.3.1. Methodology in accordance with ECCS

To analyze the obtained results of experimental series 2 and to derive the necessary conclusions, characterizing the inelastic behavior of the studied models under the effects of cyclic alternating static loading has been used the methodology of ECCS (Study on Design of Steel Buildings in Earthquake Zones) defined in [48]. Experimental studies of series 2 were performed by using a methodology of loading recommended in [48]. The key parameters that characterize each cycle designated by a conditional number Äi òare shown in Figure 4-22 and are explained in the exposition that follows:

$v_i^+ \; and \; v_i^-$ are the maximal displacements in cycle of number i for the appropriately accepted directions "+" and "-"; $F_i^+ \; and \; F_i^-$ are values of the measured force in reaching of maximal displacements $v_i^+ \; and \; v_i^-$; $\Delta v_i^+ \; and \; \Delta v_i^-$ are maximal occurring displacements in case of a positive value of the measured force and respectively the maximal occurring displacements in case of a negative value of the measured force. Tangential module of the system is a parameter that represents the tangential stiffness[1] measured in change of the sign (direction) of the force F from positive to negative and vice versa. For each cycle of number i shall be defined angles $\alpha_i^+ \; and \; \alpha_i^-$ and from them shall be determined $tg(\alpha_i^+) \; and \; tg(\alpha_i^-)$ which are tangential modules for the respective cycle.

[1] This term has been assumed by the statement in [48]. Could be used also the term cyclic stiffness.

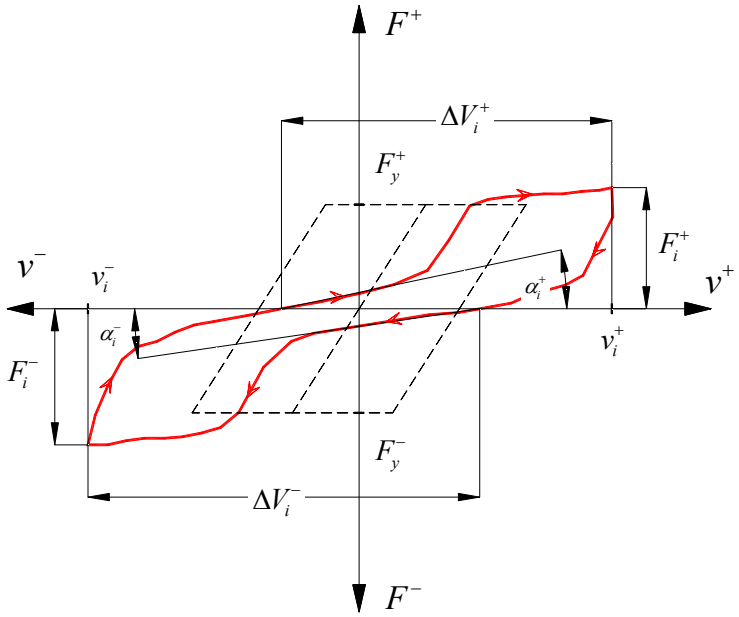

***Fig. 4-22** - defining the key parameters that characterize cyclic inelastic behavior according to [48]*

For each cycle of number i shall be defined the areas $A_i^+ \; and \; A_i^-$ matching that half-cycle. An explanation is shown in Figure 4-23.

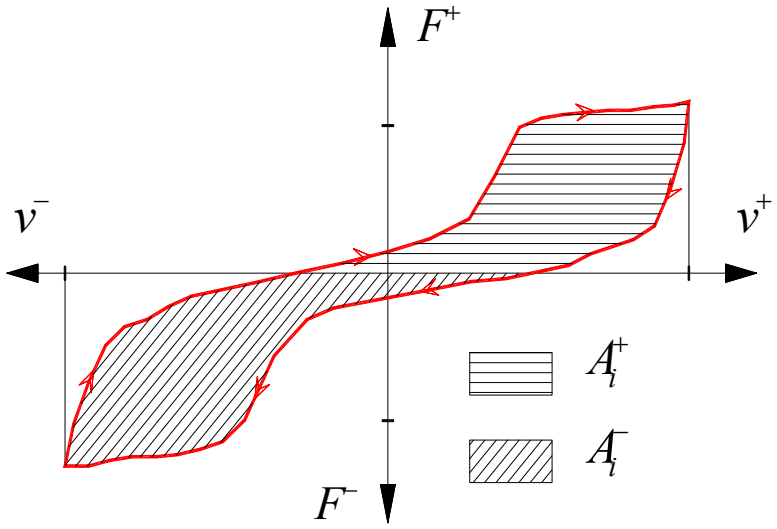

***Fig. 4-23** - defining of areas A_i^+ and A_i^- of the positive and negative half-cycle according to [48]*

So far were defined parameters that could be directly derived from the characterizing inelastic behavior graph "$F_i - v_i$" for every cycle "i". After a certain processing of these

parameters have been obtained a series of coefficients giving a numerical interpretation of the inelastic behavior of each cycle. When these coefficients are presented as a function of the displacements we obtain functions of the cyclic non-linear behavior. The key coefficients to be used for the purposes of the analysis are the following:

Partial ductility μ_0 $\mu_{0i}^{+} = \frac{v_i^{+}}{v_Y^{+}}$ and $\mu_{0i}^{-} = \frac{v_i^{-}}{v_Y^{-}}$

Full ductility μ $\mu_i^{+} = \frac{\Delta v_i^{+}}{v_Y^{+}}$ and $\mu_i^{-} = \frac{\Delta v_i^{-}}{v_Y^{-}}$

Full ductility ratios Ψ $\Psi_i^{+} = \frac{\Delta v_i^{+}}{v_i^{+} + (v_i^{-} - v_Y^{-})}$ and $\Psi_i^{-} = \frac{\Delta v_i^{-}}{v_i^{-} + (v_i^{+} - v_Y^{+})}$

Resistance ratios ε $\varepsilon_i^{+} = \frac{F_i^{+}}{F_Y^{+}}$ and $\varepsilon_i^{-} = \frac{F_i^{-}}{F_Y^{-}}$

Rigidity ratios ξ $\xi_i^{+} = \frac{tg(\alpha_i^{+})}{tg(\alpha_Y^{+})}$ and $\xi_i^{-} = \frac{tg(\alpha_i^{-})}{tg(\alpha_Y^{-})}$

Absorbed energy ratios η $\eta_i^{+} = \frac{A_i^{+}}{(v_i^{+} + v_i^{-} - v_Y^{+} - v_Y^{-}).F_Y^{+}}$ and

$\eta_i^{-} = \frac{A_i^{-}}{(v_i^{+} + v_i^{-} - v_Y^{+} - v_Y^{-}).F_Y^{-}}$ this coefficient is the ratio between the energy absorbed by the structure in the actual cycle compared to the energy that would be absorbed in ideal inelastic cycle with the same maximal displacement. Figure 4-24 shows graphical interpretation of the physical meaning of the ratio. The lower the ratio the more significant are the effects of cyclical degradation in stiffness and pinching of the hysteresis loop.

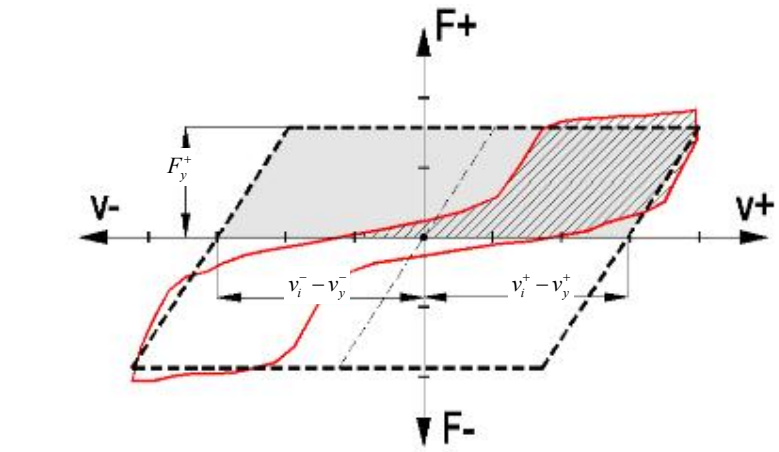

$= F_y^{+}.(v_i^{-} - v_y^{-} + v_i^{+} - v_y^{+})$

$= A_i^{+}$ $\eta_i^{+} = \frac{A_i^{+}}{(v_i^{+} + v_i^{-} - v_Y^{+} - v_Y^{-}).F_Y^{+}}$

Fig. 4-24 *- physical meaning of the absorbed energy ratio*

Yielding force F_Y has been determined for each individual experiment by looking for the maximal match between the envelope curve of all cycles "$F_{\max} - v_{\max}$" and the bilinear approximation.

4.4. Methodology for the analysis of experimental results

In analyzing the results of all experiments in series 2 has been used the following methodology:

The entire experimental record of the relationship "$F - v$" has been "cleared" by the contribution of the interference of the stand movements and then already "cleared" is divided into cycles. For each cycle are derived the respective coefficients characterizing the inelastic behavior. The resulting coefficients are presented as a function of ductility by which is defined also the relevant features of the cyclic non-linear behavior. The methodology was repeated 3 times as much is the total number of experiments in series 2.

4.5. Analysis of experimental results of experiment 3 – influence of the frame

The purpose of experiment 3 was to analyze the contribution of the frame in the overall stiffness of the structure and what is the amount of dissipation of energy by the frame response. It must be reminded that the experimental stand was designed for repeated use. Therefore the frame had to be of somewhat larger cross sections then actually needed for the experimental models. Furthermore it should be clarified that the designed joints between the members of the frame and between the frame and the experimental stand cannot be classified as pin ones. They belong to the category of semi-rigid joints.

The frame was loaded twice by applying displacement of 144 mm and by applying displacement of 96 mm. Diagrams of the records of loading and the resulting hysteresis loops are shown in Figure 4-75. In order to analyze the degree of participation of the frame in the dissipation of energy in inelastic work of the studied models was used the following methodology. For each cycle of applied displacement were derived the maximal averages of displacements $= (v^+ + v^-)/2$ and the average of the dissipated energy by cycles $= (A_i^+ + A_i^-)/2$.

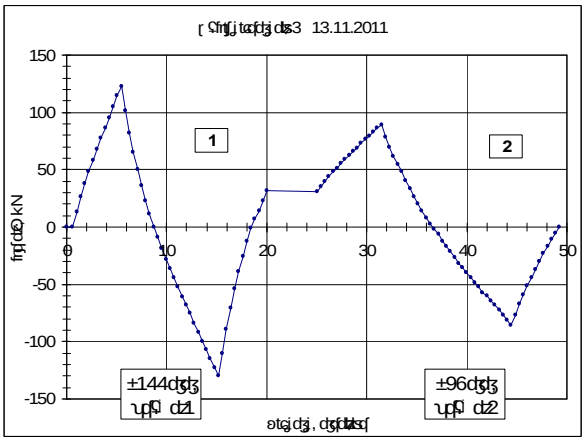

a)

Fig. 4-75 *- a) load record conducted in Experiment 3 as time function;*
b) hysteresis loop in case of applied displacement ± 144 mm in cycle 1;
c) hysteresis loop in case of applied displacement ± 96 mm in cycle 2;

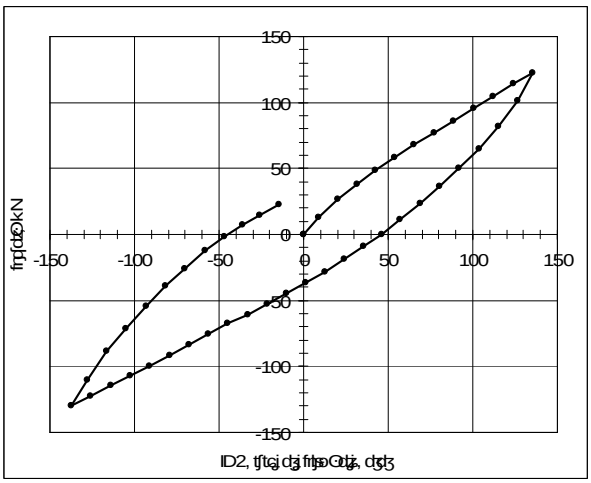

b)

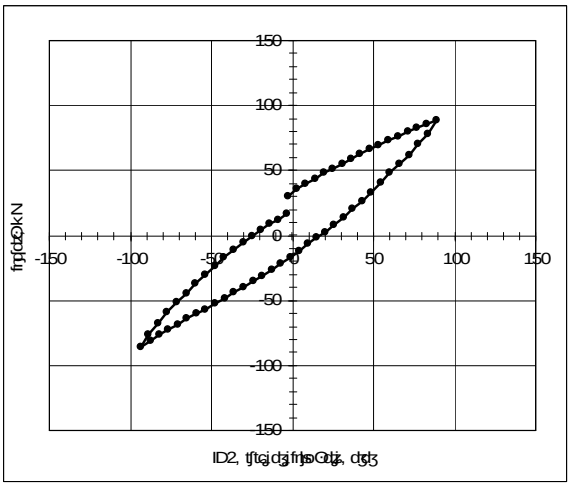

c)

When in the loading record there has three cycles in a group shall be derived the arithmetic averages of the dissipated energy. The dissipated energy itself is defined as an area of closed internal area for each half-cycle. The results are summarized in Figure 4-80 as a function of displacements and Figure 4-81 as a function of ductility. The curve (in dark brown color) in Figure 4-80 corresponds to the contribution of the frame. It is displayed with a *„trend line"* based on the available values from cycle 1 and 2 in Experiment 3. Since this curve is not based on a sufficient number of measurements its accuracy can be controversial. This is a question that cannot be fully clarified in this study due to the limited number of cycles which were held in experiment 3. However the result shown in Figure 4-80 and Figure 4-81 identifies the major pattern of the phenomenon. The contribution of the frame to the overall dissipated energy is shown in the best way in Figure 4-81. Therein on the ordinate are presented values in % reflecting the relationship $\frac{A_{frame}}{A}$ as a function of the ductility of the structure. The three curves in Figure 4-81 correspond to models H1, H2 and H3. You could say that these curves apply to CBF with slenderness of the diagonals respectively 80, 120 and 180.

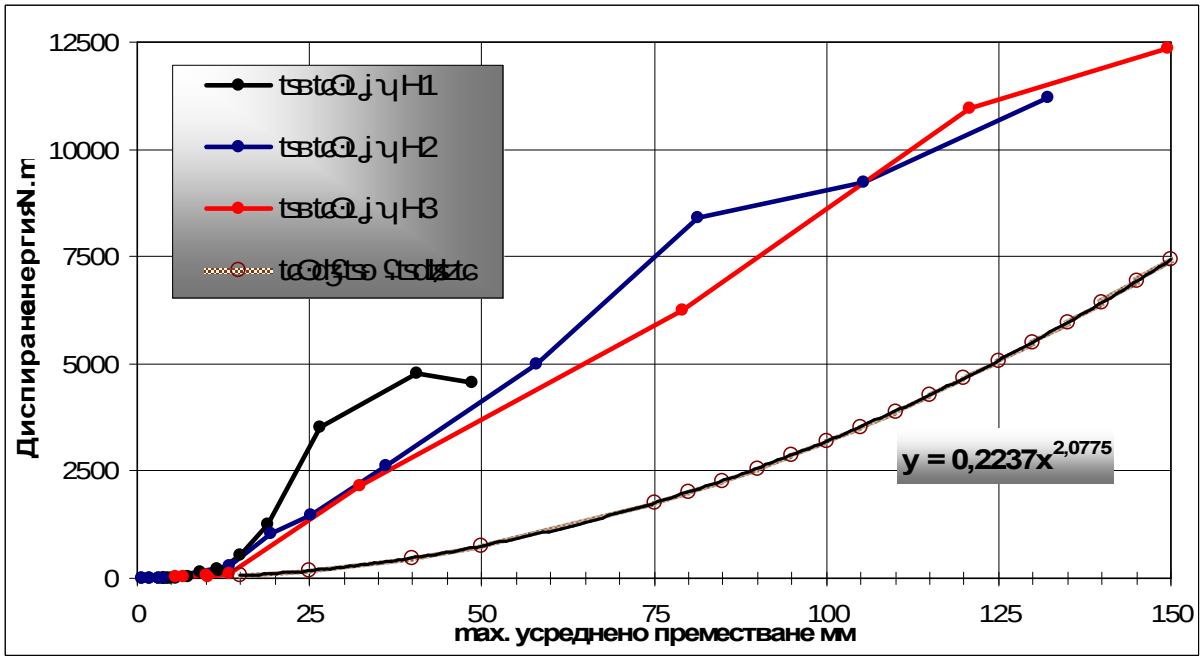

Fig. 4-80 *- a family of curves by models and one related to the frame. Each curve presents the value of dissipated energy in a half-cycle as a function of the maximal displacement for the respective cycle*

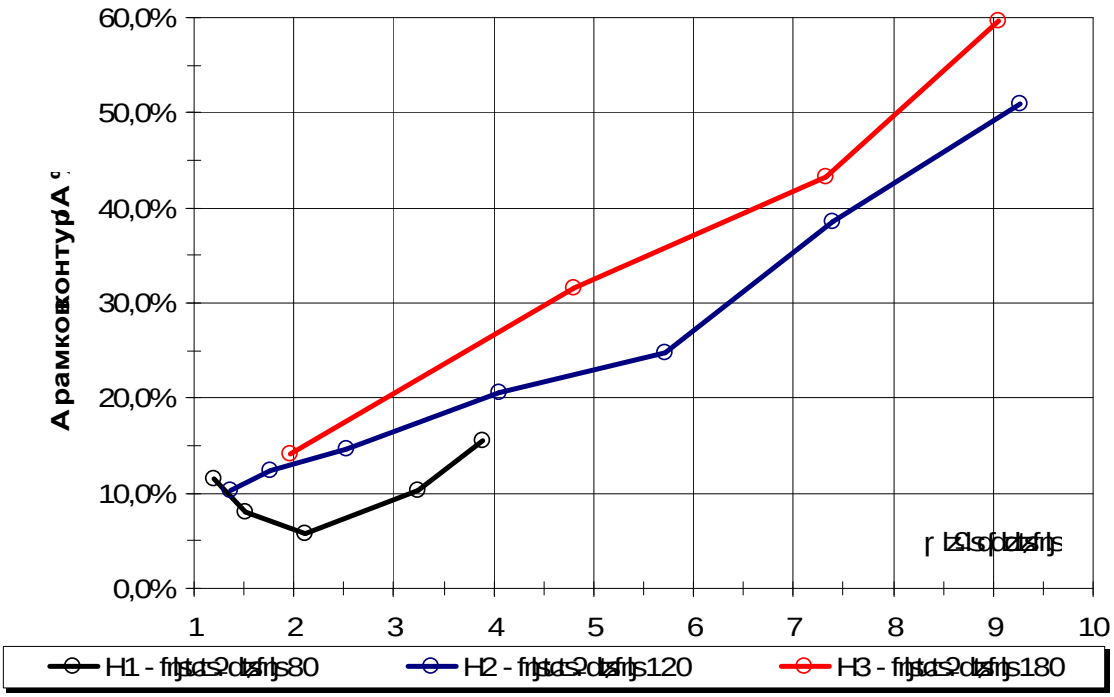

Fig. 4-81 *- contribution (in %) of the frame to the total energy dissipation as a function of the ductility of the CBF;*

particular conclusions derived by the analysis of experiment 3

From the presented analysis of the influence of the frame (the contour made of columns and beam) could be drawn the following conclusions:

- Frames in real structures virtually never have joints corresponding to ideal truss model;
- The contour frames can make a positive contribution to dissipativity of the CBF as their most important role is their contribution in the zone of zero displacements. Namely in this area of the hysteresis curve diagonals are the most inefficient and in the frame may appear the needed "supplier" of cyclic stiffness and dissipativity;
- The contribution and the role of the frame is enhanced with the increase in slenderness of the diagonals;
- The contribution of the frame is enhanced when using CBF having higher ductility ($\mu_0 \geq 4,0$);
- The contribution of the frame in the total dissipated energy in regards of the studied models for ductility ($\mu_0 < 4,0$) is as follows (Table 4-17):

Table 4-17

Model	**Effective slenderness**	**% of participation of the frame**
Designation	$\lambda_{y,eff} = \frac{L_D.\mu}{i_y}$	$\frac{A_{рамков\ контур}}{A}$
H1	**80.1**	**up to 17%**
H2	**122.0**	**up to 20%**
H3	**181.2**	**up to 27%**

- In the range of high ductility and high slenderness of diagonals the contribution of the Contour frame may reach up to 50% or even 60%.
- The Contour frame should be designed so as to enable frame's joints to allow rotations caused by large displacements to which is subjected the CBF without causing brittle forms of fracture;
- Designing of the frame and the slenderness of the diagonal must be bound. In case of more slender diagonals there must have more stringent requirements to the frame;

4.6. Defining the behavior factor q for experimental models H1, H2 and H3

The main part of the analysis of inelastic behavior of experimental models H1, H2 and H3 is the definition of the behavior factor q[♣] for each of the studied models.

In order to be determined q we will proceed from its basic definition that it depends on two key features of structural behavior - ductility and overstrength i.e. $q = q_\Omega.q_\mu$. Interpretation of this statement was made in Chapter 1, item 1.1.4, Figure 1-13 of the PhD thesis. Similar

[♣] An understanding of the concept set out in BDS EN 1998-1.

way of interpretation of the behavior factor can be found in [38, 54, 77] and Figure 4-82 shows a graphical illustration.

To determine the behavior factor will be used capacitive force-displacement diagrams obtained for each of the experimental models. Since for each model we have experimentally obtained capacitive diagram of its displacement towards "+" and "-" then for each of the experimental models we shall determine $q^+ u\ q^-$.

The final value of q will be the arithmetical average of the two i.e. $q = \frac{q^+ + q^-}{2}$.

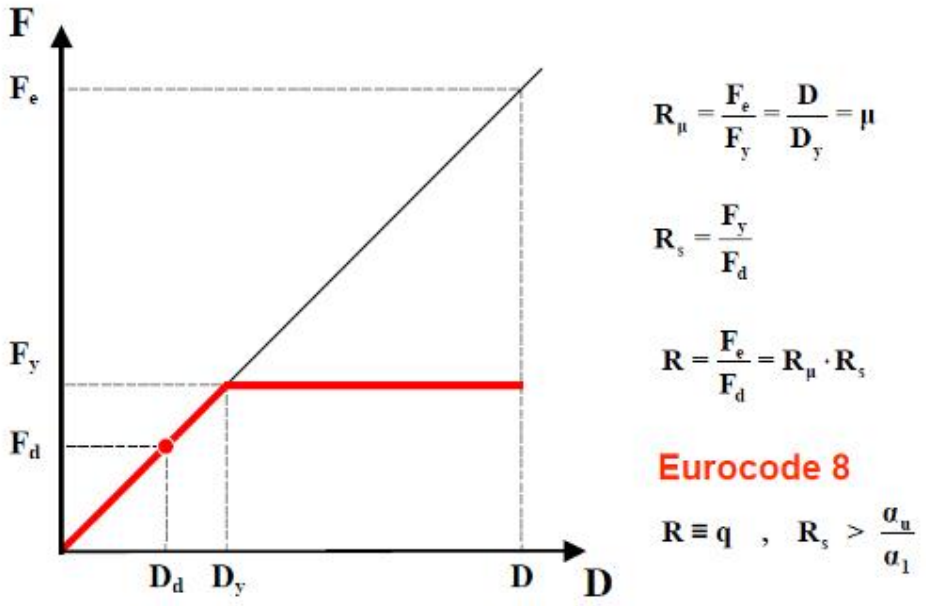

***Fig. 4-82** - interpretation of the behavior factor q made by Professor Peter Fajfar, literary source [54];*

The contribution of the overstrength will be determined by the equation $q_\Omega = \frac{F_y}{F_{y,Ed}}$. The contribution of ductility shall be determined by the well-known equation of *Newmark & Hall* [83] $q_\mu = \sqrt{2\mu - 1}$, which refers to low periodic structures. Ductility ratio μ is determined by the equation $\mu = \frac{\Delta_u}{\Delta_y}$ where Δ_u and Δ_y are defined on the basis of experimental results - see point 4.3, 4.4 and 4.5. in the PhD thesis. The author believes that for the studied by him types of structures the equation $q_\mu = \sqrt{2\mu - 1}$ is more appropriate than the rule for the equivalent displacement $q = \mu$, because the actual structures in which could be applied similar CBF belong to the category of low periodic structures. Values of μ^+ and μ^- as well as of F_Y^+ ф F_Y^- are defined for each of the experimental models respectively in items 4.3, 4.4 and 4.5. For final determination of the coefficient of behavior of each of models H1, H2 and H3 shall remain to be determined the respective values of $F_{Y,Ed}$.

Under the force $F_{Y,Ed}$ should be understood that force which is applied at the top end of the CBF. For determining of $F_{Y,Ed}$ are used rules for designing of CBF as defined in Chapter 6 of BDS EN 1998-1 [2]. The computational model of the connection includes only one diagonal and a truss system. In determining the design force $F_{Y,Ed}$ have been used actual yield strength of the flanges' and of the web's steel plates. For the determination of force $F_{Y,Ed}$ was proceeded from the computational model according to which $F_{Y,Ed} = N_{Pl,Rd}.\cos\alpha$ where:

$N_{Pl,Rd}$ - plastic bearing capacity of the tensioned diagonal which is defined by the RCS.

Plastic bearing capacity of the diagonal is defined by proceeding from the RCS and by the use of equation $N_{Pl,Rd} = A_{w,OC}.f_{y,w} + A_{f,OC}.f_{y,f}$. The results of obtained design bearing capacities of the diagonals are summarized in Table 4-19. Under $A_{w,SF}$ is meant the area of the web in the RCS and under $A_{f,SF}$ is meant the area of the flange in the RCS (Structural Fuse, SF). Naturally comes the equation $A_{SF} = A_{w,SF} + 2.A_{f,SF}$.

Table 4-19

Model	Area of the cross sections and theoretical bearing capacity of the sections					
Designation	$A_{w,SF}, mm^2$	$A_{f,SF}\ mm2$	A_{SF}, mm^2	$f_{y,w}, N/mm^2$	$f_{y,f}, N/mm^2$	$N_{Pl,Rd}, kN$
H1	320	400	1120	225.4	288.2	302.688
H2	320	300	920	225.4	288.2	245.048
H3	480	350	1180	225.4	288.2	309.932

Calculation of coefficients of behavior is shown in tabular form and summarized in Tables 4-20, 4-21 and 4-22. A graphical interpretation of the result obtained for the behavior factor for model H3 towards direction "+" is shown in Figure 4-85.

Table 4-20 Reporting the contribution of the overstrength

Model	Direction	$N_{Pl,Rd}, kN$	$\cos\alpha$	$F_{y,Ed}, kN$	F_y, kN	$q_\Omega = \frac{F_y}{F_{y,Ed}}$
H1	Ä+ò	302.688	0.6	181.61	255.2	1.405
H1	Äò	302.688	0.6	181.61	235.6	1.297
H2	Ä+ò	245.048	0.6	147.03	212.0	1.442
H2	Äò	245.048	0.6	147.03	235.0	1.598
H3	Ä+ò	309.932	0.6	185.96	262.6	1.412
H3	Äò	309.932	0.6	185.96	281.5	1.514

Table 4-21 Reporting the contribution of ductility

Model	Direction	Δ_y, mm	Δ_u, mm	$\mu = \frac{\Delta_u}{\Delta_y}$	$q_\mu = \sqrt{2\mu - 1}$
H1	Ăхò	13.0	46.6	3.58	2.482
H1	Ăò	12.0	50.4	4.20	2.720
H2	Ăхò	13.5	103.6	7.67	3.786
H2	Ăò	15.0	134.7	8.98	4.118
H3	Ăхò	17.0	139.7	8.22	3.929
H3	Ăò	19.0	164.9	8.68	4.044

Table 4-22 Determination of the behavior factor

Model	Direction	$q_\Omega = \frac{F_y}{F_{y,Ed}}$	$q_\mu = \sqrt{2\mu - 1}$	$q = q_\Omega . q_\mu$	$q = \frac{q^+ + q^-}{2}$
H1	Ăхò	1.405	2.482	3.487	3.507
H1	Ăò	1.297	2.720	3.527	
H2	Ăхò	1.442	3.786	5.459	6.020
H2	Ăò	1.598	4.118	6.580	
H3	Ăхò	1.412	3.929	5.547	5.835[2]
H3	Ăò	1.514	4.044	6.123	

In order to compare the results obtained for the coefficients of behavior has been conducted a comparison with results obtained using the method proposed by *Giuffre and Giannini* [57]. This comparison was made for the first period of own oscillations of a provisional structure with values respectively equal to 0.5, 0.6 and 0.7 seconds. The choice of these conditional first periods comes from the fact that the application of CBF of the studied types would be done in structures of buildings of low or medium-rise and thus selected first periods are a good approximation of the actual behavior of such structures. Results of the comparison made are summarized and presented graphically in Figure 4-86.

[2] It is appropriate to remind that due to the exhaustion of capabilities of the loading system the experiment was terminated without reaching the actual fracture of the researched model H3. This would mean that the real behavior ratio of model H3 would be of even higher value.

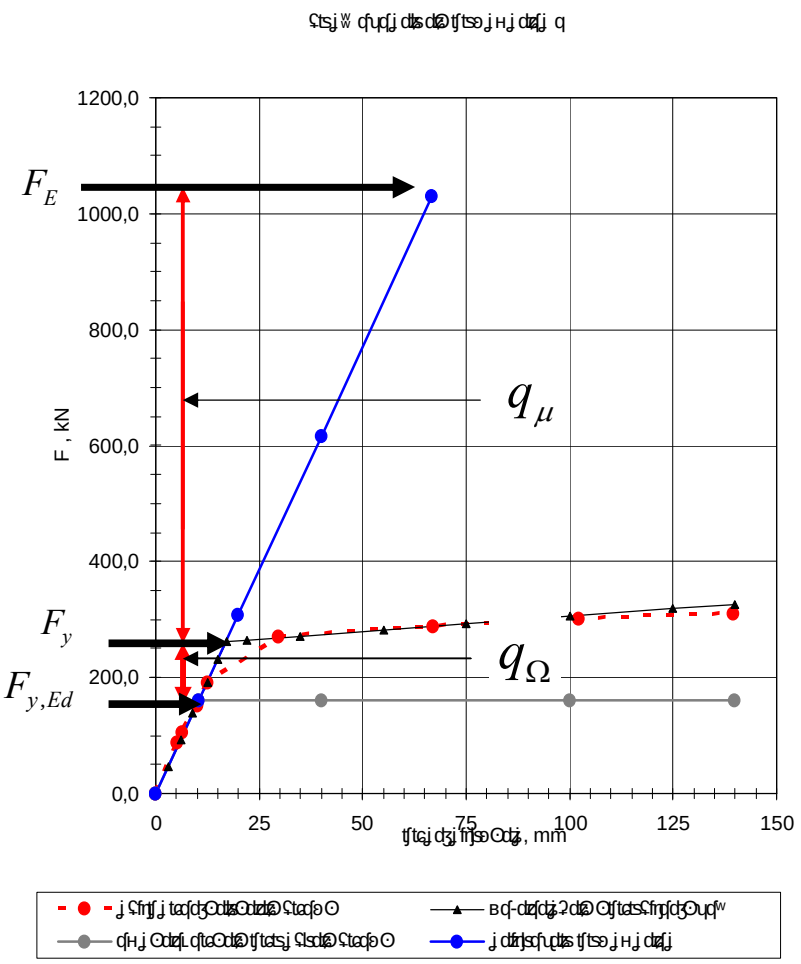

Fig. 4-85 *- graphical interpretation of the results obtained for the behavior factor q related to model H3 towards direction "+"*

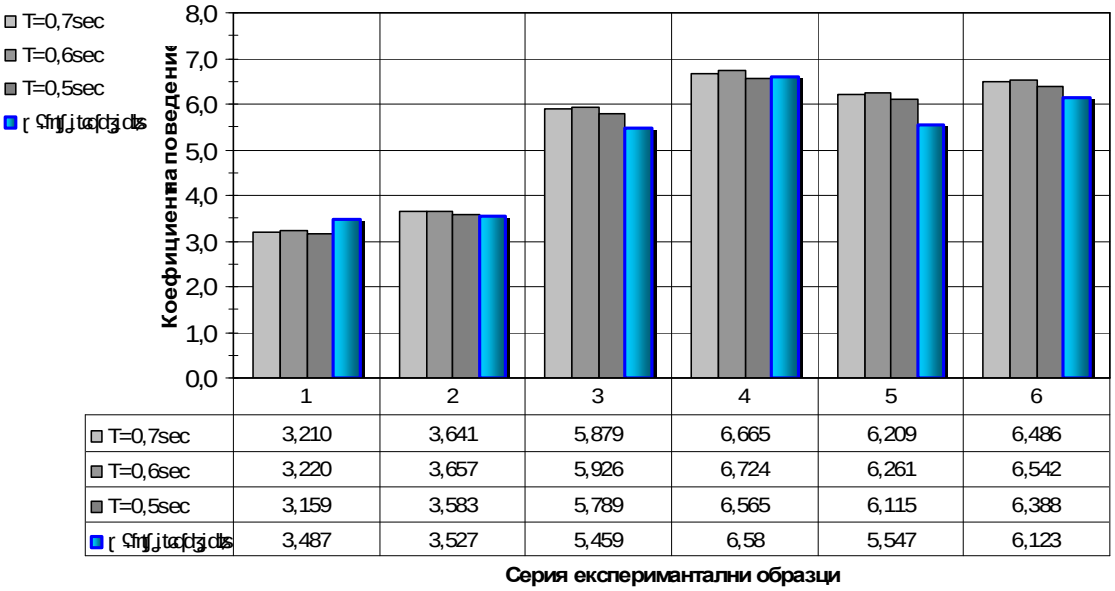

Fig. 4-86 *- Comparison of the results obtained for the behavior factor q experimentally and the results obtained by the method of Giuffre and Giannini [57].*

Legend to Figure 4-86:

Series 1 – model H1, the direction of "+"; *Series 2 – model H2, the direction of "-";*
Series 3 – model H2, the direction of "+"; *Series 4 – model H2, the direction of "-";*
Series 5 – model H3, the direction of "+"; *Series 6 – model H3, the direction of "-";*

As shown in Figure 4-86 the match of results is very good as the maximum difference of 12.8% is obtained in series 5 and the minimal difference of 2.2% is in series 4.

4.7 Particular findings derived by item 4.6.

- By conducted determining of behavior factor q for the three experimental models is obvious that for models H2 and H3 are achieved values higher than the recommended reference value of q for Concentrically Braced Frames set out in BDS EN 1998-1. The obtained values are higher also for the category of moment resisting frames combined with bracings.
- The obtained values for the behavior factor for model H1 are lower than the reference values set out in BDS EN 1998-1. This model has slenderness of diagonals 80 i.e. $\bar{\lambda} = 0.85$ and a cross-section class 1 for RCS and class 3 for the mid-section. According to the author the low slenderness of diagonals, the cross section class 3 and the use of SF in diagonals do not lead to an improvement in the inelastic behavior and just the opposite all these make the response of the CBF worse.
- Models H2 and H3 have slenderness of diagonals respectively 122 and 180 i.e. $\bar{\lambda} = 1.30$, $\bar{\lambda} = 1.92$ which falls within the recommendations of BDS EN 1998-1. The cross section for both models is Class 1. We believe that the use of the concept of RCS in diagonals designed according to Eurocode 8 leads to improvement of inelastic behavior of CBF and help to avoid the over sizing of the contour columns and beams (the contour frame).
- The obtained values of the behavior factor for model H1 can be interpreted through the prism of CBF in which diagonals must bear compression - for example Λ (lambda) or V bracings. This interpretation is not at all unnatural because slenderness of 80 is typical for diagonals of such type of CBF. Therefore if we read the results for model H1 where:

Model	Direction	$q_\Omega = \frac{F_y}{F_{y,Ed}}$	$q_\mu = \sqrt{2\mu - 1}$	$q = q_\Omega . q\mu$	$q = \frac{q^+ + q^-}{2}$
H1	Ä+ò	1.405	2.482	**3.487**	3.507
H1	Äò	1.297	2.720	**3.527**	

and rethink them using reference values for ñÝò CBF namely q=2.5, we shall see that: $q_\mu = 2.482 \approx 2.5$ and $q_\mu = 2.72 \approx 2.5$.

4.8 Analysis of the behavior of the diagonals (bracings) of experimental models H1, H2 and H3

4.8.1 General aspects of the analysis performed

In "X"-shaped CBFs (Concentrically Braced Frames) the diagonals are the main place where inelastic deformations develop (dissipative zones). Moreover since the load is cyclic and reversal diagonals are routinely subjected to tension and compression. In that structural response the diagonals pass from state of tension to compression combined with bending. The compression in the diagonals for a certain amount of axial force is causing the first buckling. In applying large frame displacements (drifts) when a given diagonal is forced to tension it develops inelastic deformation, elongates and thus changes its original length. In its reverse state of compression the diagonal buckles and thus it bends. As the length of the diagonal increases after each cycle leading to plastic elongation then at reverse compression the diagonal buckles earlier (at lower displacements applied, respectively lower forces applied). The greater the length of the bracing member the bigger the bending (curvature increases in the area of the Point of Maximum Transverse Displacement (PMTD)[1]), which leads to local buckling (LB). This entire mechanism of operation of the diagonals puts them in a situation of complex loaded and deformed state, which change over time (meaning the time when a load is applied) and which is accompanied by elongation, overlaying of effects of tension and compression internal forces with high flexural strains in PMTD and local buckling. In the behavior of the diagonals one can observes phenomena as a loss of bearing capacity due to the effects of the local buckling and high plate curvature. The loss of straightness of the cross section leads to loss of tension bearing capacity in reversal loading.

To gain an insight of how the internal forces changes in diagonals depending on the applied drift in each experimental model have been placed strain gauges (SG) in areas where it is assumed to stay elastic[2]. The location and number of strain gouges for each model differs and will be specified in respect to the specific case of study. For technical reasons the number of SG used was limited to 4 for a single diagonal or 16 in total per a model. The SGs are placed in the middle of the flanges and in the middle of the web. Thus, they cannot cover in full picture of strain in the entire cross-section and cannot provide information about the shear lag. Given the relatively small size of the cross-section the author believes that the resulting picture of the stresses in the diagonals is sufficiently representative. The obtained information about the strain in SG was transformed into information for the axial force using the following transformations:

[1] PMTD (Point of Maximum Transverse Displacement) should be understood the diagonal cross section subjected to maximum flexural deformations caused by buckling.

[2] Exception makes model H3 that was tested in experiments 2-3. On it strain gauges are installed at cross sections which subsequently plasticize.

$$\sigma_i = "datum\ STR_i".E \qquad (4.8\text{-}1)$$

where:

$"datum \quad STR_i"$ - data from strain of the i-th SG obtained in $\mu m/m$

E - modulus of elasticity of steel assumed as 210 000 N/mm^2

σ_i - normal stress corresponding to area of location of the i-th SG N/mm^2

Axial force in the corresponding diagonal is given by the expression:

$$N_d = (\frac{\sigma_{w1} + \sigma_{w2}}{2}).A_w.f_{y,w} + (\frac{\sigma_{f1} + \sigma_{f2}}{2}).A_f.f_{y,f} \qquad (4.8\text{-}2)$$

where:

A_w *u* A_f are the areas of the web and the flange of the respective model. The values of the yield strength of the flange and web steel sheets have been given in the preceding item 4.7 but for easy of reading will be reminded that they are $f_{y,w} = 225.4 N/mm^2$ and $f_{y,f} = 288.2 N/mm^2$.

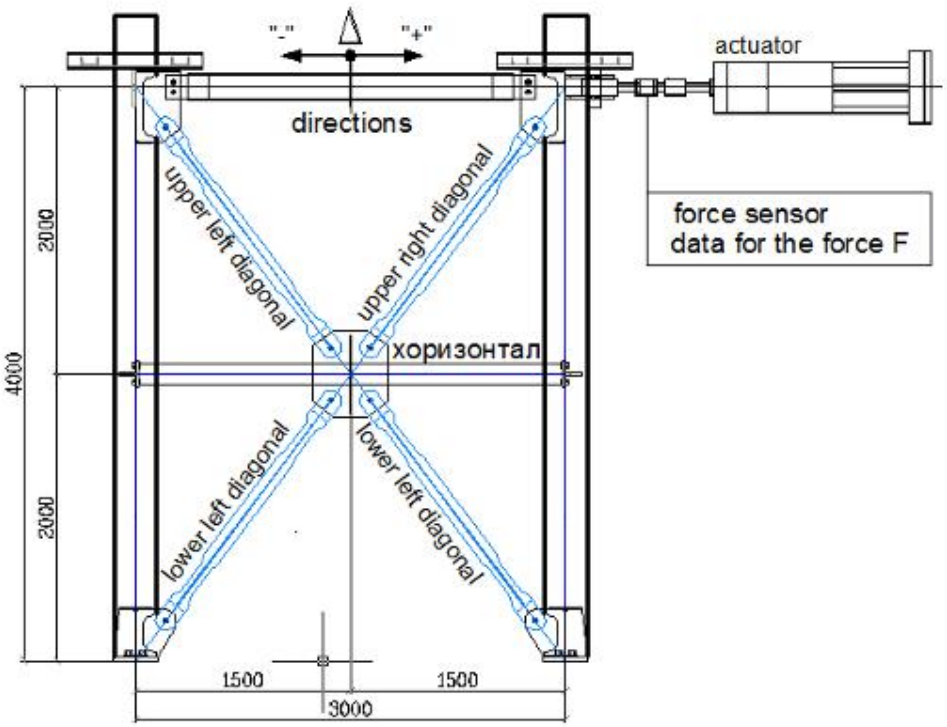

Fig. 4-87 *- assumed names of the diagonals*

σ_{wi}, σ_{fi} are the corresponding normal stresses obtained by the in expression (4.8-1).

As designed models are equipped with 4 diagonals separated by a horizontal intermediate member then for the purpose of their unambiguous identifying we will use the assumed names shown in Figure 4-87. When CBFs are subjected to horizontal

displacements as is the case with seismic impact they deform as shown on Figure 4-88. Taking that deformed position the one

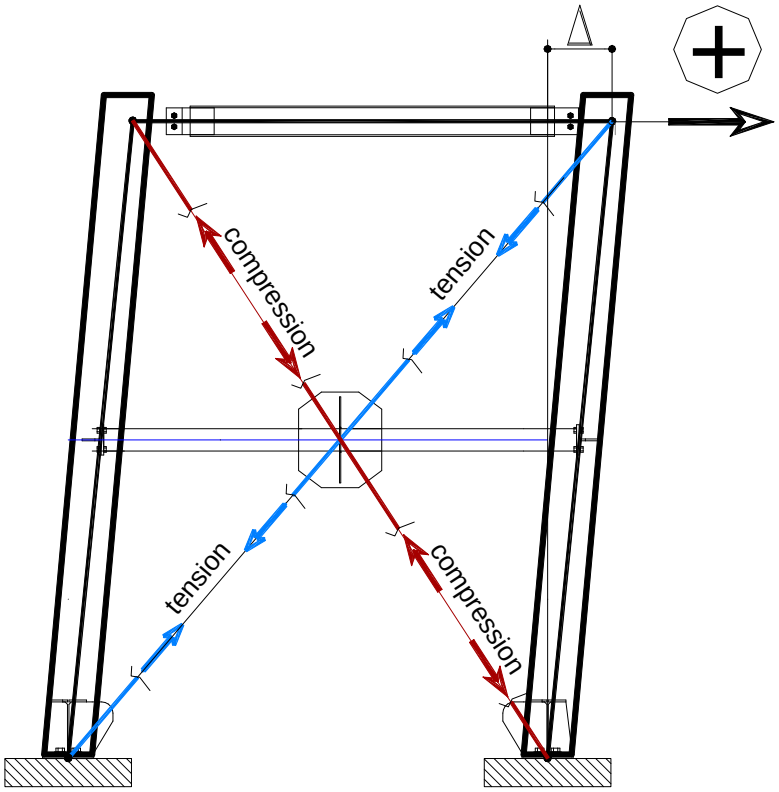

Fig. 4-88 *– deformed scheme of CBF where blue diagonals are subjected to tension and brown diagonals are subjected to compression*

pair of diagonals starts working under tension and the other pair of diagonals starts working under compression. For ease in this exposition a pair of diagonals that works identically[3] hereinafter shall be called a tandem[4]. In an idealized pin-joint structure (truss model) the elements of the supporting frame (columns, horizontal intermediate member, beam) are considered to experience only axial forces. However real structures differ from the idealized schemes by the type of their joints and connections and by the fact that the columns are continuous. The most commonly used joints such as the one used in these models are joints of the semi-rigid type according to BDS EN 1993-1-8 and in most cases the bases of the columns are close to rigid type joints. Therefore in addition to the axial forces in the elements of the frame could be expected occurrence of bending moments in columns, horizontal intermediate member and the beam. Thus stated bending moment will be of secondary importance as the dominant internal force will be the axial forces.

Several major guiding questions are covered in the study of the diagonals namely:

[3] Under the term "identical work" of a diagonals in horizontal displacement of the CBF should be understood a state when both diagonals are under compression or a state when both diagonals are under tension.

[4] Tandem appears to be lower left diagonal and upper right diagonal. Tandem are lower right diagonal and upper left diagonal.

- What are the internal axial forces in the lower and upper diagonal of each tandem?
- What is the ratio between the axial tensile forces and compressive axial forces in tandem diagonals and how this ratio changes depending on the drifts of the CBF?
- What is the behavior and the role of the horizontal intermediate member and is there interconnection between the rigidity of the horizontal intermediate member and behavior of the diagonals?
- Is there a difference between the theoretical bearing capacity (resistance) of the diagonals and the bearing capacity (resistance) established by the experiment?
- What types of final fracture have been realized?

We can distinguish the following phases in the behavior of the CBF regarding the behavior of their diagonals:

- Phase before first buckling;
- Phase after diagonal buckling (DB);
- Phases after large drifts, leading to great impacts of diagonal local buckling (LB);

In the upcoming exposition has not been followed a timeline of the ongoing experiments. The text in this item is developed by covering the results of models H2 (item 4.8.2), followed by H3 (item 4.8.3) and finally H1 (item 4.8.4). This sequence was generated by the "fertility" of the experiments and the amount of information that could be extracted. Although the three experiments were planned to be alike, in terms of the diagonals the experimental design has been changing (evolving). Because of the differences in the behavior of the models the phase to which operated the strain gauges (SG) differed. All this has reflected in diversity of data obtained and the author considered that the presented sequence of analysis of the behavior of the diagonals will be the most appropriate one.

4.8.2. Experimental model H2

To answer the guiding questions as defined in item 4.8.1 in respect to an experimental model H2 were processed the data from experiment 2-2 and the results are summarized in the respective graphs and tables. Figure 4-89 presents axial forces in the diagonals of cycle 6 relating to horizontal force F as measured by the force sensor. Cycle 6 was chosen as being a representative cycle having the greatest possible drift for the phase before first buckling. Cycle 9 was chosen since in it has been realized buckling of two compressed

diagonals. Cycle 15 is demonstrated as a typical cycle in which there is not LB in the compressed flanges and the web of the cross sections but on the other hand bracing buckling is significant. Cycle 19 is demonstrated as a typical cycle as in the preceding cycle 18 there are first signs of LB in compressed diagonal. The main characteristics resulting by the maximum displacements of all representative cycles are shown in Table 4-26.

Table 4-26

cycle	$v^{+}_{\max}\,[mm]$	$v^{-}_{\max}\,[mm]$	$\varphi^{+}=\frac{v^{+}_{\max}}{H}[rad]$	$\varphi^{-}=\frac{v^{-}_{\max}}{H}[rad]$	as part of H, direction „+“	as part of H, direction „-“
6	12,55	11,96	0,0031	0,003	$\frac{1}{319}H$	$\frac{1}{334}H$
9	16,47	20,4	0,0041	0,0051	$\frac{1}{243}H$	$\frac{1}{196}H$
15	33,36	37,4	0,0083	0,0093	$\frac{1}{120}H$	$\frac{1}{107}H$
19	55,24	60,8	0,0138	0,0152	$\frac{1}{72}H$	$\frac{1}{65}H$

As shown in Figure 4-89 in horizontal displacements up to $\frac{1}{319}H$ both diagonals are taking part in the bearing of the horizontal force. Could be noticed some asymmetry between axial forces in pressed and tensioned diagonal. From Figure 4-89 it can be concluded that the two tandems of diagonals have similar behavior.

In cycle 9 which represents the phase after DB is observed asymmetry in the axial forces between the two tandems of diagonals - Figure 4-90. This asymmetry is due to the buckling that occurred in cycle 7 in the upper right diagonal. It should be noted that in reduction of the axial force in the right upper diagonal is registered also a reduction of the force in the lower left diagonal. In other words the axial force decreases throughout the tandem though one of the diagonals in the tandem has not buckled.

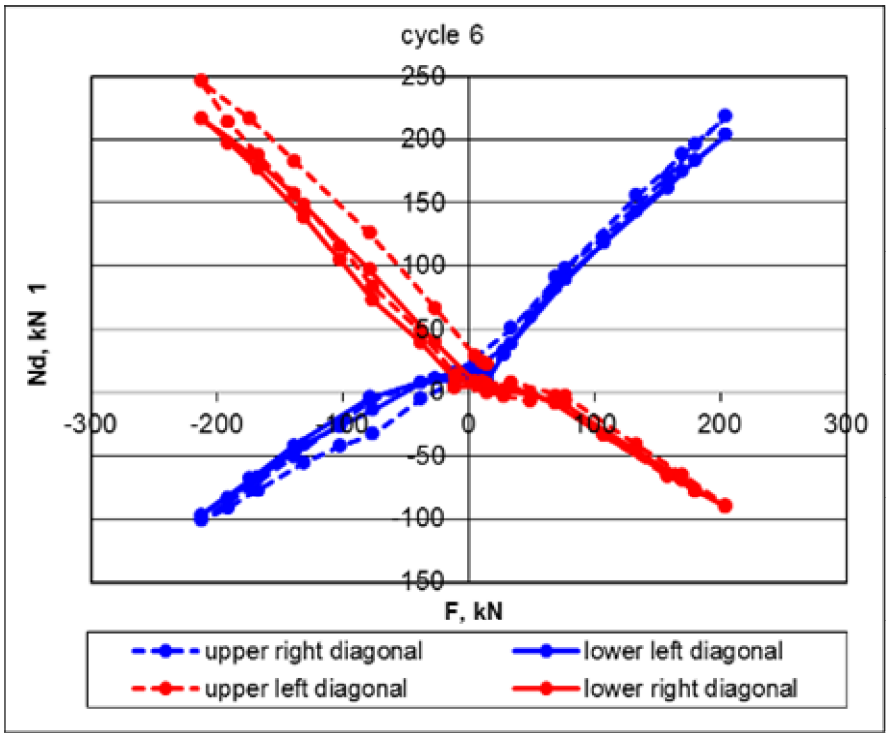

Fig. 4-89 *– model H2 in Phase before first buckling, cycle 6; Axial forces Nd in the diagonals depending on the horizontal force F;*

In cycle 18 and 19 the asymmetry in axial forces in the pressed diagonals is significant. It is observed that the bearing capacity of the pressed diagonal decreases with increasing of displacement (drifts) and at the maximum size of displacement the compression axial force in the diagonals is very small. Typical in cycle 19 is the fact that due to the occurring of LB in the pressed diagonals of the previous cycle has been noticed also a drop in the axial tensile forces in the subsequent application of tension. This could be explained by the fact that LB causes buckling in the flange plates and in the areas of those buckled part of the cross section is not straight and not working effectively. Visual presentation of the described in given in Figure 4-91.

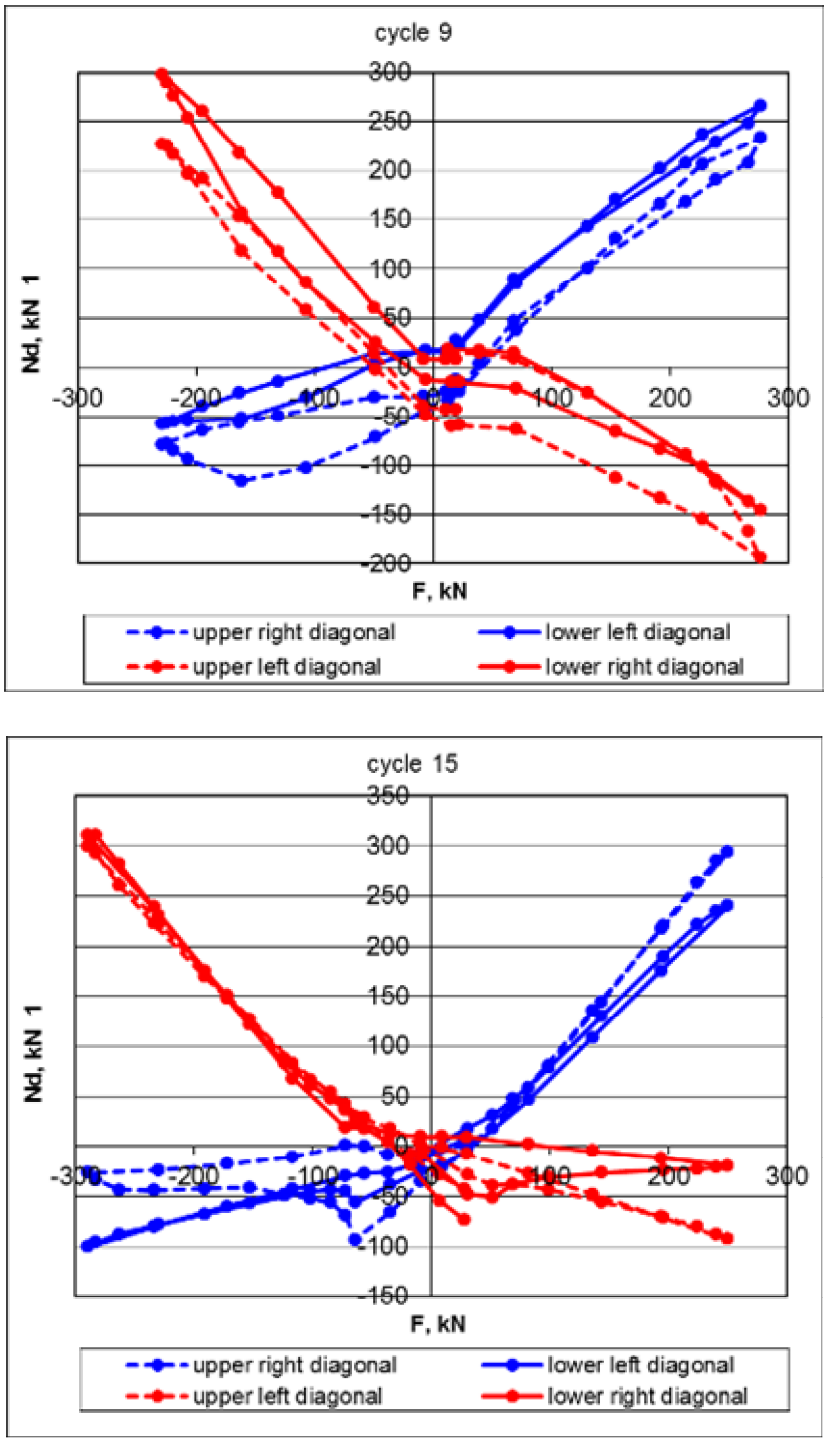

Fig. 4-90 – *model H2, axial forces Nd in the diagonals depending on the horizontal force F in;*

(upper part) cycle 9. Behavior of CBF in phases after DB; In this cycle we registered buckling in the upper right and lower right diagonal.

(lower part) cycle 15. Behavior of CBF in phases after LB and larger displacements; In this cycle we also registered buckling in the upper right and lower right diagonal. Behavior of CBF in applied displacement (drift) $\approx 2,5\Delta_Y$ *;*

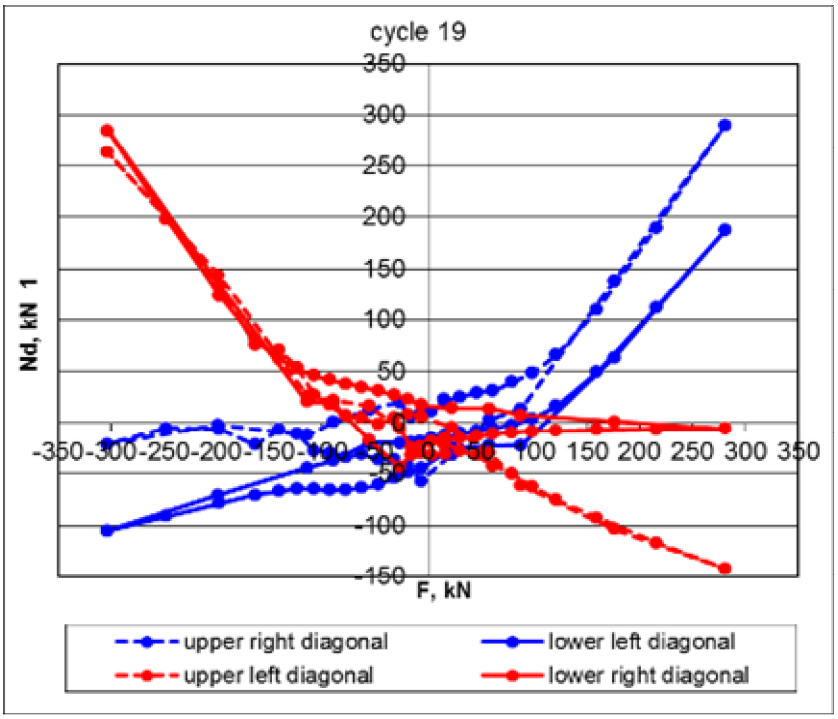

Fig. 4-91 *– model H2, axial forces Nd in the diagonals depending on the horizontal force F in cycle 19. In this cycle is registered LB (photos below, right). Behavior of CBF in applied displacement* $\approx 4{,}1\Delta_y$ *;*

In the next series of Figures 4-92, 4-93, 4-94 and 4-95 are shown the values of the forces in the diagonals depending on the maximum horizontal displacement and depending on the applied force F. Since in plastic phase cycles are repeated three times the given graphics show the first and last cycles of a group.

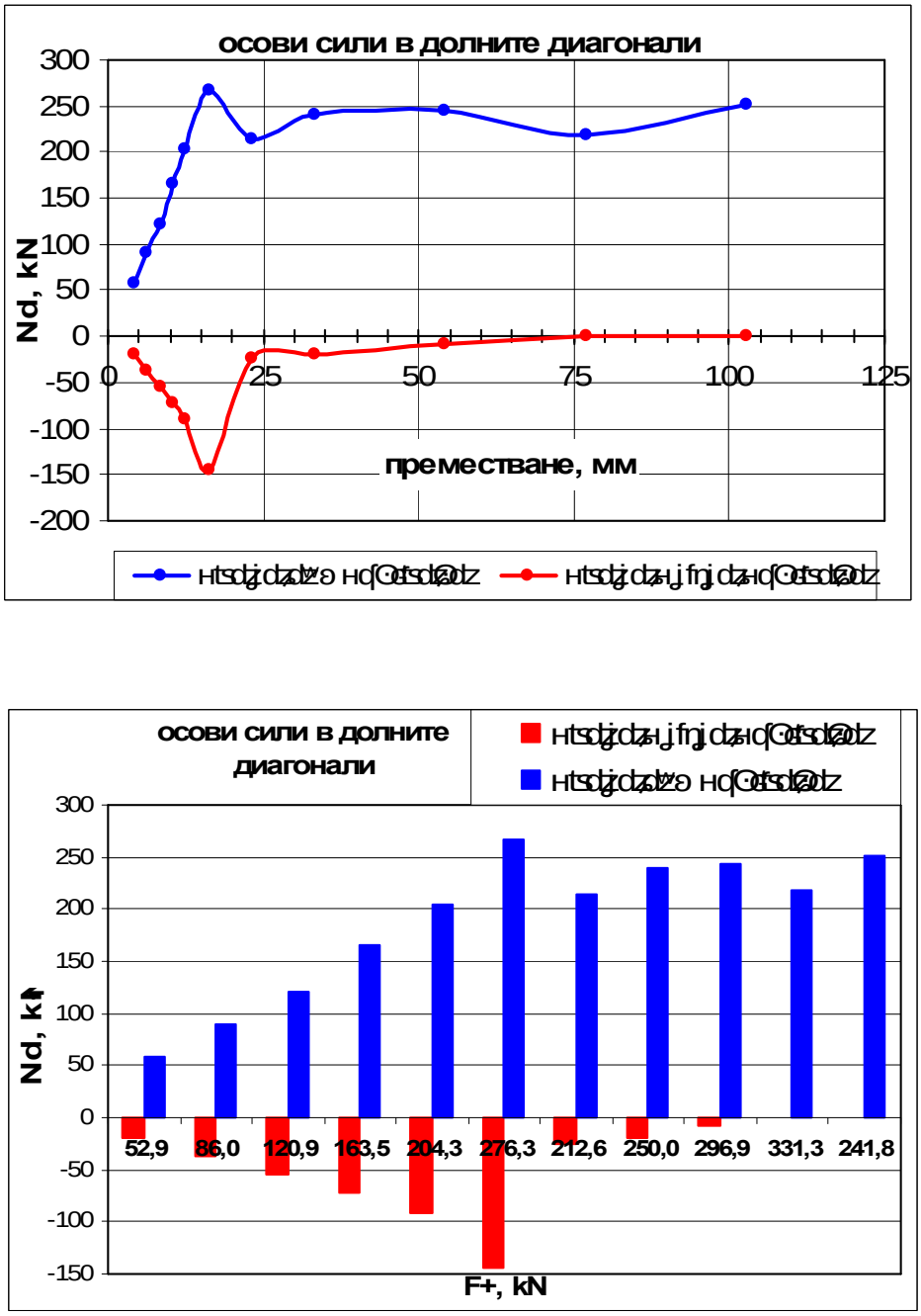

Fig. 4-92 *– model H2, axial forces Nd in the lower diagonals depending on the frame drift (diagram above) and horizontal force F (diagram below). Diagrams are formed with direction being "+" and based on the first reports in a group of cycles;*

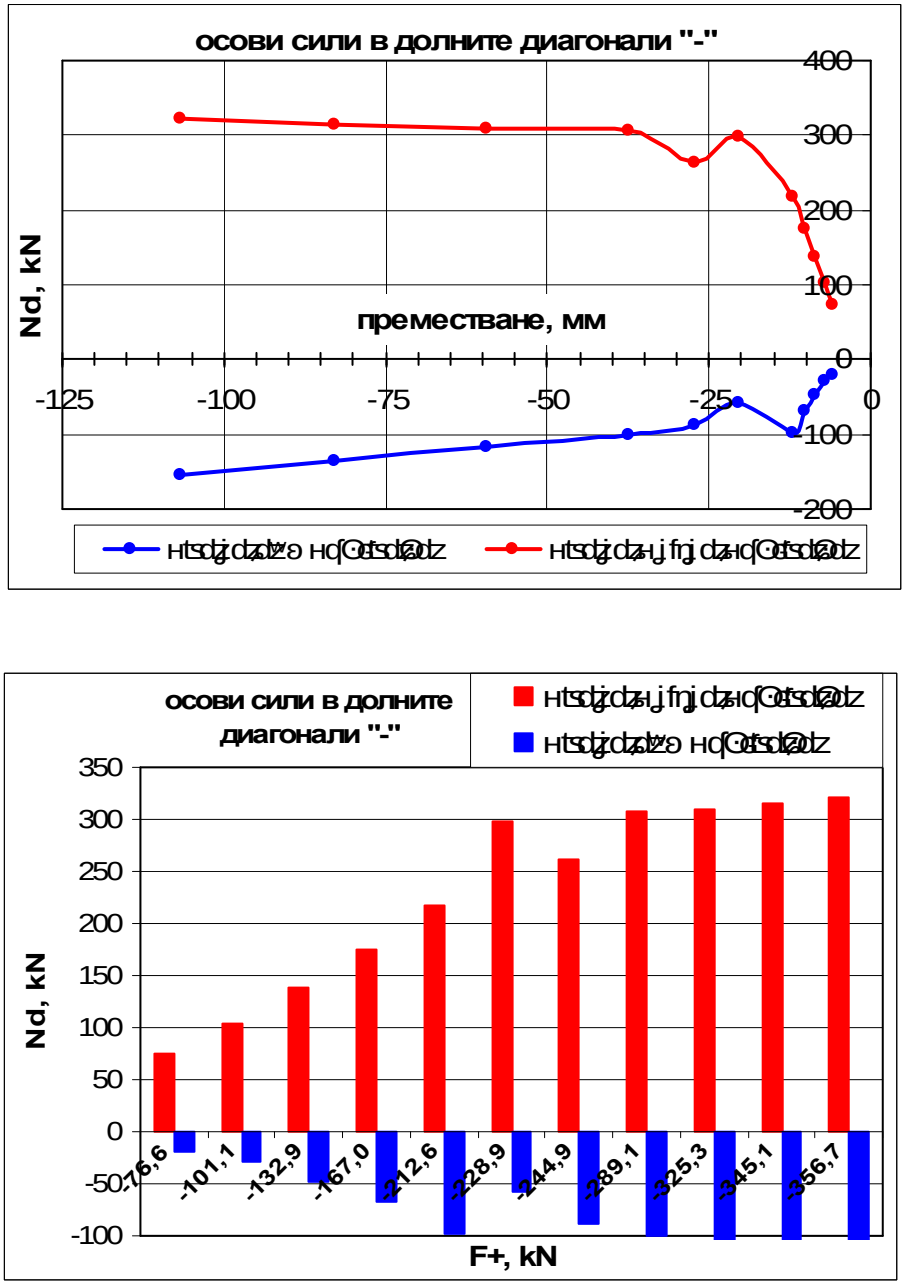

Fig. 4-93 *– model H2, axial forces Nd in the lower diagonals depending on the frame drift (diagram above) and horizontal force F (diagram below). Diagrams are formed with direction being "-" and based on the first reports in a group of cycles;*

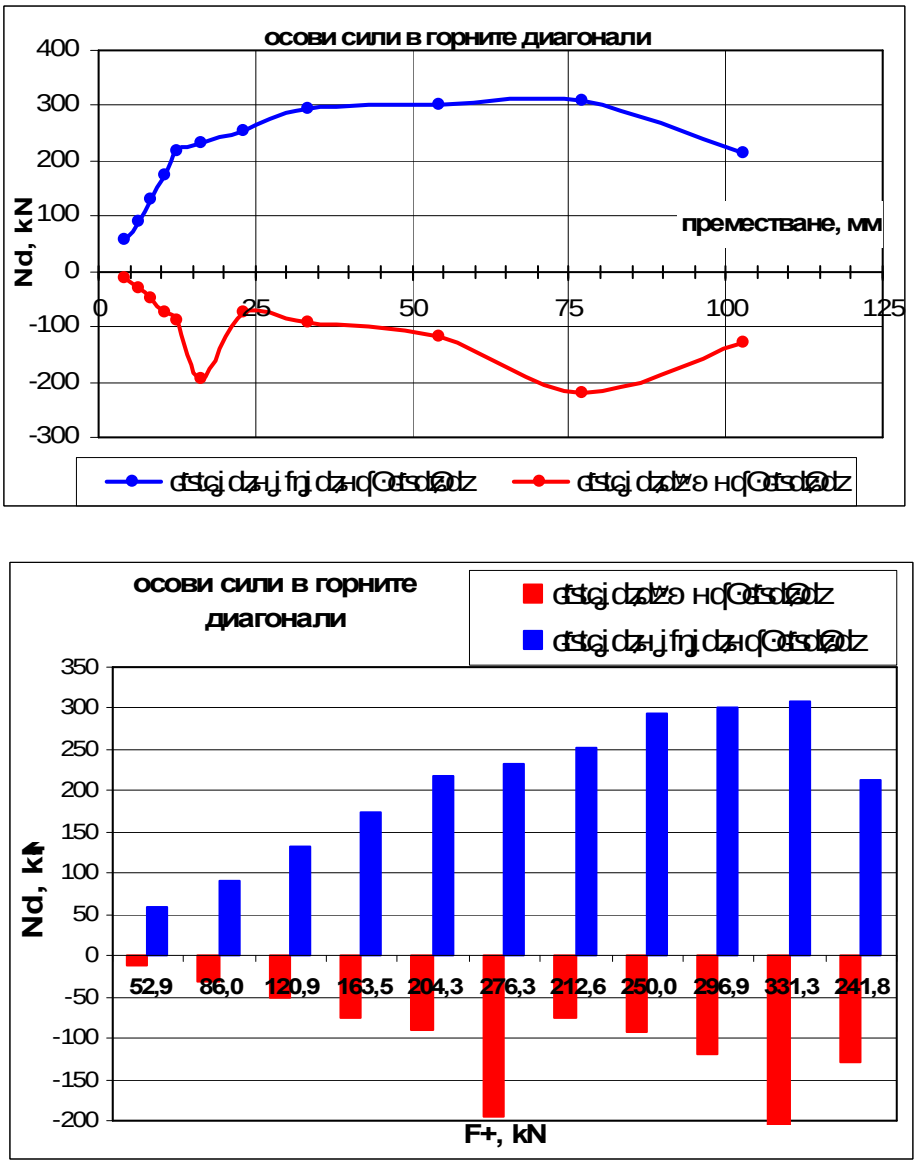

Fig. 4-94 *– model H2, axial forces Nd in the upper diagonals depending on the frame drift (diagram above) and horizontal force F (diagram below). Diagrams are formed with direction being "+" and based on the first reports in a group of cycles;*

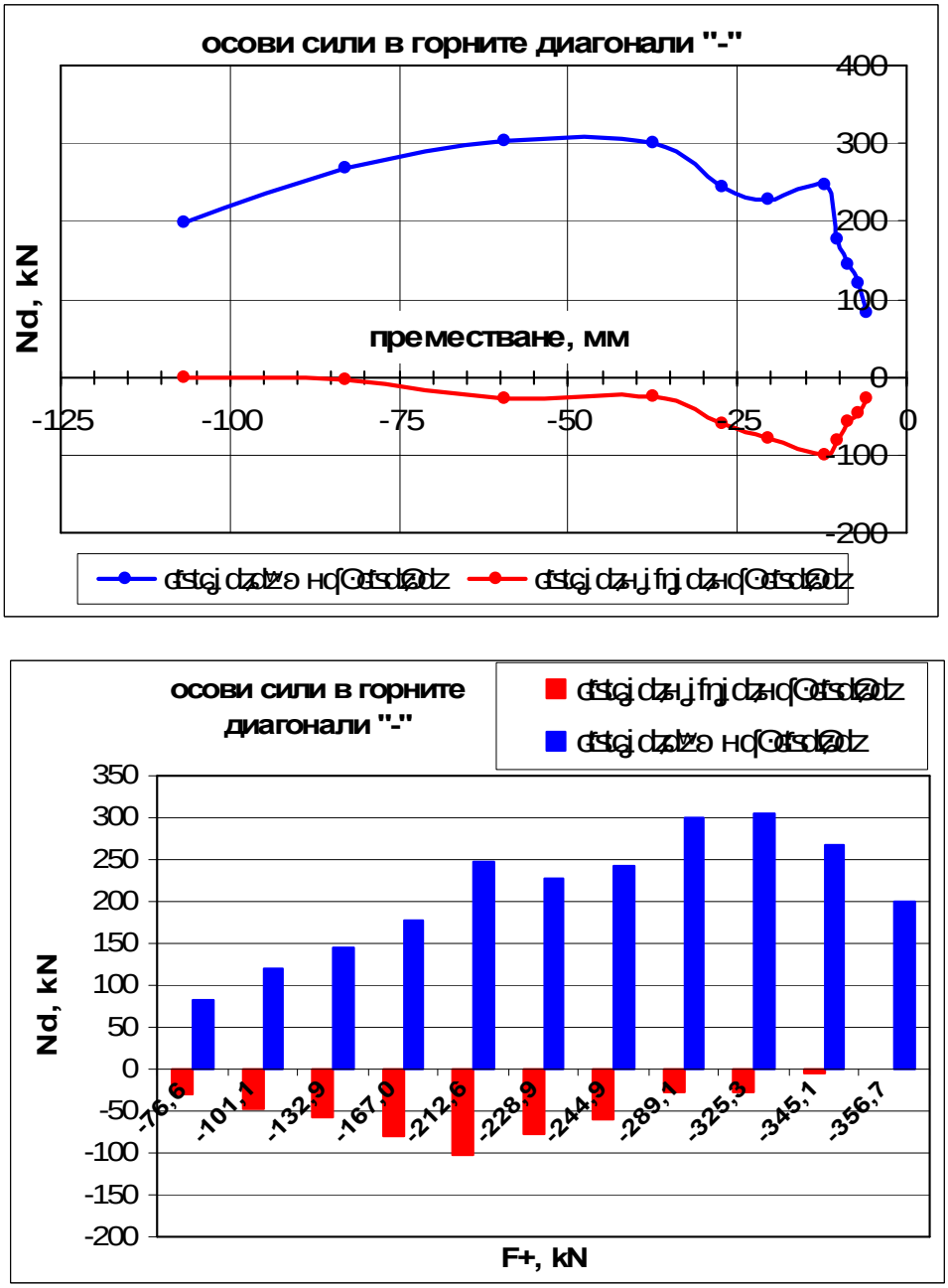

Fig. 4-95 *– model H2, axial forces Nd in the upper diagonals depending on the frame drift (diagram above) and horizontal force F (diagram below). Diagrams are formed with direction being "-" and based on the first reports in a group of cycles;*

Since in the time of implementation of a group of cycles having the same drifts could be observed decrease in axial force in diagonals and especially in the pressed diagonals as on the following Figures 4-96 and 4-97 are presented diagrams of the axial forces in the diagonals in the first and last cycle of a group of cycles.

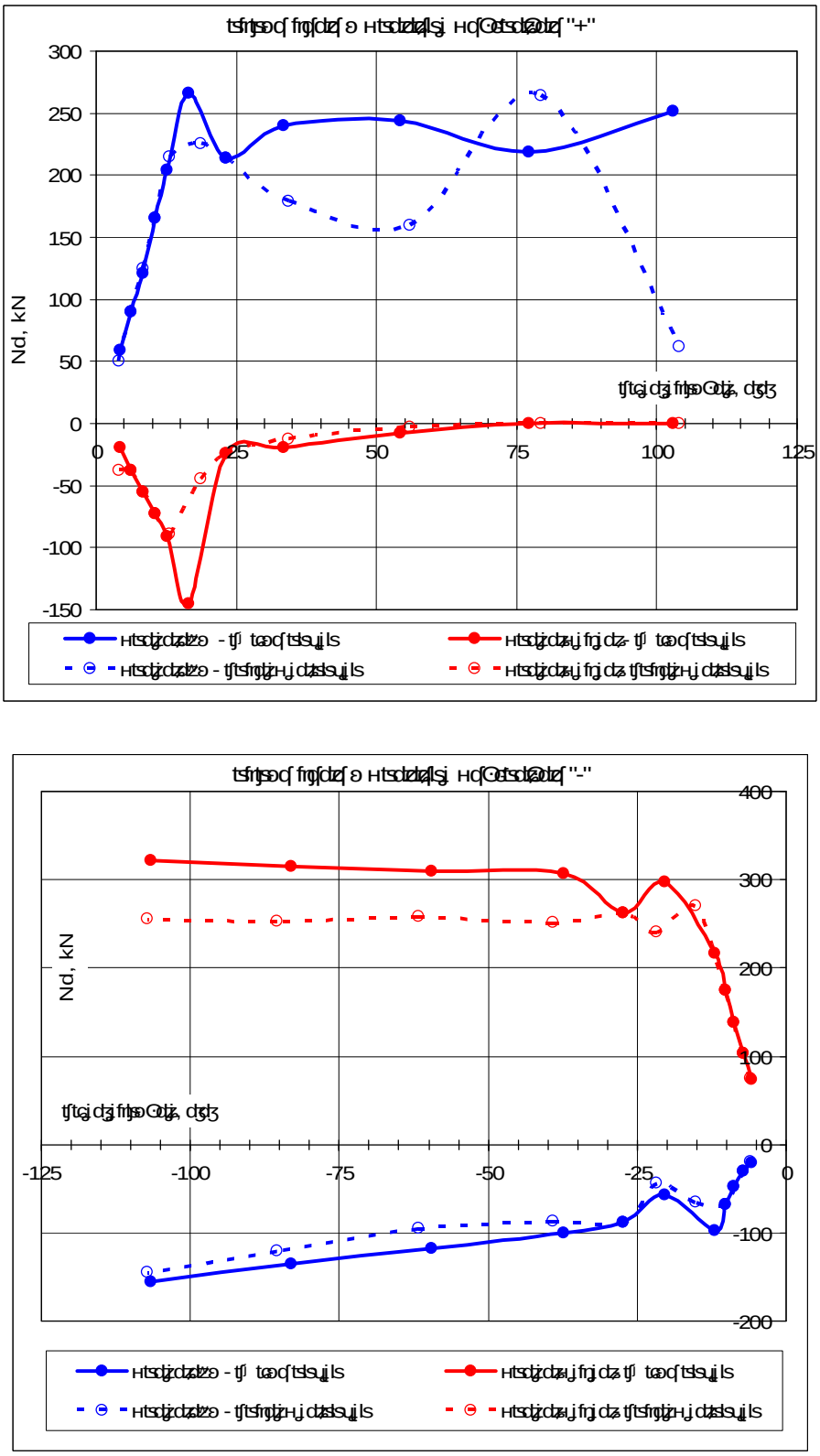

Fig. 4-96 *– model H2, axial forces Nd in the lower diagonals depending on the frame drift. Diagrams are formed having direction "+" (upper part) and "-" (lower part) and based on the first and last reports in a group of cycles;*

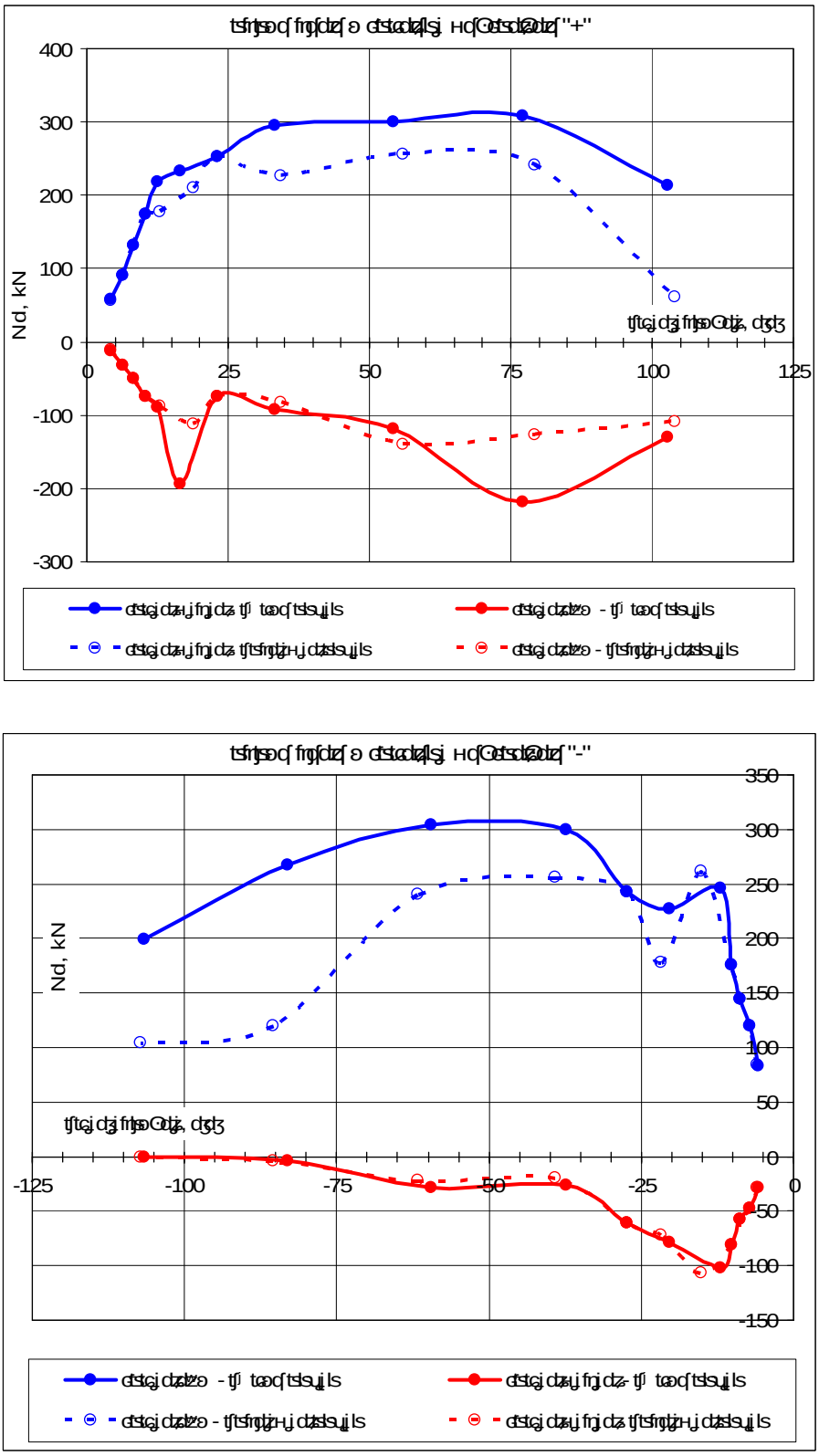

Fig. 4-97 – *model H2, axial forces Nd in the upper diagonals depending on the frame drifts. Diagrams are formed having direction "+" (upper part) and "-" (lower part) and based on the first and last reports in a group of cycles;*

Summarization of the results on axial forces change in all diagonals according to displacements (frame drift) in direction "+" and direction "-" is shown in Figure 4-98. For a clearer interpretation of the diagram has been used a color legend detailed on the Figure below the diagram.

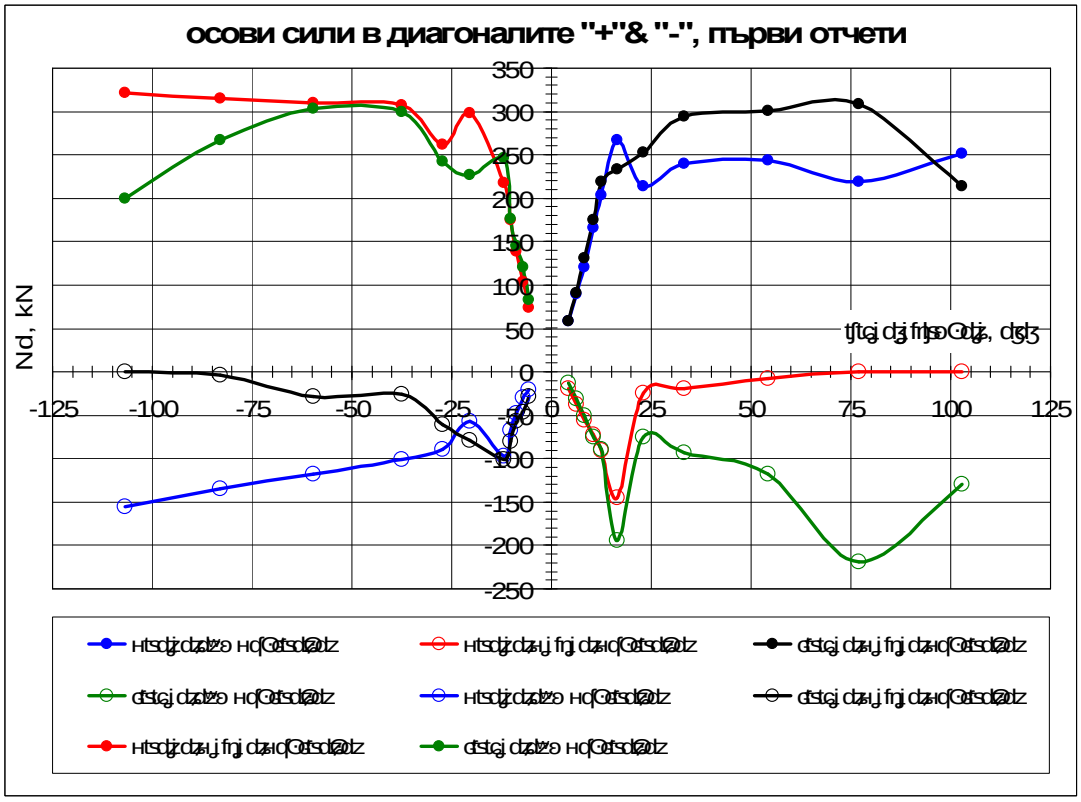

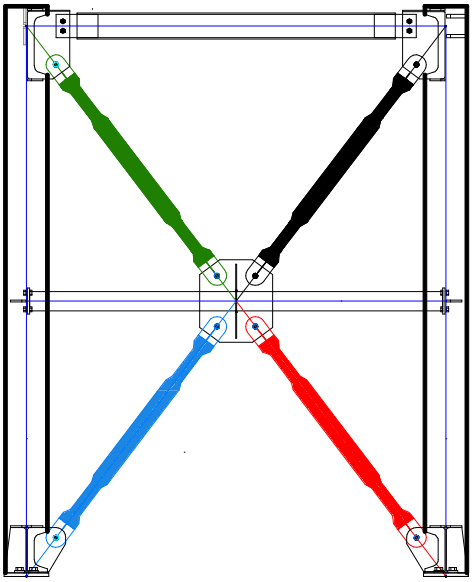

Fig. 4-98 *– model H2, axial forces Nd in all diagonals depending on the frame drift (upper part).Diagonals marked in color in the Figure (lower part) correspond to the color of the curves (upper part). Diagrams are formed based on the first reports in a group of cycles;*

By the analysis of Figure 4-98 could be found that after the implementation of the first loss of stability of pressed diagonal (diagonal buckling, DB) is lost the symmetry in the stressed state of the diagonals. DB in model H2 is implemented in the range 10-15 mm of frame drift. The distribution of axial forces between the diagonals (tensile and compressive) after the occurrence of DB changes and this causes the formation of unbalanced vertical force in the node between the horizontal intermediate member and the diagonals. After the occurrence of local buckling in the PMTD of the pressed diagonal the difference in axial forces increases. LB at upper right diagonal (black colored in Figure 4-98) appears after applying a displacement $v^{-}_{\max} = 59,53\,mm \approx 4\Delta_Y$. Occurrence of LB in the lower right diagonal could be noticed at $v^{+}_{\max} = 78,44\,mm \approx 5,8\Delta_Y$. Figure 4-99 shows the mechanism for the onset of the unbalanced vertical force and how it can be defined if we have an information about the axial forces in the diagonals.

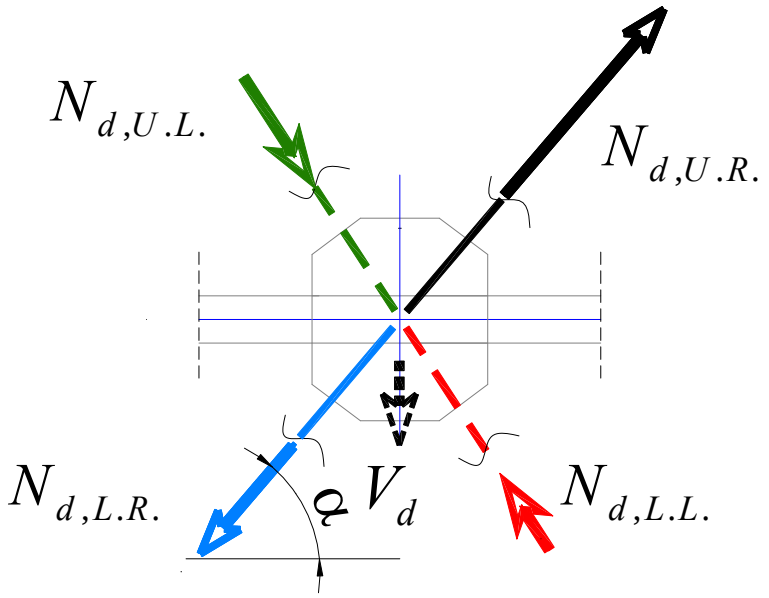

Fig. 4-99 *– model H2, mechanism for the occurrence of unbalanced vertical force in the middle of the horizontal intermediate member.*

The value of the unbalanced vertical force[5] (UVF) V_d is derived by the formula:

$V_d = \sum_i N_{d,i}.\sin\alpha$ where under the index i should be considered l.r.d (lower-right diagonal), u.r.d (upper right diagonal), l.l.d. (lower left diagonal) and u.l.d. (upper left diagonal). Figure 4-100 shows a graph of the unbalanced vertical force V_d depending on the displacement of the top of CBF. Figure 4-101 shown photographs made during the experiment with model H2 which clearly shows bending of the horizontal intermediate member due to UVF.

[5] The term "unbalanced vertical force" (UVF) has been adopted by BDS EN 1998-1, item 6.7.4.

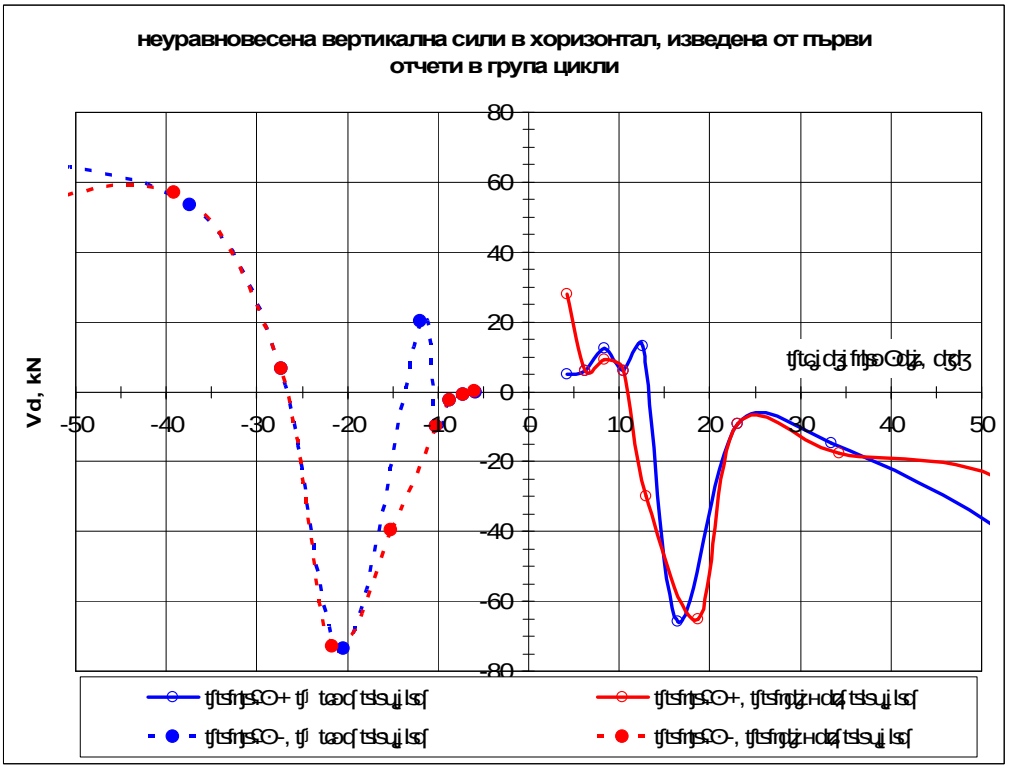

Fig. 4-100 *– model H2, diagram of the unbalanced vertical force in the middle of the horizontal intermediate member depending on the applied displacements at the top of CBF*

Fig. 4-101 *– model H2, bending of the horizontal intermediate member due to unbalanced vertical force;*

at left - cycle 15, maximum displacement $\approx 2,5\Delta_Y$ *;*

at right - cycle 24, maximum displacement $\approx 7,5\Delta_Y$ *and the occurrence of fracture in tensioned diagonal;*

The presence of unbalanced vertical force means also presence of unbalanced horizontal force (UHF) in diagonals. It can also be derived from the condition of equilibrium

of the intersection node by the formula $H_d = \sum_i N_{d,i}.\cos\alpha$. When the horizontal intermediate member is part a the floor structure this force is not a problem. When the horizontal intermediate member is used for dividing the diagonals as is the case with the proposed CBF, UHF should be borne in mind because it will force a bending moment in the columns. In this experimental study were not placed strain gauges on horizontal intermediate member. In order to prove the existence of UHF were used data from inductive sensors ID2 and ID3 (see Figure 3.67 of item 3.9.1. in Chapter 3). Inductive sensor ID3 is located opposite the horizontal intermediate member and ID2 is located against the beam. Following this logic we may conclude that if the column has not been bent by the axial force in the horizontal intermediate member the ratio of the results read by the inductive sensors will equal to 2 i.e. $K_{IND} = \frac{ID2}{ID3} = 2$. If there is a UHF in the horizontal intermediate member then it would cause a kink in the elastic line of the column and reports between ID2 and ID3 will be larger than 2. The following Figures 4-102, 4-103, 4-104 and 4-105 show force-displacement diagrams resulting from the reports in ID2 and ID3 as well as the ration of the records in cycle 18 and cycle 24.

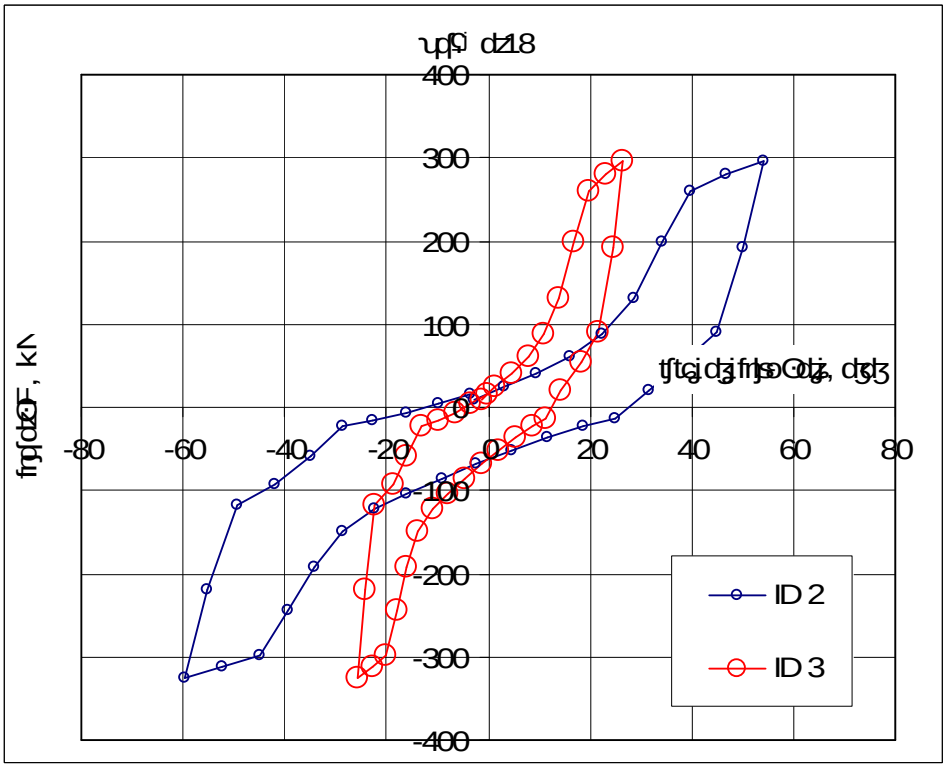

Fig. 4-102 *– model H2, cycle 18, diagram force-displacement for the upper end of the column (reports in ID2) and for the middle of the column (reports in ID3).*

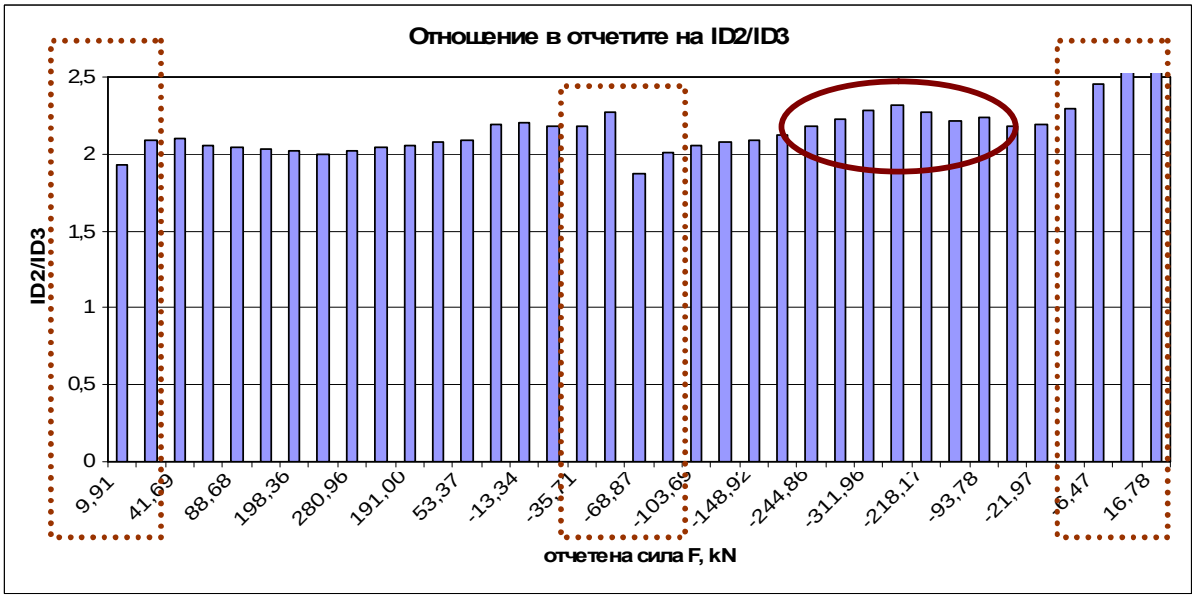

Fig. 4-103 *– model H2, cycle 18, ratio of the records ID2 / ID3; the enclosed in a rectangle reports are strongly deviating from value 2 because in drifts close to zero the effects of deformability in the joints of the frame is significant (due to the clearance between bolts and holes); Enclosed by oval outline Figures show ration of value more than 2. This happens at the maximum of displacements and proves the existence of UHF;*

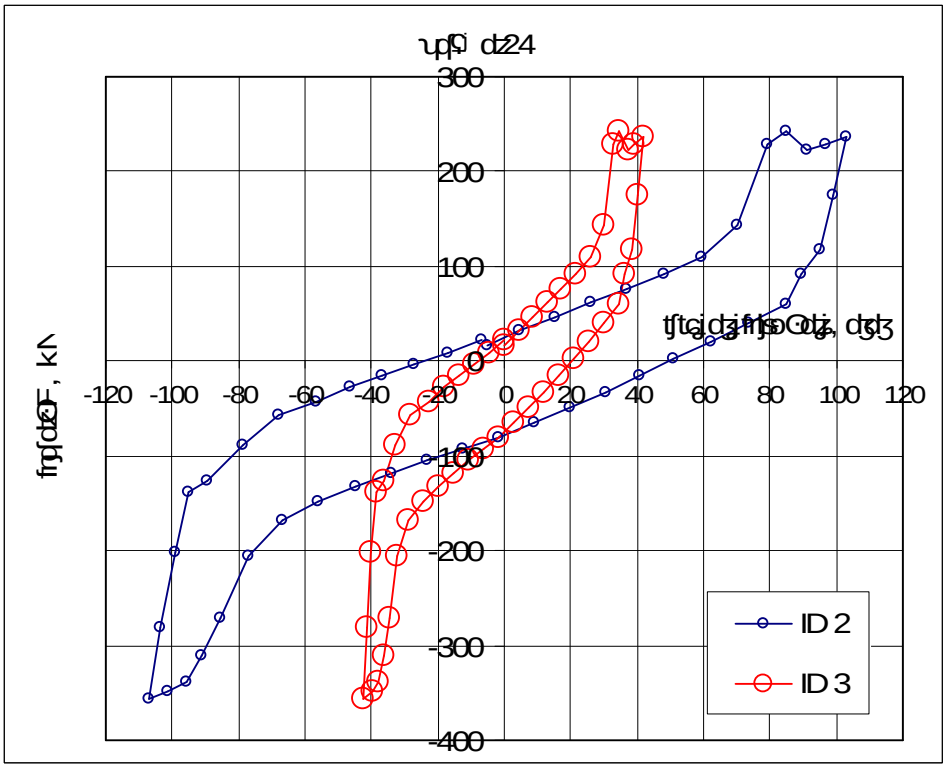

Fig. 4-104 *– model H2, cycle 24, diagram force-displacement for the upper end of the column (reports in ID2) and for the middle of the column (reports in ID3).*

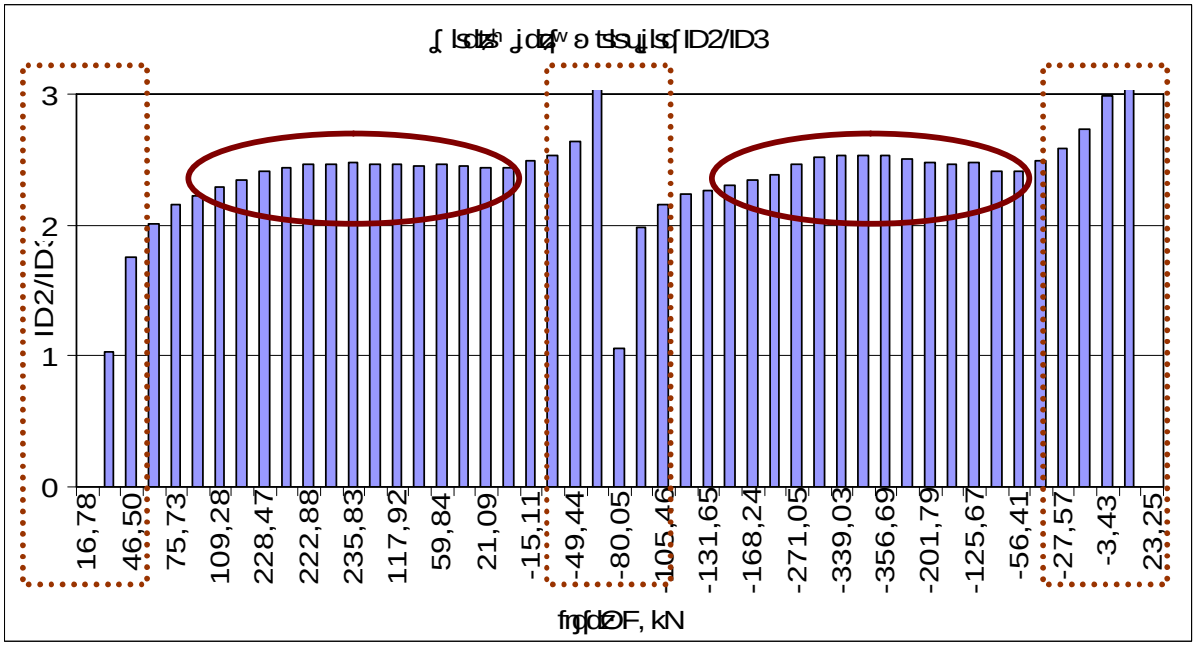

Fig. 4-105 *– model H2, cycle 24, ratio of the records ID2 / ID3; the enclosed in a rectangle reports are strongly deviating from value 2 because in drifts close to zero the effects of deformability in the joints of the frame is significant (due to the clearance between bolts and holes); Enclosed by oval outline Figures indicate deviation above 2 and prove the existence of UHF;*

By the analysis of the results shown in Figures 4-103 and 4-105 can be concluded that due to UHF columns are being bent in its middle part and that this bending should be considered in their design. The degree of bending is not great but the phenomenon exists. According to the author designing of a connection between horizontal intermediate member and the column that would allow free horizontal movement would solve the problem completely but it would deprive us of the opportunity to braced the column in the middle.

In processing the results of the experiment an analysis was also performed to determine the distribution of the total horizontal force F between the diagonal and the frame. For this purpose all reports related to direction of "+" and of "-" have been processed and averaged and has been derived an integral arithmetic average of the tensile and compressive axial forces in the diagonals. The value of the horizontal force F is measured from the force sensor (sensor 0) and thus it is considered directly obtained. The value of the axial forces in the diagonals is obtained by processing the reports of strain gauges. The difference between the horizontal projection of the sum of the axial forces in the diagonals and the force F is the shearing force in the columns of the frame. Thus was obtained the diagram in Figure 4-106. These results can be compared with the results of participation of the frame in the general absorption of energy derived in item 4.6, Figures 4-80 and 4-81. The author finds similarities in the results as meanwhile it is proper to point out that the evaluation of the contribution of the columns through the balance of forces shows smaller participation of the frame compared to the findings of item 4.6.

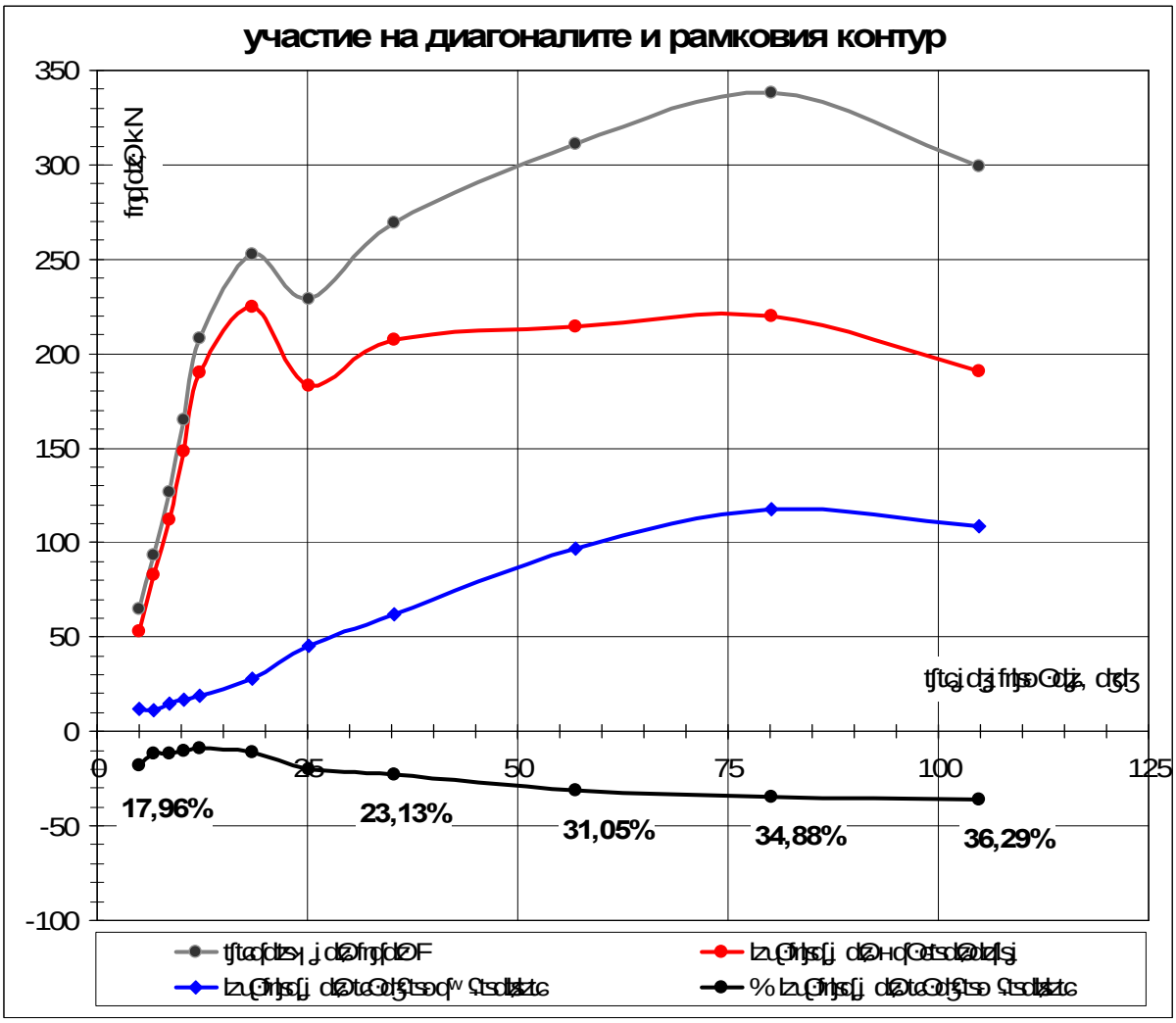

Fig. 4-106 *– model H2, participation of the frame and the diagonals in the bearing of the horizontal force F (story shear)*

Similar conclusions on the degree of participation of the columns in applying the horizontal force are defined in the comments of [31], F2 item 6d. They are based on analytical studies of the so called SCBFs arising from studies of (*Tang and Goel,* 1987, [94]) and (*Hassan and Goel* 1991, [60]). Based on the studies cited literary source [31] defines a 40% participation of columns in applying the total horizontal force. According to the graph in Figure 4-106 participation of columns is reaching 36.3%.

Entirely appreciable is also the question of the relationship between the theoretical bearing capacity of the diagonals in cases of tension and compression and the experimentally obtained axial forces in them. To make this comparison we will use dimensioning procedures under BDS EN 1993-1-1 [1] and the data on the actual yield strengths of the steel relating to the flange and web steel plates. In dimensioning procedures of Eurocode 3 all coefficients γ_{Mi}, $i = 0,1,2$ will be assumed as equal to 1.0. The Equivalent (effective) for the entire cross section actual yield strength is determined by the expression:

$$f_{y,eff} = \left(A_w.f_{y,w} + 2.A_f.f_{y,f}\right).\frac{1}{A_w. + 2.A_f} \qquad (4.8\text{-}3)$$

By applying the values for the gross cross section of the diagonal in model H2 we get:

$$f_{y,eff} = \left(480.225,4 + 2.450.288,2\right).\frac{1}{480 + 2.450} = 266,4N/mm^2$$

In the as derived equivalent yield strength the plastic tensile resistance of the reduced cross section is as follows:

$N_{pl,t,RD} = 920.266,4 = 245088 \approx 245kN$;

The diagonal tension limit force (bearing capacity) of the reduced cross section is defined by the tension resistance of the steel in the equation:

$N_{t,u} = A_{w,OC}.f_{u,w} + A_{f,OC}.f_{u,f} = (320.324 + 600.351,7).\frac{1}{1000} = 314,7kN$, this equation also comes from Eurocode 3 under the famous formula $N_{t,u} = \frac{0,9.A_{net}.f_y}{\gamma_{M2}}$ as it is assumed that γ_{M2}=1,0, and the coefficient 0.9 before A_{net} is interpreted as the coefficient of efficiency of the reduced cross section (see [55]) and is also assumed to be equal to 1.

The compression resistance (buckling capacity) of the diagonal should be defined as follows:

$$\varepsilon = \sqrt{\frac{235}{f_{y,eff}}} = \sqrt{\frac{235}{266,4}} = 0,939$$

$N_{b,Rd} = \chi\frac{A.f_{y,eff}}{1,0}$, and the buckling coefficient for efficient slenderness

$\lambda_{eff} = 122$,? $\bar{\lambda}_{eff} = \frac{122}{93,9.0,939} = 1,384$, in case of buckling curve "c" and assumed slenderness 1.384 we obtain $\chi = 0,355$

$$N_{b,Rd} = 0,355\frac{1380.266,4}{1,0} = 130509N = 130,5kN$$

Comparison of the theoretical bearing capacity and the maximum tensile and compressive forces in the diagonals obtained by the test is shown in Table 4-27

Table 4-27

diagonal	tension			compression	
	$N_{pl,t,RD}$	$N_{t,u,RD}$	experiment	theoretical	experiment[6]
upper right	245	314,7	308.49 - ***fracture***	130,5	170,04
upper left	245	314,7	303.78 ï not cut[7]	130,5	218,78
lower right	245	314,7	321.14- ***fracture***	130,5	155,31
lower left	245	314,7	not cut	130,5	*cannot be buckle*

Analysis of the results in Table 4-27 can be summarized in the conclusion that the diagonals are fractured by reaching the tensile strength of the material. Completely torn diagonal is the upper right diagonal where the tearing force is 98% of the theoretical force obtained using real properties of materials. In the lower right diagonal the force that leads to a partial tearing is of 2% higher than the theoretical force obtained using real properties of materials. Figure 4-107 shows the forms of the torn cross sections of the diagonals. The place is always at the beginning of the reduced diagonal section.

Fig. 4-107 *– model H2, forms of fracture of the tensioned diagonals; The photo on the left - upper right diagonal, the photo on the right - bottom right diagonal.*

A careful reading of the results shows that the tensile diagonals fracture due to exhaustion of the tensile strength of the material and the effects of low cyclic fatigue are of minor importance and are not dominating.

[6] This is the maximum force which has been measured when registering the loss of stability of pressed diagonal

[7] To this diagonal cannot be applied greater force as the other diagonal in the tandem is fractured. There are no significant signs of Local Buckling in the area where flexure occurs due to diagonal buckling in PMTD. There are no signs of a dominant role of low cyclic fatigue.

From the analysis of the results related to experimentally derived bearing capacity of the pressed diagonal it can be concluded that the theoretical bearing capacity is always less than the actual one. Table 4-28 presents the resultant differences and the same table shows that the actual bearing capacity is greater than the theoretical one with average of 38,9%. This is probably due to the fact that we use a methodology for sizing based on Eurocode 3 which is developed to ensure reliability of 95% in which have been set out larger initial imperfections in the geometry of the elements.

Table 4-28

	theoretical bearing capacity	result from the experiment	difference %	averaged difference in %
upper right	130,5	170,04	30%	38,9%
upper left	130,5	218,78	67,6%	
lower right	130,5	155,31	19%	
lower left	130,5	*N A*		

PARTICULAR CONCLUSIONS DERIVED BY THE ANALYSIS OF THE BEHAVIOR OF THE DIAGONALS OF EXPERIMENTAL MODEL H2

By the analysis made in item 4.8.2. could be drawn the following particular conclusions and generalizations:

- Both tandems of diagonals have the same behavior (in application of displacement force towards direction "+" and towards direction "-") only to the first appearing of loss of stability of a pressed diagonal (first diagonal buckling);
- The behavior of the tensioned diagonals is similar to the time of occurrence of local buckling. After occurrence of LB, behavior of the tensioned diagonal and the behavior of the pressed diagonal are in interactive relationship. Effects of LB appear to be initial imperfections (kinks) in applying pressing force thus leading to a steady degradation in the bearing capacity of the diagonal subjected to compression. Meanwhile the warps of the cross section due to LB influence in such manner that part of the cross section, does not work effectively also if subjected to tension. This gives rise to a mechanism of degradation in the bearing capacity of the diagonal if subjected to tension. The degradation of bearing capacity in tension is much smaller than the degradation of the bearing capacity in compression;
- In decline of the force in one of the diagonals in a given tandem declines also the force in the other diagonal of the tandem;

- After the occurrence of DB (diagonal buckling) lacks symmetry in axial forces in the diagonals. The lack of symmetry is enhanced along with buckling of the diagonal;
- The lack of symmetry in the stressed state of the diagonals causes the onset of unbalanced vertical force (UVF);
- UVF bends the horizontal intermediate member and may cause appearance of inelastic flexural deformations (plasticization) in it;
- The slenderness of the diagonals (as a measure of their stiffness) should always be linked to the flexural stiffness of the horizontal intermediate member. We believe that the horizontal intermediate member must be chosen so as to "force" both tandem diagonals towards buckling. Should be defined relationship between the stiffness of the horizontal intermediate member and the slenderness of the diagonal. We suggest the following equation for UVF $V_d = (0,1.N_{d,t} + N_{d,c})\sin\alpha$;
- The presence of UVF generates also UHF which in turn bends the column. This phenomenon either must be secured by a capacity design or should be designed a connection detail (between horizontal member and the column) allowing free horizontal movement between the column and the horizontal intermediate member;
- Shear forces carried by the columns do not exceed 37% of the total horizontal force. To a similar conclusion was reached in the researches performed by (*Tang and Goel*, 1987, [94]) and (*Hassan and Goel* 1991, [60]) and there has been stated 40%;
- When given diagonal buckles residual post-buckling compressive force therein is between 0 and 20% of its bearing capacity. In case of larger displacements that residual force tends to zero;
- If for some reason the diagonal is not losing its stability (does not buckle) it retains its compressive bearing capacity by the end of the test. This means that a plastic mechanism is implemented characterized by strong diagonals and weak horizontal intermediate member.

4.8.3. Experimental model H1

Experimental model H1 was first in line experiment of series 2 of experiments. Strain gauges (SG) through which were recorded the data related to the strains in the cross sections were placed in gusset plates of the lower left and lower right diagonal. Their location and numbering are shown in Figure 4-107. These cross sections of the diagonals are supposed to stay with elastic behaviour until the end of the experiment since in the process of their design was applied the capacity design strategy of ñstrong nodes week diaginalsò The specifics of the as chosen is that therein arises local bending due to the fact that each gusset plate is connected to the column using a single fit bolt - Figure 4-108 (see the full text of the disertation) and moreover the closeness of the bolt to SG leads to non equal deformations along the width of the cross section. 22

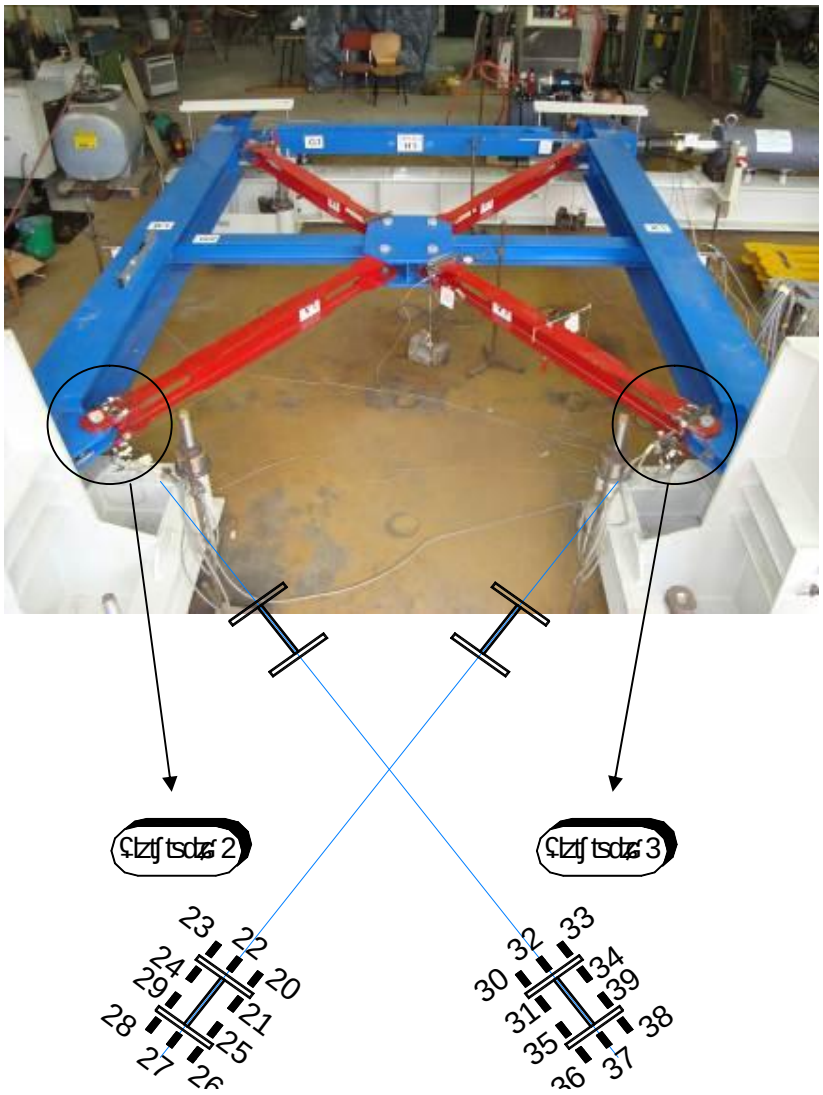

Fig. 4-107 *– model H1, location and numbering of the SG*

To overwhelm the effect of local bending in location places of SG and in orde to obtain information only for the axial force the following approach has been applied. This approach is detailed in the full text of the PhD Thesis.

In order to minimize local bending was proposed instead of two bolts to be used a common stud bolt and an internal tube spacer. The improved solution is shown in Figure 4-113. It would minimize the effect of bending without unduly complicating the note.

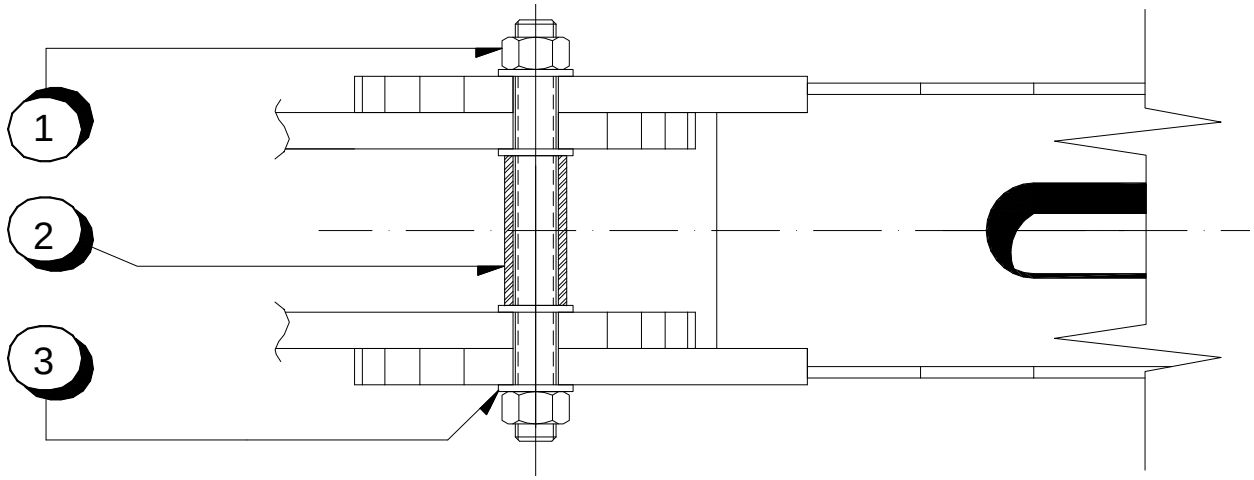

Fig. 4-113 *- eventual solution of the connection that would minimize the effect of local bending;*

1 - nut; 2 - tube spacer; 3 - washer;

By analogy with the analysis of model H2 within this item will be analyzed and summarized the data on the behavior of the diagonals in the respective graphs and tables. Specifics related to the experiment with model H1 is the disadvantage that we have available records only for lower left and lower right diagonal. This is so because SG were places only therein. As an advantage which by technical reasons could not be implemented in the rest of the experiments is that fact that inductive sensor ID9 is located in the axis of the diagonals and therefore provides reliable information about the axial displacements. More typical is that ID9 was located along side the entire length of a tandem of diagonals and could be used to assess the shortening and lengthening of the whole diagonal depending on the applied displacement at the top of the frame.

Figure 4-114 presents axial forces in the diagonals of cycle 10 relating to horizontal force F as measured by the force sensor. Cycle 14 was chosen as being a representative cycle having the greatest possible drift in work phase before first diagonal buckling. Cycle 15 was chosen since in it has been realized loss of stability of the lower left diagonal (buckling). Cycle 18 is demonstrated as a typical cycle where has been noticed lose of stability of the upper left diagonal and began the occurrence of LB in lower left diagonal. Cycle 21 is demonstrated as a typical cycle as in it there has a significant occurrence of LB in pressed diagonals but there are also missing any fractures in the cross section. The last representative cycle of the experiment is cycle 24 which shows also the occurrence of

fracture in the cross section. The main characteristics of the maximum displacements of all representative cycles are shown in Table 4-30.

Table 4-30

cycle	$v_{max}^{+}\ [mm]$	$v_{max}^{-}\ [mm]$	$\varphi^{+} = \frac{v_{max}^{+}}{H}\ [rad]$	$\varphi^{-} = \frac{v_{max}^{-}}{H}\ [rad]$	as part of H, direction Ă+ñ	as part of H, direction Ăñ
14	13,26	16,53	0,0033	0,0041	$\frac{1}{303}H$	$\frac{1}{244}H$
15	16,46	23,17	0,0041	0,0058	$\frac{1}{243}H$	$\frac{1}{172}H$
18	23,64	25,15	0,0059	0,0063	$\frac{1}{169}H$	$\frac{1}{159}H$
21	36,79	42,95	0,0092	0,0107	$\frac{1}{108}H$	$\frac{1}{93}H$
24	45,39	49,12	0,0113	0,0123	$\frac{1}{88}H$	$\frac{1}{81}H$

As shown in Figure 4-114 in horizontal displacements up to $\frac{1}{244}H$ both diagonals are taking part in the bearing of the horizontal force. Could be noticed some

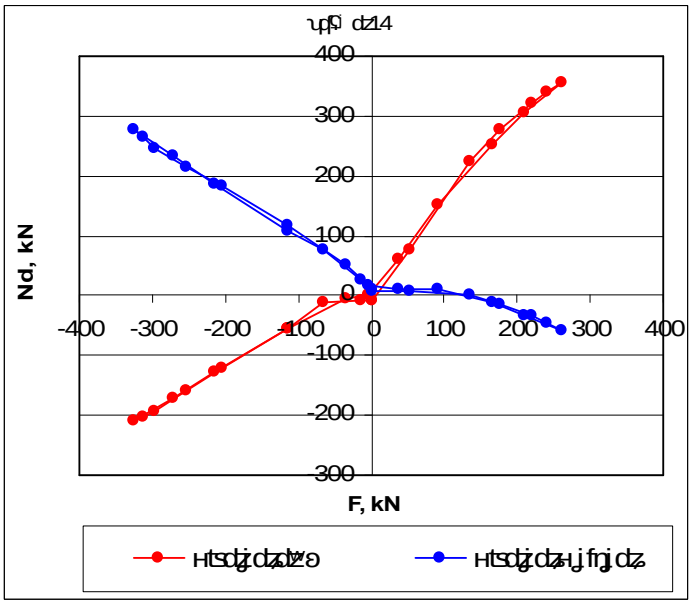

***Fig. 4-114** – model H1, cycle 14 - axial forces in the lower diagonals*

asymmetry between axial forces in pressed and in tensioned diagonal. A comment related to the small asymmetry in the compression force in the actuator will be given in item 4.8.4. and the author believes that this explanation is also valid here. The asymmetry is

particularly evident in respect to the tensile force in the piston of the loading system. The explanation that could be given is the significant clearances (gaps)[1] in the bolt connection between the beam and columns that we had in this first experiment - Figure 4-115.

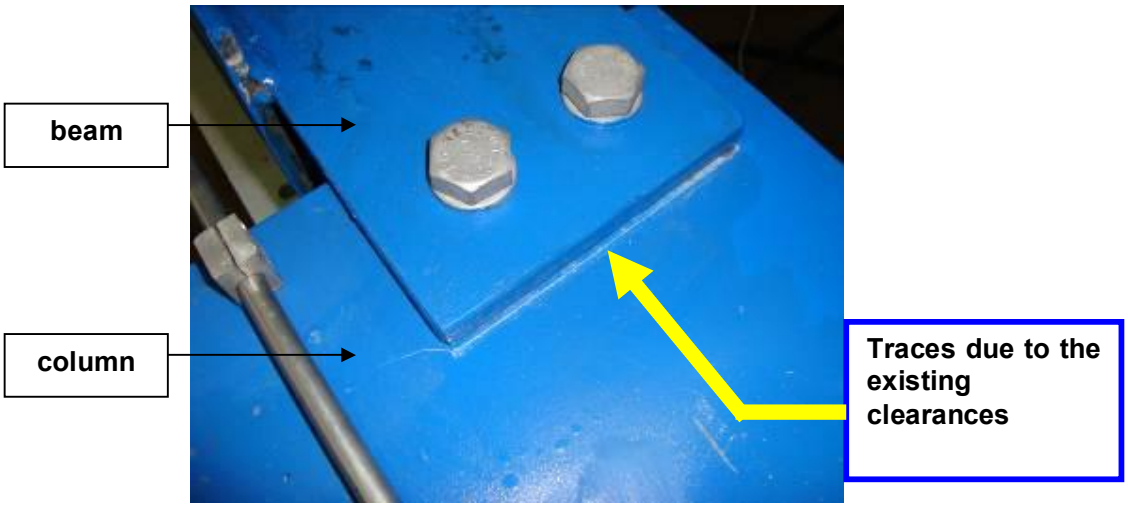

Fig. 4-115 *– model H1, the presence of clearances in the bolt connection between a beam and a column*

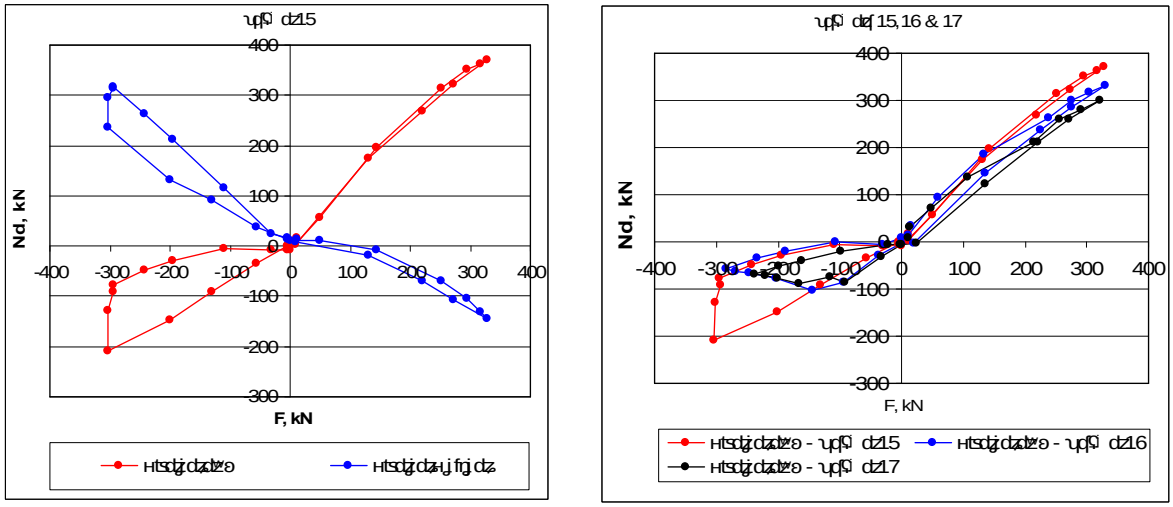

Fig. 4-116 *– model H1, cycle 15 – left, could be seen the effect of buckling of the lower left diagonal and the probable first occurrence of partial inelastic deformations in the tensioned diagonal; right - diagram of axial forces in the entire group of cycles*

[1] Clearances between the column and the beam are result of the fact that the model was performed using ordinary bolts and in this joint occurred major slip of about 4 mm. Since the diagonals are connected by fit bolts and their gusset plates are welded to the columns therefore one of the diagonals operates without the presence of clearance and the other diagonal operates in presence of such clearance. This situation increases the differences between the axial forces in the diagonals.

In cycle 15 and subsequent cycles 16 and 17 which represent the phase after DB could be observed asymmetry in the axial forces between the two diagonals - Figure 4-116. This asymmetry is due to the occurred buckling in cycle 15 in lower right diagonal. The lack of linear relationship in lower right diagonal when being subjected to tension shows the occurrence of first realized partial inelastic defomations of the cross section in the lower right or upper left diagonal. It should be noted that once lost its compression resistance the diagonal may no longer recover it - see Figure 4-116 at right.

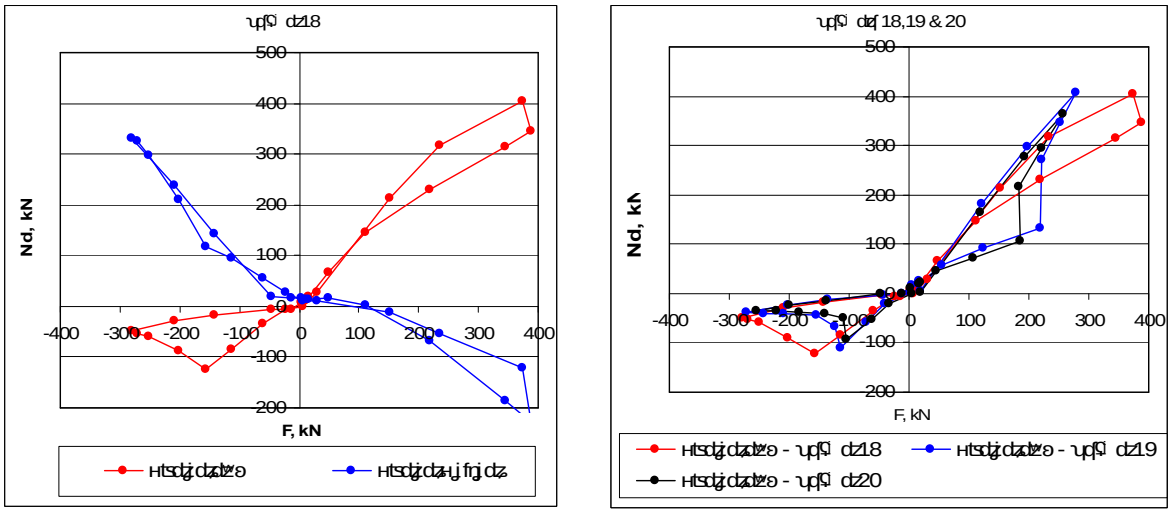

Fig. 4-117 *– model H1, cycle 18 – left, could be seen the effect of cross section plasticizing in the tensioned left diagonal; right - diagram of axial forces in the entire group of cycles. There is a decline in the bearing capacity of the diagonal when subjected to tension*

Cycle 18 is characterized by the fact that both left diagonals has lost their stability. It should be noted that by examining the entire group of cycles 18, 19 and 20 (Figure 4-117) is evident the loss of bearing capacity in case of compression and also start of loss of bearing capacity in case of applying a tensile force. <u>According to the author the latter is due to the overlapping of the effects of bending and tensioning in one and the same cross section.</u>

Cycle 21 is characterized by the fact that the residual bearing capacity of the diagonal subjected to compression is very small and begins a process of lost of bearing capacity in the cross section when subjected to tension. This can be seen in Figure 4-118 at left which represents the situation in lower right diagonal (the blue line). Significant effects of local loss of stability lead to the effect of significant local bending (wraping) of the cross section. In reversal cycle it leads to post buckling redistribution of tensial normal stresses within the cross section. Finally we achive degradation in bearing capacity for tensile forces also. Figure 4-118 at right shows these areas of the wraped parts of the cross section of upper left diagonal. Since the upper left and lower right diagonals operate in tandem, then the decline in the bearing capacity of the diagonal in it when subjected to tension is registered by the recording system using the sensors placed lower left diagonal. To illustrate the

effects as described has been performed overlaying of the graphs of axial forces in the diagonals of cycle 18 and of cycle 21. It is shown in Figure 4-119.

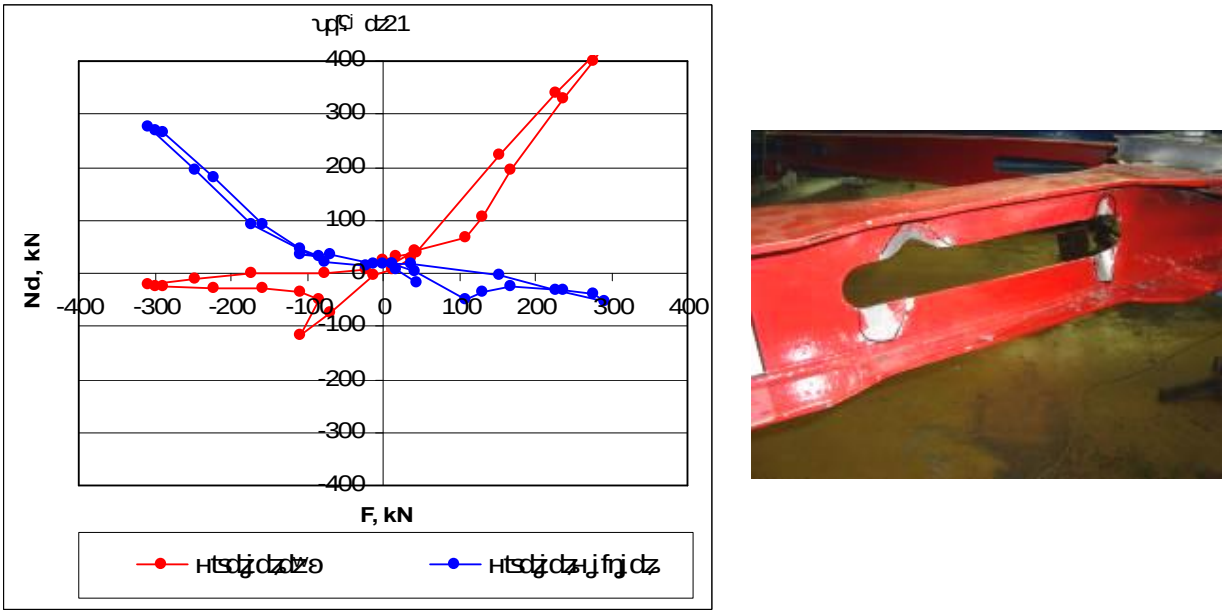

Fig. 4-118 *– model H1, cycle 21 – left, could be seen the effect of the decline in the bearing capacity of the lower right diagonal when subjected to tension; right - effects of local bending (wraping) and exclusion of the most wraped areas in subjecting to tension.*

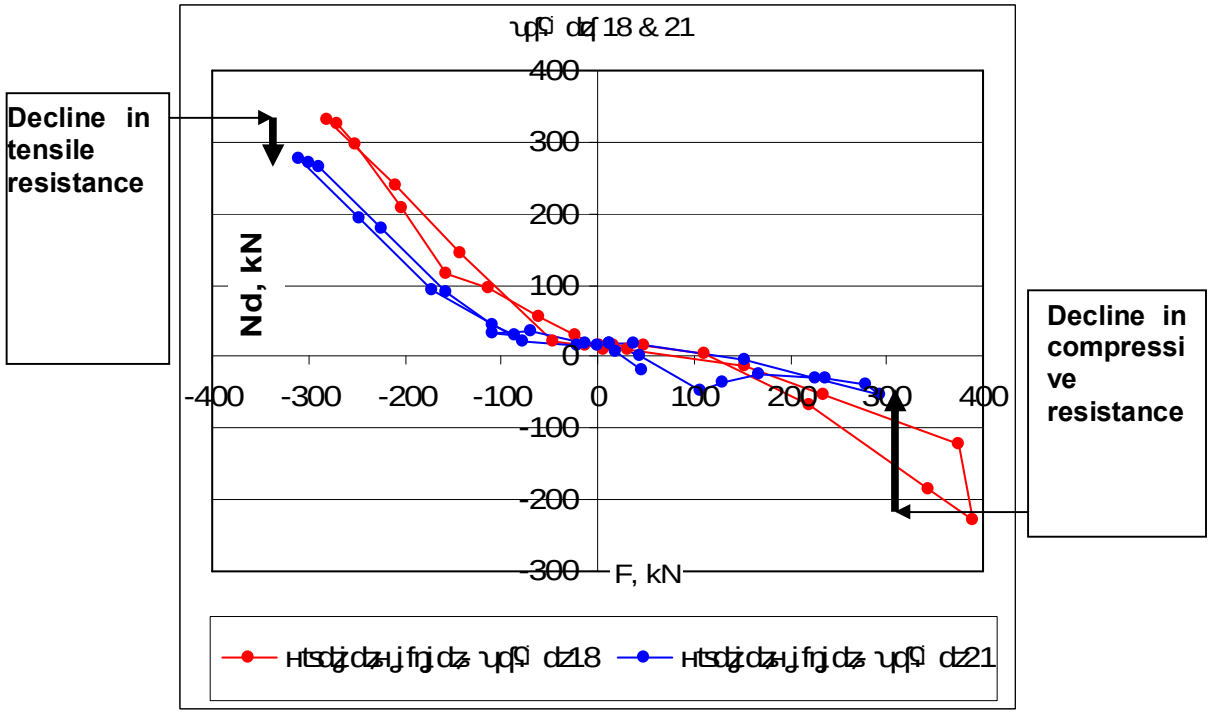

Fig. 4-119 *- model H1, cycle 18 and cycle 21 could be seen the effect of decline in the bearing capacity in tension and in compression.*

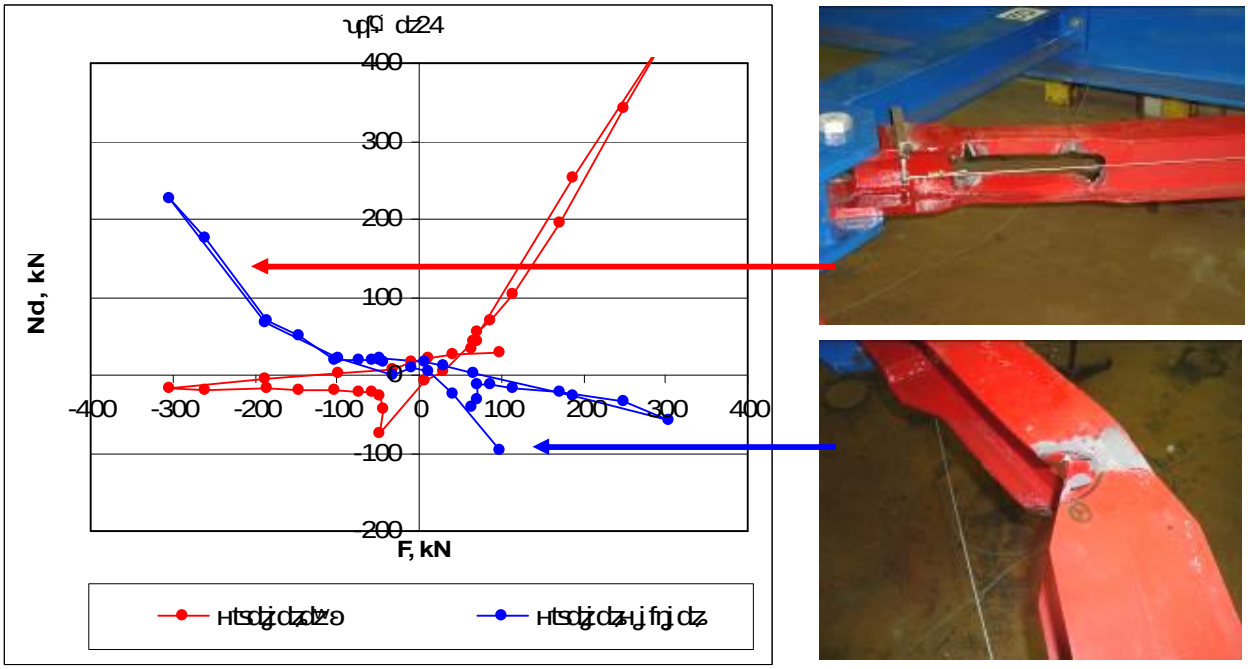

Fig. 4-120 *- model H1, cycle 24, could be seen the effect of decline in the bearing capacity in tension and in compression.*

The behaviour of the diagonals during cycle 24 is shown in Figure 4-120. It is evident the significant decline of the bearing capacity in compression. By the analysis of Figures 4-118, 4-119 and 4-120 we may generalize that after occurrence of LB the behaviour of the diagonal in tension and the behaviour of the diagonal in compression are in interactive relationship. Effects of LB appear to be initial imperfections in applying pressing force thus leading to a steady decline in the bearing capacity of the diagonal subjected to compression. Meanwhile the flange warpings due to LB influence in such manner that part of the cross section, so it does not work effectively (because of stress redistribution) also if subjected to tension (Fig.4-118 at right). This gives rise to a mechanism of decline in the bearing capacity of the diagonal if subjected to tension in case of large story drifts. The decline of bearing capacity in tension is much smaller than the decline of the bearing capacity in pressed state (Fig. 4-119).

In the next series of Figures (from 4-121 to 4-126) are shown the values of the forces in the diagonals depending on the maximum horizontal displacement and depending on the applied force F. Since inelastic cycles are repeated 3 times the given graphics show the first and last cycles of a group. It has been also analyzed the change in graphics between the first and the last report - Figure 4-126.

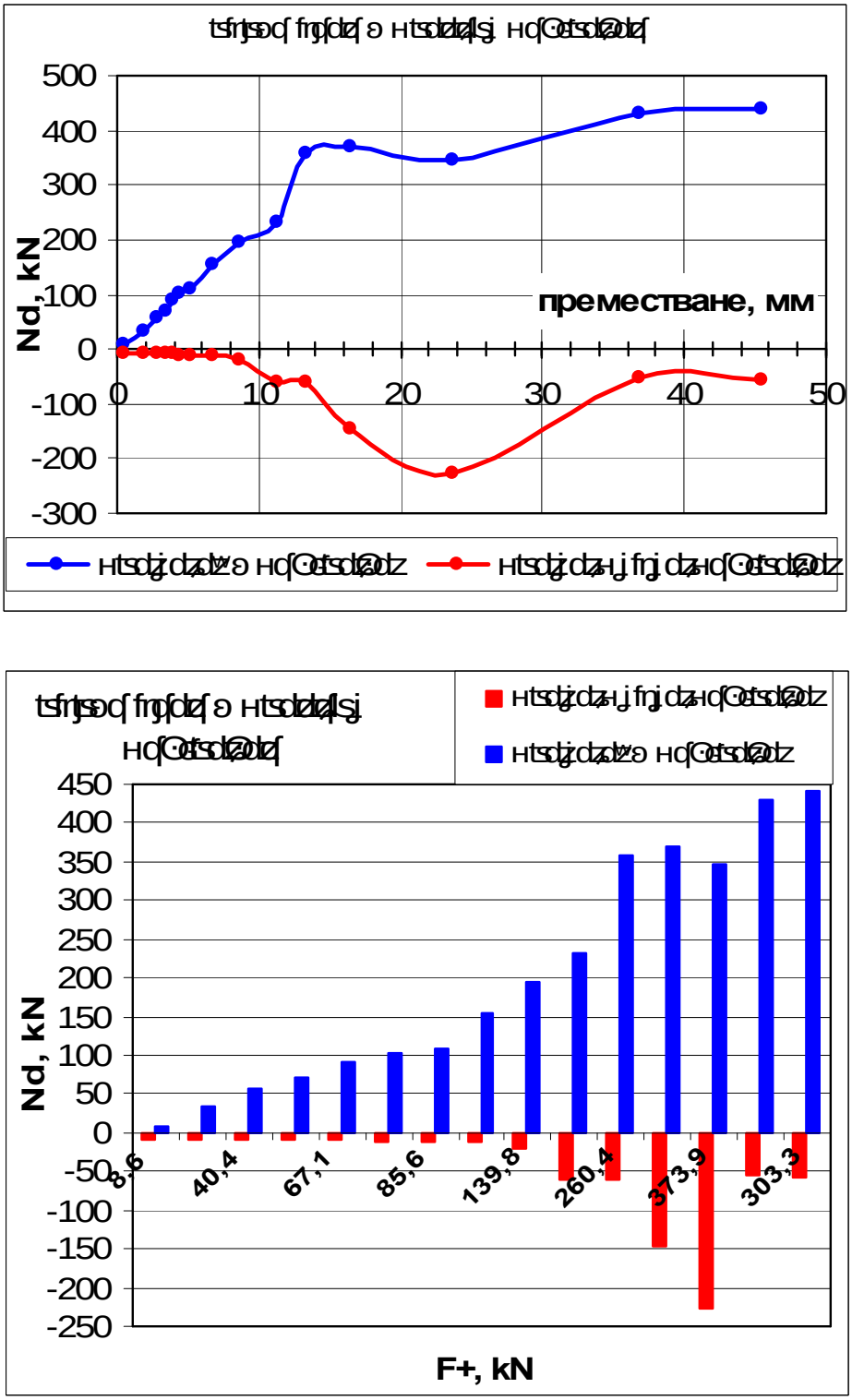

Fig. 4-121 *– model H1, axial forces Nd in the lower diagonals depending on the frame drift (diagram above) and horizontal force F (diagram below). Diagrams are formed with direction being "+" and based on the fisrt reports in a group of cycles;*

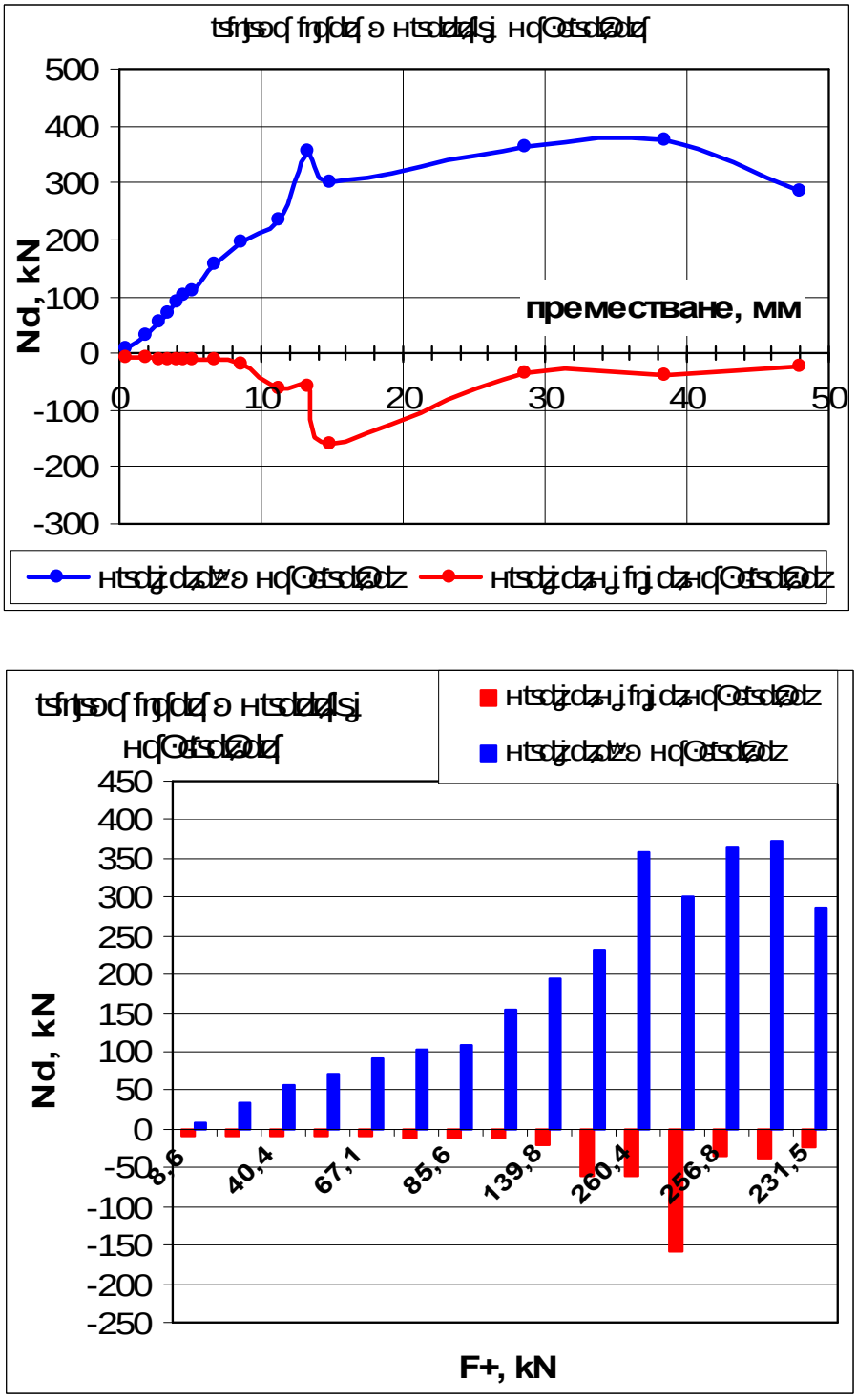

Fig. 4-122 *– model H1, axial forces Nd in the lower diagonals depending on the frame drift (diagram above) and horizontal force F (diagram below). Diagrams are formed with direction being "+" and based on the last reports in a group of cycles;*

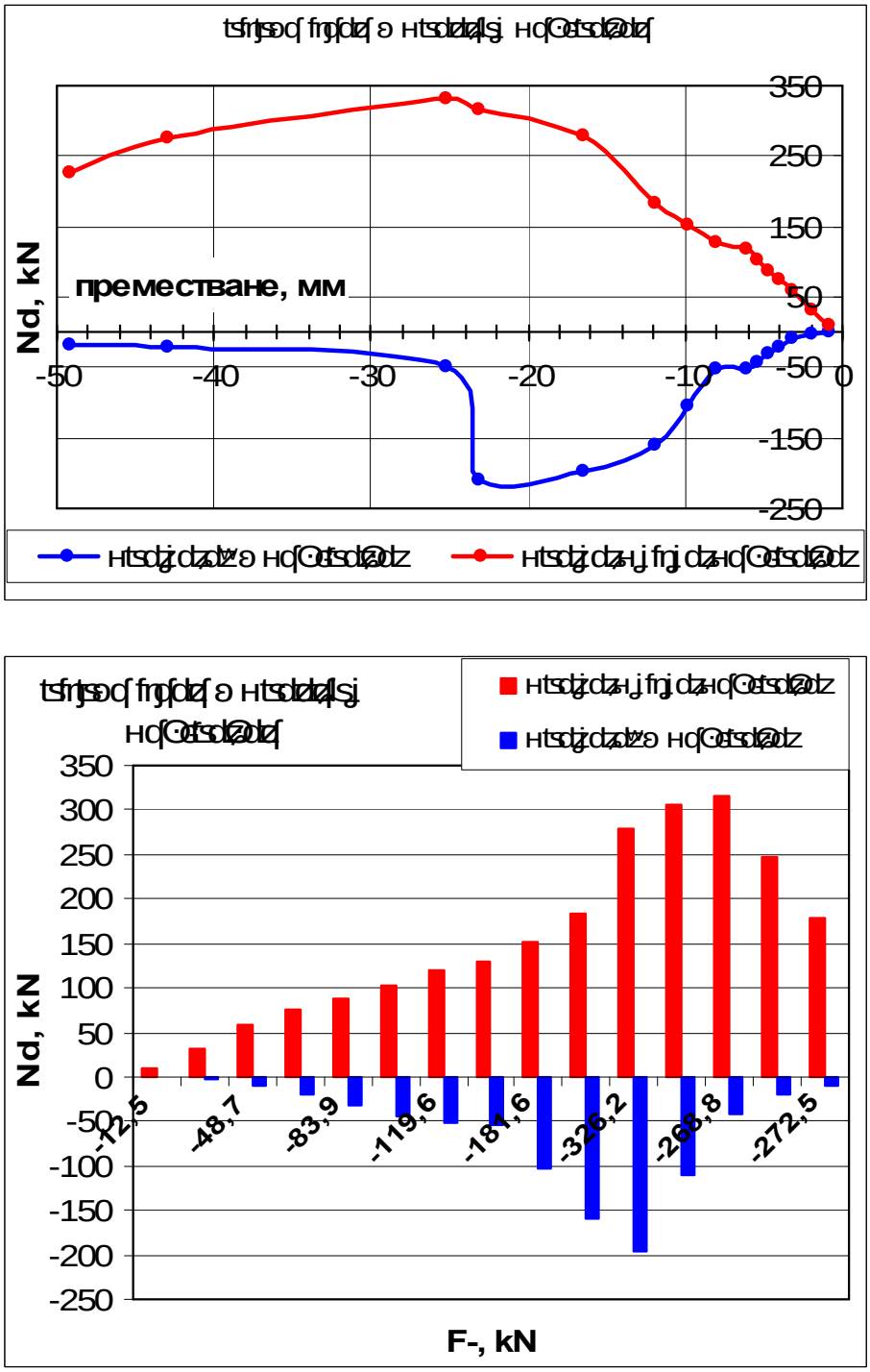

Fig. 4-123 *– model H1, axial forces Nd in the lower diagonals depending on the frame drift (diagram above) and horizontal force F (diagram below). Diagrams are formed with direction being "-" and based on the fisrt reports in a group of cycles;*

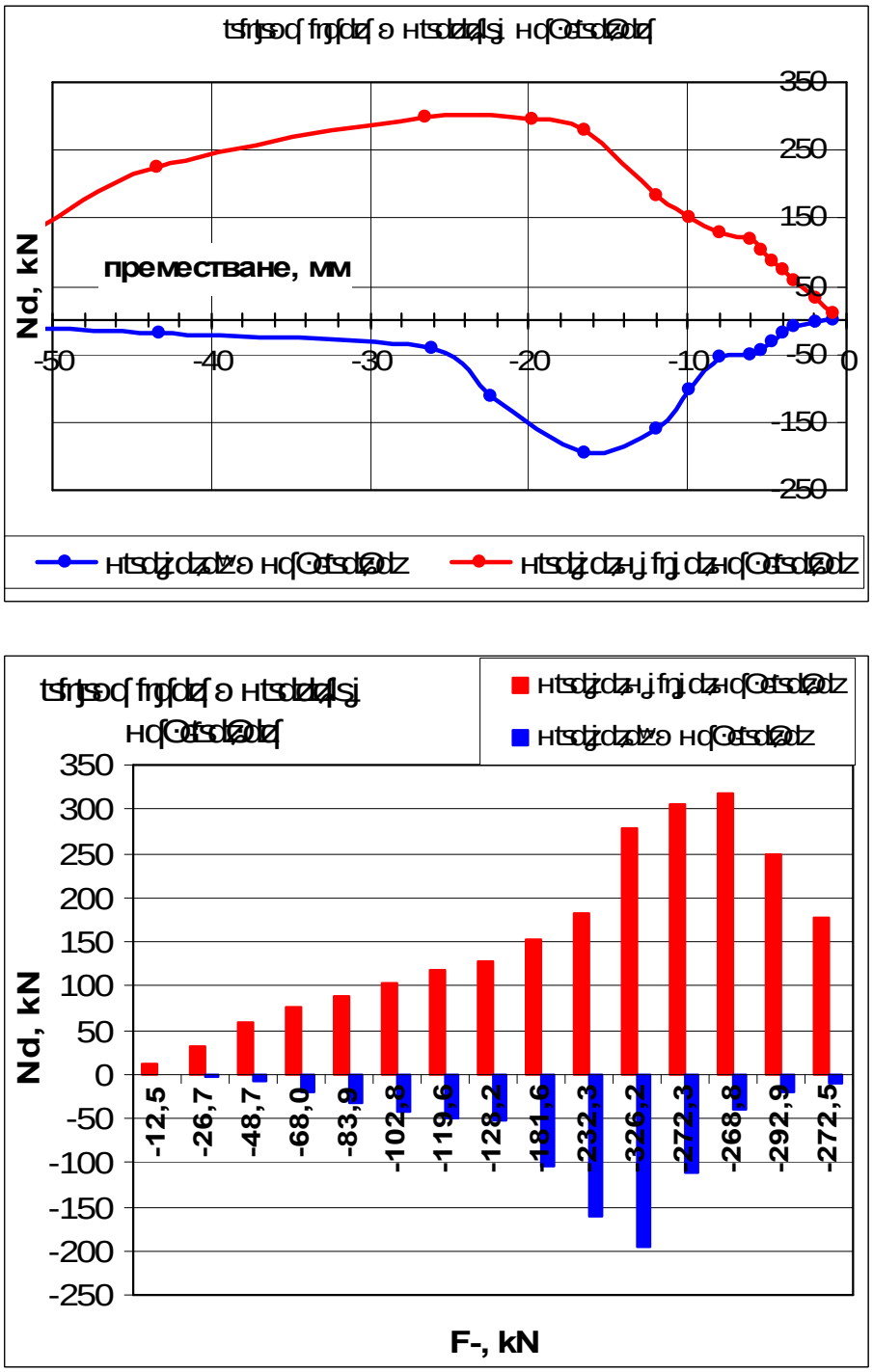

Fig. 4-124 *– model H1, axial forces Nd in the lower diagonals depending on the frame drift (diagram above) and horizontal force F (diagram below). Diagrams are formed with direction being "-" and based on the last reports in a group of cycles;*

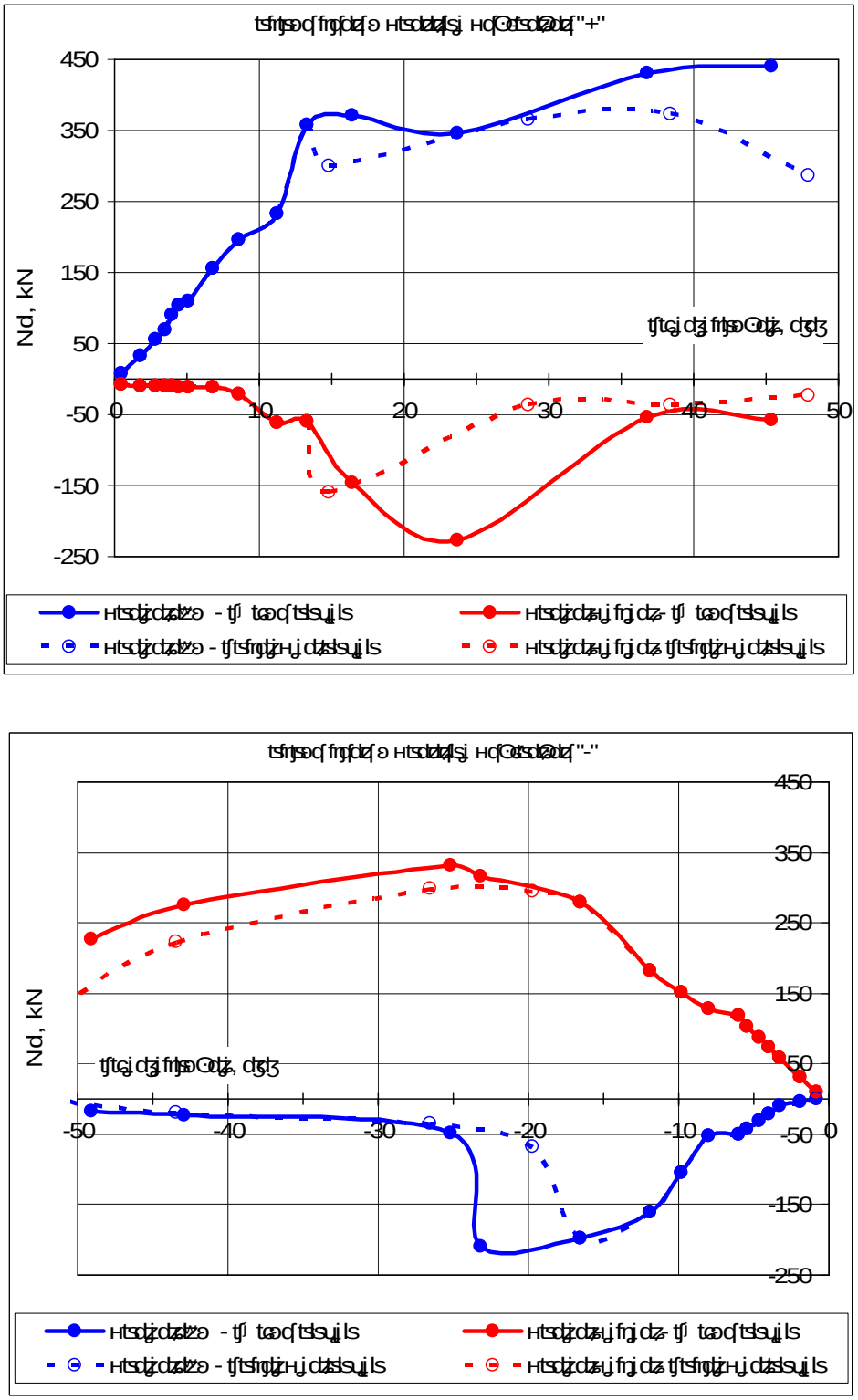

Fig. 4-125 *– model H1, axial forces Nd in the lower diagonals depending on the story drift. Diagrams are formed having direction "+" (upper part) and "-" (lower part) and based on the first and last reports in a group of cycles;*

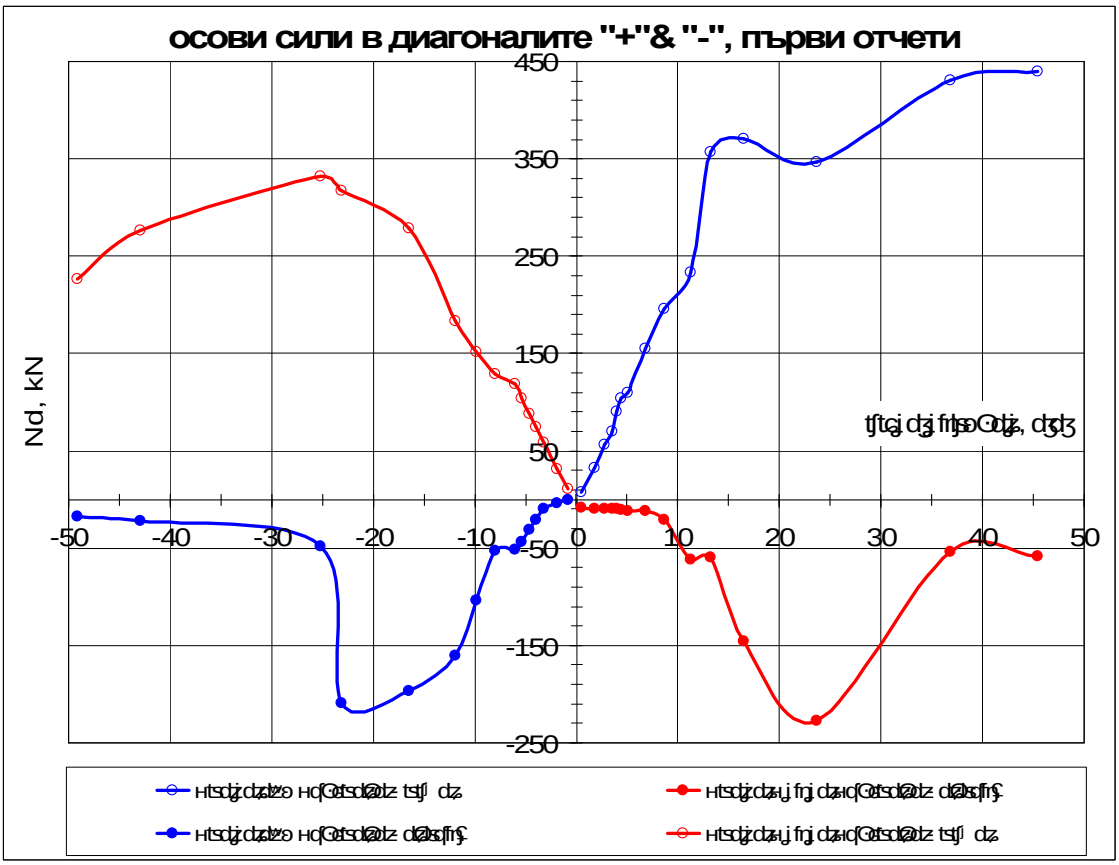

Fig. 4-126 *– model H1, axial forces Nd in the lower diagonals depending on the frame drift (above). Diagonals marked in colour in the Figure (below) correspond to the colour of the lines (in the upper graph). Diagrams are formed based on the fisrt reports in a group of cycles;*

As mentioned in the exposition above inductive sensor ID9 was mounted in the axis of the member thus allowing measurement of the axial displacements within the diagonal. Figure 4-127 presents the graph of the relationship "axial force - axial displacement" in tandem comprised of upper left and of lower right diagonal. The graph includes cycles in which there is post-buckling behavior of the diagonal. From the Figure becomes clear that after the occurrence of the first buckling of a pressed diagonal a decrease of the bearing capacity in compression follows. With each performed cycle the decline in bearing capacity increases and in last loading cycles the diagonal virtually does not obtain bearing capacity when subjected to compression. It can also be pointed out that with increasing the amplitude of the applied displacement pressed diagonal begins to lose its bearing capacity even at positive values of the displacements. This can be explained by the fact that in its previous tensile cycle the diagonal has elongated and therefore diagonal compression force apears prior reaching of the frame its neutral position. This phenomenon is not new. It can be observed also in the results of experiment 1 or in literary sources [39, 42].

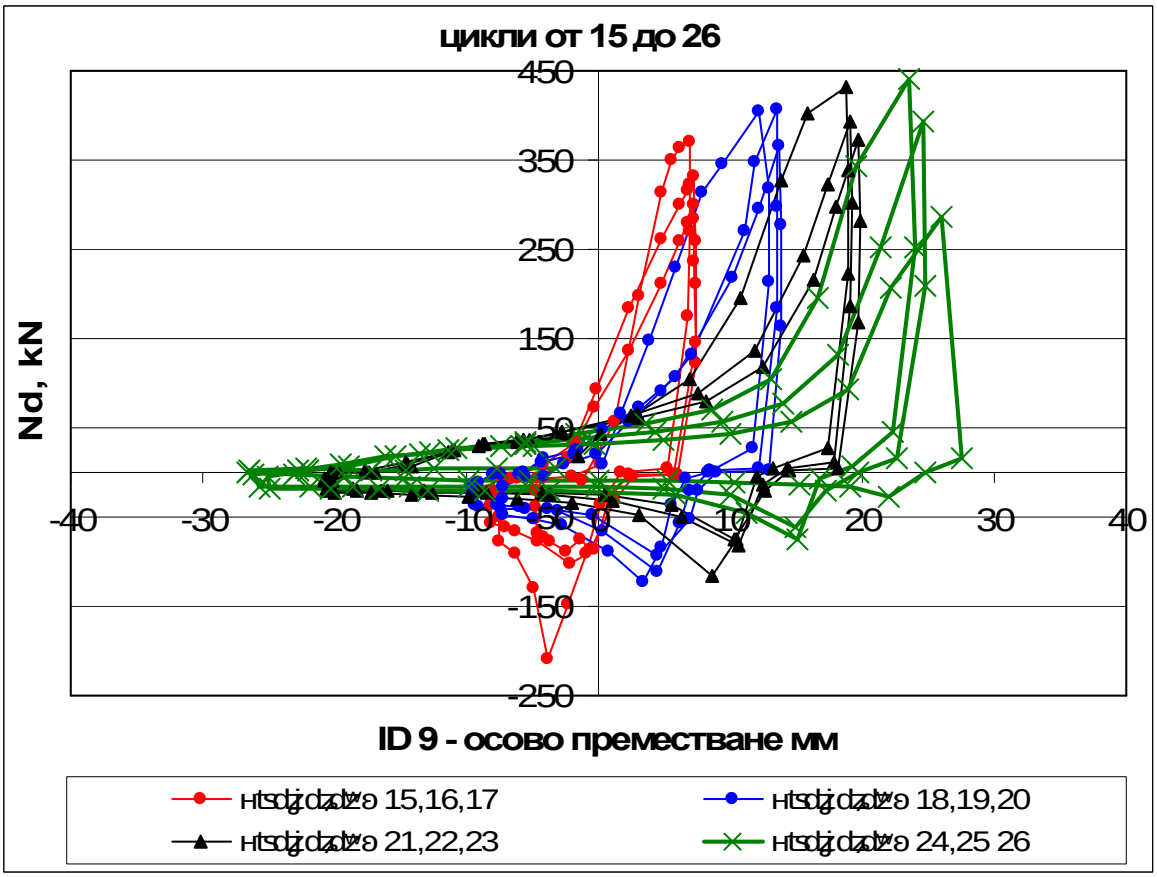

Fig. 4-127 *– model H1, graph of the relationship between the axial force Nd against the axial displacement (shortening and elongation) of the upper right and lower left diagonal. The Figure includes all elasto-plastic cycles from 15 to 26.*

Similar relationships between the axial force and axial displacements of the members subjected to cyclic tension and compression have been published in the literature. Figure

4-128 represents two relationships derived from *Black, Wenger and Popov* in the first such experiment conducted in EERC at the University of Berkeley in the year of 1980. As can be seen from the comparison in Figure 4-127 and 4-128 similarity of resulting graphs is obvious. In graphs of *Black, Wenger and Popov* (1980) [39] are shown only the first cycles of a group having the same amplitudes i.e. the experimental result is filtered. The author has shown just two of the results contained in literary source [39], where the shape of the cross section is similar to the diagonal cross section of model H1 as the slenderness of the diagonal is similar. Graphs shown in Figure 4-128 are for members having slenderness of value 80 and the values of the slenderness of the diagonals in model H1 equal to 80.1. Both values of slenderness are virtually identical.

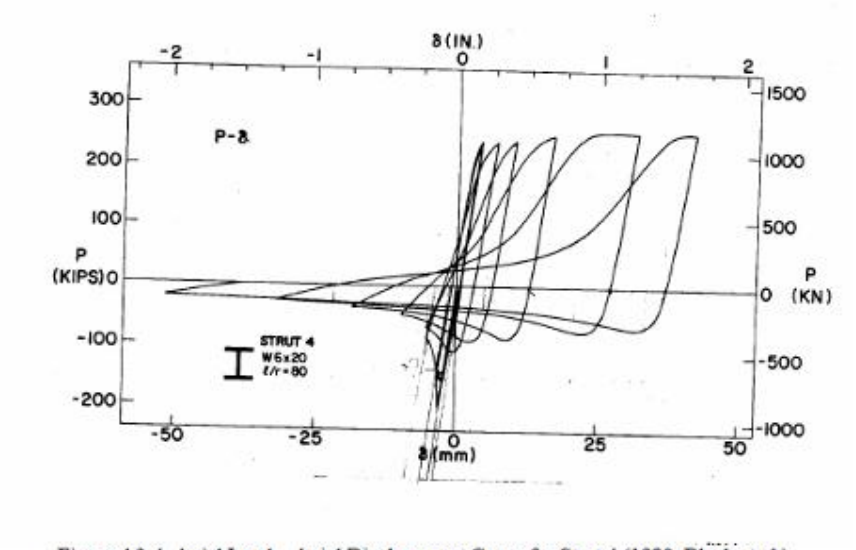

Figure A2-4. Axial Load – Axial Displacement Curve for Strut 4 (1980, Black et al.)

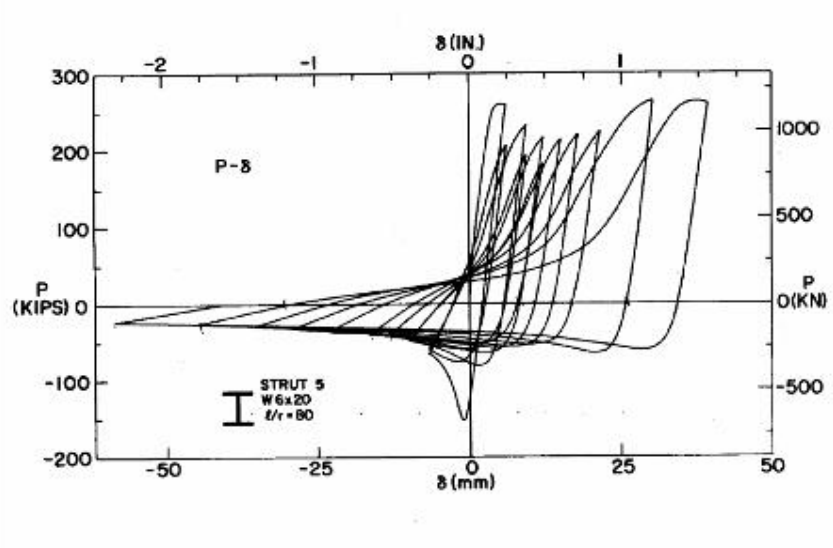

Figure A2-5. Axial Load – Axial Displacement Curve for Strut 5 (1980, Black et al.)

Fig. 4-128 *- graph of the relationship of axial force Nd against axial displacement obtained by Black, Wenger and Popov, literary source [39];*

About the role of the horizontal intermediate member. The following Figure 4-129 shows the relationship axial force - axial displacement of the diagonals of the tandem comprised of upper left diagonal and of lower right diagonal. A characteristic feature of the behaviour of these diagonals is that lower right diagonal retained its straight form to the very end of the ongoing experiment. This is evident also by the type of the graph given in Figure 4-129. Lower right diagonal (blue line) is not involved in energy absorption.gg

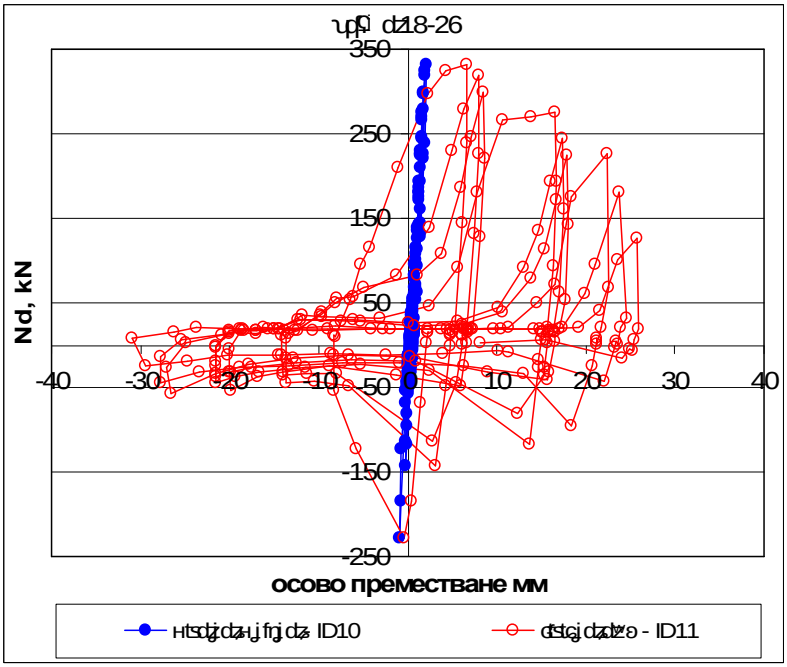

Fig. 4-129 *– model H1, graph of the relationship of axial forces Nd against axial displacement (shortening and lelongation) of upper left and lower right diagonal (the graph above). A photo showing buckling of upper left diagonal and preservation of the straight form of lower right diagonal (below).*

According to the author this effect of buckling of one of the diagonals in the tandem and the lack of buckling in the other diagonal is highly undesirable. This leads to a concentration of the entire elasto-plastic behaviour under compression only in restricted zone. It is clearly seen on Figure 4-129 that all plastic tensile deformations and the effects of loss of stability are concentrated only in the upper left diagonal. The author highlights the negative impact of such concentration with the argument that thus are enhanced the amplitudes in warping caused by LB, there is a concentration of plastic strains in the walls of the cross section subjected to compression and in less value of the frame drift v (or φ) is reached the end of inelastic behaviour of the diagonal because of the low cycle fatigue. Such a phenomenon is described in the studies of *El-Tayem and Goel* (1986) [51] and in the summary made by *Bruneau* [42] relying on proprietory researches and by citing other researchers. They reported a case when "X" CBF the both halves of pressed diagonal buckle in elastic phase but in plastic phase could be observed an effect in which one half concentrated plastic deformation and the other half did not participate. The phenomenon is the same as the described in the passage above. *Bruneau* [42] explains this with the upcoming progressive degradation of the bearing capacity of the pressed diagonal (see Figures 4-127, 4-128, 4-129) and the resulting decline in compressive force in the entire diagonal (in our case in the entire tandem). A way to avoid this negative phenomenon the author sees in the proposed by him composition of CBF (configuration utilizing horizontal intermediate member) and the correct selection of the slenderness of the diagonal and the stiffness of the horizontal intermediate member. Of particular importance is that the horizontal should be of sufficient flexural stiffness so as to force the other pressed diagonal of the tandem to buckle also as well. Analysis of this question is proposed in item 4.8.4.

Concerning the relationship storey drift - local ductility. In this experiment the location of sensor ID9 handed us the opportunity to explore the relationship between the axial displacement of the diagonal δ and the storey drift of the frame $v(\Delta)$. Prooving of such a relationship experimentally is important thus by forecasting the behaviour of the frame to reach information about the degree of development of plastic strains in the diagonals. Such relationship allows to evaluate the relationship between the global ductility of the CBF and the corresponding requirement for the local ductility of the diagonals. Figure 4-130 presents the main inductive sensors ID2 and ID9 through which is gained the information on the storey drift v and the elongation (respectively shortening) of diagonal *δ.* On the following Figure 4-131 are presented graphs of the axial displacement of the diagonal as a function of the storey drift of the frame. Selectively are shown the same characteristic cycles of the experiment as presented in Table 4-30 and was added cycle 10 as a prominent representative of the fully elastic behaviour. We have to remind that in item 2.1. of this PhD thesis were derived some theoretical formulas on the relationship of the axle diagonal displacement against the storey drift. In comparison on Figures 4-131 and 4-132 will be overlaid the graph of equation (2.1-3) from Chapter 2 which for convenience has been written here one more time.

$\delta = \Delta.\cos\alpha$ (2.1-3).

ŭ - axial elongation or shortening of the diagonal

$\Delta \equiv v$ - storey drofy (Inter-floor displacement) of CBF, conditional symbol v is taken to be consistent with the symbols and abbreviations adopted in [48, ECCS].

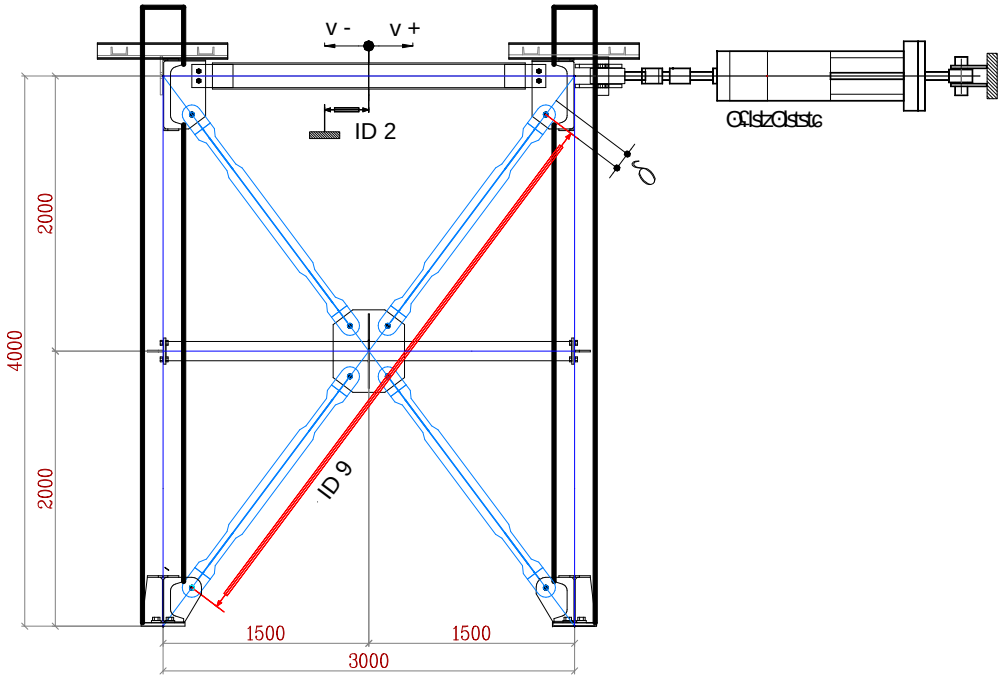

Fig. 4-130 *– model H1, scheme of the sensors for determining the storey drift v (ID 2) and axial displacement (shortening and elongating) δ (ID 9) of the tandem comprised of upper right and lower left diagonal.*

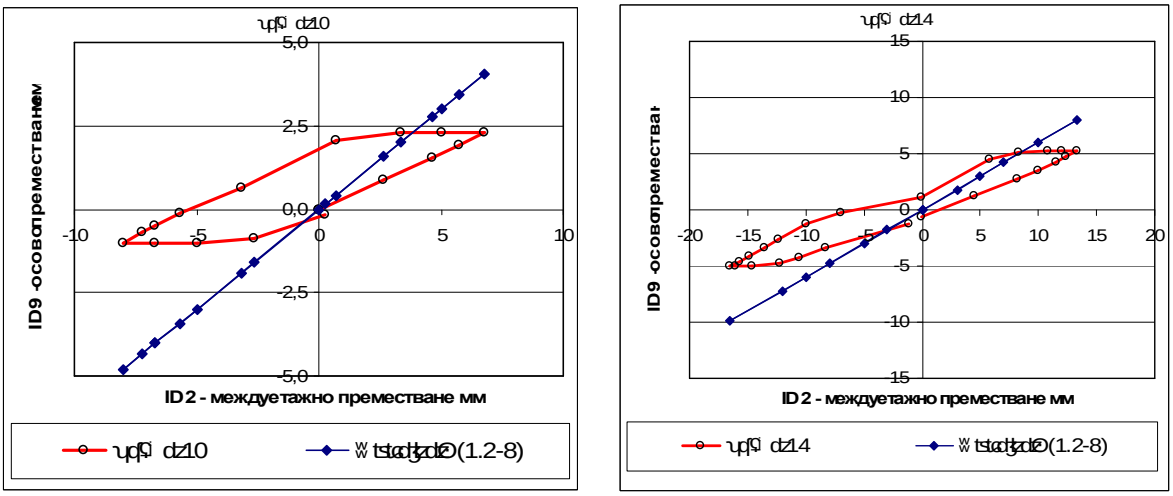

Fig. 4-131 *– model H1, graph of the relationship between the storey drift v (ID 2) and axial displacement δ (ID 9) of the tandem comprised of upper right and lower left diagonal for cycles 10 and 14.*

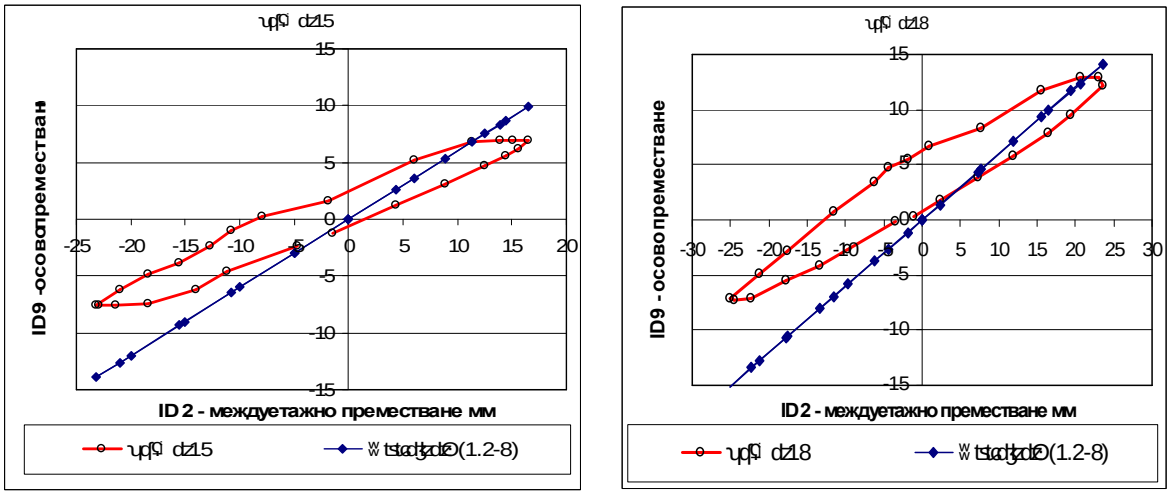

Fig. 4-131 – continued. *model H1, graph of the relationship between the storey drift v (ID 2) and axial displacement δ (ID 9) of the tandem comprised of upper right and lower left diagonal for cycles 15 and 18.*

From the analysis of the loops shown in Figure 4-131 can be concluded that the theoretical formula deviates significantly from the experimental results in cycle 10. It has been observed that cycle 14 is close to the results but again the difference stays significant. By entering the plastic phase (cycle 15 and especially cycle 18) the experimentally obtained relationship and the theoretical formulas start seeming alike. The similarity is mostly evident towards direction "+" in cycle 18. For example, if we follow direction "+" we will find that the differences in the maximum values obtained by the experiment and by the theoretical formula are 76% for cycle *№10*, 53% for cycle *№14*, 43% for cycle *№15* and 16.7% for cycle *№18*. Larger differences are recorded in cycles with fully elastic behaviour. Explanation on the latter we may obtain in two ways. The first is that ID 9 measures displacements between the physical beginning and end of the diagonals and its base (working length) equal to 4185 mm while formula (2.1-3) is derived for the entire axial length of the diagonal (which is 5000 mm). In other words to the result of the experiment should be added also the elastic deformations in the frame's joints. One possible explanation for the difference in results is that formula (2.1-3) has been derived in the prerequisite of non-lengthening feature of the frame. Prerequisite which is obviously comfortable but unreal. Therefore in the elastic phase of deformation of CBF differences between theoretical and experimental results are significant. Here we should emphasize that the purpose of the formula (2.1-3) is not the performance of analysis in elastic phase. Elastic phase could be reliably interpreted by modern software. Of interest is the plastic phase and this is where we will focus our attention. For the purpose in Figure 4-132 are added graphs similar to those presented in Figure 4-131 but covering cycles 21 and 24. These last two cycles are characterized by a significant elasto-plastic behaviour.

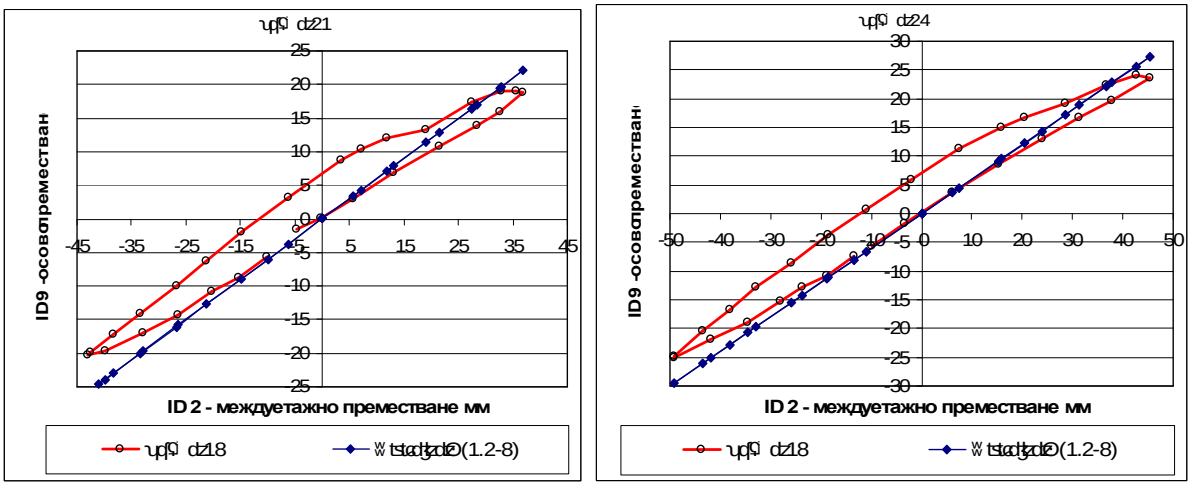

Fig. 4-132 *– model H1, graph of the relationship between the storey drift v (ID 2) and axial displacement δ (ID 9) of the tandem comprised of upper right and lower left diagonal for cycles 21 and 24 in the circumstances of significant plastic deformations.*

From the analysis of the loops shown in Figure 4-132 could be concluded that with the increase of storey drift theoretical formula begins matching the experimental results. For example, in plastic phase in cycle 21 maximum values in direction "+" obtained by the experiment and by theoretical formulas differ by 17.3% and for cycle 24 this difference equals to 15.8%. Here the author adds his personal assessment that in even greater drifts matching of the results obtained by the experiment and by theoretical formula will constitute a difference not larger than 5%. Unfortunately in the rest of the experiments where the drifts are appropriate the placement of sensors ID9, ID10, ID11 & ID12 was distanced from the axis of the diagonals thus "introducing" the effects of rotation of the diagonals in the reports received. Therefore the above statement cannot be proven by experimental results within this PhD thesis.

To achieve matching of the theoretical to the experimental results the author proposes formula (2.1-3) to be corrected by a reduction ratio of 0,90 being transformed to the form:

$$\delta = 0,9.\Delta.\cos\alpha \qquad (4.8\text{-}6)$$

ŭ - axial elongation or shortening of the diagonal

$\Delta \equiv v$ - storey drift of the CBF;

The following Figures 4-133, 4-134, 4-135 show a comparison of theoretical results obtained from equation (4.8-6) with the experimental results. The comparison is made only using the maximum values of inter-floor displacements. When in the experiment persisted a group of cycles then is used the arithmetic average report thereof.

	6,754	8,604	11,253	13,262	15,492	23,944	37,669	46,589
"+"	2,300	3,000	3,750	5,200	7,167	13,150	19,167	24,700
	3,64716	4,64616	6,07662	7,16148	8,36568	12,9299	20,3414	25,1581

Fig. 4-133 *– model H1, comparison of the results for δ obtained by the experiment and by formula (4.8-6). Direction "+";*

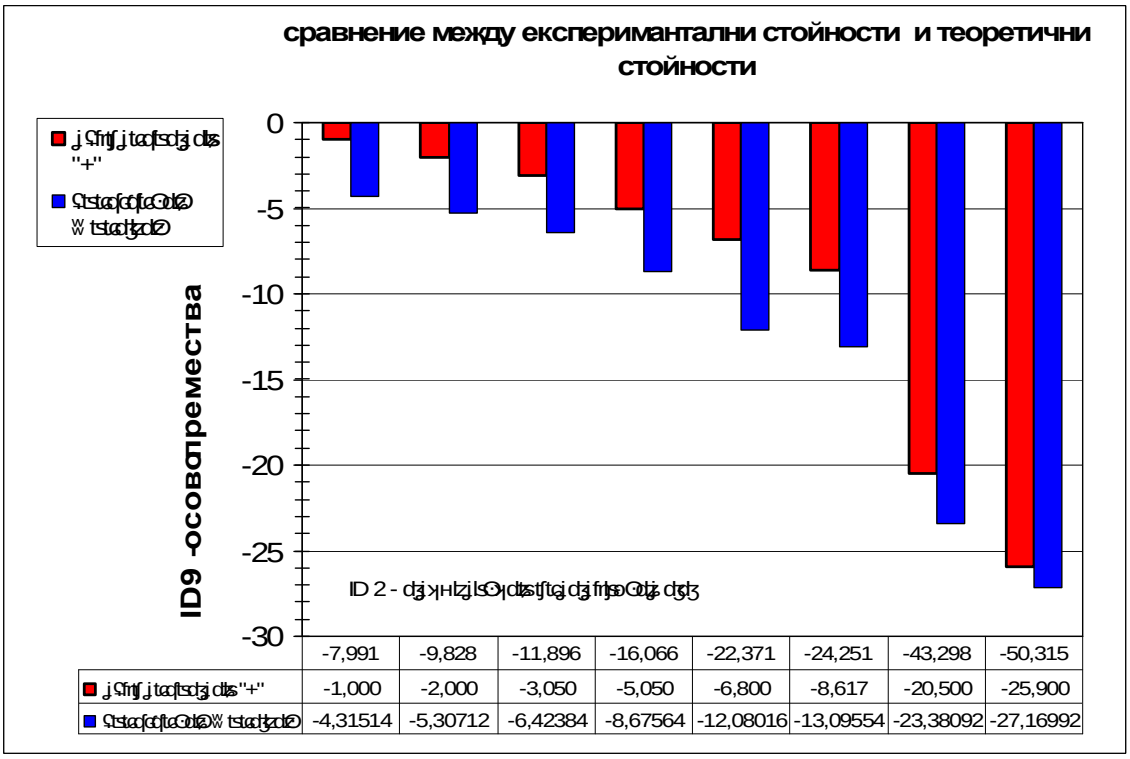

	-7,991	-9,828	-11,896	-16,066	-22,371	-24,251	-43,298	-50,315
"+"	-1,000	-2,000	-3,050	-5,050	-6,800	-8,617	-20,500	-25,900
	-4,31514	-5,30712	-6,42384	-8,67564	-12,08016	-13,09554	-23,38092	-27,16992

Fig. 4-133 *– model H1, comparison of the results for δ obtained by the experiment and by formula (4.8-6). Direction "-";*

The resulting maximum differences in positive direction "+" and in negative direction "-" are respectively 1,8% and 4,9%.

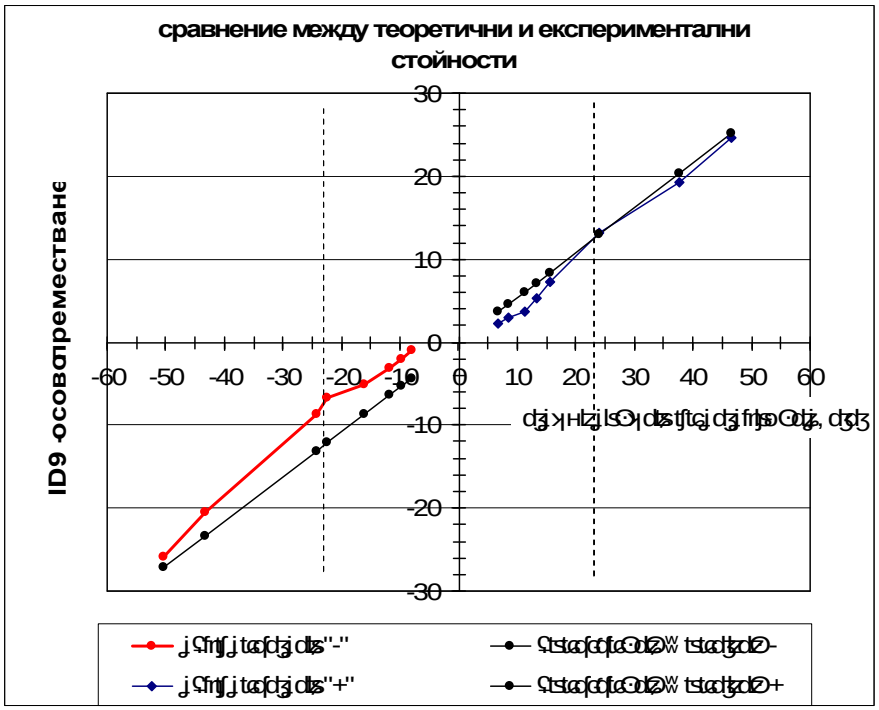

Fig. 4-135 *– model H1, graph of maximum values of δ obtained by experiment and by formula (4.8-6).*

Figure 4-135 presents graphical overlay of the maximum arithmetic average values for displacement ŭ obtained by experimental measurements and by formula (4.8-6). The area enclosed between the dotted lines is the phase of the elastic response (this concerns the tensioned tandem of diagonals) of the model. It is obvious that there the differences are most significant. In elasto-plastic phase corrected theoretical formula gives very good results. The author believes that the achieved matching is much better and the derived formula (4.8-6) is easy to implement from the initial phase of designing of the CBFs.

Comparison of the experimentally obtained bearing capacity with the forces defined in [1]. One of the important guiding questions in the analysis performed related to the behavior of the diagonals is the comparison between the theoretical bearing capacity obtained based on [1] and the experimentally obtained bearing capacity of the diagonals in tension and compression.

Theoretical bearing capacity of the diagonals of model H1 in tension and compression are determined under BDS EN 1993-1-1. As before and here all ratios γ_{Mi} will be assumed equal to 1. The equivalent to the entire cross section actual yield strength is determined by the equation (4.8-3), which in respect to model H1 is as follows:

$$f_{y,eff} = \left(480.225,4 + 2.600.288,2\right).\frac{1}{480 + 2.600} = 270,3N/mm^2$$

Plastic tensile resistance of the reduced cross section is as follows:

$N_{pl,t,RD} = 1120.270,3 = 302736 \approx 303kN$;

The design resistance (bearing capacity) of the reduced cross section is defined by the limit tensile force of the steel in the equation:

$$N_{t,u,RD} = A_{w,OC}.f_{u,w} + A_{f,OC}.f_{u,f} = (320.324 + 800.351,7).\frac{1}{1000} = 385,04kN$$

Design buckling resistance (bearing capacity) of the compressed diagonal should be defined as follows:

$$\varepsilon = \sqrt{\frac{235}{f_{y,eff}}} = \sqrt{\frac{235}{270,3}} = 0,932$$

$N_{b,Rd} = \chi \frac{A.f_{y,eff}}{1,0}$, and the buckling ratio for efficient slenderness

$\lambda_{eff} = 80,1$, $\bar{\lambda}_{eff} = \frac{80,1}{93,9.0,932} = 0,915$ and in case of buckling curve "c" for assumed slenderness 0,915 has been defined $\chi = 0,5906$

$$N_{b,Rd} = \chi \frac{A.f_{y,eff}}{\gamma_{M1}} = 0,5906 \frac{1680.270,3}{1,0} = 268193,8N = 268,2kN \qquad (4.8\text{-}7)$$

As seen in first reading it is noteworthy that the bearing capacity in compression obtained by formulas under BDS EN 1993-1 exceeds the experimentally obtained bearing capacity (see Figures 4-121 and 4-123). This result is not logical since the dimensioning procedures of Eurocode are taking into consideration a number of other negative factors that have not occurred in the experiment H1.

The author makes the following comment on the above finding. Since the diagonals of model H1 have slenderness of 80 which implies buckling in plastic phase and considering the presence of areas of reduced cross sections therein, then it is fully expected that the first plastic deformations that occur in the member to be caused by the tension in it. We expect them to occur in the transition between the reduced cross section and the non-reduced cross section. Therefore the formula that is embedded in [1] cannot be applied directly because the studied member has plasticized in tension and then was subjected to compression. This effect for which we have a background of deformations in plastic phase is known as the effect of Baushinger [6] and it can explain the phenomenon registered. Such an approach based on the effect of Baunshinger is applied in studies conducted by *Black, Wenger and Popov* (1980) [39] and *Zayas, Popov and Mahin* (1980) [103]. In order to finish this statement of ours we will cite a graph relationship shown at [39] (Figure 50, page 85) - Figure 4-136. From this Figure becomes clear that in members of slenderness about 80 there is a decline of the bearing capacity in compression of about 75% which corresponds to the case studied by us.

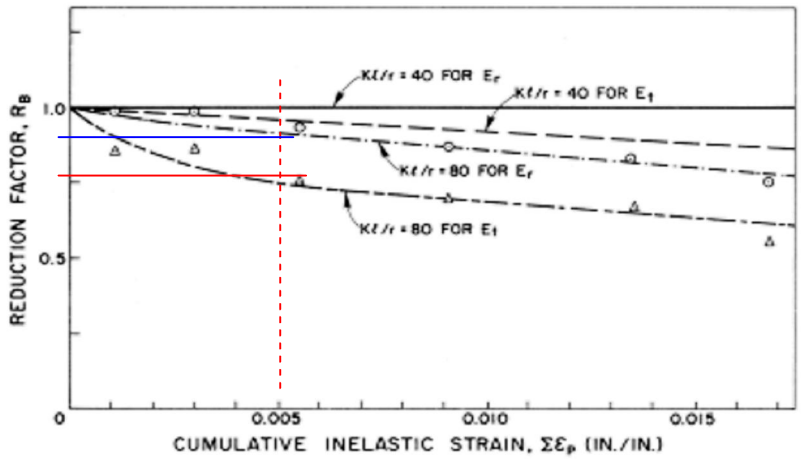

Fig. 4-136 *- decline of the bearing capacity in compression in the presence of pre-plastification caused by tension (effect of Baushinger) – literary source [39].*

In the exposition below we will introduce also another approach that relies entirely on [1]. Presence of long reduced areas is an important factor. The net cross section (that of the reduced zone) covers a length of 250 mm and is implemented in two places in the member. Therefore the theoretical bearing capacity of the diagonal in compression could be determined by the net cross section and not by the gross one as was done in equation (4.8-7). If the correct the value of the cross-sectional area shall be obtained the folowing:

$$N_{b,Rd} = \chi \frac{A.f_{y,eff}}{\gamma_{M1}} = 0,59\frac{1120.270,3}{1,0} = 178614,2N = 178,6kN \qquad (4.8\text{-}8)$$

The value obtained using (4.8-8) is 66% of the value obtained using (4.8.-7) which is conservative but secure. Comparison of theoretical bearing capacities in equation (4.8-8) and the maximum tensile and compressive forces in the diagonals obtained in the experiment is presented in Table 4-31.

Table 4-31

diagonal	**tension**			**compression**	
	$N_{pl,t,RD}$	$N_{t,u,RD}$	experiment	theoretical acc.to[2] (4.8-7)	experimental[3]
lower right	303	385,04	cannot be cut	-201,2	cannot be buckled
lower left	303	385,04	440,08	-201,2	-227,8
upper right	303	385,04	cannot be cut	-201,2	cannot be buckled
upper left	303	385,04	332,06	-201,2	-209,18

[2] If we use the value obtained by the equation (4.8-7) and we reduce it by 0,75 as indicated by Figure 4-136, then compressive resistance equals to 201,2 kN.

[3] This is the maximum force which has been measured in the respective lower diagonal of the tandem in case of buckling.

Analysis of the results in Table 4-31 can be summarized in the conclusion that the fracture in the diagonals appear for various reasons. The probable cause of the fracture of lower left diagonal is reached tensile strength of the material. The reason for the fracture of the upper left diagonal more likely is the low cycle fatigue that has occurred in the unexpected form of loss of stability of the member. Here should be recalled that in this experiment were measured forces only in the lower diagonals therefore direct transfer of the measured values for the upper diagonals is only indicative. However the author believes in the existence of a low cycle fatigue in the upper left diagonal. To illustrate this statement of his, has been made a kind of photoreport in Figure 4-137 on the mechanism of occurrence of lockal buckling and cross section fracture. Inelastic deformations in this diagonal occurred in cycle 18 and in cycle 26 was observed fracture in the cross section of webs and flanges.

Of interest is the question why in the upper left diagonal occurred such an "unexpected" form of loss of stability (buckling). We named it unexpected since premilinary sizing of model H1 and conducted solution of the equation of stability by FEM, showed that the first mode of buckling of the diagonals should be in the plane of the frame. A major factor that has contributed to the occurrence of the so-called unexpected form of buckling is the prevented rotation of the bolt joint. A registered fact is that the bolts were significantly tightened in the assembly of experimental model H1. This inevitably led to a partial restraining of the rotation of the diagonal end section. The second factor that according to the author is more significant, is the fact that the slenderness of the diagonal is of low value and prior the occurrence of the loss of stability of the member has occurred partial plasticization in the zone of transition between the reduced and the non-reduced cross section. Plasticization affected most significantly the web because the web material has appreciably[4] lower yield strength.

cycle 18 - first buckling in the diagonal

significant forms of LB, cycles 21-23

Fig. 4-137 - *(see also next page)*

[4] The steel plate by which has been made the web has yield strength of 25% lower than the yield **strength of the flange steel plate.**

cycles 24-26, a sequence of local buckling in the reduced area accompanied by local warpingg of the web. Follows straightening in tension and fracture of the mostly bent parts of the cross section

Fig. 4-137 continued – *model H1, photo report of the mechanism of development of plastic deformations in the member.*

- *cycle 18 - upper left*
- *cycles 21, 22 and 23 - upper right*
- *cycles 24, 25 and 26 - lower left*
- *cycles 24, 25 and 26 - lower right.*

In overlaying the two mentioned factors we face partial end rotation restraining that modifies the first mode of buckling and causes occurrence of partial plastification in the web. The analysis conducted in Chapter 2 shows that the first plastic deformations occur in transitional areas from the reduced to the non-reduced cross section. To verify this assumption was prepared FEM model and it was solved the equation of stability. Transitional zone of the reduced cross section was modeled using FE with a lower modulus of elastic deformations. Actually thus has been modelled the phenomenon of partial plasticization (as a state) by the use of elastic analysis means. The solution was performed using SAP 2000 V15.5 Advance. The results of the solution are shown in the following Figures 4-138 and 4-139.

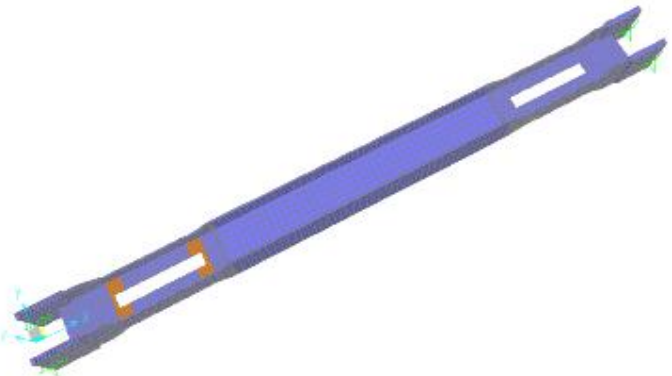

Fig. 4-138 *- Model developed using* SAP 2000 V15.5 ϕdvance*.* Orange areas are the areas in which the material has 10 times lower E modulus.

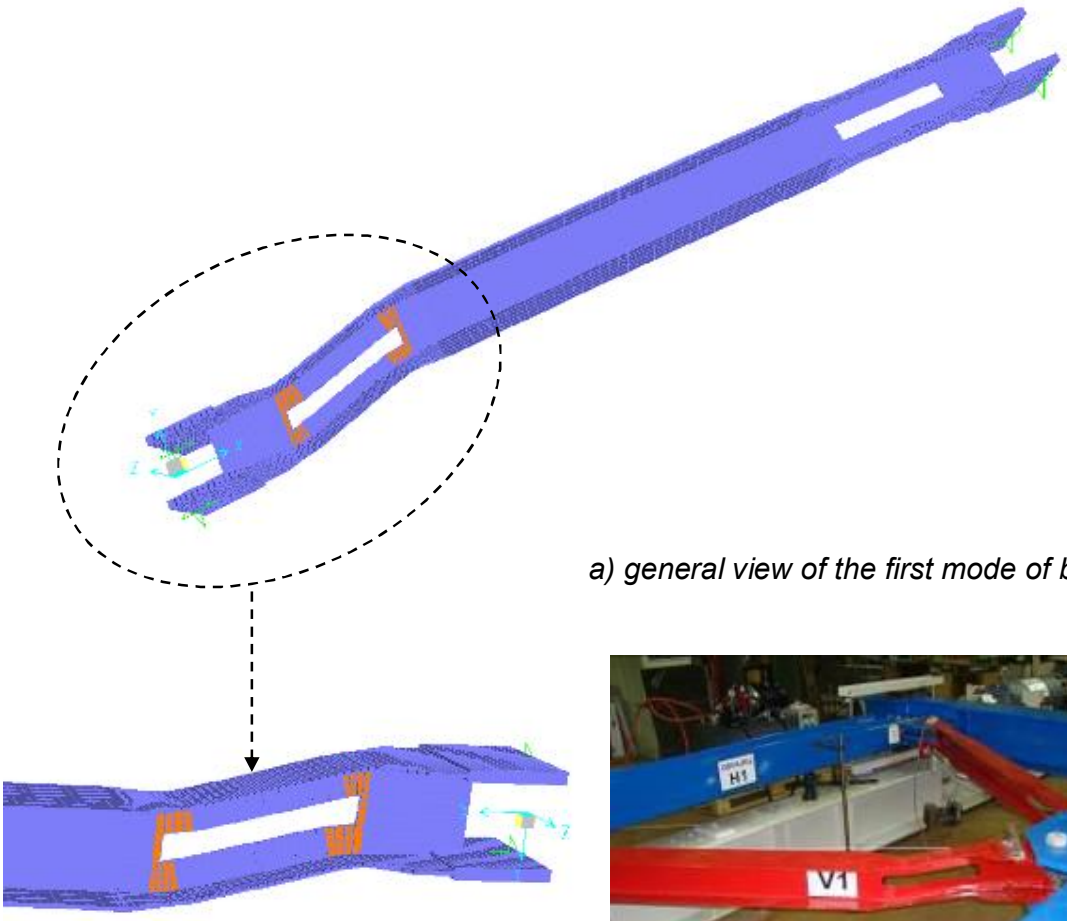

a) general view of the first mode of buckling

b) fragment - a result of the FE model

c) frament – a result of the experiment

***Fig. 4-139** – FE Model developed using SAP 2000 V15.5 Advance; First mode of buckling*

The author believes that performed decision using FE model conducted by SAP 2000 V15.5 Advance and the obtained analogy between the experimental result and numerical simulation shown in Figure 4-139 are sufficially convincing. In summary this shows that the overlapping of the effects of partial end rotation restraining of the diagonals, the low value of slenderness of the diagonals and the effect of Baushinger caused occurrence of buckling out of the plane of the frame. We pay particular attention to this fact because the initial concept for the use of RS (Reduced Sections) in the diagonals requires the letter to buckle in the plane of the frame.

PARTICULAR CONCLUSIONS DERIVED BY THE ANALYSIS OF THE BEHAVIOUR OF THE DIAGONALS OF EXPERIMENTAL MODEL H1

By the analysis made in item 4.8.3. could be drawn the following particular conclusions and generalizations:

- When the diagonals are of low slenderness they buckle in plastic phase. Then the behaviour becomes modified and it is possible the form of loss of stability of a pressed diagonal to concentrate on the reduced section area. This is an adverse effect because it leads to overlaying of effects of plasticization caused by the tensile and compressive force.

- When plastic deformations concentrate in the reduced cross section zone and the diagonal buckle out of the frame plane, then occurs effects of low cycle fatigue. This was the case in the upper left diagonal of model H1.

- Low value of slenderness of the diagonals (in this case $\lambda = 80$) in respect to the proposed CBFs should be avoided. Minimum slenderness should be the recommended one by Eurocode 8. Using slenderness of value less than 120 will lead to worse behaviour of the CBFs having reduced cross sections.

- The mechanism of the occurrence of degradation in bearing capacity is shown in Figures 4-118, 4-119 and 4-120. It can be summarized as follows:

  After occurrence of LB, behavior of the diagonal in tension and the behaviour of the diagonal in compression are in interactive relationship. Effects of LB appear to be initial imperfections in applying compression axial force thus leading to a steady decline in the bearing capacity of the diagonal subjected to compression (Fig. 4-127). Meanwhile the warpings of the cross section lead to redistribution of normal stresses if subjected to tension. This gives rise to a mechanism of decline in the inelastic bearing capacity of the diagonal if subjected to tension. The decline of bearing capacity in tension is much smaller than the decline of the bearing capacity in pressed state (Fig. 4-119).
- In presence of diagonals of low slenderness, it is necessary that the horizontal intermediate member should have significant stiffness in order to be able to ñforceò both tandem diagonals to buckle in the post buckling phase. If this did not happen shall emerge a mechanism of strong diagonals and a weak horizontal intermediate member. This leads to a redistribution of the internal forces. As a result plastic deformations shall concentrate in one cross sections resulting to reduction of the plastic behaviour of diagonals and lost of ductility of the CBF.

- The lack of symmetry in the stressed state of the diagonals causes the onset of unbalanced vertical force.

- Once a diagonal buckles in subsequent cycles of loading shall be obtained steady degradation in the buckling bearing capacity. The residual post-buckling bearing capacity in compresion is between 0 and 20% of the initial one - Figure 4-127. For large displacements that force tends to zero.
- Inter-relationship between storey drift and shortening or elongation of the diagonal are described reliably using the corrected equation (4.8-6). The equation gives good results in the phase of inelastic deformations of the CBF. In case of larger drifts the equation is expected to be even more accurate.
- Theoretical bearing capacity of a diagonal from the investigated type of CBFs, having low slenderness (below 120) and reduced cross section areas can be determined as in the formula of Eurocode 3 shall used the net cross section.
- It is a must to provide no sliping bolted connections between the members of the frame. Bolted connections employing standard non-pretensioned bolts and standard hole clearances lead to unintended redistribution of internal forces.

4.8.4. Experimental model H3

To clarify the approach that was used in the experimental model H3 will have to remind that the reduced cross sections of this model are the dominant part of the length of the diagonal. Middle cross-section is designed with a larger cross-sectional area and smaller bending stiffness. We named it modified cross section. Due to the above reasons both in the reduced cross section and in the middle modified cross section is expected the occurrence of plastic deformations but caused by different reasons. The reduced cross section will plasticize in tension and modified cross section in bending. This specific in the behavior of the diagonals of models H3 limits the possibility of finding a suitable place for location of the strain gauges and ensuring their functioning[1] by the end of the experiment.

Strain Gauges (SG) were located in the middle of the areas of reduced cross section of each diagonal. This is described in Chapter 3, Figure 3-96. Being such installed SG provided information about the strains until the occurrence of the first plastic deformations. That is why in this chapter are proposed figures only up to cycle ¯ 5. The rest of the analysis is based on visual observations, photographs and notes kept by the author during the experiment.

Figure 4-140 presents the diagrams of axial forces in the diagonals in cycle 1, 4 and 5. The charts show that in both directions "+" and "-" there is symmetry in the behavior of the diagonals. It is also obvious that there is considerable asymmetry in the behavior

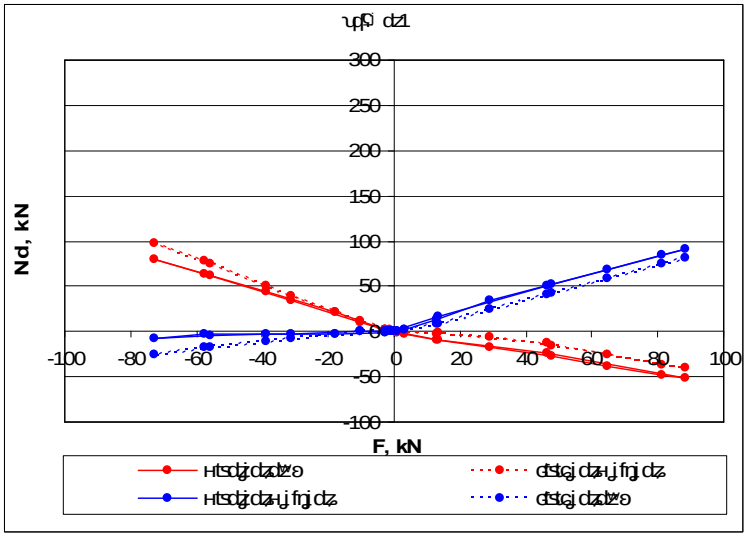

Fig. 4-140 *– model H3, axial forces Nd in the diagonals depending on the horizontal force F at the first cycle of the experiment*

[1] Strain gauges may operate until the moment of yielding in the area where these are glued.

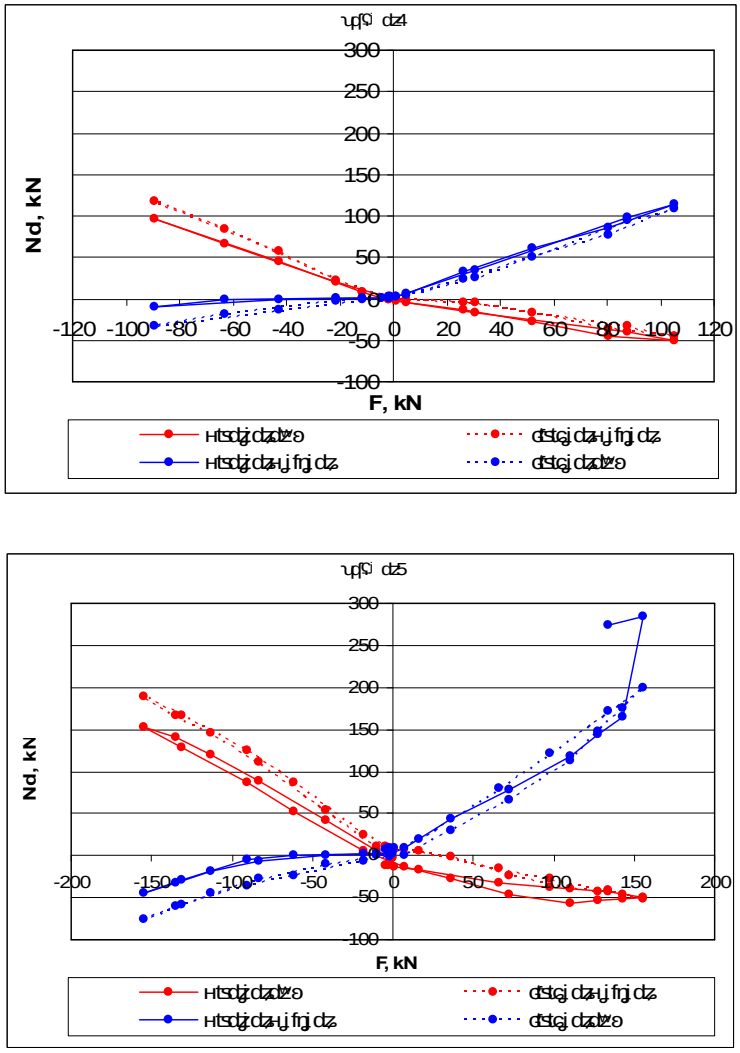

***Fig. 4-140** – continuation, loading cycles 4 and 5*

of tensioned and compressed diagonals yet in cycle 1 although there has not been registered buckling of the compressed diagonal. Here is the place to point out that such a difference in the behavior of the diagonals is registered also in model H2 (see Figure 4-116). The author gives the following explanation of this behavior of the structure. The diagonals of all experimental models are designed and manufactured as welded, built-up "H"-shaped cross sections. Their dimensions are 130 mm in height of the cross section and 60 to 90 mm width of the flange. This size of the cross sections does not allow the use of technological stands for serial production of built-up beams. The manner for composing the cross sections is through the use of manual devices (vices for general use) and also manual locksmith work for alignment the web and flanges. In its entirety this simpler production technology leads to the possibility of occurrence of initial imperfections which appear to be most severe in the most slender diagonals (these of model H3). Moreover in model H3 the web is interrupted in the middle because there should be inserted the thicker steel plate for the intermediate modified cross section. This part of the cross section requires the execution of butt welds in a short sector and this in turn leads to welding

deformations causing initial non-linearity (geometric imperfection) of the member. A similar comment on the impact of initial imperfections can be found also in [58].

In order to verify the thesis for the origin of the different stiffness of the compressed diagonal and the tensioned diagonal at the phase before First Diagonal Buckling (FDB) has been used computer simulation. The computational model is based on beam FE (finite elements). In all diagonals of the model were set initial imperfections. Since before the experiment were not performed measurements of the linearity of the diagonals as recommended by BDS EN 1993-1 was set initial geometrical imperfection in the middle of a diagonal of 9,6 mm (which is $f_0 = \frac{1}{200} = \frac{1920}{200} = 9,6mm$). The shape of the initial imperfection follows a sine wave with amplitude f_0. A Push-over non-linear analysis was done by SAP 2000 Advanced 14.1. General view of the used model is shown in Figure 4-141 and deformed scheme obtained by the solution is shown in Figure 4-142. Diagram of the relationship between the axial forces in the diagonals and the total horizontal force is shown in Figure 4-143. It is clear from Figure 4-143 that there is a similarity with the diagrams in Figure 4-140.The study was conducted only for value of the initial imperfection $f_0 = \frac{1}{200}$ since the purpose of the study is not to be determined the influence of initial imperfection but to prove that the reason of the asymmetry shown in Figure 4-140 is due to this initial imperfection. On the basis of conducted numerical modeling and analysis the author repeats his thesis and states that in the phase before FDB initial imperfections in diagonals are the reason for the different participation of the tensioned and pressed diagonals in resistance to the horizontal force. In pressed tandem of diagonals initial imperfections contribute to the occurrence of bending moments while in tensioned diagonals, tensile axial force acts in a direction of reducing the bending moments. Namely this effect is the reason for the differences in axial forces in the pressed and tensioned diagonal. After the occurrence of the first loss of stability of the diagonal the initial imperfections increase and the asymmetry in the behavior of the diagonals becomes even greater.

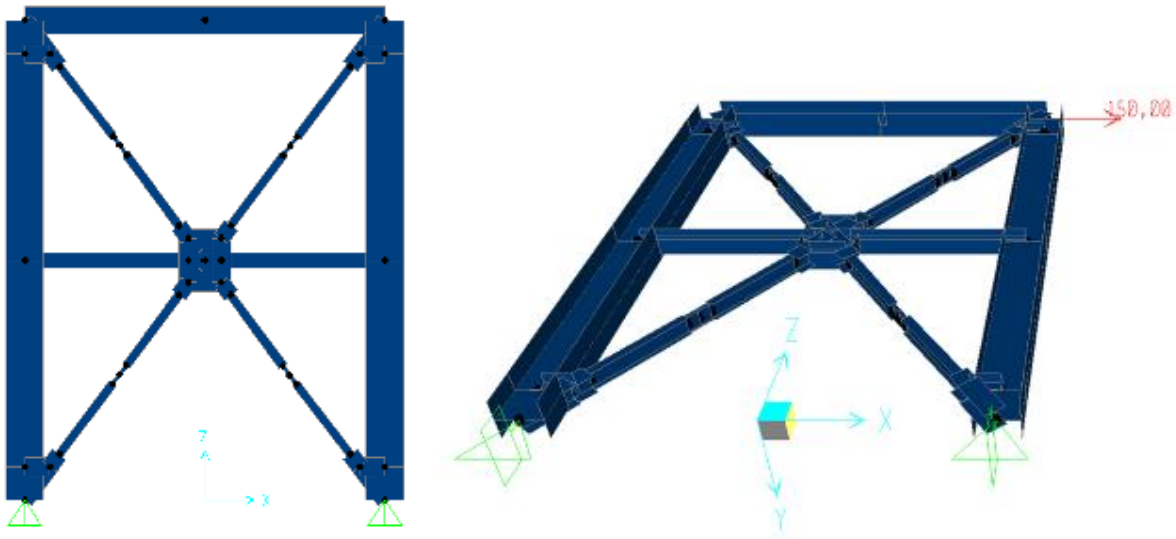

Fig. 4-141 *– general view of the FE computational model*

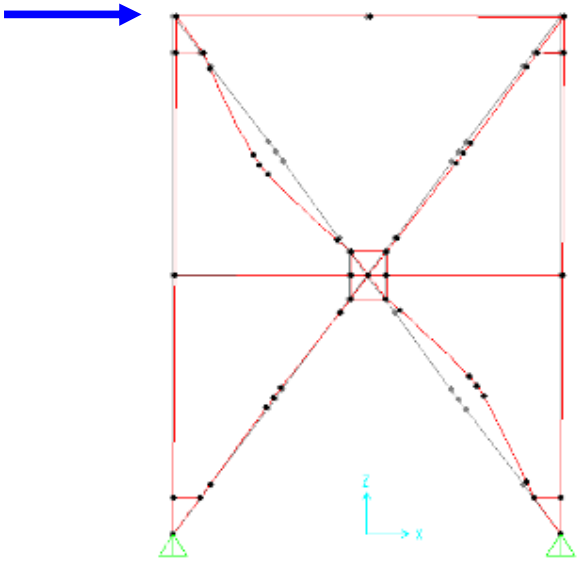

Fig. 4-142 *– deformed scheme. It is clearly shown how transverse displacements (transverse in respect to the axis of the non-deformed axis of the diagonal) of the pressed tandem of diagonals are much larger than the transverse displacement of the tensioned tandem.*

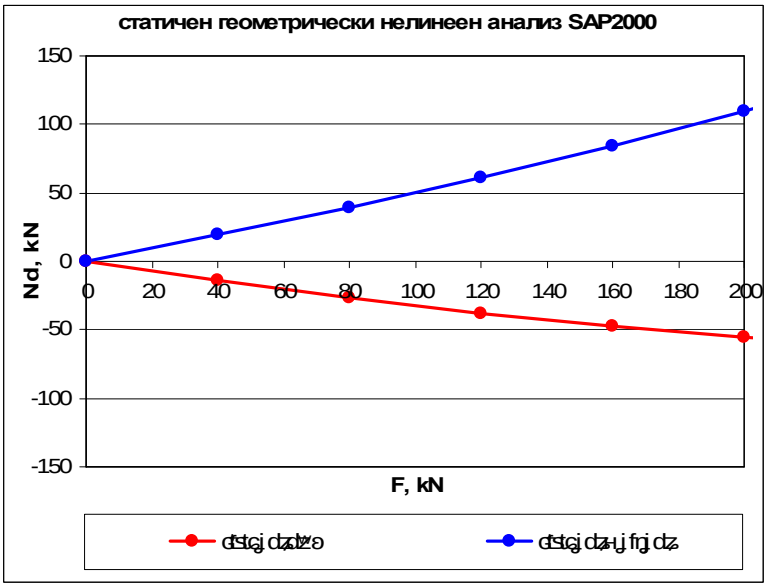

Fig. 4-143 *– model H3 - numerical experiment, axial forces in the diagonals Nd depending on the horizontal force F obtained by geometrically non-linear static analysis. Upper left diagonal is pressed and upper right diagonal is tensioned.*

Early occurred inoperative state of strain gauges prevented to be drawn a detailed picture of the axial forces in the diagonals as was drawn for model H2 and H1. However significant development of inelastic deformations in the diagonals allowed being conducted a visual inspection which is summarized in the Figures below. Characteristic point is that in this experiment all four diagonals buckled in pressed state. Chronology of this buckling is shown in Figures 4-144 and 4-145 below.

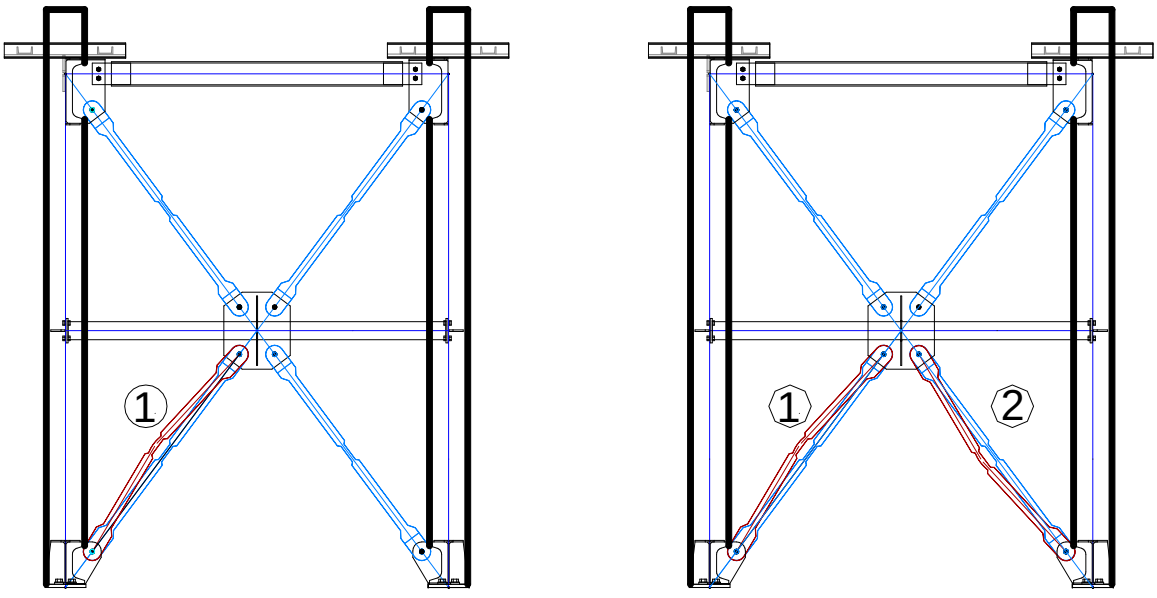

Fig. 4-144 *– model H3, buckling of pressed diagonals;*

Figure 4-144 at the left shows buckling of lower left diagonal. It occurred in the second cycle in the application of displacement of the top of the frame equal to 5,385 mm. Such displacement corresponds to $\frac{1}{742}H$ or $\varphi = 0,00135rad$. On the same figure at the right is shown the buckling of lower right diagonal. It occurred in cycle 5 in the application of displacement of the top of the frame equal to 10,065 mm. Such displacement corresponds to $\frac{1}{397}H$ or $\varphi = 0,0025rad$. Numbers placed next to diagonals in Figure 4-144 show the sequence of occurrence of buckling.

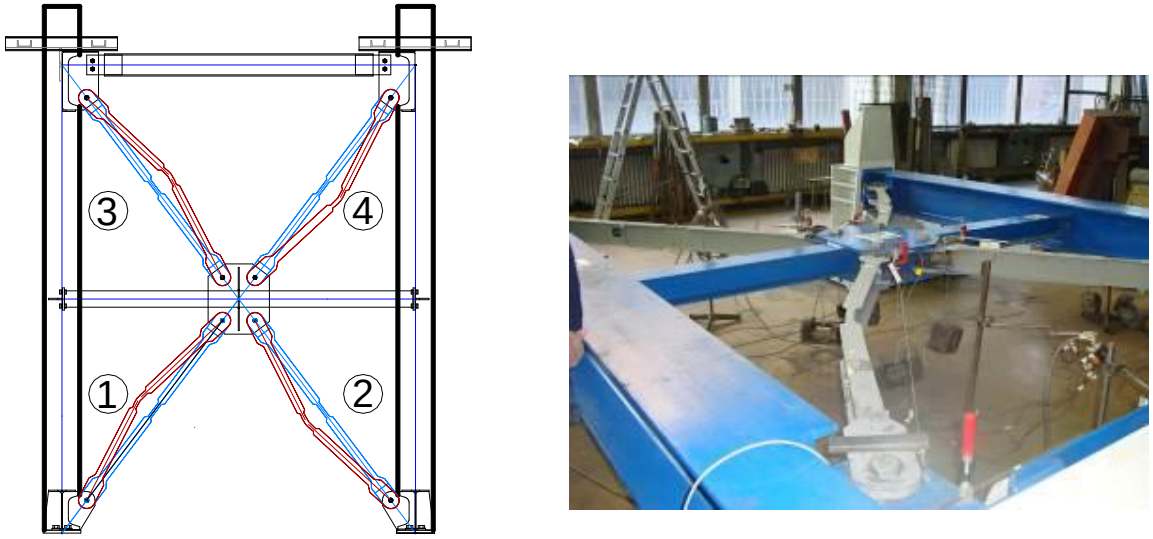

Fig. 4-145 *– model H3, sequence of buckling of upper pressed diagonals (at left). Pressed tandem of diagonals during cycle 12 of experiment 2-3 (at right).*

Buckling of upper left diagonal occurred in cycle 12 which is the second in the group of three cycles. The applied displacement at the top of the frame equals to 28,976 mm. Such displacement corresponds to $\frac{1}{138}H$ or $\varphi = 0,0072rad$. Last buckled upper right diagonal. This happened throughout the course of cycle 12. Buckling occurred in the application at the top of the frame of displacement of value 34,365 mm. Such displacement corresponds to $\frac{1}{116}H$ or $\varphi = 0,0086rad$.

Numbers placed next to diagonals in Figure 4-145 show the sequence of occurrence of buckling. The photo at the right of the same figure is made in course of cycle number 12 when buckling occurred in upper right diagonal. Generalization of these data is made in Table 4-32 and the maximum value of occurred displacements is summarized in Table 4-33.

Table 4-32

diagonal	cycle in which occurred FDB	$v_{\max}\,[mm]$	$\varphi = \frac{v_{\max}}{H}\,[rad]$	as part of H
Lower left	2	5,385	$\varphi = 0,00135$	$\frac{1}{742}H$
Lower right	5	10,065	$\varphi = 0,0025$	$\frac{1}{397}H$
Upper left	12	28,976	$\varphi = 0,0072$	$\frac{1}{138}H$
Upper right	12	34,365	$\varphi = 0,0086$	$\frac{1}{116}H$

Table 4-33

tandem of diagonals	Last cycle	$v_{\max}\,[mm]$	$\varphi = \frac{v_{\max}}{H}\,[rad]$	as part of H
l.r + u.l	22	149,16	$\varphi = 0,0373$	$\frac{1}{26,8}H$

About the role of the horizontal intermediate member. As shown in the analysis of the diagonals of model H2 when there is a difference in the stressed state of the pressed diagonals compression force in them is different. Therefore the balance in the node of intersection of the diagonals is lost and appears unbalanced vertical force (UVF). Exactly this moment with the occurrence of UVF is shown in Figure 4-146 above and is explained in the same figure below. Exactly in this phase of the deformation of the frame the stiffness of the horizontal intermediate member has a decisive importance for the subsequent distribution of plastic deformations in cross sections. If the horizontal intermediate member is of enough stiffness it will "force" the non-buckled diagonal to lose stability. It will establish the mechanism of week diagonals and strong frame. If the horizontal intermediate member is not of enough stiffness only one of the pressed diagonals in the tandem shall buckle and therefore this diagonal concentrates in it larger bending moments (greater curvature). If only one of the diagonals in a tandem is buckled this leads to a concentration of plastic deformations only in one cross section and to premature exhaustion of the bearing capacity of the diagonal (see also item 4.8.3., page 395,396). Much beneficial is the effect of buckling of both diagonals in the tandem thus distributing among each other plastic deformations. In this sense the horizontal intermediate member should play a redistributive role by "forcing" both diagonals in the tandem to lose stability. Since diagonals in model H3 are more flexible this means that the horizontal intermediate member was stiff enough and has played its redistributive role.

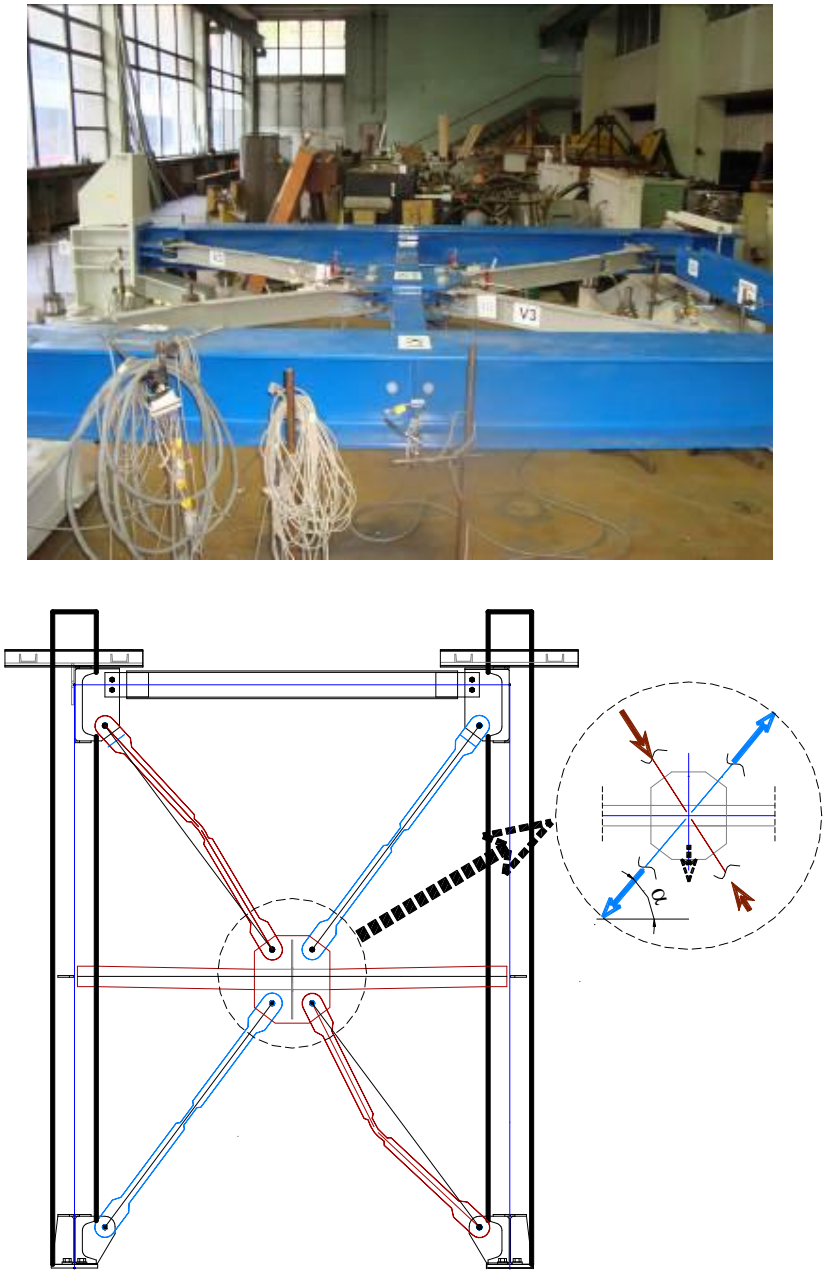

Fig. 4-146 *– model H3, state of buckling of a pressed upper left diagonal and the occurrence of VUF (Vertical Unbalanced Force) in the horizontal intermediate member*
(above) - photos that clearly shows the horizontal curvature caused by the VUF.
(below) - a mechanism for the occurrence of VUF

Further on the behavior of the diagonals of model H3 is studied by visual inspection of the places where plastic deformations develop. Such locations are the modified middle cross section shown in Figure 4-147 and the reduced cross section (area) shown in Figure 4-148. Modified cross section is designed not to plasticize when subjected to tension but to bend and to plasticize if subjected to compression. This can be seen clearly from Figure 4-147 where there are visible traces of yielding of the cross section. Plasticizations are

caused by bending of the cross section in buckling of the pressed diagonal. Traces of plasticization can be seen through the cracks in primer which was used to cover the steel member. From the experience gained by experimental series 1 we can say that the visual cracks in the primer becomes evident after the occurrence of axial deformations $\varepsilon \geq 1,5\%$. During the entire experiment there were no patterns of Local Buckling (LB) in the middle cross section. It should be remembered that the experiment was terminated due to the exhaustion of the technical capacity of the loading system and not because of failure of model H3.

Another typical cross section of the diagonal is the so called by the author reduced cross section[2] (structural fuse). In this cross section could be observed also visible signs of inelastic deformations. Such consists in paint cracking. The most visible cracking is in the connection area of the flange with the web. Cracking should be understood as lines at 45 degrees to the axis of the cross section in two opposite directions. Plastic deformations exist also in the web where all the glued signatures of the diagonals or the sensors fell. At the end of the experiment were measured also the transverse shrinkage of the cross-section. The initial width of the cross section was 70 mm and at the end of the experiment were measured widths between 68 and 69 mm. Figure 4-148 shows a case of measured width of 68.49 mm.

***Fig. 4-147** – model H3, middle modified cross section, plastic deformations, no LB*

[2] Perhaps the term "area of reduced cross section" is more correct because it does not refer to only one cross section and for whole area of certain length exceeding the height of the cross section of the member

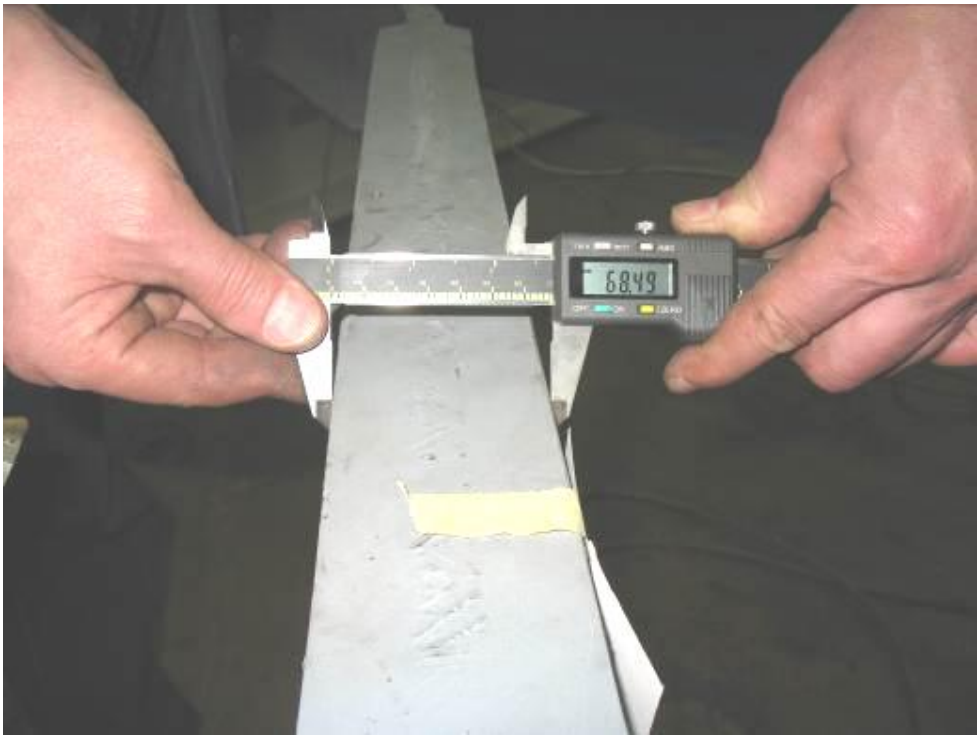

Fig. 4-148 *– model H3, reduced cross section. Visible signs of plastic deformations. Transverse shrinkage is due to the effect of Poisson.*

Comparison of the experimentally obtained bearing capacity with the design forces specified in accordance with [1]. Theoretical bearing capacity of the diagonals in model H3 when being subjected to tension and compression was calculated under BDS EN 1993-1-1. Here once again all coefficients γ_{Mi} will be assumed equal to 1. The equivalent for the entire cross section actual yield strength is determined by the equation (4.8-3) and for model H3 it is:

$$f_{y,eff} = \left(480.225,4 + 2.350.288,2\right).\frac{1}{480 + 2.350} = 262,6N/mm^2$$

Plastic tensile resistance (bearing capacity) of the reduced cross section is:

$N_{pl,t,RD} = 1180.262,6 = 309868 \approx 310kN$;

The Maximum resistance tensile force of the net cross section is defined by tensile strength of the steel pursuant to equation:

$$N_{t,u,RD} = A_{w,OC}.f_{u,w} + A_{f,OC}.f_{u,f} = (480.324 + 700.351,7).\frac{1}{1000} = 401,7kN$$

Buckling resistance force of pressed diagonal is defined as follows:

$$\varepsilon = \sqrt{\frac{235}{f_{y,eff}}} = \sqrt{\frac{235}{262,6}} = 0,946$$

$N_{b,Rd} = \chi\frac{A.f_{y,eff}}{1,0}$, and the coefficient of buckling χ in effective slenderness

$\lambda_{eff} = 181,2$, $\bar{\lambda}_{eff} = \frac{181,2}{93,9.0,946} = 2,04$, in case of use of buckling curve "c" for assumed slenderness 2,04 is determined to be $\chi = 0,19$. Then

$$N_{b,Rd} = 0,19\frac{1180.262,6}{1,0} = 58874,9N = 58,9kN$$

Unfortunately at this place could be done comparison only between theoretical buckling resistance by spreading up to cycle number 5. After this cycle SG become inoperable. Such a comparison is made in Table 4-34.

Table 4-34

diagonal	**Tension, kN**			**Compression, kN**	
cycle	$N_{pl,t,RD}$	$N_{t,u,RD}$	experiment	theoretical	experiment
upper right cycle 5; and FDB is in cycle 12	310	401,7	*tearing not achieved*	-58,9	-51,18
upper left cycle 5, and FDB is in cycle 12	310	401,7	*tearing not achieved*	-58,9	-76,23
lower right cycle 5	310	401,7	*tearing not achieved*	-58,9	-44,64
lower left cycle 2	310	401,7	*tearing not achieved*	-58,9	*-48,54*

From the last column of Table 4-34 could be seen that in 3 of the 4 cases the theoretical bearing capacity is greater than the bearing capacity in compression obtained in the experiment. This the author comments as follows. The theoretical bearing capacity is determined by the so-called effective yield strength rather than the nominal one. Safety factors of materials are equated to 1. If we strictly observe the procedure in Eurocode 3 we will receive

$\varepsilon = \sqrt{\frac{235}{f_y}} = \sqrt{\frac{235}{235}} = 1$, $\lambda_{eff} = 181,2$, $\bar{\lambda}_{eff} = \frac{181,2}{93,9.1,0} = 1,929$, in case of buckling curve "c" and assumed slenderness of 1,929 we define $\chi = 0,208$,

$N_{b,Rd} = 0,208\frac{1180.235}{1,1} = 52434,9N = 52,4kN$.

The arithmetic average of the buckling bearing capacity obtained during the experiment is 55,14 kN which is a value of 5% higher than the theoretical value.

The second and more important comment is that the diagonals have significant manufacturing tolerances above the allowable one. According to [26] the allowable tolerance is $\pm l_d/750$ and according to the team which has conducted the experiment the alignment offset is estimated of about $f_0 \approx \frac{l_d}{200} \div \frac{l_d}{400}$. The allowable tolerance according to EN 1090-2 is exceeded and therefore dimensioning procedure of Eurocode 3 is not in the

range of validity. It is this feature of slender diagonals in model H3 that the author would like to highlight and adds that in experimenting with computer models compressive bearing capacity should be determined by non-linear static analysis and assumed initial imperfection $f_0 = \frac{1}{200}$ or should be used the formula from Eurocode 3 by setting a reduction factor of 0,75.

To a tearing due to the application of tensile force was not reached in experiment 2-3 because of the exhaustion of the technical ability of the loading system (reached limit of piston stroke).

Once again we have to emphasize that due to the innovative design of the diagonals there have never been reached forms of Local Buckling. For the same reason we cannot mention also the effects of low cycle fatigue. Such effects in this model are not present.

Experiment 2-3 allowed measuring buckling amplitude f in loss of stability of the compressed diagonal. We will remind that under the term "buckling amplitude" the author understands Maximum Displacement in Transverse Direction between deformed line of the buckled bar and its non-deformed line - Figure 4-149. A theoretical model for determining the buckling amplitude of a pressed diagonal depending on the relative inter-floor displacement $\vartheta = \frac{v_{max}}{H}$ was presented in Chapter 2 item 2.1. There has been shown how to derive equation (2.1-7) but for convenience it will be presented also here.

$$\bar{f} = \frac{\sqrt{\sin\alpha.\cos\alpha}}{2}.\sqrt{\theta} \qquad (2.1\text{-}7).$$

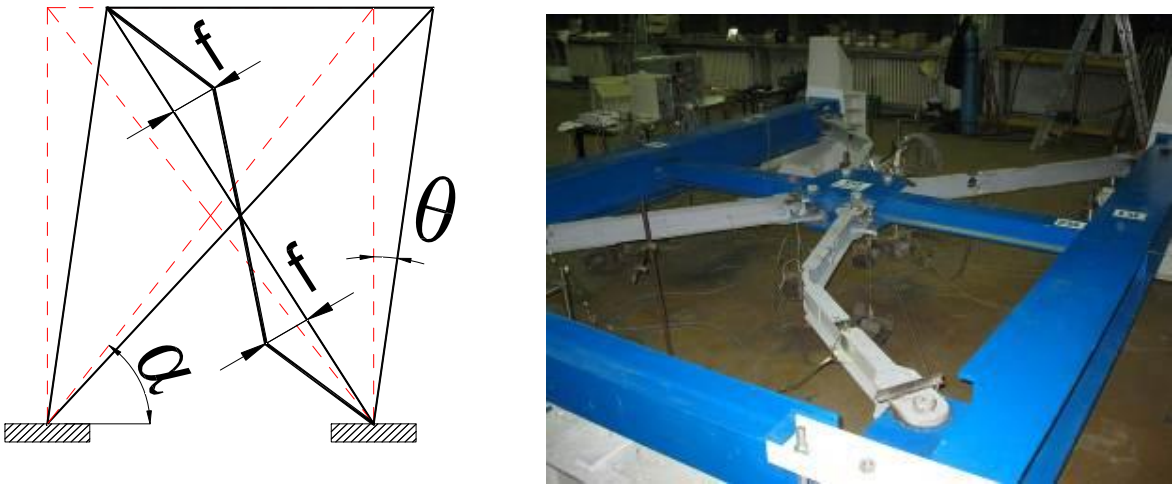

***Fig. 4-149** - a theoretical model for determining the buckling amplitude in case of buckling – at left. A photo of the actual occurrence during an experiment 2-3 – at right.*

Buckling amplitudes were measured manually and therefore there is no complete data for all cycles. Measurement results are shown in Table 4-35.

Table 4-35

	buckling amplitude f, mm	
	diagonal	
cycle -	lower left	lower right
1	4	
4	14	
5	36	
9	46	24
12	90	77
15		146
18	306	
21	335	

Through experiment 2-3 was performed a verification of the theoretical model. Theoretical results were compared with the actually measured buckling amplitudes. Summary of the comparison is shown in Figure 4-150.

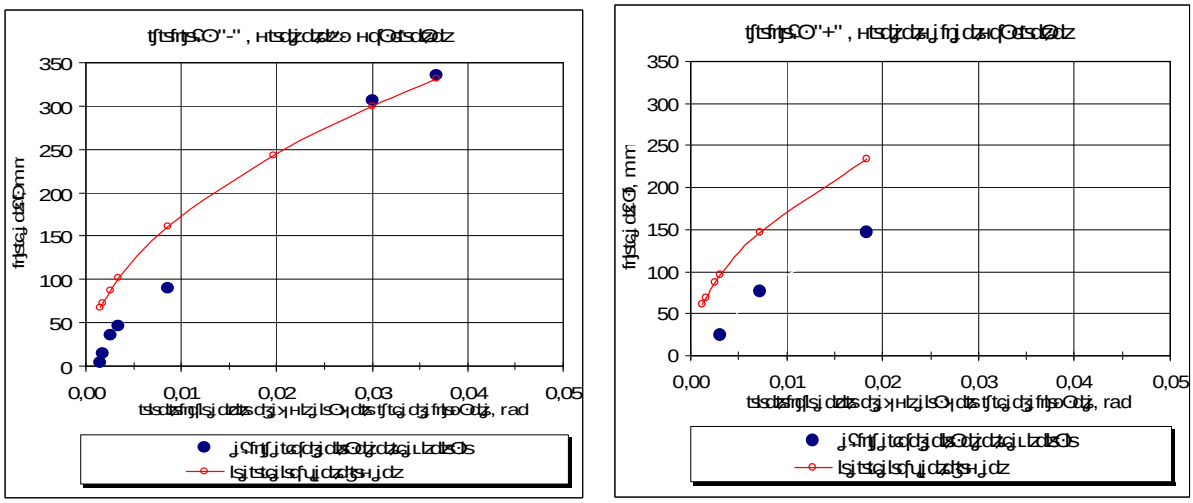

Fig. 4-150 *- comparison of the results of a theoretical model for determining the buckling amplitudes and measured ones during the experiment 2-3*

From the analysis of the results shown in Figure 4-150 is clear that for small values of the relative inter-floor displacements (less than 0,01 rad) the theoretical model provides significantly greater results. For the mid range from 0,01 to 0,025 rad is missing sufficient data from the experiment but for the single report which we have the theoretical result is about 60% higher than the experimental. For the range after 0,03 rad is observed an excellent match between the experimental data and the theoretical model. The difference is reduced to 1.9% in the one case and 0.9% in the other case. The author believes that the convergence between theoretical and experimental results with an increase in the relative inter-floor displacement is not accidental. It is due to the fact that at large displacements the deformed line of buckled diagonals more and more approximates to the

assumed theoretical polygonal line. Also with the increase of inelastic deformations is formed a kink in the middle of the diagonal and the rest of the diagonal remains almost straight. Thus the actual behavior of the compressed diagonals approximates to the theoretical model. All this allows us to conclude that formula (2.1-7) is suitable for determining buckling amplitudes for the relative inter-floor displacements over 0,025 rad. This is the range that would be of interest to design engineers. In the other cases the formula is on the safe side as for $\theta \leq 0.01\,rad$ it raises the result more than twice.

After completion of experiment 2-3 all diagonals were dismantled from the frame. They were in deformed but unbroken form - Figure 4 151. This made possible to perform measurements of the residual buckling amplitudes f_{res} and thereby to be obtained information about the occurred elongations in diagonals and the occurred inelastic deformations. The information for measured residual buckling amplitudes (BA) can be found in Table 3-23 of Chapter 3. In order to follow the methodology by which has been achieved to the residual elongations we will remind what is the initial geometry of the diagonals of an experimental model H3. It is shown in Figure 4-152. By the experience that has been gained from experimental series 1, we have the reason to presuppose that all plastic deformations develop in the reduced cross sections. From Figure 4-152 is evident that the axial length of the diagonal is 1920 mm and the length of the reduced cross section is $L_{OC} = 2x555 = 1110 мм$. Assuming that the deformed line is equilateral triangle whose height is the residual BA f_{res} and the sum of the legs is the length

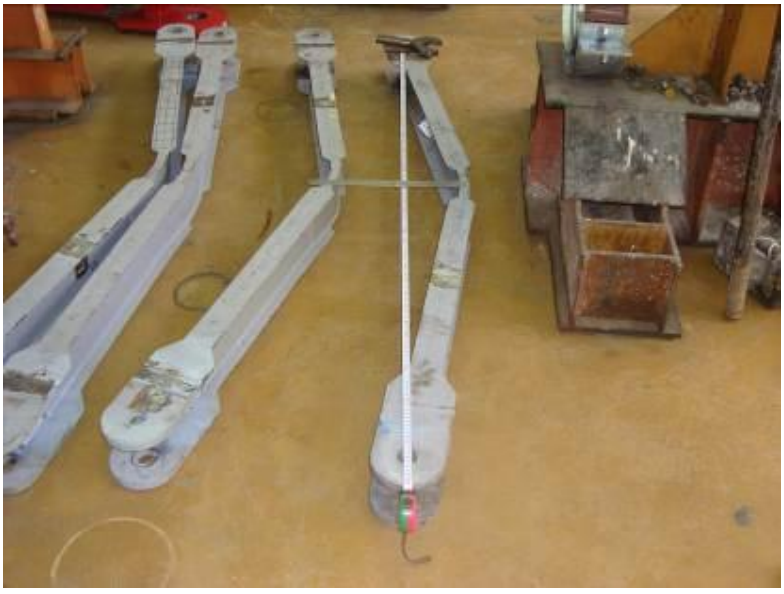

Fig. 4-151 *- residual BA in diagonals in model H3. Measurement after the test using a precision ruler.*

of the elongated diagonal. Then the third side of the triangle represents the length of the non-deformed diagonal. With the use of this geometric set-up we may easily derive via Pythagorean theorem the residual elongation of the diagonal $\delta_{\max}$. The maximum plastic

deformation that has occurred in the diagonal is obtained by the equation $\varepsilon_{\max,pl} = \frac{\delta_{\max}}{L_{OC}}$.

The results of these calculations are shown in Table 4-36.

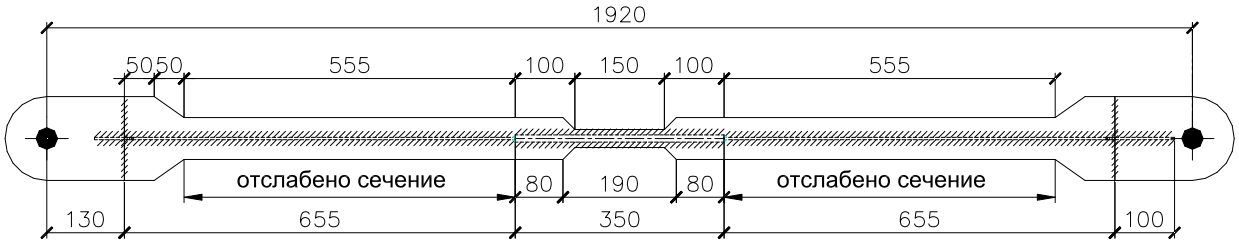

***Fig. 4-152** – geometry of the non-deformed diagonals in experimental model H3*

Table 4-36

Diagonal	Residual BA f_0, mm	Initial length of the diagonal, mm	Length of the RCS, mm	Residual elongation $\delta_{\max}$, mm	Maximum strain $\varepsilon_{\max,pl}$,%
Lower left	*210*	1920	1110	45,4	4,09
Upper left	*135*	1920	1110	18,89	1,70
Lower right	*225*	1920	1110	52,0	4,69
Upper right	*165*	1920	1110	28,15	2,54

It is interesting to compare the chronology of buckling of separate diagonals with the calculated strains therein. This is done in Figure 4-153 where the numbers next to the diagonals show the sequence of buckling in the course of the experiment and the numbers inside the rectangles are the strains in the respective diagonal. It is evident from Figure 4-153 that diagonals whose buckling occurred later on suffered less strains. It is also apparent that the difference between the maximum and minimum strains is 2.75 times. If we sum residual elongations in diagonals and determine the average strain in each tandem we will obtain the following picture. For the first tandem (lower left and upper right diagonal) $\varepsilon_{средно,\,pl}^{тандем\,1} = 3,315\%$. For the second tandem (lower right and upper left diagonal) $\varepsilon_{средно,\,pl}^{тандем\,2} = 3,195\%$. The difference between the two averaged conditional strains is 3.8%.

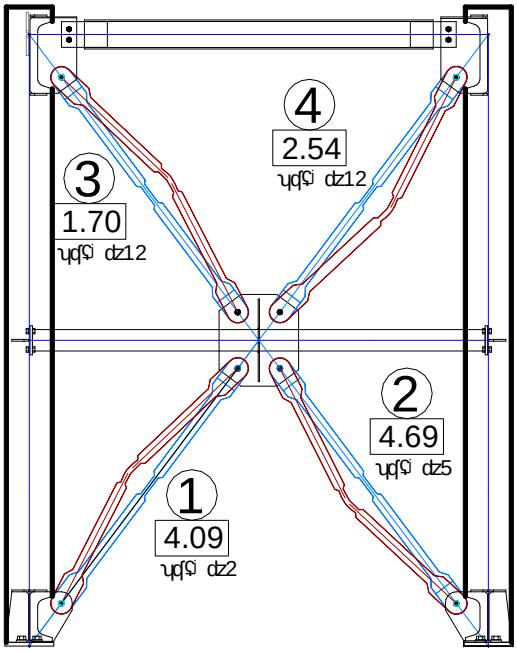

Fig. 4-153 *– a scheme of the sequence of buckling of the diagonals in experimental model H3, plastic strains in the corresponding diagonal and the number of the cycle where buckling occurred. The number in the rectangular frame is the plastic strains in the diagonal in %.*

About the sequence of diagonal buckling the author believes that the actual manufacturing tolerances and their magnitude are the main factor that predetermines the picture. This factor is complex and depends on many parameters such as production technology, degree of control, qualification of the manufacturer and etc. It will remain beyond the scope of this study.

PARTICULAR CONCLUSIONS DERIVED BY THE ANALYSIS OF THE BEHAVIOUR OF THE DIAGONALS OF EXPERIMENTAL MODEL H3

By the analysis performed in item 4.8.4 could be draw the following particular conclusions and generalizations:

- The author believes that the use of innovatively designed details applied in model H3 and aiming to define medium modified cross section having reduced bending stiffness and increased bearing capacity of axial forces is a new approach that helps to be avoided overlapping of inelastic tensile and compressive strains, extends the durability of the member in respect to low cycle fatigue and significantly improves the ductile behavior of the diagonals.
- For model H3 when diagonals are of assumed slenderness $\bar{\lambda}_{eff} \approx 2,0$, the horizontal intermediate member plays its redistributive role and "forces" all diagonals to buckle. This effect leads to a distribution of the plastic deformations on longer cross sections and the avoidance of concentrations of inelastic strains.
- In model H3 has been also registered asymmetry in the stressed state of the diagonals and the occurrence of unbalanced vertical force. The adequate stiffness of the horizontal intermediate member helped to overcome the asymmetry and for homogenizing the behavior of all diagonals.
- During the experiment 2-3 with a model H3 have not been registered any forms of Local Buckling.
- Initial imperfections (manufacturer's alignment offset) in two of the diagonals lead to a difference in stiffness of pressed and tensioned diagonal even in elastic phase of behavior. Diagonal compression force can be from 18% to 60% of the diagonal tensile force. Variation of the compression force depends on the degree of initial imperfection.
- Theoretically obtained compressive bearing capacity should be reduced by a factor of 0,75 in order to be accounted the effects of initial imperfections or should be used methodology of geometrical non-linear static analysis with initial imperfections.
- Formula (2.1-7) is suitable for determining the buckling amplitude for the relative inter-floor displacements over 0,025 rad and for the rest of the cases it gives results on the safe side.
- In all the diagonals of the frame there is a development of plastic strains. Plastic strains between the diagonals differ by up to 2,75 times but the difference between tandem diagonals is limited to only 3.8%.
- Diagonals that have lost stability earlier develop larger plastic strains.

4.9. Investigation on the influence of the slenderness of the diagonal on the overall inelastic behavior of CBFs

Experimental models H1, H2 and H3 were conceived, designed and manufactured so that the frame (columns, beam and horizontal intermediate member) shall remain unchanged while the diagonals of each model will have a different slenderness - Table 4-37. This intention embedded on purpose in the experiment is due to the fact that the prevailing researchers' understanding on the behavior of CBFs was that the slenderness of the diagonal is a key parameter that affects the dissipativity of this type of structures [34,39,41]

Table 4-37

Model	Slenderness of the diagonal		Effective slenderness	Equivalent yield strength	ε	Normalized slendernes s
	$\lambda_y = \frac{L_D}{i_y}$	$\lambda_Z = \frac{L_D}{i_Z}$	$\lambda_{y,eff} = \frac{L_D.\mu}{i_y}$	$f_{y,eff}$ N/mm^2,	$\varepsilon = \sqrt{\frac{235}{f_{y,eff}}}$	$\bar{\lambda} = \frac{\lambda_{y,eff}}{93,9.\varepsilon}$
H1	**65,6**	**34,3**	**80,1**	**270,3**	**0,932**	**0,915**
H2	**91,4**	**35,3**	**122,0**	**266,4**	**0,939**	**1,384**
H3	**123,2**	**36,2**	**181,2**	**262,6**	**0,946**	**2,040**

For the purpose of evaluating the influence of the slenderness of the diagonals on the inelastic behavior of the studied CBFs were tracked the main functions of cyclic inelastic behavior as derived in items 4.3, 4.4 and 4.5. There have been made a series of summary charts demonstrated in Figures 4-154, 4-155, 4-156, 4-157 and 4-158.

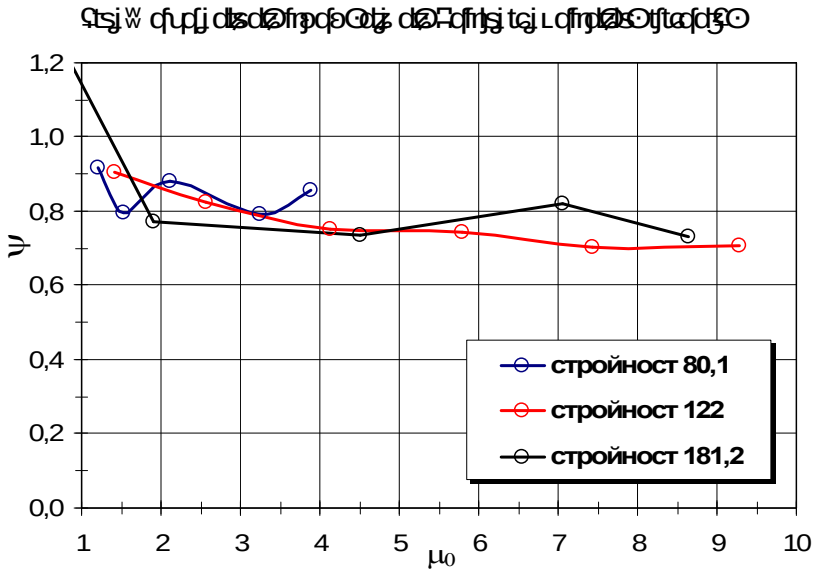

Fig. 4-154 *- variation of the* ***full ductility ratio*** *as a function of the ductility of the frame and the slenderness of the diagonals*

In the summarizing charts are used averaged results in way of direction "+" and direction "-" of participating parameters. Arithmetic averaging is used.

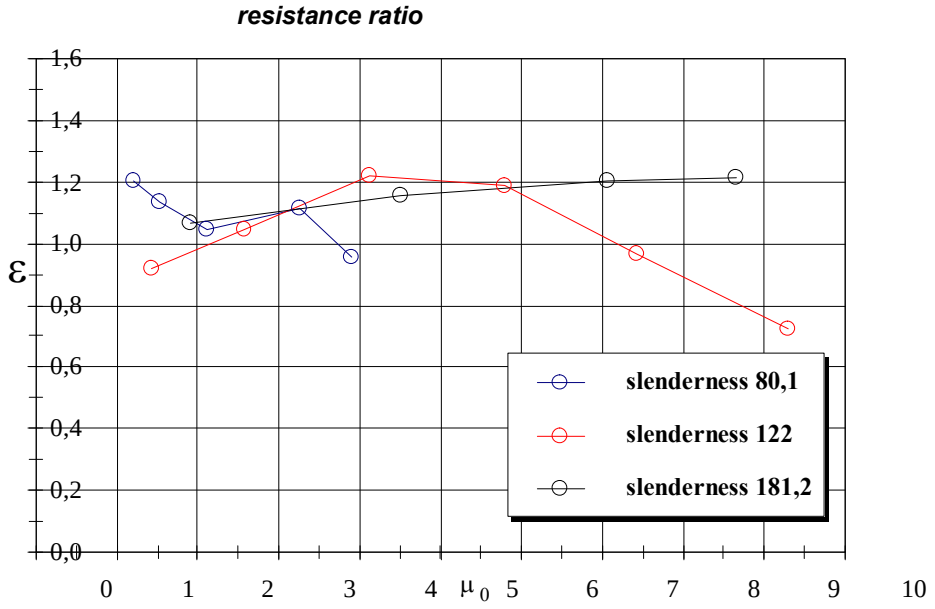

Fig. 4-155 *– variation of the* ***resistance ratios*** *as a function of the ductility of the frame and the slenderness of the diagonals*

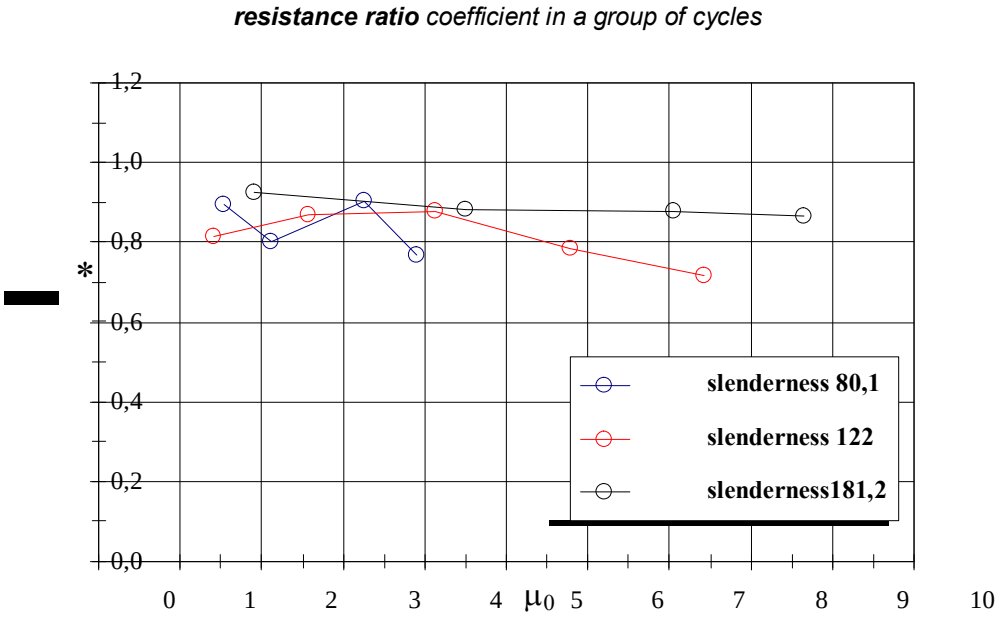

Fig. 4-156 *– variation of the* ***resistance ratio*** *in a group of cycles as a function of the ductility of the frame and the slenderness of the diagonals*

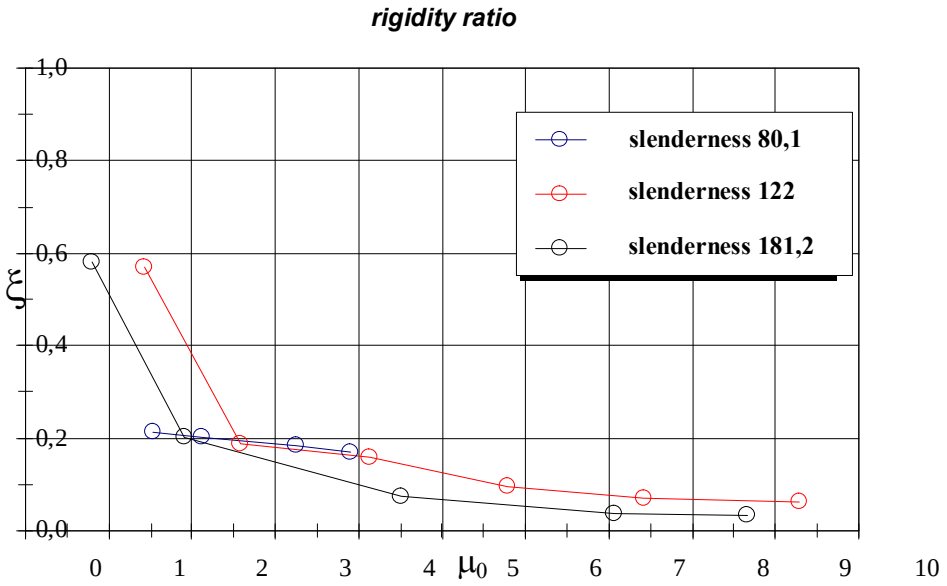

Fig. 4-157 *– variation of the* ***rigidity ratio*** *as a function of the ductility of the frame and the slenderness of the diagonals*

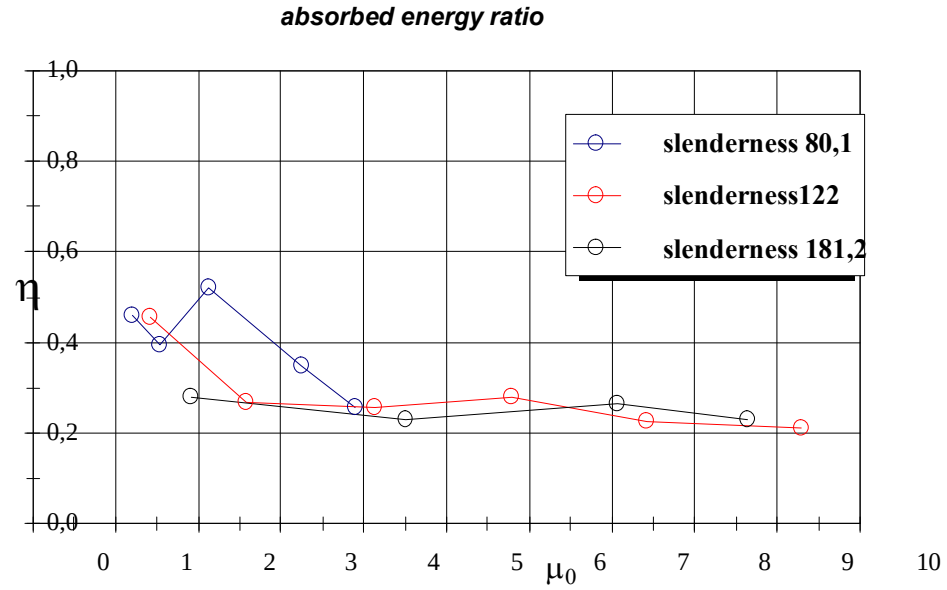

Fig. 4-158 *– variation of the* ***absorbed energy ratio*** *as a function of the ductility of the frame and the slenderness of the diagonals*

The careful study of the results of Figures 4-154, 4-155, 4-156, 4-157 and 4-158 shows that the slenderness of the diagonals introduces its effect but the diagram of the

cyclic inelastic behavior of various models is similar. Still it is possible to define the following differences:

In respect to the full ductility ratio Ψ

We may consider two ranges of the inelastic behavior, ductility $\mu_0 \leq 4$ and ductility $\mu_0 > 4$. In the first range $\mu_0 \leq 4$ by increasing slenderness of the diagonals the value of Ψ reduces as the difference in values reaches up to 15%.

In the second range $\mu_0 > 4$ the diagonals having the utmost slenderness demonstrate the highest values of Ψ. The experimental model H1 equipped with diagonals of slenderness $\lambda = 80.1$ is not able to reach ductility greater than 4. We must generalize that at the required value of ductility $\mu_0 > 4$, slenderness of the diagonals is not essential in respect to the studied type of CBFs. If the diagonals are within the range of the normalized slenderness recommended by Eurocode 8, namely $1,3 \leq \bar{\lambda} \leq 2,0$ then the value of the coefficient Ψ varies in the range $\psi \approx 0,7 \div 0,8$.

Reference on the resistance ratio ε

Resistance ratio varies within the range $\varepsilon \approx 1,1 \div 1,2$ in case CBF respond within the range of its limit ductility[1]. When the limit ductility is surpassed shall occur decrease in frame bearing capacity. The decrease is related to the development of effects of local buckling and interactive reduction in the bearing capacity of the diagonals when subjected to tension and compression - for further details please see item 4.8.3 and 4.8.2. If CBF respond within the range of its limit ductility then coefficient ε increases with the increase of inelastic deformations (ductility).

Reference on the resistance ratio in a group of cycles ε^*

The author believes that coefficients ε and ε^* are interrelated. Therefore, the coefficient ε^* directly depends on the limit ductility and indirectly by the slenderness of the diagonals. When CBF responds within the range of its limit ductility resistance ratio in a group cycles has the following value $\varepsilon^* \approx 0,8 \div 0,9$. If CBF surpasses its limit ductility then coefficient ε^* decreases. In the study performed for model H3 has not been observed any decrease of the coefficient ε^* due to the fact that the limit ductility of the CBF has not been surpassed.

Reference on the rigidity ratio ξ

Coefficient of ***rigidity ratio*** is affected by the slenderness of the diagonals in respect to the studied type of CBFs and reduced cross-sections. By increasing the slenderness of the diagonals decreases coefficient ξ.

Reference on absorbed energy ratio η

[1] Term "limit ductility" is defined later on in the exposition on page 129.

In the stage of large inelastic deformations the ***absorbed energy ratio*** η is not affected by the slenderness of the diagonals. The summarization is valid for the studied type of CBFs.

To complete the picture of the analysis of the influence of the slenderness of the diagonals, has been derived relationship between the full ductility and the partial ductility of the studied structures. One more time have been used arithmetic averaging of the results in way of direction "+" and direction "-". The diagram is shown in Figure 4-159. Could be easily noticed a practical invariance of full ductility compared to the slenderness of the diagonals. Moreover could be mentioned that for the three studied models full ductility is very close to a linear function of partial ductility. This gave rise to seek an analytical expression (4.9-1) by which could be defined full ductility. The author proposes the following relationship:

$$\mu = 1,34\mu_0 - 0,3 \qquad (4.9\text{-}1)$$

Comparison between the proposed analytical expression and the experimental results is shown in Figure 4-160. According to the author the achieved accuracy is completely satisfactory. Expression (4.9-1) could be used to establish an analytical model of inelastic behavior of the investigated type of CBFs.

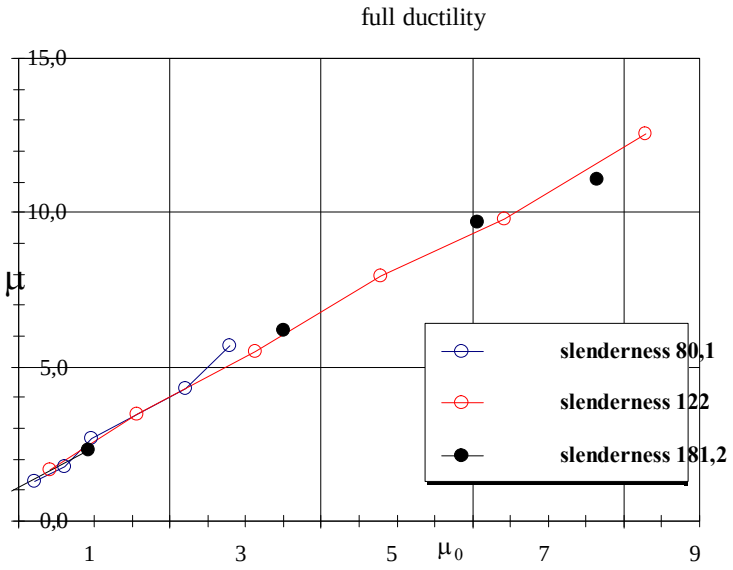

Fig. 4-159 *– variation of the full ductility coefficient as a function of the partial ductility of the frame and the slenderness of the diagonals. Virtually full ductility does not depend by the slenderness of the diagonals. This statement refers to the studied type of CBFs and the respective range of slenderness of the diagonals.*

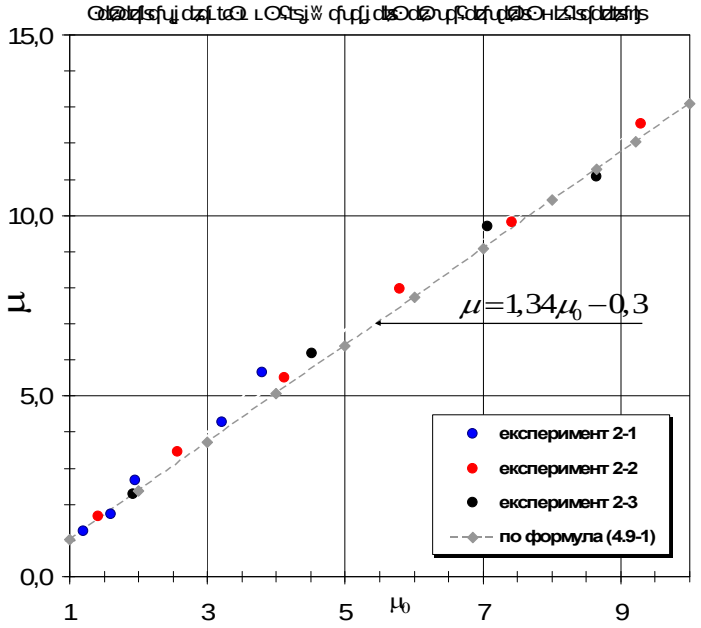

Fig. 4-160 *- comparison between the results obtained by formula (4.9-1) and the experimental results related to the full ductility coefficient as a function of the ductility of the frame.*

To complete the assessment of the influence of slenderness of the diagonals on the dissipativity of the studied CBFs, have been performed comparison of the amount of energy dissipated. In order to ensure comparability of results the amount of energy dissipated was presented as a function of cumulative displacement at the top of the frame. A similar approach has been used by other authors such as in literary source [90], item 3.3. The diagram of obtained results is presented in Figure 4-161.

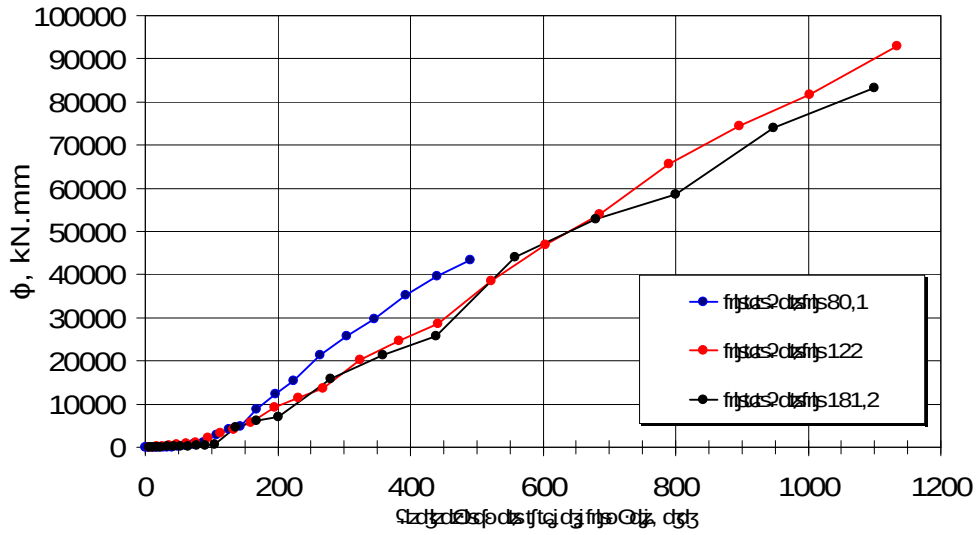

Fig. 4-161 *– a family of curves representing the dissipated energy as a function of cumulative displacement at the top of the frame and depending on the slenderness of the diagonals*

Figure 4-161 shows that by increasing the slenderness of the diagonals the dissipated energy decreases. Thus for example within the range of ductility $\mu_0 \leq 4$ the dissipated energy by model H1 equals to 39723kN.mm, dissipated energy by model H2 is 28705kN.mm and dissipated energy by model H3 is 25800kN.mm. The amount of dissipated energy for model H1 is 53.4% more than dissipated energy for model H3 and 11.3% more than dissipated energy for model H2. These figures apply for relatively small inelastic deformations. Within the range of large inelastic deformations fall only experimental models H2 and H3. In this range again could be noticed that lower slenderness of diagonals of model H2 reflects in more dissipated energy but the difference is limited to 8%.

In the above stated (page 126) has been used the scientific term "limit ductility". By using the term "limit ductility" the author understands the maximum value of the ductility coefficient at which the resistance ratio is greater than one ($\varepsilon \geq 1,0$). Graphically in Figure 4-162 are defined the ñlimit ductilityò of various experimental models. Thus for example limit ductility for experimental model H1 equal to 3.7, for experimental model H2 limit ductility is 7.3 and for experimental model H3 the latter has not been reached. By increasing the slenderness of the diagonals increases also limit ductility.

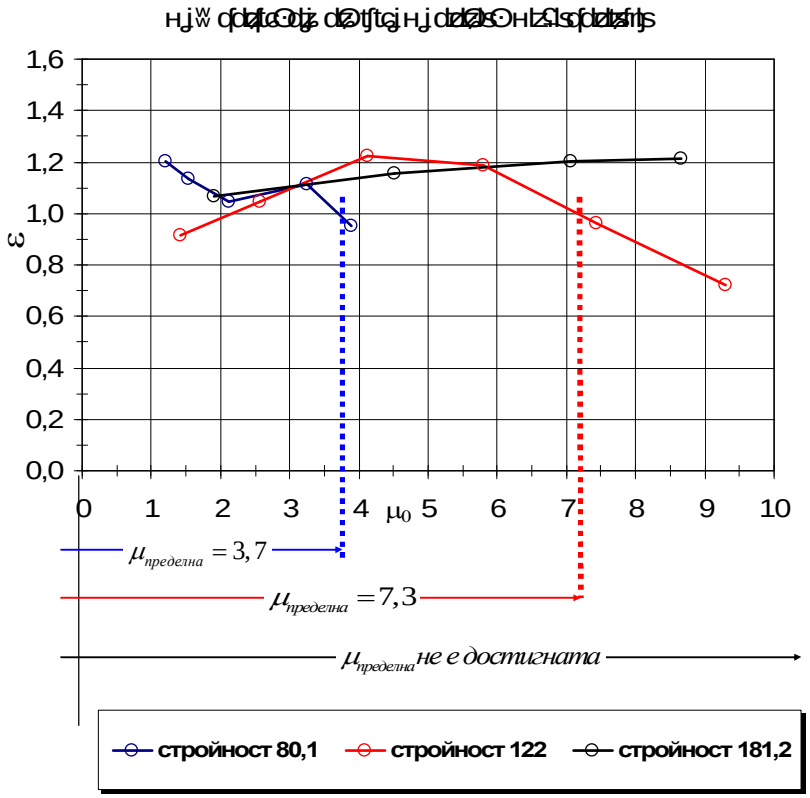

Fig. 4-162 *- limit ductility as a function of the slenderness of the diagonals*

PARTICULAR CONCLUSIONS DERIVED BY ITEM 4.9.

By the analysis made in item 4.9. could be drawn the following particular conclusions and generalizations:

- Inelastic behavior of the studied type of CBFs improves when diagonals obtain slenderness that falls within the range recommended by Eurocode 8 $1,3 \le \bar{\lambda} \le 2,0$ due to the substantially improved ductility and small decrease in bearing capacity. If the diagonals are of less slenderness (as it was the case with H1) this leads to a concentration of inelastic deformations in a specific cross-section along with the development of the effects of local buckling (buckling of flanges and web steel plates) and occurrence of low cycle fatigue. This is why studied model H1 failed to achieve demanded ductile behavior. Similar conclusion could be found in the works of *Walpole* (1995) [100].

- Slenderness of the diagonals has a direct influence on the ductility of CBF. At low slenderness of diagonals the frame obtains limit ductility that equals to 3.7 and in case of slenderness within the range $1,3 \le \bar{\lambda} \le 2,0$ limit ductility ranges from 7.3 to over 10.

- Slenderness of the diagonals has a direct influence on the rigidity ratio. Frames having diagonals of higher slenderness experience bigger drop of cyclic stiffness. In their hysteresis loops could be observed pinching. Frames having lower slenderness of the diagonals (model H1) experience less drop of cyclic stiffness and hence their hysteresis loop is not that pinched.

- In all studied models pinching of the hysteresis loops is a characteristic feature. This phenomenon the author explains by the used range of slenderness of the diagonals and believes that pinching of the hysteresis loops is specific and inevitable characteristic of cyclic inelastic behavior of CBFs designed according to Eurocode 8.

- Slenderness of the diagonals of the studied type CBFs has little influence on the full ductility ratio Ψ of the hysteresis loop.

- Slenderness of the diagonals of the studied type CBFs does not affect the full ductility. Full ductility could be determined with sufficient accuracy by the proposed equation $\mu = 1,34\mu_0 - 0,3$ (4.9-1).

- Slenderness of the diagonals of the studied type CBFs affects the amount of dissipated energy. When CBF responds within the range of minor inelastic deformations $\mu_0 \le 4$ at low slenderness of the diagonals $\lambda \approx 80$, the amount of dissipated energy is more than 50% bigger than in case of slenderness of the diagonals with $\lambda \approx 180$. Therefore slenderness has significant influence. When CBF

responds within the range of large inelastic deformations $\mu_0 > 6$ at slenderness of the diagonals $\lambda \approx 120$, the amount of dissipated energy is around 10% bigger than in case of slenderness of the diagonals with $\lambda \approx 180$. Therefore slenderness has certain influence but not that significant.

- CBFs of studied type has resistance ratio $\varepsilon \geq 1,0$ at limit ductility $\left(\mu_{\lim it}\right)$ as follows;
  - $\lambda = 80,1 \qquad \bar{\lambda} = 0,915 \qquad \mu_{\lim it} = 3,7$
  - $\lambda = 122 \qquad \bar{\lambda} = 1,384 \qquad \mu_{\lim it} = 7,3$
  - $\lambda = 181,2 \qquad \bar{\lambda} = 2,04 \qquad \mu_{\lim it} = more\ than\ 10$
- Studied types CBFs with reduced cross-sections in the diagonals demonstrate the best inelastic behavior when slenderness of diagonals is between values 120 and 180. At higher values of slenderness of the diagonals, hysteresis behavior of the frame is such that a higher ductility is achieved and hence higher dissipation of the structure. Such a conclusion could be found in the works of *Goggins, Broderick and Elghazouli* (2005) in literary source [58]. We should say that in this format of the study have not been considered the second order effects (P-φeffects).

Chapter 5. General conclusions and summary of research done

This thesis involves performance of numerical studies presented in Chapter 2 and experimental studies of which analysis is performed in Chapter 4. Chapter 5 will present the final conclusions and summary to which the author reached. Subject of the thesis are Concentrically Braced Frames (CBFs) with shaped structural fuses (areas of reduced cross section) of the diagonals. Therefore always in the exposition of Chapter 5 when it comes to CBFs should be understood that these are frames of the studied type and a subject of the thesis.

5.1. Conclusions and summary of numerical studies in Chapter 2

As a result of the numerical parametric study performed the author formulates the following general conclusions and generalizations:

- The reduction in cross section as proposed (see Figure 5-1) does not act as a concentrator and allows plastic deformations to develop in the area of reduced cross section (RCS). The presence of a RCS reduces plastic deformations between 25 and 45% depending on the reduction ratio $k = \frac{A_{OC}}{A}$. However this plastic phase is absolutely sufficient for obtaining of dissipative behavior relying on ductile work. The reduction of the cross section of the web practically does not change the inelastic behavior of the member.

- The length of the area of reduced cross section directly affects the ductility of the member. Too short length of the area of RDS may act as a stress concentrator leading to the reduction of plastic work of the member. The study confirms that the minimum length of the area of reduced cross section could be determined by the equation $L_{OC,\min} = 5.65\sqrt{A_{OC}}$. A similar recommendation was given also by Professor *Vincenzo Piluso* et al in [84]. The author offers also a second criterion $L_{OC,\min} = 1.5H$.

- The degree of trimming of the cross section, the degree of development of plastic deformations, the length of the area of implemented RCS and the hardening caused by the presence of the Structural Fuses are in interaction. In significant reduction of the cross section, hardening may ignore the effect of trimming. Proper setting of the behavior could be obtained by increasing the length of the area of reduced cross section.

- Connecting the dissipative member and the non-dissipative frame is realized in joints. To ensure elastic behavior of the frame should be kept in mind the occurrence of potential hardening in the dissipative member. This should become

with the use of coefficient γ_{SH} called a coefficient of strain-hardening. On the value of the coefficient of strain-hardening according to the author influence the following factors:

- Hardening caused by the operation of material within the reduced cross section zone, after reaching the end of plastic plateau;
- Hardening caused by the shape of the cross section and of the layout of the joint ribs and connections;
- Hardening due to the strain rate in seismic situation;
- Hardening dependent on the class of ductility of the designed structure (DCH or DCM);

The author proposes for structures or members sensitive to overloading the value of the coefficient in question to be $\gamma_{SH} = 1,3$. The author believes that value 1,1 set out in the European code is undervalued and should have more differentiated form in accordance with the factors described above. Such a conclusion is also well supported in study [58], where Goggins, Broderick and Elghazouli report about forces of 20% higher than the expected one and explain the difference with the dynamic nature of the study.

❖ Of the studied 5 different designs of the area reduced in cross section the proposed version (Figure 5-1) has the best impact on the inelastic behavior of the member. The variants related to reduction of the cross section through drilling of openings act as stress concentrators. The variant related to reduction of the cross section by the implementation of trimming of type "dog bone" is not acting as a stress concentrator but reduces the plastic work of the member.

***Fig. 5-1** - the most appropriate variant for shaping the area with RCS*

❖ By introducing reduced cross sections along the diagonal is affected the slenderness of the member. Trimming of the web (parameter W) affects negligibly and in practice could be ignored. Trimming of the flange (parameter F) affects significantly the slenderness of the diagonal and this effect should be taken into consideration in determining the equivalent slenderness λ_{eq}. The length of the trimmed cross section is a geometrical parameter that significantly affects the equivalent slenderness of the diagonal. In order to take into account the impact of the reduced cross section has been derived an analytical equation (2.2-1) which covers cases of practical interest of such type of diagonals with RCS.

$$\mu = \frac{\lambda_{eq}}{\lambda} = \left(0.42\frac{L_{OC}}{L} + 0.89\right)\left(\frac{I_{Z,OC}}{I_Z}\right)^{-(\frac{L_{OC}}{L}+0.14)} \geq 1.0 \qquad (2.2\text{-}1)$$

The equation has a range of validity $0.95 \geq k = \frac{A_{OC}}{A} \geq 0.50$ and $0.25 \geq \frac{L_{OC}}{L} \geq 0.10$.

The accuracy of the equation is compared with the results obtained through solution derived by the FEM (Finite Elements Method) and has been proven for cross section of height of 130 mm, width of 120 mm, flange thickness of 5 mm and web thickness of 4 mm. The equation always gives values on the safe side. The average deviation of the values obtained by equation (2.2-1) is 4.46% and the maximum deviation is 8.65%. The proposed equation is compared with the equation proposed by *Vincenzo Piluso* et al in [84]. The results are published in Appendix 2.3 of this thesis.

5.2. Conclusions and summary of experimental studies

5.2.1. Experimental series 1

After performance of the experiments of series 1 and the subsequent processing and analysis of the results the author reaches the following general conclusions and generalizations:

❖ Designing the structural fuse (RDS) within diagonals by the use of two classes of steel is wrong and ineffective. The proper decision is to design the area of the structural fuse of steel S235J2 having the best possible plastic properties and guaranteed maximum value of the yield strength. The key parameter that determines the plastic behavior of the material is the residual elongation. The structural fuse should be designed using steel sheet of the same thickness and made from the same cast of steel. Thus will be achieved almost simultaneous occurrence of plastic deformations in all parts (web, flange) of the structural fuse.

❖ Inelastic deformations in diagonals of the studied types of CBFs develop within the structural fuses (areas of reduced cross sections) and within transition areas in front

and behind them and elastic deformations occur within the entire diagonal. The contribution of the transitional areas in the final inelastic deformations of the diagonal is up to 8%. The proposed form of shaping of the structural fuse by narrowing the flange and forming an elongated opening in the web by itself does not develop concentration of inelastic deformation and are acceptable for implementation in a dissipative member. The maximum inelastic deformations that the material may develop (by standard tensile test) and inelastic deformations that the structural fuse may develop are different.

- Inelastic deformations that could develop a diagonal having structural fuses when subjected to tension and accompanying compression (as it was done in the experimental set-up of series 1) and inelastic deformations that the diagonal may develop in cyclic tensile and compressive loading accompanied by buckling of the diagonal (as it was done in the experimental set-up of series 2) differ significantly. The author explains this difference as follows. When in a given section superimpose effects of plasticization in tension and occurrence of local buckling under compression within the cross section emerge warpings (local buckling waves) of flange steel plates. Once occurred warpings may not be completely strengthened in reverse loading. Warpings make so that cross section may not work fully effective when it is subjected to tension (there is a stress redistribution) and thus they play the role of a kind of concentrator of inelastic deformation. In reverse loading warpings appear to be an initial geometric imperfection in the cross section leading to a decline in the bearing capacity in case of compression. In every subsequent application of compression warping amplitudes increase and enhance the mechanism of decline in bearing capacity in tension and thereafter in compression. In the end we have an **interactive mechanism of degradation of the plastic work of the diagonal member** and hence of the entire CBFs. The author believes that the mechanism as described is not even a question of whether in the diagonal there has RCS or not. It is a matter of matching at the area of occurrence of inelastic strains incurred by tension and compression. The end of the structural fuse for models H1 and H2 is a place where inelastic deformations are concentrated. The reduced cross section even has a positive effect because the slenderness of compressed walls of the flanges decreases and thus increases the compactness[1] of the place where plastic deformations develop.

5.2.2. Experimental series 2 and experiment 3

Experimental series 2 and experiment 3 made it possible to study thoroughly the inelastic behavior of the proposed type of CBFs. For this reason the conclusions will be grouped thematically.

[1] This means that the cross section is of class 1 according to BDS EN 1993-1.

Concerning the design composition and details of the proposed type of CBFs

- Conducted experimental study of the proposed type of CBFs and structural fuses in the diagonals (RCS) confirmed the original intent. Inelastic deformations occurred in the designated areas and the form for development of plastic strains was in accordance with the design concept. Exception made upper left diagonal of model H1. The reasons for this exception are analyzed in item 4.8.3.

- The proposed structural detail by increasing the gusset plate of the diagonal and by the use of bolt connection with fitted bolts provides elastic behavior of frame connections (non-dissipative members) and provides free diagonal rotation without leading to plasticization in the gusset plate. The proposed types of CBFs belong to the category "weak diagonals ï strong gusset plates."

- The detail of connection of the column to the diagonal by pair of gusset plates and two bolts causes local bending in bolts and in the plates. Local bending can be avoided if it is used common stud bolt and tube spacer as suggested by Figure 4-113.

- The lack of direct intersection of the diagonals by inserting a horizontal intermediate member avoids the interaction between tensioned and pressed diagonal. This separation requires a more detailed study of the role of the horizontal intermediate member and in particular the relationship between bending stiffness of the horizontal intermediate member and the slenderness of diagonals.

- The proposed type of ñHò-shaped built-up welded cross section used in diagonals is appropriate for the following range of reasons:

  - The cross section is built-up by steel plates and the provision of steel sheets having guaranteed maximum value of yield strength is a task that is feasible in Europe[2].

  - In an established European practice[3] of the manufacturers of hot-rolled sections HEA, HEB, IPE, the delivery of steel profiles that are of class S235 and having guarantee maximum value of yield strength is not possible. In Europe are not available hot-rolled profiles HEA, HEB, IPE of class S235.

  - Through built-up cross section the engineer may specify the required cross sections of the diagonals of multi-story CBFs as required by the design. The smooth change of the cross sections of the diagonals in height is entirely

[2] In the author's personal practice the provision of steel plates with limited upper yield strength has happened several times in the past two years i.e. this is virtually feasible.

[3] In Europe all profiles of types HEA, HEB, IPE are produced from steel grade not lower than S275.

under the control of the designer. It is not the same if one uses hot-rolled cross sections because there are limitations in standard sizes on the one hand and of the actual market availability of sizes on the other hand.

Concerning the specifics of the hysteresis behavior of the proposed type of CBFs

- Inelastic behavior of CBFs in experimental models H1, H2 and H3 is characterized by the development of the hysteretic loop which has an expressed form of pinching and a significant cyclic decrease in stiffness.

- The main characteristic of inelastic behavior is the ductility of the structure. In this regard CBFs of more slender diagonals have higher limit ductility. We remind that under limit ductility the author understands the maximum value of ductility coefficient up to which there is no decline in resistance ratio below 1.0. The performed study showed that the limit ductility for all three frames participating in the study are as summarized in Table 5-1:

Table 5-1

Model	Slenderness of the diagonals	Classification of the slenderness of the diagonals	Effective slenderness of the diagonals with RCS	Limit ductility
Ɩ 1	$\lambda = 80,1$	low slenderness	$\bar{\lambda} = 0,915$	$\mu_{\textit{пределна}} = 3,7$
H2	$\lambda = 122$	medium slenderness	$\bar{\lambda} = 1,384$	$\mu_{\textit{пределна}} = 7,3$
H3	$\lambda = 181,2$	high slenderness	$\bar{\lambda} = 2,04$	$\mu_{\textit{пределна}} = \textit{над}\,10$

i.e. by increasing the slenderness of the diagonals increases also limit ductility. This statement has been verified experimentally for a range of slenderness of the diagonals from 80 to 180.

- If the diagonals are within the range of the normalized slenderness recommended by Eurocode 8, namely $1,3 \le \bar{\lambda} \le 2,0$ then the value of the full ductility ratio Ψ varies in the range $\psi = 0,7 \div 0,8$.

- All three models in the study have a "resistance ratio" over 1 but it changes depending on the development of inelastic deformations. CBF of model H1 (of the lowest slenderness of the diagonals) obtains a descending branch of the function of the "resistance ratio" and the values are ranging from 1.2 to 1.0 approaching limit ductility. CBF of model H2 (of the medium slenderness of the diagonals) has an ascending branch of the function of the "resistance ratio" to the limit ductility and

subsequent descending branch. CBF of model H3 (of the highest slenderness of the diagonals) obtains only ascending branch of the function of the "resistance ratio" which is not exhausted in the study - Figure 4-155.

- Inelastic behavior of CBF is characterized by a decline in rigidity ratio ξ with increasing inelastic deformations. This ratio is influenced by the slenderness of diagonals. By increasing the slenderness of the diagonals decreases ξ.

- All studied models show similar characteristics in terms of the absorbed energy ratio which can be defined in respect to its average value as $\eta = 0,25$ - Figure 4-158.

- Despite the differences in the slenderness of the diagonals and the type of shaping of the RCS, CBFs have similar relationship between partial ductility and full ductility and they are described by the equation $\mu = 1,34\mu_0 - 0,3$ (4.9-1).

- Slenderness of the diagonals has a direct influence on the ductility of CBFs. At low slenderness of diagonals the frame obtains limit ductility that equals to 3.7 and in case of slenderness within the range $1,3 \le \bar{\lambda} \le 2,0$ limit ductility ranges from 7.3 to over 10.

- Slenderness of the diagonals of the studied type of CBFs affects the amount of dissipated energy. When CBF responds within the range of minor inelastic deformations $\mu_0 \le 4$ at low slenderness of the diagonals ($\lambda \approx 80$) the amount of dissipated energy is more than 50% bigger than in case of slenderness of the diagonals with $\lambda \approx 180$. Therefore slenderness has significant influence. When CBF responds within the range of large inelastic deformations $\mu_0 > 6$ at slenderness of the diagonals $\lambda \approx 120$ the amount of dissipated energy is around 10% bigger than in case of slenderness of the diagonals with $\lambda \approx 180$. Therefore slenderness has certain influence but not that significant.

- Inelastic behavior of the studied type of CBFs and diagonals of slenderness that falls within the range recommended by Eurocode 8 $1,3 \le \bar{\lambda} \le 2,0$ is better due to the substantially improved ductility and small decrease in bearing capacity. If the diagonals are of less slenderness (as it was the case with H1) this leads to a concentration of inelastic deformations in a specific cross-section along with the development of the effects of local buckling (buckling of flanges and web steel plates) and occurrence of low cycle fatigue. This is why studied model H1 failed to

achieve demanded ductile behavior. Such a conclusion could be found in the works of *Walpole* (1995) [100].

SUMMARY

We can formulate the summary that the relatively constant ability of CBF for dissipation of energy is due to its excellent ductility and small decline in bearing capacity on one hand and pinching of the hysteretic loop and the cyclical decline of stiffness on the other hand. The first two factors act in a positive direction and the latter two factors deteriorate the cyclic inelastic behavior of the structure. With the increase of slenderness of the diagonals improves the contribution of ductility and the reserve of bearing capacity but become worse the cyclic decline of stiffness and the pinching of the hysteretic loop. Thus is reached a dissipativity equal to about 25% of the dissipativity in perfect inelastic cycle. Full ductility coefficient does not depend by the slenderness of the diagonals.

Concerning the design of Reduced Cross Sections

Differences in design of RCS affect differently the development of forms of local buckling (LB). In the frame with diagonals of low slenderness as model H1 the mechanism of development of LB rapidly evolved and occurred concentration of plastic deformations in the places where the LB has led to warping of the walls of the cross section. Once originated this phenomenon leads to the development of an interactive mechanism of decline in bearing capacity (resistance) of the diagonals and the failure of the relevant diagonal.

In frames with diagonals of greater slenderness as in model H2 the mechanism of occurrence of LB and the concentration of plastic deformations is present but it is not developing as fast as in model H1. Again there is a presence of an interactive mechanism of decline in bearing capacity of the diagonals and their destruction but the process is not as intense as in model H1.

In frames with diagonals of the highest slenderness as in model H3 where have been introduced modified middle cross section in the diagonal was not observed occurrence of LB. Mid-section is subjected to inelastic deformations caused by bending of buckled diagonal. The RCS (structural fuse) is subjected to inelastic deformations by tension. There is no mechanism that can lead to the occurrence of low cycle fatigue. Throughout the study has not been reached a fracture of the model. The proposal for separation of the sections in the place of development of inelastic deformations improves inelastic behavior of the CBF.

The final conclusion is that if the diagonals of CBFs of the studied type are within the recommended range of slenderness acc. to BDS EN 1998-1 namely $1,3 \le \bar{\lambda} \le 2,0$, inelastic behavior of the studied type of CBFs improves. This is proven by the derived behavior factors *q* that has the following averages - Table 5-2. When dealing with diagonals of low slenderness behavior of CBFs deteriorates.

Table 5-2

Model	Slenderness	Behavior ratio
H1	$\lambda = 80,1$	3.507
H2	$\lambda = 122$	6.020
H3	$\lambda = 181,2$	5.835[4]

The use of a modified midsection as was shown in model H3 is an innovative proposal that solves the problem of separation of the places for the development of inelastic deformations caused by tension and compression. With the introduced innovative proposal SF is a zone where the member will plasticize if subjected to tension and the middle modified section is where the member will plasticize due to bending in occurrence of buckling in the diagonal.

CONCERNING the role and influence of the frame

The frame (F) in practice is never a truss system. It is a participant in dissipation of seismic energy through the development of inelastic deformations in the semi-rigid frame joints. The contribution of the frame in the overall energy dissipation is very important for the part of the hysteretic loops in the zone of zero displacements. The more slender the diagonals are the more important is the contribution of the frame. The latter should reflect in more stringent rules for designing of frame joints where it should be a must:

- To be designed joints and connections so that there should not be any clearances allowing unrestrained deformations;
- To be designed joints so that they could follow the rotation between the beams and columns caused by the frame drift.

The use of structural details such as the applied once in the frames of the tested models is a possible good design solution.

The contribution of the frame in the total dissipated energy in regards of the tested models for ductility ($\mu_0 < 4,0$) is as follows:

Model	Effective slenderness	% of participation of the frame in the dissipation of energy
Designation	$\lambda_{y,eff} = \frac{L_D . \mu}{i_y}$	$\frac{A_{frame}}{A}$
H1	80.1	up to 17%
H2	122.0	up to 20%
H3	181.2	up to 27%

[4] It is appropriate to remind that due to the exhaustion of capabilities of the loading system the experiment was terminated without reaching the actual failure of the researched model H3. This would mean that the real behavior ratio of model H3 would be of higher value.

In the range of high ductility $\mu_0 > 6,0$ and high slenderness of diagonals $\lambda = 181,2$, the contribution of the frame may reach up to 50% or even 60%. Shear forces borne by columns do not exceed 37% of the total horizontal force. To a similar conclusion was reached in the researches performed by (*Tang and Goel*, 1987, [94]) and (*Hassan and Goel* 1991, [60]) and there has been stated the value of 40%.

CONCERNING the role and behavior of the diagonals

The behavior and role of the diagonals can be summarized as follows. Diagonals are the main place where inelastic deformations develop in CBF. Inelastic deformations develop by buckling of the diagonals and the induced by it bending and by tensile inelastic elongation. In models H1 and H2 bending caused by buckling occurs in the more remote from the joint end of the RCS. In the stage of first loss of stability of the pressed diagonal the diagonal buckles following a sine wave (or similar). With increasing the frame drifts a kink appear and the rest of the member straightens. In models H1 and H2, the kink is always in the end of the RCS. In model H3 bending occurs in the middle modified cross section. Tensile plastic strains occur always in the areas of reduced cross section. The inelastic strains of all areas of reduced cross section in a given tandem of diagonals are not the same.

The conducted studies led to the following conclusions:

- The upper and lower diagonal having the same angle of inclination form a tandem. Each CBF has two tandems and they have identical behavior. For example if decline of the force in one of the diagonals in a given tandem declines also the force in the other diagonal of the tandem. Behavior of the diagonals is identical only to the first diagonal buckling of a compressed diagonal.

- The behavior of the tensioned diagonals is similar until the time of occurrence of local buckling (LB). After occurrence of LB behavior of the tensioned diagonal and the behavior of the pressed diagonal are in interactive relationship. Effects of LB appear to be initial imperfections in applying compression force thus leading to a steady decline in the bearing capacity of the diagonal subjected to compression (fig. 4-127). Meanwhile the warpings due to LB lead to normal stress redistribution within the flange width so the whole cross section does not work effectively also if subjected to tension . This gives rise to a mechanism of decline in the bearing capacity of the diagonal if subjected to tension. The decrease in tensile resistance is much smaller than the degradation in compressive resistance (Figure 4-119). The interactive mechanism of onset of decline in bearing capacity (resistance) is shown in Figures 4-118, 4-119 and 4-120.

- When a diagonal loses its stability and CBF continues to develop inelastic deformations the residual post-critical compressive force in the diagonal is between 0 and 20% of its bearing capacity - Figure 4-127. For large displacements that residual force tends to zero. If for some reason the diagonal is not buckled it retains its compressive bearing capacity by the end of the experiment. This means that a plastic mechanism is implemented characterized by strong diagonals and weak horizontal intermediate member.

- When the diagonals are of low slenderness they buckle in plastic phase. Then the behavior in compression becomes modified and it is possible the buckling mode of the diagonal to be concentrated in the area of reduced cross section. This is an adverse effect because it leads to overlaying of effects of local buckling and global one. In such a scenario occur effects of low cycle fatigue. This was the case in the upper left diagonal of model H1.

- Low value of slenderness of the diagonals (in this case $\lambda = 80$) and classes of cross sections 3 should be avoided. Minimum slenderness should be the recommended one by Eurocode 8. Using slenderness of value less than 120 will lead to worse behavior of the CBF and reduced cross sections.

- The author believes that the use of innovatively designed applied in model H3 with implementation of middle modified cross section with reduced bending stiffness and increased bearing capacity of axial forces is a new approach that helps to be avoided overlapping of plastic tensile and compressive deformations and significantly improves the ductile behavior of diagonals. During the experiment 2-3 with model H3 have not been registered any forms of local buckling.

- When using middle modified cross section initial imperfections (manufacturer's alignment offset) should be considered. The study showed that in two of the diagonals even in the elastic phase of behavior there is a difference in stiffness in compression and in tension. Diagonal compression force can be from 18% to 60% of the diagonal tensile force. A similar conclusion was formulated by *Goggins, Broderick and Elghazouli* in [58]. Variation of the compressive force depends on the degree of initial imperfection. Theoretically obtained compressive resistance should be reduced by a factor of 0,75 in order to be accounted the effects of initial imperfections or should be used non-linear static analysis with initial imperfections.

- In all the diagonals of frame H3 there is a development of inelastic deformations. Inelastic deformations between the diagonals differ by up to 2,75 times but the difference between tandem diagonals is limited to only 3.8%. A diagonal that buckles earlier develop larger inelastic deformations.

CONCERNING the role of the horizontal intermediate member

- After the occurrence of first buckling of compressed diagonal lacks symmetry in axial forces in the diagonals. The lack of symmetry increase along with the enhancement of buckling of the diagonal; The lack of symmetry in the stressed state of the diagonals causes the onset of Unbalanced Vertical Force (UVF) in the horizontal intermediate member. UVF bends the horizontal intermediate member and may cause plastic hinge in it. The slenderness of the diagonals (as a measure of their stiffness) should always be related to the bending stiffness of the horizontal intermediate member. The author believes that the horizontal intermediate member must be chosen so as to "force" both tandem diagonals towards buckling. Should be defined relationship between the stiffness of the horizontal intermediate member and the slenderness of the diagonal; Has been proposed the following formula for UVF $V_d = (0,1.N_{d,t} + N_{d,c})\sin\alpha$ - Chapter 4, item 4.8.2 - particular conclusions. The lower the slenderness of the diagonals is, the greater the bending stiffness of the horizontal intermediate member should be. The presence of UVF generates also UHF which in turn bends the column. This phenomenon either must be secured by a capacity design or should be designed a connection detail (between horizontal member and the column) allowing free horizontal movement between the column and the horizontal intermediate member;

- The horizontal intermediate member should have the necessary bending stiffness in order to be able to redistribute the forces arising in the post buckling phase. If this did not happen (if the horizontal intermediate member may not redistribute) shall emerge a mechanism of strong diagonals and a weak horizontal intermediate member. This leads to a redistribution of the internal forces. As a result plastic deformations shall concentrate in the same cross sections resulting to reduction of the inelastic work of diagonals and decline of partial ductility of CBF.

- For model H3 when diagonals are of assumed slenderness $\bar{\lambda}_{eff} \approx 2,0$, the horizontal intermediate member plays its redistributive role and "forces" all diagonals to buckle. This effect leads to a distribution of the plastic deformations on more cross sections and the avoidance of concentrations of plastic deformations.

- In model H3 has been also registered asymmetry in the stressed state of the diagonals and the occurrence of unbalanced vertical force. The adequate stiffness of the horizontal intermediate member helped to overcome the asymmetry and for homogenizing the behavior of all diagonals.

Relationship between inter-storey drift and axial elongations in the diagonal (relationship between global and local ductility)

- The relationship of shortening or lengthening of the diagonal in respect to inter-storey drift could be described reliably through the corrected formula (4.1-1) which was proven experimentally.

$$\delta = 0,9.\Delta.\cos\alpha \qquad (4.1\text{-}1)$$

The formula gives good results in the phase of inelastic CBF response. In case of larger drifts the author expects that the equation will be even more accurate.

- Formula (1.2-12) is suitable for determining the buckling amplitude for CBF of the type of model H3.

$$\bar{f} = \frac{\sqrt{\sin\alpha.\cos\alpha}}{2}.\sqrt{\theta} \qquad (1.2\text{-}12).$$

For the relative drifts above 0,025 rad it is of sufficient accuracy and in the rest of the cases it gives results on the side of safety. The formula was proved also experimentally.

Scientific contributions (Findings)

According to the contents of the conducted analytical and experimental study the author believes that he has contributed to the advancement of knowledge on the behavior of concentrically braced frames with X-shaped configuration of diagonals and lays claim to the following scientific contributions:

I. Has been proposed an idea for designing of Concentrically Braced Frames (CBFs) and Reduced Cross Sections in diagonals enabling:

   a. Implementation according to the Bulgarian construction practices and traditions in steel construction;

   b. Implementation of Reduced Cross Sections in diagonals enable decrease of the sizes of the columns and beams of the frame and decries the connections design forces, when following the capacity design procedure under BDS EN 1998-1, item 6;

II. Has been planned and realized an experimental program of 6 experiments covering models in geometrical scale of 1:0,5. The program is aimed at

clarifying the hysteretic behavior of the proposed CBFs. Has been made an overall analysis of the experimental results according to the procedure of ECCS by deriving all the features of the inelastic behavior;

III. Has been proposed an idea and was carried out experiment 2-3 for frame with diagonals having middle modified cross section targeting to predetermine the shape of the mode of buckling and separation of cross sections plasticizing through tension and cross sections plasticizing by bending in case of buckling.

IV. Has been performed an analytical study on determining the optimal shape of the Reduced Cross Section (Structural Fuse) and determining the factors influencing the reduction of plastic strains and the accompanying hardening - Chapter 2, item 2.2.6. Has been analyzed the stressed state in the RCS and the mechanism for the development of inelastic deformations in the web and flanges.

V. Has been performed an analytical study and was derived a family of curves for determining the effective slenderness of members with Reduced Cross Sections. Has been proposed an analytical formula (2.2-1) reflecting the influence of the length of the area of RCS and the reduction ratio on the slenderness of the element.

VI. Through the experiments held were checked two proposed theoretical formulas. It has been experimentally proven the applicability of formula (1.2-12) for large inter-storey drifts. Has been checked formula (2.1-3) showing the relation between the inter-storey drift and axial elongation of the diagonal. It has been made a comparison between the theoretical data and the experimental ones. As a result was proposed an improved corrected version of formula (4.8-6);

VII. Has been studied the influence of the frame (columns and beams), the presence of unbalanced vertical forces in the horizontal intermediate member and the behavior of the diagonals of the proposed CBFs. Has been drawn the necessary graphs characterizing the behavior of the diagonals through which could be created analytical models. Has been demonstrated a mechanism for introduction of unbalanced vertical force, have been analyzed the effects thereof and was proposed same to be considered in designing the horizontal intermediate member (Chapter 4, item 4.8.2 - particular conclusions);

VIII. Has been suggested values for the behavior factors q (Chapter 4, item 4.7) of the three types of studied frames and has been proposed a methodology for their determination based on experimental results;

IX. Has been proposed a theoretical model (analytical bi-linear model) on the autonomous behavior of the area of reduced cross section in case of available data on the used steel and its inelastic properties - (Chapter 4, item 4.1.4).

Directions for future research

Conducted analytical and experimental study inevitably raises new research questions. They cannot be detailed in this work. Systematization of questions and problems addressed in future studies might be:

A. Structural fuse (SF)

Exploration of the possibility of designing structural fuses through (Reduced Cross Section) a single thickness of steel sheet. Development of a structural fuse detail made of steel castings for use as a pre manufactured element inserted within a diagonal of CBF.

Investigation of the influence of the RCS (structural fuse) on the stiffness of the structure.

B. Modified middle section

Developing on the idea of the use of a modified midsection in order to predetermine the mode of buckling and separation of cross sections plasticizing through tension and cross sections plasticizing through bending in buckling.

- Study on the influence of the middle modified cross section on the type of the form of buckling;
- Study on the influence of the middle modified cross section on the slenderness of the member;
- Determination of the minimum required length of the middle modified cross section;

C. Connection detail between the diagonal and the frame

Development of an alternative connection detail between the diagonal and the frame through gusset plate and predetermined bending in it.

D. Horizontal intermediate member

Investigation on the stiffness of the horizontal intermediate member depending on the slenderness of the diagonals in order to achieve equal distribution of plastic deformations among all diagonals;
Refining the formulation for determining unbalanced vertical forces in the middle of the horizontal intermediate member.

E. Computational models and numerical studies

Creating a computational model based on plastic hinges that reliably interprets the inelastic behavior of the studied CBF. Calibration of the model with experimental results.
Performance of series of dynamic non-linear analyses in respect to buildings of low and medium-rise (up to 6 or 8 floors) aimed to obtain:

- Behavior factor;
- Type of the global yielding mechanism;
- Obtaining the ratio of overloading of the frame by the effects of redistribution of internal forces in the development of plastic zones in the diagonals;

F. Other options for application

Exploring the option of applying the concept of *separation of cross sections plasticizing through tension and cross sections plasticizing through bending in buckling* of CBFs with "V" and "ə" configuration of the diagonals.

G. Design recommendations

Development of design recommendations and development of a methodology for designing of CBFs with Reduced Cross Sections in diagonals.

Acknowledgments

I express my deepest filial gratitude to my parents Snezhana and Stefan Georgievi for the mannered person that they made me for the education that my family provided me and for their significant moral support.
I thank my wife Albena for the stoicism in sharing difficulties, for the faith and support she continually showed and for the harmonious family environment which also turned to a source of strength and inspiration in my work.

Like any modern scientific study this one also has been accomplished with the help of a number of professionals and organizations. I will use the following lines to express my personal gratitude to them.

I take this opportunity to thank Prof. Dr. Eng. Petar Sotirov who is a scientific advisor of this PhD thesis and also my teacher and instructor in the field of seismic engineering. I cordially thank for the professionalism, deep knowledge shared, human and professional model and patience and confidence by which was accompanied our long professional work.

I want to express my deepest gratitude to the Heads of Department "Steel, Timber and Plastic Structures" for the opportunity and support granted for the time during which were conducted the experimental studies and the preparation of the PhD thesis. I thank Associate Prof. Dr. Eng. Georgi Linkov for the skilled guidance and belief in my abilities. I thank Associate Prof. Dr. Eng. Nikolay Rangelov for his support and confidence in the value of the performed study.

I extend my most sincere gratitude for the support and sponsorship I received from Prof. Dr. Eng. Mihail Tzankov, Eng. Yasen Vuchkov and Eng. Konstantin Zhelyazkov. Without their moral support, commitment and trust this PhD thesis couldn't be realized.

I thank Chief Assist. Prof. Eng. Ognyan Ganchev who is a head of the Teaching and Research Laboratory of Department "Steel, Timber and Plastic Structures" in the UACEG for the excellent organization and technical and software support of the experiments held.

I thank Eng. Ismet Haji for the assistance in obtaining numerical results from the analytical study conducted in Chapter 2.

I thanks to the internal reviewer Prof. Dr. Eng. Stefan Tzachev for the profound reading, relevant comments and notes and overall interest in the study.

LIST OF REFERENCES

1. *БДС EN 1993-1.* [illegible] 3: [illegible]

2. *БДС EN 1998-1.* [illegible] 8: [illegible] 1: [illegible]

3. *Белев Б.,* [illegible], 5-6, 1997.

4. *Белев Б.,* [illegible], 2002.

5. *Бонев З., Благов Д., Таушанов А.*, [illegible] 2008-2009, [illegible] VI, 2009.

6. *Брайнов М., Венков Л.* [illegible], 1991.

7. *Венков Л., Белев Б., Пенелов Ч.,* [illegible] 3[illegible], 2009.

8. *Върбанов Хр., Тепавичаров Ан., Ганев Т.,* [illegible], 1992.

9. *Ганчева Р.* "[illegible]", [illegible] 2007.

10. *Георгиев Цв.*, [illegible] 2010, [illegible] VII, 2010.

11. *Георгиев Цв., Хаджи И.*, [illegible] 5, [illegible] 2011.

12. *Даков Д.*, [illegible], 2004.

13. *Драганов Н.*, [illegible] 3[illegible], 2006.

14. *Казаков К.*, [illegible], 2010.

15. *Линков Г., Рангелов Н., Белев Б., Ганчев О., Георгиев Ц., Гюров В.,* [illegible], 2011.

16. *Милев Й.,* [illegible] 8. [illegible] - [illegible], 2012.

17. [illegible] 1987.

18. [illegible] 2, [illegible] 2007.

19. *Пенелов Ч.* "[illegible] 8 [illegible]", [illegible] 1, [illegible], 2011.

20. *Попов Хр.,* [illegible], 1966.

21. *Рангелов Н., Енчев Ал., Милев Й., Сотиров П.,* [illegible] 60 [illegible] 3, [illegible] 181-189, [illegible] 2002.

22. *Сотиров П., Георгиев Цв., Рангелов Н.,* [illegible] 60 [illegible] 3, [illegible] 209-220, [illegible] 2002.

23. *Сотиров П., Игнатиев Н., Михалева Д., Павлов И.* [illegible] ([illegible]), [illegible], 2012.

24. *Хаджиянева И., Белев Б., Ганчев О.,* [illegible] - [illegible], 15-16 [illegible] 2010.

25. *Хаджиянева И.* "[illegible]", [illegible], 2010.

26. *Цанков М.*, [illegible] 3 [illegible] EN 1090-2, [illegible], 2011.

27. *Цачев С.,* [illegible] 1, 3 [illegible] 8 [illegible], 2011.

28. *Чуканов С. Б.,* [illegible] - [illegible], 1990.

29. *Корчински И. Л., Бородин Л. А., Дузенкевич М. С., Короленко Н. А.,* [illegible]

ƏtsLHɉ ʔfrʃsɘɖʷ fŋ lzɥɉ lststdʒ tsʙtɕʘLtsɘʘdʑʷ tʃdʑʘfrʃsɖʮɉ frʆɖ ʰ ʘtɕdʑʃtɕtsɘò, ʮdʑʃɖtʃtɕtsɉ ʕlsfrʃsʘdz ʕtsdʑʃstɕdzʕʮɖʷ, ʆ tsfrʆɘʘ, ʉ lstɕtsʔɖLHʘls, 1974.

30. *AISC.,* ñSeismic provisions for Structural Steel Buildingsò, ANSI/AISC 341-05, Chicago: American Institute of Steel Construction, 2005.

31. *AISC., “*Seismic provisions for Structural Steel Buildingsò, ANSI/AISC 341-10, Chicago: American Institute of Steel Construction, 2010.

32. *Applied Technology Council,* ñTentative Provisions for the Development of Seismic Regulations for Buildingsò, ATC 3-06, National Bureau of Standards, U.S., Department of Commerce, Washington, D.C., 1984.

33. *Aslani, Farhang; Goel, Subhash C*. ñExperimental and analytical study of the inelastic behavior of double angle bracing members under severe cyclic loadingò, UMCE 89-5, Ann Arbor, Department of Civil Engineering, University of Michigan, 1989.

34. *Astaneh-Asl A. , Goel S.C., and Hanson R.D.,* ñCyclic in-plane buckling of double-angle bracingò, Journal of Structural Engineering, ASCE, 1985.

35. *Astaneh-Asl A. , Goel S.C., and Hanson R.D.,* ñCyclic out-of-plane buckling of double-angle bracingò, Journal of Structural Engineering, ASCE, 1985.

36. *Astaneh-Asl A. , Goel S.C., and Hanson R.D.,* ñEarthquake-resistant design of double-angle bracingò, Engineering Journal, American Institute of Steel Construction, 1986.

37. *Astaneh-Asl A.* ĂSeismic behavior and Design of Gusset Platesò Structural Steel Educational Council, TIPS, December 1998.

38. *Bertero V.V., Uang C.M., Whittaker A.S.,* ñEarthquake simulator testing of concentrically braced steel structureò, Report No 86/10, UCB/EERC, 1986.

39. *Black G., Wenger W, Popov E.,* ñInelastic Buckling of Steel Struts under Cyclic Load reversalsò, Report No 80/40, UCB/EERC, 1980.

40. *Broderick B.M., Elghazouli A.Y., Goggins J., “*Cyclic Behaviour of Hollow and Filled Axially-loaded Membersò, Paper No. 2589, 13th WCEE, Vancouver, August, 2004.

41. *Bruneau M., Uang Ch.M., Whittaker A*. "Ductile design of steel structures", first edition, The McGraw-Hill Companies, Inc., 1998.

42. *Bruneau M., Uang Ch.M., Sabeli R*. "Ductile design of steel structures", second edition, The McGraw-Hill Companies, Inc., 2011.

43. *Canadian Standards Association.* ñCSA-S16-09, Design of Steel Structuresò, Willowdale, 2009.

44. *Castiglioni C.A., Brescianini J.C., Crespi A., Dell'Anna S, Lazzarotto L*, ñINERD Two Innovations for Earthquake Resistant Designò ECSC Contract n, 7210-PR-316, Final report 2, Detailed report of experimental activity ñDissipative connections for concentric

bracing systems for steel frames in seismic areasò, Politecnico di Milano, Structural Engineering Department, October 2004.

45. *Diceli M., Calic E.,* ñPhysical Theory Hysteretic Model for Steel Bracesò, Journal of Structural Engineering, ASCE, vol 134, no.7, 2008.

46. *Dominic J. Kelly, David R. Bonneville And Stacy J. Bartolett,* ñ1994 Northridge Earthquake Damage to a four-story Steel Braced Frame Building and its Subsequent Upgradeò, proceeding of 12 WCEE, Auckland New Zealand, 2000.

47. *Dubina D.*, ñExperimental Evaluation of q Factorsò, Proc. of 7Th Greek National Conference of Steel Structures, volume I, Invited papers, Volus, 2011.

48. *ECCS*, ñStudy of Design of Steel Buildings in Earthquake Zonesò, Technical Committee 1 ï Structural Safety and Loadings; Technical Working Group 1.3 ï Seismic Design. 1986.

49. *Elghazouli A.Y.,* ñSeismic Design of Buildings to Eurocode 8ò, Spon Press, 2009.

50. *Elghazouli, A.Y., Broderick, B.M., Goggins, J., Mouzakis, H., Carydis, P., Bouwkamp, J. And Plumier, A.,* ñShake table testing and seismic performance evaluation of bracing membersò, Paper No. 2589, 13th WCEE, Vancouver, 2004.

51. *El-Tayem A.A., Goel S.C.,* ñEffective length factor for the design of X-braced systemsò, Engineering Journal, American Institute of Steel Construction, 1986.

52. *Englekirk R. E.,* Steel Structures: controlling behavior through design. John Wiley & Sons, Inc., 1994.

53. *EQE International,* ñThe January 17, 1995 Kobe Earthquake an EQE Summary Report April 1995ò, 1995.

54. *Fajfar P.*, ñModeling and analysisò, Eurocode 8 Background & Applications, Lisbon, 2011.

55. *Gaylord E.H., Gaylord Ch.N. , Stallmeyer J. E.,* ñDesign of Steel Structuresò, Third edition, McGraw-Hill, Inc., pp. 137-146, 1992.

56. *Gelinas A., Tremblay R., Davaran A.* ñSeismic behavior of Steel HSS X-Bracing of the Conventional Construction Categoryò, Proceeding of Structural Congress, SEI, Chicago Illinois, March 2012.

57. *Giuffre A., Giannini R.*, ñLa Duttilit delle Structture in Cemento Armatoò, ANCE-AIDIS, Roma, 1982.

58. *Goggins J., Broderick B., Elghazouli A.,* ñSeismic behaviour and design of bracing membersò, Eurosteel 2005, volume C, p.5.2-123, 2005.

59. *Gugerli H., Goel S. C.,* ñInelastic Cyclic Behavior of Steel Bracing Membersò, Report UMCE 82-R1, University of Michigan, Department of Civil and Environmental Engineering, 1982.

60. *Hassan O., Goel S. C.,* ñSeismic Behavior and Design of Concentrically Braced Steel Structuresò, Report UMCE 91-1, University of Michigan, Department of Civil and Environmental Engineering, 1991.

61. *Hussain S., Benschoten P.V., Satari M., Lin S.,* " Buckling Restrained Braced Frame (BRBF) Structures: Analysis, Design and Approvalsò

62. *Huang Y., Mahin S. A.,* ñEvaluation of Steel Structure Deterioration with Cyclic Damaged Plasticityò, 14th World Conference on Earthquake Engineering, Beijing, China, October 12-17, 2008.

63. *Ikeda K., Mahin S.A., Dermitzakis S.N.,* ñPhenomenological Modeling of Steel Braces under Cyclic Loadingò, Report No 84/09, UCB/EERC, 1984.

64. *Ikeda K., Mahin S.A.,* ñA Refined Physical Theory Model for Predicting the Seismic Behavior of Braced Framesò, Report No 84/12, UCB/EERC, 1984.

65. *Imanpour A., Tremblay R., Davaran A.,* ñSeismic performance of steel concentrically braced frames with bracing members intersecting columns between floorsò, Stessa 2012 Mazzolani & Herrera(eds), Santiago Chile, 2012.

66. *ICB,* International Conference of Building Officials., ñUniform Building Codeò, Whittier, California, 1985.

67. *Jain A.K, Goel S.C, and Hanson R.D*., ñInelastic response of restrained steel tubesò, Journal of the Structural Engineering, ASCE, 1978.

68. *Jain A.K, Goel S.C, and Hanson R.D*., ñHysteretic cycles of axially loaded steel membersò, Journal of the Structural Division, ASCE, 1980.

69. *Kahn F.L, Hanson R.D,* ñInelastic cycles of axially loaded steel membersò, Journal of the Structural Division, ASCE, 1976.

70. *Khatib I., Mahin S., and Pister K.,* ñSeismic Behavior of Concentrically Braced Steel Framesò, Report No. UCB/EERC ï 88/01, University of California, Berkeley, 1988.

71. *Kitagawa Y., Hiraishi H*., ñOverview of the 1995 Hyogo-Ken Nanbu Earthquake and Proposals for Earthquake Mitigation Measuresò, Journal of Japan Association for Earthquake Engineering, Vol.4, No.3 (Special Issue), 2004.

72. *Krawinkler H.,* ñEarthquake Design and Performance of Steel Structuresò, Pacific Conference of Earthquake Engineering, November 1995.

73. *Lee S., Goel S.C.,* ñSeismic Behavior of Hollow and Concrete-Filled Square Tubular Bracing Membersò, Report No UMEE 87-11 Ann Arbor, MI: Department of Civil Engineering, University of Michigan, 1987.

74. *Lehman D. Roeder C.,* ñImproved Seismic Design of Concentrically Braced Frames and Gusset Plate Connectionsò, ASCE, 2008.

75. *Liu Z., Goel S.C.,* ñInvestigation of Concrete-Filled Steel Tubes under Cyclic Bending and Bucklingò, Report No UMCE 87-3 Ann Arbor, Department of Civil Engineering, University of Michigan, 1987.

76. *Longo A., Montuori R., Vincenzo Piluso V.,* ñPlastic design of seismic resistant Mbraced framesò, Eurosteel 2005, volume C, p.5.2-41, 2005.

77. *Mazzolani F. et al,* ñMoment Resistant Connections of Steel Frames in Seismic Areas, Design and reliabilityò, edited by Mazzolani F. , E&FN SPON, 2000.

78. *Mazzolani F.M., Piluso V. R*. "Theory and Design of Seismic Resistant Steel Frames", first edition, E&FN SPON, 1996.

79. *Medhekar M., Laurie Kennedy D.J,* ñSeismic evaluation of steel buildings with concentrically braced framesò, Structural Engineering Report ¯ 219, University of Alberta, 1997.

80. *Milev J., Petkov Z.B., Sotirov P., Rangelov N. and Georgiev Tz.,* ñEnergy based methods and time history response analysis for behaviour factor evaluation of moment-resisting steel framesò, Proceedings of the 6th International Colloquium on Stability & Ductility of Steel Structures, (edited by D. Dubinâ and M. Iványi), pp. 421-428, Timiкoara, September 1999.

81. *Milev J., Sotirov P. and Rangelov N.,* ñEnergy based methods for evaluation of behaviour factor for moment resisting framesò, Proceedings of the Third International Conference ñBehaviour of Steel Structures in Seismic Areasò (STESSA 2000) pp. 619ï 626, Montréal, August 2000, ed. by F.M. Mazzolani & R. Tremblay, Balkema, Rotterdam, 2000.

82. *National Research Council of Canada.* ñNational Building Code of Canadaò, 13 th edition, Ottawa, 2010.

83. *Newmark N.M., Hall J.W*. ñProcedures and Criteria for earthquake Resistant Designò, Building Practice for Disaster Mitigation, Building Science Series 45, National Bureau of Standards, Washington, pp. 94-103, 1973.

84. *Piluso V., Longo A., Montuori R.,* ñAn Innovative Conception for Bracing Members: The Reduced Brace Section Solutionò, Eurosteel 2005, 4th European Conference on Steel Structures, Maastricht, 8-10 June 2005.

85. *Plumier A.*, "New idea for safe structures in seismic zones", IABSE Symposium, Mixed structures including new materials, Brussels, 1990.

86. *Plumier A.*, **"**The Dogbone**:** Back to the Future**,"** Engineering Journal, Vol. 34, No. 2, pp. 61-67, AISC. Seismic Provisions for Structural Steel Buildings (1997), 2nd Edition, AISC, Chicago, IL.1997.

87. *Plumier A., Degee H., Somja H.*, ñSpecific Rules for Design and Detailing of Steel Buildings, Illustrations of Designò EUROCODE 8 Background and Applications, Lisbon 2011.

88. *Plumier A., Doneux C. , Castiglioni C. , Brescianini J., Crespi A. , Dell'anna , Lazzarotto L., Calado L., Ferreira J., Feligioni S., Bursi O. , Ferrario F., Sommavilla M., Vayas I., Thanopoulos P., Demarco T.,* ĂTwo INnovations for Earthquake Resistant Design The INERD Projectò, CEC Agreement No7210-PR-316, Final Report, 2004.

89. *Scawthorn C., Bruneau M., Eguchi R., Holzer T., Johnson G., Mander J., Mitchell J., Mitchell W., Papageorgiou A.., Webb G., "*The Marmara, Turkey Earthquake of August 17, 1999: Reconnaissance Reportò, MCEER Project Number 99-9001, 2000.

90. *Sotirov P., Rangelov N., Ganchev O., Georgiev Tzv., Milev J., Petkov Zdr.*, ñImproved beam-to-column joints for moment-resisting frames ï an experimental studyò, INCO-Copernicus Joint Research Project RECOS, Progress report, UACG, Sofia May 1999.

91. *Sotirov P., Rangelov N., Ganchev O., Georgiev Tz., Petkov Z.B. and Milev J.,* ñImproved beam-to-column joints for moment-resisting frames ï an experimental studyò, Proceedings of the 6th International Colloquium on Stability & Ductility of Steel Structures, (edited by D. Dubinâ and M. Iványi) , pp. 241-248, Timiкoara, September 1999.

92. *Sotirov P., Rangelov N., Ganchev O., Georgiev Tzv., Milev J., Petkov Zdr.,* ñInfluence of Haunchingò point 3.3 from ñMoment Resistant Connections of Steel Frames in Seismic Areas, Design and reliabilityò, edited by Mazzolani F. , E&FN SPON, 2000.

93. *Sotirov P., Rangelov N. and Milev J.*, ñImprovement of seismic behaviour of beam-to-column joints using tapered flangesò, Proceedings of the Third International Conference ñBehaviour of Steel Structures in Seismic Areasò (STESSA 2000) pp. 265ï 270, Montréal, August 2000, ed. by F.M. Mazzolani & R. Tremblay, Balkema, Rotterdam, 2000.

94. *Tang X., Goel S. C.,* ñSeismic Analysis and Design Consideration of Braced Steel Structuresò, Report UMCE 87-4, University of Michigan, Department of Civil and Environmental Engineering, 1987.

95. *Timler P., Prion H., Tremblay R., Bouatay N.*, ĂDuctile Fuses for HSS Seismic Bracing of Low-rise Buildingsò CISC - Ecole Polytechnique ï UBC Collaborative Project, in progress, 2011.

96. *Tremblay R., Timler P., Bruneau M., Filiatrault A.,* ñPerformance of Steel Structures during the January 17, 1994, Northridge Earthquakeò, Canadian Journal of Civil Engineering, vol 22, no. 2, 1995.

97. *Tremblay R., Bruneau M., Nakashima M., Prion H., Filiatrault A. and DeVall R.,* ñSeismic design of steel buildings: lessons from the 1995 Hyogo-ken Nanbu earthquakeò, Canadian Journal of Civil Engineering, vol 23, no. 3, 1996.

98. *Uang C.M. , Bertero V.V.,* ñEarthquake simulation tests and associated studies of a 0,3-scale model of a six-story concentrically braced steel structureò, Report No 86/10, UCB/EERC, 1986.

99. *Vayas I., Thanopoulos P., Castiglioni C., Plumier A., Calado L.*, ÄBehaviour of Seismic Resistant Braced Frames with Innovative Dissipative (INERD) Connectionsò, Eurosteel 2005, 4th European Conference on Steel Structures, Maastricht, 8-10 June 2005.

100. *Walpole W. R.,* ñBehaviour of cold formed steel RHS members under cyclic loadingò, Proceedings of the NZNSEE Conference, Rotorua, New Zealand, New Zealand national Society for Earthquake Engineering, Waikanae, New Zealand, 1995.

101. *Xu P., Goel S.C.,* ñBehavior of Double Chanel Brace Members under Large Cyclic Deformationsò, Report No UMCE 90-1 Ann Arbor, Department of Civil Engineering, University of Michigan, 1990.

102. *Yang T. Y., Moehle J. P.,Stojadinovic B.,* ñPerformance Evaluation of Innovative Steel Braced Framesò, PEER Report 2009/103, PEERC, UCB, August 2009.

103. *Zayas V. A., Popov E. P., Mahin S. A.,* ñCyclic Inelastic Buckling of Tubular Steel Bracesò, Report No 80/16, UCB/EERC, 1980.